



Universiteit
Leiden
The Netherlands

The role of glomerular filtration and active tubular secretion in predicting renal clearance of drugs in children using population pharmacokinetic and physiology-based pharmacokinetic modeling approaches: unspinning the yarn

Cristea, S.

Citation

Cristea, S. (2021, June 16). *The role of glomerular filtration and active tubular secretion in predicting renal clearance of drugs in children using population pharmacokinetic and physiology-based pharmacokinetic modeling approaches: unspinning the yarn*. Retrieved from <https://hdl.handle.net/1887/3188573>

Version: Publisher's Version

License: [Licence agreement concerning inclusion of doctoral thesis in the Institutional Repository of the University of Leiden](#)

Downloaded from: <https://hdl.handle.net/1887/3188573>

Note: To cite this publication please use the final published version (if applicable).

Cover Page



Universiteit Leiden



The handle <https://hdl.handle.net/1887/3188573> holds various files of this Leiden University dissertation.

Author: Cristea, S.

Title: The role of glomerular filtration and active tubular secretion in predicting renal clearance of drugs in children using population pharmacokinetic and physiology-based pharmacokinetic modeling approaches: unspinning the yarn

Issue Date: 2021-06-16

**THE ROLE OF GLOMERULAR FILTRATION AND
ACTIVE TUBULAR SECRETION IN PREDICTING
RENAL CLEARANCE OF DRUGS IN CHILDREN
USING POPULATION PHARMACOKINETIC
AND PHYSIOLOGY-BASED PHARMACOKINETIC
MODELING APPROACHES**

Unspinning the yarn

Sînziana Cristea

Printing of this thesis was financially supported by the Leiden Academic Centre for Drug Research.

Cover design: Georgiana & Sergiu Popa

ISBN: 978-94-6332-756-5

The research described in this thesis was performed at the Systems Biomedicine and Pharmacology division of the Leiden Academic Centre for Drug Research (LACDR), Leiden University (Leiden, The Netherlands).

© S. Cristea, 2021

All rights reserved. No part of this thesis may be reproduced in any form or by any means without permission of the author.

**The role of glomerular filtration and
active tubular secretion in predicting
renal clearance of drugs in children using
population pharmacokinetic and
physiology-based pharmacokinetic modeling
approaches**

Unspinning the yarn

Proefschrift

ter verkrijging van
de graad van Doctor aan de Universiteit Leiden,
op gezag van Rector Magnificus prof. mr. C.J.J.M. Stolker,
volgens besluit van het College voor Promoties
te verdedigen op woensdag 16 juni 2021
klokke 16:15 uur

door

Sînziana Cristea

geboren te Suceava, Roemenie
op 11 juli 1988

Promotores: Prof. dr. C.A.J. Knibbe
Prof. dr. K. Allegaert (KU Leuven, Belgium)

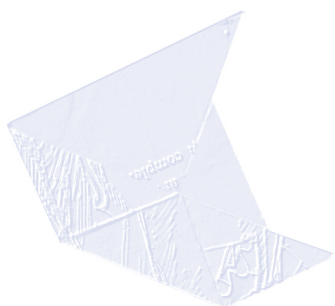
Copromotor: Dr. E.H.J. Krekels

Promotiecommissie: Prof. dr. H. Irth, voorzitter
Prof. dr. J.A. Bouwstra, secretaris
Prof. dr. A.Rostami-Hodjegan
Manchester University
Prof. dr. S.N. de Wildt
RadboudUMC
Prof. dr. A. Vermeulen
University of Ghent
Prof. dr. M. Danhof
Dr. J.G.C. van Hasselt

Table of contents

SECTION I	BACKGROUND AND INTRODUCTION TO MODELING RENAL CLEARANCE OF DRUGS	
Chapter 1	General introduction and scope	9
SECTION II	POPULATION PHARMACOKINETIC MODELING TO GUIDE DOSING OF RENALLY EXCRETED DRUGS IN PRETERM NEONATES	
Chapter 2	Amikacin pharmacokinetics to optimize dosing recommendations in neonates with perinatal asphyxia treated with hypothermia	23
Chapter 3	Larger dose reductions of vancomycin required in neonates with patent ductus arteriosus receiving indomethacin versus ibuprofen	37
SECTION III	PBPK-BASED DOSING OF DRUGS CLEARED BY GLOMERULAR FILTRATION IN CHILDREN	
Chapter 4	The predictive value of GFR-based scaling of pediatric clearance and doses for drugs eliminated by glomerular filtration with varying protein binding properties	55
SECTION IV	ONTOGENY OF RENAL TRANSPORTERS AND ITS IMPACT ON RENAL CLEARANCE OF DRUGS IN CHILDREN	
Chapter 5	The influence of drug properties and ontogeny of transporters on pediatric renal clearance through glomerular filtration and active secretion: a simulation-based study	91
Chapter 6	Estimation of ontogeny functions for renal transporters using a combined population pharmacokinetic and physiology-based pharmacokinetic approach: application to OAT3	117
SECTION V	SUMMARY, CONCLUSION, AND PERSPECTIVES	
Chapter 7	Summary, conclusion, and perspectives	137
Chapter 8	Nederlandse samenvatting	155
SECTION VI	APPENDICES	
	Curriculum vitae and list of publications	162
	Affiliations of authors	164
	Acknowledgements	167

Section I. Background and introduction to modeling renal clearance of drugs in children



Chapter 1

General introduction and scope

1.1 General introduction

Pharmacokinetic (PK) modeling describes drug absorption, distribution, metabolism and excretion by mathematical equations [1]. The parameters of these equations can be used to compare and evaluate different models and their performance as well as to predict drug exposure through PK profiles [2]. Drug exposure needs to be accurately captured as it relates to the pharmacologic effects of a drug [1].

Differences in size and physiological development between adults and children influence drug disposition as well as pharmacological effects. When differences in drug exposure between children and adults can be attributed entirely to differences in PK, necessary pediatric dose adjustments are generally driven by drug clearance as drug exposure is inversely proportional with clearance at steady-state [3]. PK modeling approaches have been used to estimate and describe the impact of developmental changes on PK parameters, often together with other patient and treatment related factors.

In population PK models, developmental changes that affect clearance are captured using descriptive covariate models. Covariate models capture the correlations between individual deviations from typical model parameters and patient or treatment related variables (i.e. covariates) to describe and predict some of the random variability between individual patients [4]. Covariate analyses are used to identify covariates that are clinically relevant and can be used as a basis for dose adjustments. In pediatric research, patient demographics (e.g. bodyweight, postnatal age, etc.) are the most commonly used covariates to describe changes with development whereas other covariates can be related to patient and treatment related factors (e.g. organ failure, intubation period, drug-drug interactions). In part due to ethical constraints, the number of clinical studies in children is typically limited. The majority of pediatric data comes from prospective or retrospective studies in small pediatric age-groups conducted in clinical practice where covariates such as disease, organ failure, inflammation markers or co-therapy are routinely included in covariate models and used for dose adjustments.

When pediatric PK data is scarce with a limited number of patients per age group and limited sparse sampling for a specific drug that does not support the development of a covariate model, clearance can be scaled from adults to children using empirical approaches. To do so, linear and exponential relationships based on bodyweight are regularly used. These methods are applied to 13-30% of drugs used in pediatric primary care and to 49-87% of drugs used to treat children in hospitals [5]. However, particularly in younger age groups, differences in bodyweight can capture the developmental differences in clearance between adults and children only partially which could lead to biased predictions. Physiologically-based PK models offer a better alternative, as they use system-specific parameters with physiological meaning which are separated from drug-specific parameters. With the inclusion of maturation functions, these system-specific parameters can be scaled from adults to children by describing the changes in developing physiology throughout the pediatric age-range. Based on this information together with drug-specific information (e.g. molecular weight, pH, logP, etc.), pediatric PBPK models can predict clearance values and PK profiles for any drug and any child.

This thesis focuses on drugs cleared by renal excretion for which pediatric doses are scaled based on changes in renal clearance (CL_R). Glomerular filtration (GF), active tubular secretion (ATS), reabsorption, and renal metabolism are processes that contribute to CL_R . Of the top 200 drugs prescribed in the US in 2010, 30% were renally eliminated of which 92% relied, at least partially, on ATS [6]. However, the expression and activity of renal transporters, and their contribution to ATS and CL_R remain understudied in adults as well as in children. Therefore, ATS and its contribution to CL_R in children needs to be better understood before being able to accurately predict CL_R of renally excreted drugs subject to active secretion. Once the age-dependent changes in CL_R are accurately captured throughout the pediatric age-range, it can be used to guide dose selection in children for renally excreted drugs, including those subject to active secretion.

1.2 The role of population PK approaches in predicting pediatric CL_R and guiding pediatric dosing

For pediatric patients for which off-label dosing is common practice [5], covariate models can be used to develop dose regimen that reach an effective and safe exposure from the start of therapy. Vulnerable subpopulations such as preterm neonates, especially those undergoing concomitant treatments (e.g. co-medication, hypothermic treatment, etc.) may require additional dose adjustments on top of the ones correcting for maturational changes. In this thesis, antibiotic agents used for (suspected) neonatal sepsis that are cleared renally by GF will be used to exemplify how to predict CL_R in such special populations using covariate models (Chapters 1 and 2). For these patients, co-therapy is expected to have an influence on CL_R , and therefore the impact of treatment related factors is quantified in addition to the maturation of CL_R . The identified covariate model can then be used to personalize drug dosing for each patient.

In the absence of the data required to build and validate a new covariate model, existing models can be used for extrapolations. For example, covariate models can be extrapolated to younger or older children than the age-range they were developed and validated on to obtain initial CL_R estimates for the drug of interest. When only adult CL_R values are known for the drug of interest, empirical methods based on changes in bodyweight (i.e. allometric and linear scaling) can be used for extrapolation to children. However, these methods have been proven to be inaccurate in some cases, including when used to extrapolate CL_R for drugs cleared by GF to certain pediatric age-groups [7,8]. This behavior indicates that weight-related changes are not sufficient for CL_R scaling, and that more information about developmental changes is required for accurate scaling (e.g. maturation functions) [9].

1.3 The role of physiologically-based PK approaches in predicting pediatric CL_R and guiding pediatric dosing

PBPK modelling approaches use system-specific parameters that reflect the human physiological system and are informed by diverse and abundant literature data, usually following an extensive meta-analysis. System-specific parameters are calculated using anthropometric measures that capture differences between individuals using equations that are dependent on patient demographics, and are drug independent. Drug-specific parameters are integrated in PBPK models based on physicochemical properties. Some drug-specific parameters are sensitive to variations in physiology, e.g. the fraction unbound is dependent on concentrations of plasma proteins, blood to plasma ratio is dependent on hematocrit levels, and clearance by active secretion is dependent on transporters abundance and the number of proximal tubule cells per g kidney. Pediatric PBPK models are obtained by accounting for developmental changes in physiology by applying maturation functions to the system-specific parameters. In addition, drug-specific parameters that are sensitive to changes in physiology are expected to change with age.

Recently, physiologically-based PK (PBPK) modelling approaches were acclaimed for accurately predicting CL_R throughout the pediatric age-range for a few example drugs [10]. However, the exact contribution of different processes involved in pediatric CL_R is not yet entirely understood. By using a pediatric PBPK model for predicting CL_R , the contribution of the underlying system- and drug-specific parameters to CL_R can be separated and investigated. The PBPK model for CL_R [11] (equation 1) can be studied in isolation from the full PBPK model. In this thesis, CL_R resulting only from the contribution of GF and ATS [11] will be considered, assuming no contribution of tubular reabsorption, passive diffusion or renal metabolism.

$$CL_R = CL_{GF} + CL_{ATS} = GFR \times f_u + \frac{(Q_R - GFR) \times f_u \times CL_{sec}}{Q_R + f_u \times \frac{CL_{sec}}{BP}} \quad [1]$$

As shown in equation 1, CL_R through GF and ATS is dependent on GF rate (GFR), fraction unbound (f_u), renal blood flow (Q_R), secretion clearance (CL_{sec}), and blood-to-plasma ratio (BP).

Table 1.1. The level of characterization (well, partially, poorly) for system-specific parameters and drug-specific parameters sensitive to changes in system-specific parameters included in the PBPK-based model for CL_R through GFR and ATS (equation 1). Demographic characteristics used as input for the maturation functions of these parameters are included as well.

Characterization of maturation	Parameters of the PBPK model for CL_R through GFR and ATS	Demographic characteristics for maturation functions of system-specific parameters
	Glomerular filtration rate	$GFR_{maturation} = f(WT, PMA)$
	Fraction unbound	$f_u = f(P)$, with $[P]_{maturation} = f(AGE)$
	Renal blood flow:	$Q_R = f(CO, fr)$, with $CO_{maturation} = f(BSA, AGE)$ $fr_{maturation} = f(AGE, GENDER)$
	Blood-to-plasma partitioning:	$BP = f(HEMAT, f_u, K_p)$, with $HEMAT_{maturation} = f(AGE, GENDER)$
	Secretion clearance:	$CL_{sec} = f(KW, PTCPGK, CL_{intT}, ont_T)$, with
	Kidney weight:	$KW_{maturation} = f(\rho_{kidney}, WT)$
	Proximal tubule cells per gram kidney (PTCPGK)	Unknown maturation
	Transporter-mediated intrinsic clearance	$CL_{int,T} = f(\text{transporters activity} + \text{exposure}, ont_T)$
	Ontogeny of transporters	$ont_T = f(AGE)$

green - well characterized; orange - partially characterized; red - poorly characterized;

WT – body weight; **PMA** – postmenstrual age; **P** – plasma protein; **CO** – cardiac output; **HEMAT** – hematocrit; **fr** – fraction of cardiac output; **K_p** – blood to plasma partition coefficient; **ρ_{kidney}** – kidney density; **PTCPGK** – proximal tubule cells per gram kidney.

1.4 Towards pediatric dosing for drugs cleared exclusively by glomerular filtration

Urine formation begins with GF, the main passive route involved in renal excretion of small molecules, including drugs. CL_R through GF is dependent on GFR and on protein binding, as only the free fraction of a drug is available to be cleared through this process [12] (see CL_{GF} in equation 1).

GFR has been extensively investigated in adults as well as in children. Various methods have been published for quantifying GFR *in vivo*. GFR can be derived based on endogenous markers (e.g. serum creatinine [13], cystatin C [14,15]), exogenous markers (i.e. inulin, mannitol, etc.) [16–20] or clearance of drugs mainly eliminated by GF (e.g. antibiotics [21]). As such, data on different markers for GFR have been collected throughout the pediatric age-range and used to develop mathematical functions to characterize the maturation of this process. Dependent on the marker used for quantifying GFR, but also on the quality and quantity of data used for development, different maturation functions for GFR have been published. However, it has not been established yet what the best published GFR maturation function is.

In adults, CL_R through GF is proportional to changes in the unbound fraction of the drug in plasma (see CL_{GF} in equation 1). Developmental changes in plasma protein concentrations are known to influence protein binding in children, especially in newborns and infants [22]. In older children human serum albumin and α -acid glycoprotein levels approach adult levels. However, the influence of maturation in the concentration of plasma proteins on drug binding and, implicitly, on pediatric CL_R has not been systematically investigated yet.

1.5 Towards pediatric dosing for drugs cleared by glomerular filtration and active tubular secretion together

In addition to GF, ATS contributes to CL_R by extracting a drug from blood into urine through membrane bound transporters [12]. Transporters involved in tubular secretion (e.g. OAT1/3, OCT2, OCTNs, MATE1, etc.) are located on the apical and basal sides of proximal tubule cells with secretion capacity changing alongside the proximal tubules. Hydrophilic and ionizable drugs are most likely to be substrates for active transporters. Such drugs can have a broad spectrum for transporter affinity, meaning that they can be transported by one or more renal transporters [23]. Hence, ATS of a drug is dependent on physicochemical properties such as lipophilicity, ionization, but also on plasma protein binding and on affinities to one or more renal transporters [23].

There is limited published information about the contribution of active secretion transporters and their ontogeny to ATS and, subsequently, to total CL_R in adults or in children. By performing global sensitivity analyses on PBPK models for CL_R , the contribution of the different transporters and their ontogeny to predicting CL_R for various drugs can be systematically investigated. Such an approach could determine essential system- and drug-specific parameters to accurately predicting CL_R when active secretion processes are involved.

Equation 1 shows a PBPK-based model for CL_R where GF and ATS are included in series, with ATS as a process following GF. All the (system-specific) parameters included in this PBPK-based model together with the demographic characteristics required to derive the maturation functions for each of these parameters are included in Table 1.1. Drug-specific parameters that are influenced by maturation in system-specific parameters (e.g. the concentration of plasma proteins available for drug binding thereby influencing fraction unbound changes with age) are also included in Table 1.1.

The color-coding in Table 1.1 indicates how well the maturation of the system-specific parameters included in the PBPK-based model for CL_R is characterized at the moment, with green being well characterized, orange – partially characterized and red – poorly characterized. Maturation of GFR, plasma proteins, renal blood flow, hematocrit levels, and kidney weight are well characterized. However, pediatric CL_R predictions for drugs that are actively secreted are currently still based on adult values for the number of proximal cells per gram kidney, as there is limited information on (potential) maturation of this parameter. Furthermore, the transporter-mediated intrinsic clearance ($CL_{int,T}$) reflects both the activity and expression of the transporters. *In vivo* ontogeny functions for ATS have previously been based on the quantification of *in vivo* net secretion as the aggregated functionality of one or more secretion and/or reabsorption pathways [19,24]. However, different transporters can have different ontogeny profiles throughout the pediatric age-range that cannot be identified using this method. Furthermore, net secretion implies the quantification of the resultant between active secretion and reabsorption, both of which may involve one or more active transporters. Therefore, separating between different transporters and between the different processes allows for a better understanding of the underlying physiological processes and of their contribution to CL_R . Fortunately, the protein expression of a few renal transporters (i.e. OAT1/3, OCT2, Pgp) was measured in post-mortem kidney samples to characterize their ontogeny throughout the pediatric age-range [25]. However, there is no information yet on how well the ontogeny of protein expression reflects the ontogeny of transporter activity *in vivo* and whether it remains constant with age.

Drug-specific parameters that characterize the drug kinetics for renal transporters (i.e. transporter-mediated intrinsic clearance) are commonly obtained from *in vitro* experiments. The *in vitro* value needs to be extrapolated to its corresponding *in vivo* value to obtain the correct parameter required for the calculation of secretion clearance (CL_{sec}), a key parameter in obtaining clearance through ATS. Even if the methodology for *in vitro* – *in vivo* extrapolation is continuously being refined, *in vitro* measurements are

not available for all drugs that undergo active secretion, and can be biased or reported with incomplete information that could eventually lead to a biased *in vitro-in vivo* extrapolation [26].

1.6 A combined population and physiologically-based PK modeling approach to derive key parameters and *in vivo* ontogeny functions for renal transporters

The contribution of model parameters in equation 1 to CL_R predictions can be established by performing sensitivity analyses. As shown in Table 1.1, the ontogeny of two system-specific parameters is partially or poorly characterized (orange or red color), i.e. ontogeny of renal transporters and PTCPGK (the number of proximal tubule cells per gram kidney), respectively. If the results of a sensitivity analysis show that (one of) these parameters have impact on CL_R predictions at certain pediatric ages and/or for particular drugs, then quantifying the maturation of these parameters becomes essential to obtain accurate pediatric CL_R predictions of those drugs.

Poorly and partially characterized ontogeny profiles for certain parameters can be derived *in vivo* by using a combined approach between population PK and PBPK modelling thereby maximizing the use of available data in children. The information included in a PBPK model that relies on well-established system-specific parameters and their corresponding maturation functions, can be leveraged when combined with the information captured by individual PK parameters to derive those parameters that rely on limited prior information or that are difficult to measure throughout the whole pediatric age-range.

1.7 Conclusion

Population PK methods, such as covariate analyses, are currently used to characterize the maturation of CL_R (such as glomerular filtration) and propose dose adjustments in vulnerable pediatric sub-populations for which sufficient PK data is available. When PK data is scarce or unavailable pediatric CL_R can be obtained using PBPK methods. Such methods allow the study of physiological processes in isolation to find parameters that play a key role in predicting pediatric CL_R . By combining the two methodologies- population PK and PBPK- poorly characterized ontogeny functions can be derived from data collected *in vivo*. By making use of the available data and the current methodologies individual dosing of renally cleared drugs is facilitated and can be further improved.

1.8 Scope of this thesis

The primary scope of this thesis is to apply population pharmacokinetic (popPK) and physiologically-based pharmacokinetic (PBPK) approaches to investigate the influence of glomerular filtration (GF) and active tubular secretion (ATS) on renal clearance (CL_R) in children including assessing the importance of developing accurate maturational functions for various pharmacokinetic processes used in predictions of CL_R in children. For this investigation, the contributions of passive (i.e. GF) and active (i.e. ATS) processes to CL_R are considered. Both processes contribute to pediatric CL_R and are expected to be influenced by developmental changes. Hence, the extent to which these developmental changes impact CL_R is explored in pediatric populations using clinical data of existing drugs, and using a PBPK-based framework for hypothetical drugs with an array of different properties excreted by either GF or both GF and ATS. The projects were performed to meet the following research objectives:

1. Extend existing popPK models by characterizing the development in CL_R for drugs excreted by GF in (pre)term neonates and quantify the influence of disease and co-therapy on CL_R . These covariate models are to be used to propose dosing recommendations (**section II**).
2. Establish a general scaling method for CL_R from adults to children for drugs eliminated by GF and systematically investigate how maturation of plasma protein concentration influences the unbound fraction of drugs, and subsequently, scaling of pediatric CL_R and drug doses (**section III**).
3. Use a pediatric PBPK-based model for CL_R to systematically investigate the influence of transporter ontogeny on the contribution of ATS to CL_R and illustrate how a combined population PBPK approach could be used to derive ontogeny functions for renal transporters involved in ATS (**section IV**).

To meet the stated research objectives, first, dose adjustments will be proposed for preterm neonates treated with antibiotics mainly eliminated by GF, using covariate functions from popPK models that describe the changes in CL_R with development. Secondly, based on a PBPK model the best method for scaling CL_R through GF from adults to children will be identified and this method will be used further for dose scaling. By using PBPK modelling approaches to predict pediatric CL_R throughout the pediatric age-range for hypothetical drugs excreted exclusively by GF that differ in fraction unbound, the influence of maturation on plasma protein expression and the accuracy of the scaling methods will be investigated. Lastly, a PBPK model for CL_R including GF and ATS, will be used to predict pediatric CL_R for an array of hypothetical drugs, to investigate the influence of renal transporter ontogeny on CL_R . More information on renal transporter ontogeny is required, as the only data available is based on a limited sample of post-mortem kidneys [1]. By using a combined PBPK and popPK approach, the information that is included in the PBPK model can be leveraged to estimate parameters that are poorly or partially characterized. The PBPK model for CL_R through GF and ATS has the potential to be used for scaling CL_R from adults to children and for extrapolations between different substrates for the same transporter.

The current section (**Section I**) places our analysis in the context of the current research, highlighting the research questions that will be addressed in our studies.

Section II focuses on extending existing popPK models for optimizing dosing regimens of antibiotics cleared mainly by GF. These antibiotics are administered to (pre)term neonates with (suspected) septicemia who are co-treated for complications such as perinatal asphyxia or patent ductus arteriosus, with therapeutic hypothermia or non-steroidal anti-inflammatory drugs (NSAIDs; ibuprofen or indomethacin), respectively. Previously published models that characterize the PK of the same antibiotics in (pre)term neonates treated only with the antibiotic are extended to include (pre)term neonates with these complications for which they receive co-treatments. Either the complications or the co-treatment or both are expected to affect CL_R . The quantified changes in CL_R of the antibiotic between (pre)term neonates with and without co-therapy (i.e. hypothermia or NSAIDs) serve as basis for drug dosing adjustments for this special population. Dosing adjustments are proposed based on the results

obtained from performing simulations with the popPK models that describe the antibiotic data the best. The efficacy of the treatment is assessed from the trough concentration levels that are correlated to the drug exposure. In **Chapter 2**, the influence of perinatal asphyxia treated with hypothermia is quantified on amikacin CL_R and used for developing dose recommendations in (pre)term neonates. In **Chapter 3**, the influence of co-administrating either of two different NSAIDs to induce closure of patent ductus arteriosus is quantified on vancymcin CL_R and used for dosing recommendations in this neonatal population.

While **section II** focused on using popPK approaches to characterize the development of CL_R and to optimise dosing, the following sections (**sections III** and **IV**) present general methods to scale CL_R and dosing from adults to children in the absence of PK data. In this situation, researchers often use empirical scaling methods based on bodyweight. Recently PBPK approaches became available to serve this purpose as well. PBPK methods are gaining momentum as they have been successfully used to predict pediatric PK parameters [2].

Section III is directed to establish a scaling method for CL_R of drugs eliminated by GF that is accurate throughout the pediatric age-range. CL_R through GF is dependent on GFR and the unbound fraction of the drug. By generating hypothetical drugs cleared exclusively by GF that differ in unbound fraction and type of binding plasma protein (i.e. human serum albumin, α -acid glycoprotein), a systematic investigation was performed to establish how the maturation of plasma proteins impacts scaling CL_R throughout the pediatric age-range. To do so, in **chapter 4**, first, published maturation functions for GFR were compared to observed inulin or mannitol CL_R data reported in literature throughout the whole pediatric age-range to establish the best available function for GFR maturation. Then, this function was used to describe GFR maturation in a PBPK-based model and to scale CL_R from adults to children for all hypothetical drugs. The PBPK-based model for CL_R considered changes in both GFR and protein binding throughout the pediatric age-range. By systematically comparing PBPK predicted CL_R to GFR-based scaled CL_R the impact of maturation of plasma proteins on CL_R predictions was studied in isolation from other contributing factors. In addition to GFR-based scaling, the performance of scaling CL_R with empirical scaling methods (i.e. linear scaling and 0.75 allometric scaling based on bodyweight) was investigated throughout the entire pediatric age-range.

As PBPK models are also useful to increase our understanding of the underlying physiology, in **section IV** we explore a PBPK-based model for CL_R that includes ATS in addition to GF. In **chapter 5**, the influence of the ontogeny of secretion transporters on the contribution of GF and ATS to CL_R was systematically investigated for an array of drugs with various properties, as information about renal transporters ontogeny is limited. While GF is a passive excretion pathway, ATS relies on several transporters for drug excretion. So far, ontogeny functions for renal secretion have been obtained either from *in vivo* clearance, in which case they reflect net secretion clearance by all active renal excretion and reabsorption processes, or from protein expression profiles for individual transporters, in which case it is unknown how protein expression relates to *in vivo* activity. Ontogeny of transporters remains less explored and could influence the predictions of pediatric CL_R with PBPK models of drugs that are actively secreted, making them less reliable. To understand more about the influence of ontogeny, a pediatric PBPK model for GF and ATS is used to predict CL_R for hypothetical drugs with an array of realistic properties. The influence of ontogeny of secretion transporters on CL_R is explored by assuming different extents of transporter ontogeny at various pediatric ages. To quantify the impact of transporter ontogeny we compared the CL_R predictions with or without ontogeny of secretion transporters. Drugs with properties that lead to inaccurate pediatric CL_R predictions in the absence of transporters ontogeny are highly influenced by transporters and their ontogeny. These drugs are expected to be suitable probes to investigate transporters ontogeny further.

In **chapter 6**, ontogeny of *in vivo* renal secretion transporter activity was derived using a combined

popPK and PBPK approach. This method allows the leverage of the physiology-related data integrated in the PBPK model and inform unknown parameters, in this case the ontogeny of OAT3, based on clinically observed drug clearance values. To do so, PK data on clavulanic acid –a drug mainly eliminated by GF – and amoxicillin – a drug mainly eliminated by GF and ATS by OAT3 – that were administered simultaneously to pediatric patients with ages between 1 month and 15 years was used. The individual post-hoc CL_R values obtained with the population PK models for each of the two drugs were fitted with a PBPK-based model for CL_R . All established maturation functions in the PBPK-based model were fixed to literature values so that the maturation of active CL through the transporters could be estimated. This allowed the estimation of OAT3-mediated intrinsic clearance and its ontogeny profile. Once the ontogeny of OAT3 is identified, it could be used in a PBPK model to predict CL_R for other substrates of the same transporter. Hence, CL_R for piperacillin and cefazolin was scaled to different pediatric ages. Accuracy of these predictions was assessed against typical CL_R predictions obtained from reported population PK models for each drug. Once the ontogeny of individual transporters is well characterized, for instance with the methodology developed here, the use of PBPK models can be extended to predict CL_R of drugs that are actively secreted in children.

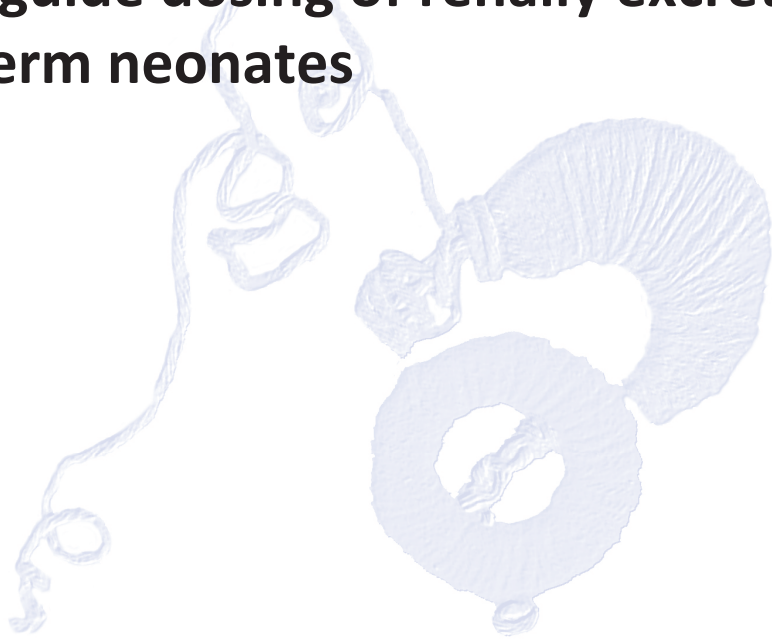
Lastly, **section V** summarizes the main findings and concludes the investigations of this thesis. Perspectives and future applications of popPK methods to determine how the relationship between trough concentrations and drug exposure changes with age and dosing frequency are also addressed. In addition, the accuracy with which empirical relationships based on bodyweight can predict PBPK CL_R of actively secreted drugs will be systematically explored to propose general guidelines for pediatric CL_R scaling. Such tools can be further extended by including additional elimination pathways (i.e. reabsorption and metabolism) to understand more about the influence of the development of renal functionality on CL_R throughout the pediatric age-range.

1.9 References

1. Levy, G. Kinetics of pharmacologic effects. in *Clinical Pharmacology and Therapeutics* (1966). doi:10.1002/cpt196673362
2. Bonate, P. L. Pharmacokinetic-Pharmacodynamic Modeling and Simulation. *Pharmacokinetic-Pharmacodynamic Modeling and Simulation* (2011). doi:10.1007/978-1-4419-9485-1
3. Benet, L. Z. & Zia-Amirhosseini, P. Basic principles of pharmacokinetics. in *Toxicologic Pathology* (1995). doi:10.1177/019262339502300203
4. Mould, D. R. & Upton, R. N. Basic concepts in population modeling, simulation, and model-based drug development- Part 2: Introduction to pharmacokinetic modeling methods. *CPT Pharmacometrics Syst. Pharmacol.* (2013). doi:10.1038/psp.2013.14
5. Kimland, E. & Odland, V. Off-label drug use in pediatric patients. *Clinical Pharmacology and Therapeutics* (2012). doi:10.1038/clpt.2012.26
6. Miners, J. O., Yang, X., Knights, K. M. & Zhang, L. The Role of the Kidney in Drug Elimination: Transport, Metabolism, and the Impact of Kidney Disease on Drug Clearance. *Clin. Pharmacol. Ther.* (2017). doi:10.1002/cpt.757
7. Krekels, E. H. J., Calvier, E. A. M., van der Graaf, P. H. & Knibbe, C. A. J. Children Are Not Small Adults, but Can We Treat Them As Such? *CPT Pharmacometrics Syst. Pharmacol.* (2019). doi:10.1002/psp4.12366
8. Calvier, E. et al. Allometric scaling of clearance in paediatrics: when does the magic of 0.75 fade? *Clin Pharmacokinet.* 56, 273–285 (2017).
9. Strougo, A. et al. First dose in children: Physiological insights into pharmacokinetic scaling approaches and their implications in paediatric drug development. *J. Pharmacokinet. Pharmacodyn.* (2012). doi:10.1007/s10928-012-9241-9

10. Zhou, W. et al. Predictive performance of physiologically based pharmacokinetic and population pharmacokinetic modeling of renally cleared drugs in children. *CPT Pharmacometrics Syst. Pharmacol.* (2016). doi:10.1002/psp4.12101
11. Rowland Yeo, K., Aarabi, M., Jamei, M. & Rostami-Hodjegan, a. Modeling and predicting drug pharmacokinetics in patients with renal impairment. *Expert Rev Clin Pharmacol* 4, 261–274 (2011).
12. Taft, D. R. Drug Excretion. *Pharmacology* (Elsevier Inc., 2009). doi:10.1016/B978-0-12-369521-5.00009-9
13. Cockcroft, D. W. & Gault, M. H. Prediction of creatinine clearance from serum creatinine. *Nephron* (1976). doi:10.1159/000180580
14. Hoek, F. J., Kemperman, F. A. W. & Krediet, R. T. A comparison between cystatin C, plasma creatinine and the Cockcroft and Gault formula for the estimation of glomerular filtration rate. *Nephrol. Dial. Transplant.* (2003). doi:10.1093/ndt/gfg349
15. Larsson, A., Malm, J., Grubb, A. & Hansson, L. O. Calculation of glomerular filtration rate expressed in mL/min from plasma cystatin C values in mg/L. *Scand. J. Clin. Lab. Invest.* (2004). doi:10.1080/00365510410003723
16. Mahmood, I. Dosing in children: A critical review of the pharmacokinetic allometric scaling and modelling approaches in paediatric drug development and clinical settings. *Clin. Pharmacokinet.* 53, 327–346 (2014).
17. Rhodin, M. M. et al. Human renal function maturation: A quantitative description using weight and postmenstrual age. *Pediatr. Nephrol.* 24, 67–76 (2009).
18. Johnson, T. N., Rostami-Hodjegan, A. & Tucker, G. T. Prediction of the clearance of eleven drugs and associated variability in neonates, infants and children. *Clin. Pharmacokinet.* 45, 931–956 (2006).
19. Hayton, W. L. Maturation and growth of renal function: dosing renally cleared drugs in children. *AAPS PharmSci* 2, E3 (2000).
20. Salem, F., Johnson, T. N., Abduljalil, K., Tucker, G. T. & Rostami-Hodjegan, A. A re-evaluation and validation of ontogeny functions for cytochrome P450 1A2 and 3A4 based on in vivo data. *Clin. Pharmacokinet.* (2014). doi:10.1007/s40262-014-0140-7
21. De Cock, R. F. W. et al. Simultaneous pharmacokinetic modeling of gentamicin, tobramycin and vancomycin clearance from neonates to adults: Towards a semi-physiological function for maturation in glomerular filtration. *Pharm. Res.* 31, 2643–2654 (2014).
22. McNamara, P. J. & Alcorn, J. Protein binding predictions in infants. *AAPS PharmSci* (2002). doi:10.1208/ps040104
23. Fagerholm, U. Prediction of human pharmacokinetics- renal metabolic and excretion clearance. *J. Pharm. Pharmacol.* (2007). doi:10.1211/jpp.59.11.0002
24. DeWoskin, R. S. & Thompson, C. M. Renal clearance parameters for PBPK model analysis of early lifestage differences in the disposition of environmental toxicants. *Regul. Toxicol. Pharmacol.* 51, 66–86 (2008).
25. Cheung, K. W. K. et al. A Comprehensive Analysis of Ontogeny of Renal Drug Transporters: mRNA Analyses, Quantitative Proteomics, and Localization. *Clin. Pharmacol. Ther.* (2019). doi:10.1002/cpt.1516
26. Yoon, M., Efremenko, A., Blaauboer, B. J. & Clewell, H. J. Evaluation of simple in vitro to in vivo extrapolation approaches for environmental compounds. *Toxicol. Vit.* (2014). doi:10.1016/j.tiv.2013.10.023

Section II. Population pharmacokinetic modelling to guide dosing of renally excreted drugs in preterm neonates



**Amikacin pharmacokinetics to optimize dosing
recommendations in neonates with perinatal asphyxia
treated with hypothermia**

S Cristea*, A Smits*, A Kulo, CAJ Knibbe,
M van Weissenbruch, EHJ Krekels, K Allegaert

Antimicrob Agents Chemother.
2017 Dec; 61(12): e01282-17

* authors contributed equally

2.1 Abstract

Aminoglycosides pharmacokinetics (PK) is expected to change in neonates with perinatal asphyxia treated with therapeutic hypothermia (PATH). Several amikacin dosing guidelines have been proposed to treat neonates with (suspected) septicemia, however, none provide adjustments in the case of PATH. Therefore, we aimed to quantify the differences in amikacin PK between neonates with and without PATH to propose suitable dosing recommendations.

Based on amikacin therapeutic drug monitoring data collected retrospectively from neonates with PATH, combined with a published dataset, we assessed the impact of PATH on amikacin PK using population modelling. Monte Carlo and stochastic simulations were performed to establish amikacin exposures in neonates with PATH after dosing according to the current guidelines and according to proposed model-derived dosing guidelines.

Amikacin clearance was decreased by 40.6% in neonates with PATH, with no changes in volume of distribution. Simulations showed that, increasing the dosing interval with 12 hours results in a decrease in percentage of neonates reaching toxic trough levels (> 5 mg/L) from 40–76% to 14–25%, while still reaching efficacy targets, compared to current dosing regimens.

Based on this study, a 12-hour increase in amikacin dosing interval in neonates with PATH is proposed to correct for the reduced clearance, yielding safe and effective exposures. As amikacin is renally excreted, further studies into other renally excreted drugs may be required as their clearance may also be impaired.

2.2 Introduction

Aminoglycosides are administered to treat neonates with (suspected) septicemia. Aminoglycosides display a concentration-dependent effect and are almost entirely eliminated by glomerular filtration [1]. Recently, a population pharmacokinetic (PK) model-derived dosing regimen for amikacin [2] was prospectively evaluated in 579 neonates, showing predictive effective and safe amikacin exposure across the entire neonatal population [2, 3]. However, for neonates diagnosed with perinatal asphyxia and treated with therapeutic hypothermia (PATH), prediction of accurate amikacin disposition remains a challenge [2]. This might be due to asphyxia-induced renal impairment with or without the influence of therapeutic hypothermia which is used as standard of care treatment for moderate to severe hypoxic ischemic encephalopathy in (near) term neonates.

Hypothermia reduces the basal and cerebral metabolic rates, decreases the process of excitotoxicity and results in improved neurodevelopmental outcome [1,4,5]. Furthermore, it may alter pharmacologic characteristics of drugs [5,6]. Drug PK profiles do not only depend on drug-specific characteristics (e.g., molecular weight, lipophilicity, etc.), but also on system-specific (physiological) characteristics of the patients (e.g., cardiac output, organ perfusion, glomerular filtration [5], etc.). The system-specific characteristics are known to be affected by the pathophysiological changes that occur during both perinatal asphyxia and hypothermia [7]. This specific combination of patient-related factors impairs the elimination of aminoglycosides, as previously documented for gentamicin [8, 9, 10]. Data on amikacin PK in neonates with PATH are, to our knowledge, not yet available.

The aim of the current study (AMICOOL) was to use population PK modelling and simulation approaches to further characterize amikacin disposition in neonates by quantifying the impact of PATH on amikacin PK. Therefore, PK data collected from neonates with PATH were analyzed together with data from a large and heterogeneous group of neonates without PATH [11]. The findings were used to determine suitable adjustments of the most recent amikacin dosing regimens to improve the exposure in this special population. As amikacin clearance is considered a surrogate for glomerular filtration, the results may provide guidance for other drugs undergoing renal excretion.

2.3 Materials and methods

2.3.1 Data Collection

Amikacin therapeutic drug monitoring (TDM) data from routine clinical care were retrospectively collected from January 2010 to December 2015 from neonates with PATH admitted to the Neonatal Intensive Care Units (NICUs) of UZ Leuven (Belgium) and VUmc Amsterdam (The Netherlands) and receiving amikacin for (suspected) septicaemia. Both centres applied the standard criteria to initiated whole-body hypothermia in term neonates [12]. A total of 83 samples were retrieved, of which 75 were obtained during the hypothermic treatment period, with a median of 1.5 samples per patient (samples range between 1 and 3). Data from neonates participating in other trials (i.e., Pharmacool trial [13]) were excluded.

The study protocols were evaluated and approved by the local institutional review boards: the UZ Leuven ethics committee approved the study protocol, and a waiver for ethical approval was obtained in VUmc according to the Dutch law on research with human participants.

Clinical characteristics at birth and at the time of amikacin TDM were extracted retrospectively from patients' files. Each NICU used separate dosing protocols, summarized in Table 2.1. Effective peak concentrations were considered to be within the 24–35 mg/L interval. To avoid side effects, trough concentrations were preferably below 3 mg/L (target trough level) and strictly under 5 mg/L (toxic trough level).

At UZ Leuven, as part of routine clinical care, amikacin TDM was collected just before administration of the second dose. According to local clinical practice, dosing intervals could be adapted by the treating physician. At VUmc Amsterdam, the first routine amikacin TDM was collected at least 6, but preferably, 12–18 hours after the first amikacin administration. Eventual dosing adaptations were suggested by the VUmc pharmacy, based on the initial amikacin dose and TDM results, according to the maximum a posteriori Bayesian fitting method, using the MW/Pharm version 3.6 (Mediware, Groningen, the Netherlands).

2.3.2 Blood sample analysis

In both centres, amikacin concentrations were initially measured using fluorescence polarization immunoassay (Abbott TDx kit, Abbott Laboratories, Diagnostics Division, Abbott Park, IL, USA) with a lower limit of quantification (LLOQ) of 0.8 mg/L and a coefficient of variation (CV) below 5%. From May 31st 2012, amikacin quantification in UZ Leuven was based on a kinetic interaction of microparticles in solution (KIMS) immunoassay (Roche/Hitachi Cobas c systems, Roche Diagnostics GmbH, Mannheim, Germany) with a LLOQ of 0.8 mg/L and a CV below 4%. From September 2011, amikacin quantification in VUmc Amsterdam was based on a particle-enhanced turbidimetric inhibition immunoassay (PETINIA) (ARCHITECT Systems, Abbott, Abbott Laboratories Inc, Abbott Park, IL, USA) with a LLOQ of 2 mg/L and CV below 4%.

2.3.3 Modeling Dataset

TDM data from neonates with PATH were combined with a previously published dataset of amikacin PK samples taken from preterm and term neonates who were neither diagnosed with perinatal asphyxia nor underwent hypothermic treatment [2,11].

The combined modelling dataset consisted of 930 neonates of which 55 (6%) were treated for PATH. All neonates were younger than 30 days of postnatal age (PNA), and the neonates treated with hypothermia were younger than 4 days. Characteristics of patients in the combined dataset are summarized in Table 2.2. No outliers were identified during the current analysis.

TABLE 2.1 Dosing regimens used for the treatment of neonates with perinatal asphyxia treated with hypothermia (PATH) at the UZ Leuven (Belgium) and VUmc Amsterdam (The Netherlands) neonatal intensive care units (NICU)

NICU	Dosing regimen	Period in use	Regimen summary		
UZ Leuven	Langhendries et al. 1998 [19]	Up to July 2011	Duration of IV infusion: 30 minutes		
			GA (weeks)	Dose (mg/kg)	Dosing int. (h)
			< 28	20	42
			28 to < 31	20	36
			31 to < 34	18.5	30
			34 to < 37	17	24
			37–41	15.5	24
	De Cock et al. 2012 [11]	July 2011–July 2014	Duration of IV infusion: 20–30 min		
			Weight (g)	Dose (mg/kg)	Dosing int. (h)
			0–800	16	48
			800–1200	16	42
			1200–2000	15	36
			2000–2800	15	30
			≥ 2800	15	24
	Smits et al. 2015 [2]	Since July 2014	Duration of IV infusion: 20 minutes		
			Weight (g)	Dose (mg/kg)	Dosing int.(h)
			0–800	16	48
			800–1200	16	42
			1200–2000	15	36
			2000–2800	15	36
			≥ 2800	15	30
VUmc Amsterdam	-	Up to 24 March 2015	Duration of IV infusion: 1 hour		
			Dose (mg/kg)	Dosing interval (h)	
			12	24–36h*	
			* determined by TDM (cfr. methods)		
	-	Since 24 March 2015	Dose (mg/kg)	Dosing interval (h)	
			15	24–36h*	
			* determined by TDM (cfr. methods)		

TABLE 2.2 Combined dataset characteristics: Current TDM dataset with retrospectively collected data from neonates with perinatal asphyxia treated with hypothermia and published dataset [11]

Dataset	TDM**	Published [11]	Combined
Number of neonates	56	874	930
Number of HT Samples (Total)	75 (83)	0 (2174)	75 (2257)
Gestational age (weeks)	38 [35–41]	31 [24–43]	32 [24–41]
Postnatal age (days)	2 [1–4] *	2 [1–30]	2 [1–30]
Birth weight (g)	3184 [1910–4770]	1530 [385–4650]	1795 [385–4770]
Current weight (g)	3184 [1910–4800]	1560 [385–4780]	1800 [385–4800]
Co-admin. of ibuprofen	0	118	118

*one neonate in the TDM dataset did not undergo hypothermia

**cohort consists of n = 13 cases from UZ Leuven and n = 43 cases from VUmc

2.3.4 Pharmacokinetic analysis

The PK analysis and model validation were performed using NONMEM v7.3 and PsN v3.4.2, respectively, both running under Pirana v2.9.0. The results were analyzed using Rv3.3.2 running under RStudio v1.0.136.

2.3.5 Model development

For the structural model, a previously published population PK model on amikacin in a large and heterogeneous group of neonates [11] was used as a basis. This model consisted of a two-compartment model with inter-compartmental clearance (Q) estimated as fractions of clearance (CL) and peripheral volume of distribution (V2) equal to the central volume of distribution (V1), respectively and with a combined additive and proportional error model [11]. Birthweight (BW) and PNA were covariates on CL and current weight (CW) was a covariate on V1 [11]. In order to estimate the impact of PATH, we tested a discrete covariate on CL and V1. Statistical considerations were accounted for by the decrease in objective function ($-2\log$ likelihood) value with a significance level of $p < 0.05$ (likelihood ratio test) which assumes a χ^2 distribution and the precision of parameter estimates ($RSE < 30\%$). In addition, the model fits were assessed visually using goodness-of-fit (GoF) plots split for the covariate tested.

2.3.6 Model validation

To assess the robustness of the parameter estimates of the final model, a non-parametric bootstrap was performed in which the combined dataset was resampled 1000 times with replacement and with stratification on the origin of the data (TDM or published). The resampled datasets were subsequently fitted with the final model, after which median and 95% confidence intervals of the obtained estimates were calculated.

To assess the predictive properties of the model, a normalized prediction distribution error (NPDE) analysis was performed using the NPDE package in R [14]. Each observed concentration was compared to 1000 simulated values for that observation.

Potential overparameterization was evaluated by calculating the condition number, by taking the eigenvalues from the NONMEM output and dividing the largest one to the smallest one.

2.3.7 Monte Carlo and stochastic simulations

To compare the exposures that would be obtained upon dosing according to three closely related and previously published dosing regimens [2, 11 (Table 2.3), the final model was used to simulate peak (1 hour after start of infusion) and trough (just before the subsequent dose) concentrations. For details regarding the three closely related previously published dosing regimens (Table 2.3) we refer to Smits et al. [2].

The final model was then used to determine, for neonates with PATH, an effective and practical dosing adjustment that would lead to target peak and trough concentrations. For this purpose, different doses and dosing intervals were explored to determine the regimen reaching the predefined peak and trough targets in the highest possible percentage of patients, while keeping in mind its feasibility in clinical practice. For all simulations, target peak and trough concentrations were above 24 mg/L and

TABLE 2.3 Summary of analyzed dosing regimens in model-based simulations

Dosing regimen Reference	De Cock 2012 (11)	Smits 2015a (2)	Smits 2015b (2)	Proposed dosing regimen
Description	Original model based dosing regimen	Simplified model based dosing regimen	Current dosing regimen	Current dosing with 12-hours interval increase
Current weight (g)				
1200–2000	15 mg/kg, 36h	15 mg/kg, 36h	15 mg/kg, 36h	15 mg/kg, 48h
2000–2800	13 mg/kg, 30h	15 mg/kg, 30h	15 mg/kg, 36h	15 mg/kg, 48h
> 2800	12 mg/kg, 24h	15 mg/kg, 24h	15 mg/kg, 30h	15 mg/kg, 42h

below 5 mg/L, respectively. In all simulations, neonates received two consecutive doses of a dosing regimen, assuming hypothermic treatment throughout the dosing intervals, without intermediate dose adjustments.

For both Monte Carlo (MC) simulations and stochastic simulations (SC), the demographic characteristics (PNA, BW, CW, gestational age) of the neonates with PATH from the TDM dataset were used. For the MC simulations, 2500 individuals were sampled with replacement from this subpopulation, taking time-varying changes and correlations in the demographics into account. For the SC simulations, 4 neonates that are treated with HT were generated. Each had a PNA of 1 day and BW equal to the mean (3093 g), median (3000 g), 5th percentile (1965 g) or 95th percentile (4220 g) of the BW of the neonates with PATH from the TDM dataset. For the SC simulations, for each of the 4 neonates, 2500 individual clearance values were sampled from the frequency distribution of the clearance values obtained in the pharmacometric analysis.

2.4 Results

2.4.1 Population pharmacokinetic model

The CL in neonates with PATH was found to be decreased by 40.6% (9% RSE) as compared to CL in neonates without PATH. The addition of the covariate accounting for PATH on CL led to a reduction in objective function with 73 points ($p < 0.05$) and reduced the unexplained inter-individual variability on CL from 0.116 to 0.104 (10% decrease). PATH was not found to influence any of the other model parameters. The final population PK parameters and bootstrap results are summarized in Table 2.4.

The bootstrap analysis confirmed the precision of parameter estimates of the final model, as the bootstrap medians were very similar to the parameter estimates and within the 95% prediction interval. The GoF

TABLE 2.4 Final population PK parameters and bootstrap results

Parameter estimates	Units	De Cock et al. 2012 (11)	Model Estimates (%RSE)	Bootstrap Median	95% Prediction Interval
Structural Model					
Clearance	L/h/kg	0.0493 (2.2%)	0.0495 (2%)	0.0497	0.048–0.052
Central Volume of Distribution*	L	0.833 (1.34%)	0.832 (1%)	0.826	0.808–0.845
Intercompartmental Clearance (as a fraction of CL)	L/h	0.415 (12.3%)	0.45 (11%)	0.482	0.402–0.575
Covariates					
Hypothermic treatment	g	-	0.594 (9%)	0.587	0.498–0.673
Birthweight	g	1.34 (2.04%)	1.34 (2%)	1.344	1.294–1.391
Current weight	g	0.919 (2.46%)	0.926 (2%)	0.923	0.884–0.960
Postnatal Age	days	0.213 (9.81%)	0.22 (8%)	0.222	0.198–0.255
Ibuprofen	-	0.838 (3.88%)	0.838 (4%)	0.836	0.779–0.894
Inter-individual Variability				[Shrinkage %]	
Clearance	CV%	30% (14.9%)	32% (13%) [17%]	0.105	0.082–0.127
Residual variability					
Additive	mg/L	0.267 (27.2%)	0.305 (24%) [15%]	0.505	0.277–0.758
Proportional	%	0.061 (8.19%)	0.0606 (8%) [15%]	0.057	0.050–0.065

*Central Volume of Distribution = Peripheral Volume of distribution;

plots of the final model did not show any trends or bias which would indicate model misspecifications (Figure 2.1). The NPDEs of the predictions had a mean of 0.025 which was not significantly different from 0 ($p = 0.24$) and a standard deviation of 1.02 which was not significantly different from 1 ($p = 0.49$). Visual inspection of the results did not suggest bias in the model predictions (Figure S2.1). The NPDEs have similar distributions for both populations, with or without PATH (Figure S2.2). The condition number was 39, well below the threshold of 1000, suggesting that the model was not overparameterized and well supported by the data.

As the results of the PK model showed that only CL is influenced by PATH, for neonates with PATH it was proposed to use the most recently published and extensively validated dosing regimen (Smits et al.) with

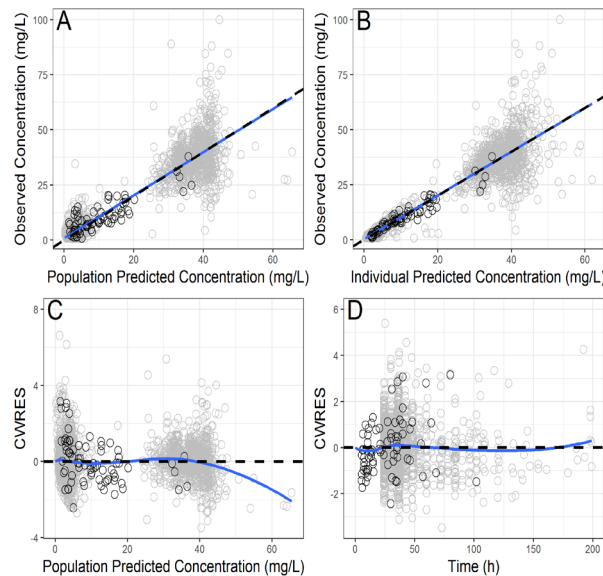


FIGURE 2.1 Population predicted concentration (A) and individual predicted concentration (B) vs. observed concentration; Conditional Weighted Residuals vs. Population predictions (C) and vs. Time after dose (D); Black circles - TDM dataset: asphyxia with hypothermia; Grey circles - Published Dataset

an increased dosing interval of 12 hours, while keeping the same doses (mg/kg). The previously published and the proposed dosing regimens are summarized in Table 2.3.

2.4.2 Monte Carlo (MC) and stochastic simulations (SC)

The results of the MC simulations upon dosing according to the three closely related dosing regimens (2, 11) for amikacin and the proposed regimen for PATH are shown in Figure 2.2. In the figure percentages of peak and trough concentrations within predefined target concentration ranges in neonates with PATH, split by the three weight groups used for dosing (Table 2.3), are shown. Results are presented upon the second amikacin dose, as then the target body temperature for hypothermia is mostly achieved.

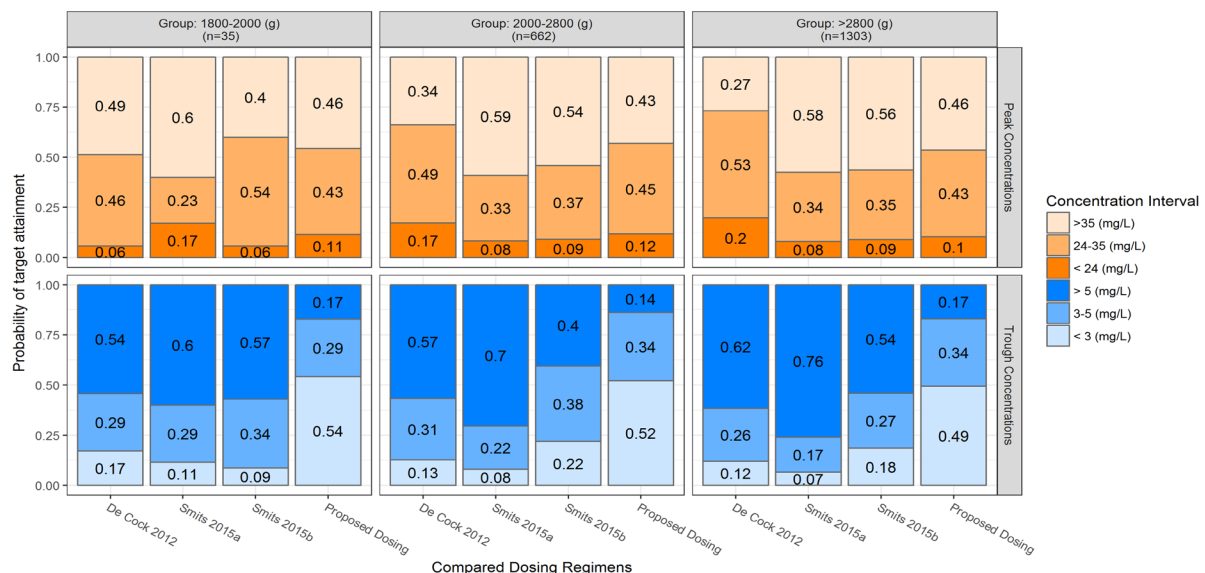


FIGURE 2.2 Stacked bar plots of the Monte Carlo simulations ($n = 2500$) presenting the results on target peak (upper panels) and trough (bottom panels) concentration attainment after the second amikacin dose. Results are split by three weight groups according to which the doses were calculated (Table 2.3) (left, middle and right panel). In each panel, the three columns on the left show the results obtained with the closely related and previously published dosing regimens [2, 15] whereas the column on the right shows the results of the newly proposed dosing regimen. All simulations were performed for neonates with PATH.

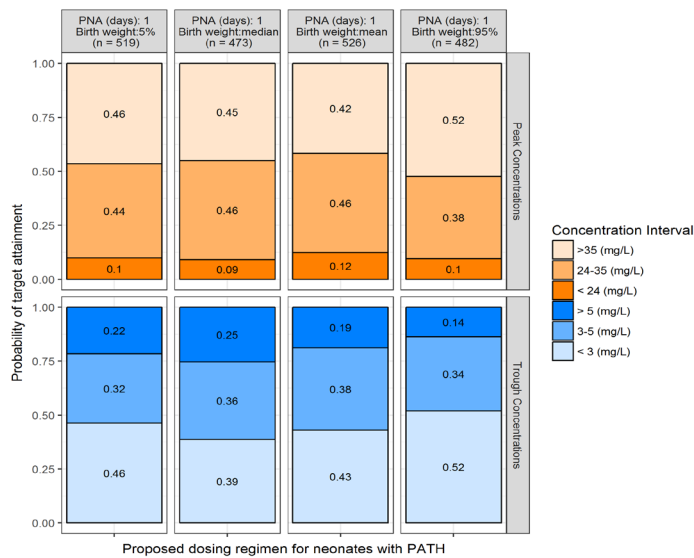


FIGURE 2.3 Stacked Bar of the Stochastic Simulations (n = 2500) presenting the results on target peak (upper panels) and trough (bottom panels) concentration attainment with the model-derived dosing interval. Results are presented after the second amikacin dose with panels for the lower (5%), median, mean and upper (95%) birthweight range of studied neonates with PATH, at the start of the hypothermic treatment

Figure 2.2 illustrates that the regimens currently used in clinical practice reached trough concentrations higher than 5 mg/L in 40% to 76% of neonates, whereas, using the proposed regimen where the dosing interval is increased with 12 hours, this percentage can be reduced to 14–17%. Peak concentrations were below the lower efficacy threshold in 10–12% of the cases only, which is in accordance with the results for the published dosing regimens, where the range was 6–17%.

Figure 2.3 comprises the results of the SC simulations showing how the proposed regimen performed when given to neonates representative of our sample, with specific demographic characteristics and PATH. In this figure, results are presented for the lower (5%), median,

mean and upper (95%) birth weights of the population of neonates with PATH. Compared to the published dosing regimens(2), the proposed dosing regimen, where the dosing interval is increased by 12 hours, yielded similar target concentrations for the four tested groups, i.e., 14 to 25% of neonates had trough concentrations above the toxic level and in less than 12% of neonates the effective peak concentrations was not reached (Figure 3).

2.5 Discussion

In this manuscript, we quantified the impact of PATH on amikacin CL in neonates, a potential surrogate for glomerular filtration, and translated this finding in a dosing recommendation tailored for neonates with PATH.

Our model-based approach showed that amikacin CL is decreased with 40.6% in neonates with PATH when compared to neonates without this condition. The model was used for simulations with targeted trough concentrations to determine an effective and practical dosing adjustment for neonates with PATH. The 12-hour increase in the dosing interval of the most recent and extensively validated dosing regimen [2], while keeping the amikacin dose (mg/kg) unchanged, had a minimal impact on the peak concentrations but improved the attained trough concentrations (Figure 2.2).

With unadjusted dosing regimen, the reduced amikacin CL led to trough concentrations above the toxic threshold for a large percentage of the neonates with PATH population (Figure 2.2), increasing the probability of developing adverse reactions such as nephro- and ototoxicity. Achieved peak concentrations were minimally impacted by the reduced CL and increased dosing interval, as these are determined by the dose and the administration rate of the IV infusion.

The MC simulations allowed for a comparison between the performances of the published dosing regimens [2, 11] and the proposed regimen in a group of patients with demographics encountered in this group (Figure 2.2), whereas the SC simulations led to a better understanding of how the proposed dosing regimen would perform in individuals with specific realistic demographic characteristics for neonates with PATH. A PNA of 1 day was considered most relevant for the studied population since

hypothermic treatment is usually started within the first 6 hours after birth and the BW mean, median, 5th and 95th percentiles were calculated for these patients of the TDM dataset (Figure 2.3).

Our results showed that the proposed dosing regimen for neonates with PATH did not impair the attainment of the amikacin treatment efficacy target, with less than 12% of the studied population reaching a suboptimal peak concentration, while the toxic effects were reduced, with less than 17% of the studied population attaining trough concentrations above 5 mg/L (Figure 2.2). This does show, nevertheless, that even with the proposed adjustment, amikacin trough TDM should still be performed as part of routine clinical care, especially in patients with PATH. It should also be noted that the validity of the traditional target concentrations for efficacy and safety of amikacin has not been established for such prolonged dosing intervals, warranting prospective evaluation of the regimen.

Although we provided the first report of amikacin PK in a dual-center cohort of neonates with PATH, other studies were performed for other aminoglycosides (i.e. gentamicin). Frymoyer et al. [8] reported improved attainment of gentamicin target trough levels in neonates with PATH, after increasing the dosing interval from 24 to 36 hours (+ 50%). In addition, peak gentamicin concentrations were minimally impacted by the increase in dosing interval. This is in concordance with our findings for amikacin, and can be explained by the fact that these compounds from the same therapeutic class, eliminated by the same pathway – glomerular filtration – actually reflect the impact of perinatal asphyxia or hypothermia (or both) on the neonatal glomerular filtration rate. De Cock et al. and others previously reported that physiological maturation of amikacin CL can be used to predict ontogeny of other compounds eliminated almost entirely by glomerular filtration [14, 15]. The current findings support this ‘semi-physiological’ concept, which could be further explored to quantify the impact of perinatal asphyxia and whole-body cooling on the CL of drugs eliminated almost exclusively by glomerular filtration.

Due to the nature of the TDM data (i.e. retrospectively retrieved from patients’ files, small number of patients with PATH, sampling during routine care), our analysis has limitations. First, we were unable to disentangle the impact of perinatal asphyxia from the impact of hypothermic treatment on amikacin CL. These are expected to have different extents, as shown in preclinical experiments in newborn pigs by Satas et al. [10] (hypoxia-ischemia) and Koren et al. [17] (hypothermia). They have also shown that, the intensity of the hypothermic treatment could be relevant, as severe hypothermia decreased gentamicin half-life with 36% (10°C temperature drop) [17], whereas, mild hypothermia (4°C temperature drop) did not have an impact on CL [10]. On the other hand, studies in neonates had contradicting results. While Liu et al. reported that 40% of gentamicin trough concentrations in neonates with hypoxic ischemic encephalopathy were above the target 2 mg/L, they could not identify an additional impact of hypothermia on CL [18]. However, Ting et al. [9] showed in neonates with hypoxic-ischemic encephalopathy that hypothermic treatment caused an increase in the half-life of gentamicin, from 7.01 hours in a normothermic group to 9.57 hours (+ 36.5%) in a hypothermic group, which suggests that the hypothermic treatment itself reduces CL as well. With this in mind, we suggest that the results of our study, including the model-derived dosing regimen, should not be extrapolated to populations other than neonates with PATH, or to other drugs, even if eliminated by the same pathway, as the validity of such extrapolations requires further research.

Another limitation is that, both at the initiation of the hypothermic treatment and initiation of the rewarming phase, the body temperature of the neonates is not constant. Since the number of samples collected during these periods was limited, it was not possible to identify a covariate relationship that reflects the dynamic changes in clearance during these periods. As a result, model-based simulations cannot be expected to be accurate for initiation of the cooling process as well as during the rewarming phase. We, therefore, only present simulation-based results for the second amikacin dose, as the body temperature is expected to be stable (33.5°C) throughout this interval.

2.6 Conclusion

To conclude, we identified a significantly decreased (40.6%) amikacin CL in (near) term neonates with PATH. Based on simulations, indicating the achievement of safe trough concentrations ($< 5\text{ mg/L}$) while still reaching optimal peak concentrations ($> 24\text{ mg/L}$), we propose a 15 mg/kg dose every 42 hours for children above 2800 g, or 48 hours for children between 1800 g and 2800 g, in this special neonatal population. As a future step, this model-based dosing proposal should undergo prospective validation and eventual clinical implementation.

2.7 Acknowledgements

The authors would like to thank Dr. Swantje Voller for carefully reviewing the code used for the modeling and simulations. The research activities were facilitated by the agency for innovation by Science and Technology in Flanders (IWT) through the SAFEPEDRUG project (IWT/SBO 130033). KA has been supported by FWO Vlaanderen (Senior Clinical Investigatorship, 1800209 N)). CAJK received support from the Innovational Research Incentives Scheme (Vidi grant, June 2013) of the Dutch Organization for Scientific Research (NWO) for the submitted work. All authors declare that they have no conflicts of interest. This work was performed within the framework of Top Institute Pharma project D2-501.

2.8 References

1. Ducher M, Maire P, Cerutti C, Bourhis Y, Foltz F, Sorensen P, Jelliffe R, Fauvel JP. 2001. Renal elimination of amikacin and the aging process. *Clin Pharmacokinet* 40:947.
2. Smits A, De Cock RFW, Allegaert K, Vanhaesebrouck S, Danhof M, Knibbe CAJ. 2015. Prospective evaluation of a model-based dosing regimen for amikacin in preterm and term neonates in clinical practice. *Antimicrob Agents Chemother* 59:6344–6351.
3. Smits A, Kulo A, van den Anker J, Allegaert K. 2016. The amikacin research program: a stepwise approach to validate dosing regimens in neonates. *Expert Opin Drug Metab Toxicol* 0:1–10.
4. Zanelli S, Buck M, Fairchild K. 2011. Physiologic and pharmacologic considerations for hypothermia therapy in neonates. *J Perinatol* 31:377–86.
5. Van Den Broek MPH, Groenendaal F, Egberts ACG, Rademaker CMA. 2010. Effects of hypothermia on pharmacokinetics and pharmacodynamics: A systematic review of preclinical and clinical studies. *Clin Pharmacokinet* 49(5):227–294.
6. Pokorna P, Wildschut E, Vobruha V, van den Anker J, Tibboel D. 2015. The Impact of Hypothermia on the Pharmacokinetics of Drugs Used in Neonates and Young Infants. *Curr Pharm Des* 21(39):5705–5724.
7. Dammann O, Ferriero D, Gressens P. 2011. Neonatal encephalopathy or hypoxic-ischemic encephalopathy? Appropriate terminology matters. *Pediatr Res* 70:1–2.
8. Frymoyer A, Shirley L, Bonifacio S, Meng L, Lucas S, Guglielmo J, Sun Y, Verotta D. 2013. Every 36-hour Gentamicin Dosing in Neonates with Hypoxic Ischemic Encephalopathy Receiving Hypothermia. *J Perinatol* 33:778–782.
9. Ting JY, Kwan E, McDougal A, Osiovich H. 2015. Pharmacokinetics of gentamicin in newborns with moderate-to-severe hypoxic-ischemic encephalopathy undergoing therapeutic hypothermia. *Indian J Pediatr* 82:119–25.
10. Satas S, Hoem NO, Melby K, Porter H, Lindgren CG, Whitelaw A, et al. 2000. Influence of mild hypothermia after hypoxia-ischemia on the pharmacokinetics of gentamicin in newborn pigs. *Biol Neonate* 77:50–57.
11. De Cock RFW, Allegaert K, Schreuder MF, Sherwin CMT, De Hoog M, Van Den Anker JN, Danhof M, Knibbe CAJ. 2012. Maturation of the glomerular filtration rate in neonates, as reflected by amikacin

- clearance. *Clin Pharmacokinet* 51:105–117.
12. Azzopardi D V, Strohm B, Edwards AD, Dyet L, Halliday HL, Juszczak E, Kapellou O, Levene M, Marlow N, Porter E, Thoresen M, Whitelaw A, Brocklehurst P. 2009. Moderate hypothermia to treat perinatal asphyxial encephalopathy. *N Engl J Med* 361:1349–1358.
 13. Bijleveld YA, de Haan TR, van der Lee HJH, Groenendaal F, Dijk PH, van Heijst A, de Jonge RCJ, Dijkman KP, van Straaten HLM, Rijken M, Zonnenberg IA, Cools F, Zecic A, Nuytemans DHGM, van Kaam AH, Mathot RAA. 2016. Altered gentamicin pharmacokinetics in term neonates undergoing controlled hypothermia. *Br J Clin Pharmacol*.81(6):1067- 1077.
 14. Comets E, Brendel K, Mentre F. 2010. Model evaluation in nonlinear mixed effect models, with applications to pharmacokinetics. *J la Société Française Stat* 151:106–127.
 15. De Cock RFW, Allegaert K, Sherwin CMT, Nielsen EI, De Hoog M, Van Den Anker JN, Danhof M, Knibbe C a J. 2014. A Neonatal amikacin covariate model can be used to predict ontogeny of other drugs eliminated through glomerular filtration in neonates. *Pharm Res* 31:754–767.
 16. Zhao W, Biran V, Jacqz-Aigrain E. 2013. Amikacin maturation model as a marker of renal maturation to predict glomerular filtration rate and vancomycin clearance in neonates. *Clin Pharmacokinet* 52:1127–1134.
 17. Koren G, Barker C, Bohn D, Kent G, Biggar WD,. 1985. Influence of hypothermia on pharmacokinetics of gentamycin and theophylline in piglets. *Crit Care Med* 13:844–847.
 18. Liu X, Borooah M, Stone J, Chakkarapani E, Thoresen M. 2009. Serum gentamicin concentrations in encephalopathic infants are not affected by therapeutic hypothermia. *Pediatrics* 124:310–315.
 19. Langhendries JP, Battisti O, Bertrand JM, Francois A, Kalenga M, Darimont J, Scalais E, Wallemacq P. 1998. Adaptation in Neonatology of the Once-Daily Concept of Aminoglycoside Administration : Evaluation of a Dosing Chart for Amikacin in an Intensive Care Unit. *Biol* 351–362.

2.9 Supplementary material

2

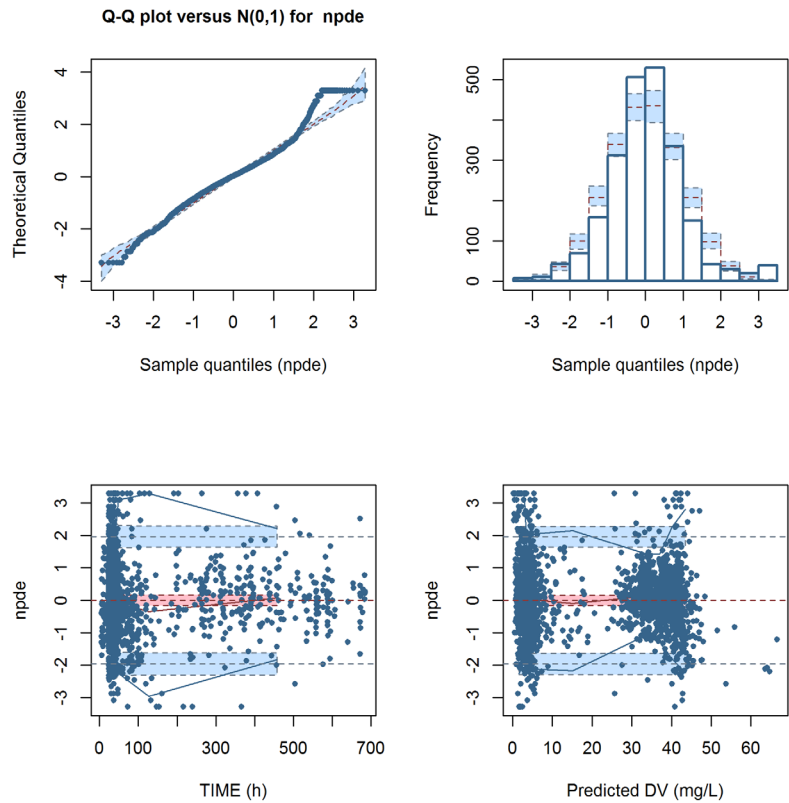


FIGURE S2.1. Normalized prediction distribution errors results of the best model (N = 1000). Both published and TDM datasets are included in the analysis. DV stands for observed amikacin concentrations.

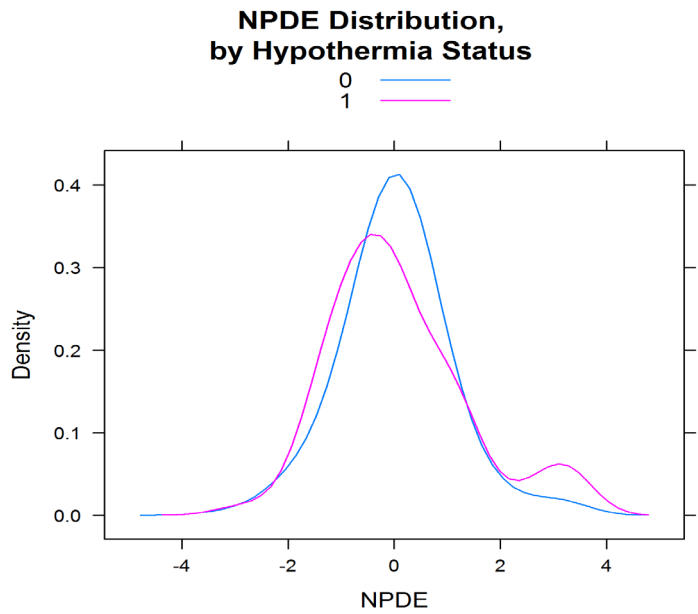


FIGURE S2.2. Normalized prediction distribution errors distribution stratified by hypothermic status: pink line – hypothermia and blue line – normothermia

2.10 Model code

```
; -----
;; 1. Based on: De Cock 2012
;; 2. Description:AMICOOL PRJ
$PROB Amikacin PK for PATH patients
$INPUT ID TIME AMT DV MDV RATE GA BW CW PNA IBU COOL
$DATA 20042016-SC-AMICOOL.NM.06.csv IGNORE=@

IGNORE (ID.EQ.182); excluded previously
IGNORE (ID.EQ.521); excluded previously
IGNORE (ID.EQ.523); excluded previously

$SUBROUTINE ADVAN3 TRANS4

$PK
FF=1
FC=1
IF(IBU.EQ.1) FF = THETA(7) ; ibuprofen coadmin as cat cov
IF(COOL.EQ.1) FC = THETA(8) ; hypothermia coadmin as cat cov
TVCL = THETA(1) * ((BW / 1750) ** THETA(4)) * (1 + (PNA / 2) * THETA(6)) *
      (FF) * (FC)
CL    = TVCL * EXP(ETA(1))
TVV1  = THETA(2) * ((CW / 1760) ** THETA(5))
V1    = TVV1 * EXP(ETA(2))
Q     = THETA(3) * CL
V2    = V1
S1    = V1

$ERROR

IPRED = F
Y      = F * (1 + ERR(1)) + ERR(2); combined error

$THETA
(0, 0.0493) ;1- CL
(0, 0.833)  ;2- V1
(0, 0.415)  ;3- Q
(0, 1.34)   ;4- BW on CL
(0, 0.919)  ;5- CW on V2
(0, 0.213)  ;6- PNA on CL
(0, 0.838)  ;7- IBU on CL
(0, 0.583)  ;8- COOL on CL

$OMEGA
0.0899      ;CL
0 FIX       ;V

$SIGMA
0.0614
0.267

$EST METHOD=1 INTERACTION NOABORT SIGDIG=3 PRINT=5 MAXEVAL=9999 POSTHOC
$COV COMP PRINT=E
$STABLE ID TIME DV MDV GA BW CW PNA IBU TVCL IPRED CL V1 V2 Q COOL IBU FC FF
ETA1 ETA2 CWRES NOPRINT ONEHEADER FILE=AMICOOL99.tab
```


Larger dose reductions of vancomycin required in neonates with patent ductus arteriosus receiving indomethacin vs. ibuprofen

S Cristea, K Allegaert, AC Falcao, F Falcao, R Silva,
A Smits, CAJ Knibbe, EHJ Krekels

Antimicrob Agents Chemother.
2019 Jul 25;63(8): e00853-19

3.1 Abstract

Ibuprofen and indomethacin are commonly used to induce ductus arteriosus closure in preterm neonates. Our group previously reported that ibuprofen decreased vancomycin clearance by 16%. In this study, we quantified the impact of indomethacin co-administration on vancomycin clearance by extending our vancomycin population pharmacokinetic model with a dataset containing vancomycin concentrations measured in preterm neonates co-medicated with indomethacin.

The modeling dataset includes concentration-time data of vancomycin administered alone or in combination with either ibuprofen or indomethacin collected in the neonatal intensive care units of UZ Leuven (Leuven, Belgium) and São Francisco Xavier Hospital (Lisbon, Portugal). The derived vancomycin pharmacokinetic model was subsequently used to propose dose adjustments that yield effective vancomycin exposure (i.e., AUC_{0-24h} between 300-550 mg·h/L, with a probability below 0.1 of sub-therapeutic exposure) in preterm neonates with patent ductus arteriosus.

We found indomethacin co-administration to reduce vancomycin clearance by 55%. Model simulations showed that the most recent vancomycin dosing regimen which was based on an externally validated model, requires a 20% and 60% decrease of the loading and maintenance dose of vancomycin, respectively, when aiming for optimized exposure in the neonatal population.

By analyzing vancomycin data from preterm neonates co-medicated with indomethacin we found a substantial decrease in vancomycin clearance of 55% versus a previously reported 16% for ibuprofen. This decrease in clearance impacts vancomycin dosing and we anticipate that other drugs eliminated by glomerular filtration are likely to be affected to a similar extent as vancomycin.

3.2 Introduction

Vancomycin is frequently used in neonates as therapy for late onset infections with coagulase-negative *Staphylococcus* or as an alternative therapy for methicillin-resistant *Staphylococcus aureus* [1]. Recently, Janssen et al. [2] proposed a vancomycin dosing regimen for both preterm and term neonates, based on an externally validated population pharmacokinetic (PK) model yielding effective and safe vancomycin exposure (i.e., an area under the curve (AUC) around 400 mg·h/L) from the start of treatment [2].

Co-medication given to preterm neonates with a patent (symptomatic) ductus arteriosus (PDA) include ibuprofen and indomethacin, which have been proven to effectively induce PDA constriction and closure [3]. Both nonsteroidal anti-inflammatory drugs (NSAIDs) are known to have renal side effects, as they suppress the vasodilatory effects of prostaglandins leading to vasoconstrictive renal hypoperfusion, even though exact quantification is incomplete [3,4]. Vancomycin clearance (CL) was shown to decrease by 16% when co-administered with ibuprofen [5], upon which it was proposed to decrease the vancomycin dosage for neonates with PDA co-medicated with ibuprofen [2]. Less is known about the impact of indomethacin on vancomycin CL. Upon quantifying the influence of indomethacin on vancomycin CL we could improve vancomycin dosing in this special population. And, since vancomycin CL is mainly eliminated by glomerular filtration, a reduction in CL of vancomycin as a result of co-administration with ibuprofen or indomethacin may also imply a reduction in CL for other drugs such as aminoglycosides [5, 6] cleared by the same pathway.

In the current analysis, our goal is to quantify the impact of indomethacin co-administration on vancomycin CL in neonates with PDA, in addition to the previously quantified impact of ibuprofen on vancomycin CL in this population. For this, vancomycin PK data collected during routine therapeutic drug monitoring (TDM) in preterm patients pharmacologically treated for PDA with indomethacin [7] were analyzed within the context of a previously published population pharmacokinetic model for vancomycin and vancomycin co-administered with ibuprofen [5]. This model has been externally validated and used to propose dosing guidelines for vancomycin in neonates(2). Model-based simulations were

subsequently used to evaluate available dosing regimen [2, 8–10] for vancomycin in preterm neonates with PDA co-medicated with ibuprofen or indomethacin and to propose dose adjustments.

3.3 Methods

3.3.1 Data exploration

For this analysis we used vancomycin PK data collected during routine TDM at two neonatal intensive care units: University Hospitals Leuven (Leuven, Belgium; hereafter referred to as UZ Leuven) and São Francisco Xavier Hospital (Lisbon, Portugal; hereafter referred to as HSFX). All preterm neonates diagnosed with PDA received either ibuprofen (UZ Leuven) or indomethacin (HSFX) together with vancomycin. Data on vancomycin without co-medication from neonates without PDA were all collected in UZ Leuven. Findings from both sets of data have been published separately before by De Cock et al. 2014 [5] (UZ Leuven) and Silva et al. 1998 [7] (HSFX). The combined dataset was used for model development in the

Table 3.1. Summary of demographic characteristics of the patients included in this analysis - mean (range) for the studied population (N = 319) treated with vancomycin only (n=263) or vancomycin co-administrated with either ibuprofen (n=23) or indomethacin (n=33).

	Vancomycin treat- ment only [5]	Vancomycin treatment with ibuprofen [5]	Vancomycin treatment with indomethacin [7]
	(N = 263)	(N = 23)	(N = 33)
Postmenstrual age (weeks)	31 (24-38)	28 (24-33)	29 (26-35)
Gestational age (weeks)	29 (23-34)	27 (24-33)	28 (25-34)
Postnatal age (days)	14 (1-28)	7 (2-12)	11 (4-30)
Birth body weight (g)	1150 (385-2550)	832 (415-1930)	1000 (570-1960)
Current body weight* (g)	1256 (485-2630)	810 (415-1930)	981 (628-1850)

* the patient’s body weight at the start of the treatment

current analysis. A summary of the demographics of the patients included in this analysis is provided in Table 3.1, which shows a large degree of similarity regarding age and weight related demographics in these preterm neonates.

3.3.2 Model development

The previously published population PK model, developed with the data collected at UZ Leuven to characterize vancomycin disposition and quantify the impact of ibuprofen on vancomycin CL [5], was used as a basis for the current analysis. Briefly, this model concerns a two-compartment model that includes birth body weight (BW), postnatal age (PNA) and ibuprofen co-administration as covariates on CL and current body weight (CW) as a covariate on the central and peripheral distribution volumes (V1, V2) [5]. This model was externally validated in a previous study [2]. In the current analysis, all population parameters describing vancomycin disposition and the influence of ibuprofen on CL were fixed to the estimates reported by De Cock et al. [5]. The combined dataset including the data from both UZ Leuven and HSFX [7] was used to quantify the influence of indomethacin co-administration as a covariate (Findo) on CL and V1.

Model selection was based on numerical and graphical criteria (e.g., decrease in objective function value > 3.84 with one more degree of freedom ($p < 0.05$), relative standard errors below 30%, and unbiased goodness-of-fit plots).

3.3.3 Model Validation

The robustness of the parameter estimates of the final model was assessed by a non-parametric bootstrap. For this, the extended dataset was resampled with replacement 1000 times and stratified on vancomycin co-medication (i.e., vancomycin without co-medication, vancomycin with ibuprofen or vancomycin with indomethacin). The resampled datasets were subsequently fitted with the final model,

Table 3.2 - Vancomycin dosing regimen according to Janssen et al.(2) (grey) and proposed vancomycin doses for ibuprofen and indomethacin co-administration (no background) resulting from model-based simulations with the final model, aiming for a target of AUC0-24h between 300 - 550 mg·h/L.

Clinical characteristics		Vancomycin Dosing(2)*		Vancomycin with ibuprofen co-administration		Vancomycin with indomethacin co-administration	
PNA (days)	BW (g)	Loading Dose	Maintenance Dose	Loading Dose	Maintenance Dose	Loading Dose	Maintenance Dose
0-7	≤700	16 mg/kg	15 mg/kg/day in 3 doses	16 mg/kg	(20% reduction)	(20% reduction)	(40% reduction)
	700-1000		21 mg/kg/day in 3 doses		12 mg/kg/day in 3 doses	13 mg/kg	9 mg/kg/day in 3 doses
	1000-1500		27 mg/kg/day in 3 doses		17 mg/kg/day in 3 doses		13 mg/kg/day in 3 doses
	1500-2500		30 mg/kg/day in 4 doses		22 mg/kg/day in 3 doses		16 mg/kg/day in 3 doses
8-14	≤700	20 mg/kg	21 mg/kg/day in 3 doses	20 mg/kg	24 mg/kg/day in 4 doses	16 mg/kg	18 mg/kg/day in 4 doses
	700-1000		27 mg/kg/day in 3 doses		17 mg/kg/day in 3 doses		13 mg/kg/day in 3 doses
	1000-1500		36 mg/kg/day in 3 doses		22 mg/kg/day in 3 doses		16 mg/kg/day in 3 doses
	1500-2500		40 mg/kg/day in 4 doses		29 mg/kg/day in 3 doses		22 mg/kg/day in 3 doses
14-28	≤700	23 mg/kg	24 mg/kg/day in 3 doses	23 mg/kg	32 mg/kg/day in 4 doses	18 mg/kg	24 mg/kg/day in 4 doses
	700-1000		42 mg/kg/day in 3 doses		19 mg/kg/day in 3 doses		19 mg/kg/day in 3 doses
	1000-1500		45 mg/kg/day in 3 doses		34 mg/kg/day in 3 doses		25 mg/kg/day in 3 doses
	1500-2500		52 mg/kg/day in 4 doses		36 mg/kg/day in 3 doses		27 mg/kg/day in 3 doses
21-28	≤700	26 mg/kg	24 mg/kg/day in 3 doses	26 mg/kg	42 mg/kg/day in 4 doses	21 mg/kg	31 mg/kg/day in 4 doses
	700-1000		42 mg/kg/day in 3 doses		19 mg/kg/day in 3 doses		19 mg/kg/day in 3 doses
	1000-1500		45 mg/kg/day in 3 doses		34 mg/kg/day in 3 doses		25 mg/kg/day in 3 doses
	1500-2500		52 mg/kg/day in 4 doses		36 mg/kg/day in 3 doses		27 mg/kg/day in 3 doses

* Janssen et al. [2] proposes a decrease of 2 mg/kg/dose of both the maintenance and loading dose when ibuprofen co-administration

after which median and 95% confidence intervals of the parameters were obtained.

The predictive properties of the model were assessed by a normalized prediction distribution error (NPDE)(11) analysis using the NPDE package in R v3.3.2. Each observed concentration was compared to 1000 simulated values for that observation to calculate the prediction error(11). The results of the NPDE were also stratified by co-medication.

3.3.4 Vancomycin dosing optimization

The final vancomycin PK model was used for Monte Carlo simulations and stochastic simulations to guide dose adjustments upon co-administration with either ibuprofen or indomethacin. For this purpose, we defined a safe and effective vancomycin target exposure, i.e. an AUC in the first 24 hours (AUC_{0-24h}) ranging between 300- 550 mg·h/L, which should lead to a median AUC/MIC of 400 mg·h/L for a minimum inhibitory concentration (MIC) of 1 mg/mL. For the recommended dose adjustments, we aimed for a probability of reaching sub-therapeutic exposures ($AUC_{0-24h} < 300$ mg·h/L) below 0.1.

As basis for our proposed vancomycin dosing adjustments, we used a recently published dosing regimen for vancomycin [2] (Table 3.2) that reaches and maintains the vancomycin target AUC_{0-24h} in children, including preterm neonates. This dosing regimen was based on an externally validated population PK model and proposed a fixed dose reduction of 2 mg/kg/dose for both the loading and the maintenance dose, upon co-administration with ibuprofen, to account for the reduced vancomycin CL. This regimen was evaluated together with other dosing guidelines for vancomycin that are currently in clinical use, but that have not been optimized for scenarios with co-administration of NSAIDs (Table S3.1 – Dutch Children’s Formulary [10], British National Formulary [9], and Neofax [8]).

Monte Carlo simulations in virtual preterm neonates pharmacologically treated for PDA

For the Monte Carlo simulations, a virtual patient population was created by resampling with replacement 1000 patients from our original sample of patients with PDA. The final model was used to simulate individual vancomycin concentration-time profiles following dosing with the different guidelines and to calculate AUC_{0-24h} values for each of the virtual patients. The results are presented as probabilities of exposure attainment within, above or below the predefined AUC_{0-24h} target range.

Stochastic simulations in hypothetical preterm neonates pharmacologically treated for PDA

For the stochastic simulations, three individuals with birth body weights representing the 1st quartile (BW = 770 g), median (BW = 1050 g), or 3rd quartile (BW = 1250 g) and postnatal ages (PNA) of 6, 9 and 12 days, respectively, were derived from the sample of patients with PDA.

For each of these individuals, 1000 stochastic simulations were performed with the final model taking inter-individual variability of the model parameters into account. Simulated individual concentration-time profiles obtained after dosing vancomycin following different guidelines were used to calculate AUC_{0-24h} for each hypothetical individual.

3.4 Results

3.4.1 Population pharmacokinetic model

Our analysis showed that indomethacin reduced vancomycin clearance by 55% (Table S3.1 - fraction of 0.447 (RSE of 14%)), while the reduction for ibuprofen was 16% [5]. Adding indomethacin co-administration as a covariate on V1 did not lead to statistically significant improvement of the model.

Figure 3.1 illustrates these findings showing the relationship between individual vancomycin CL values and body weight of patients in the overall dataset, in the presence or absence of either ibuprofen or indomethacin. Besides the systematic difference in vancomycin CL values between the three groups, a

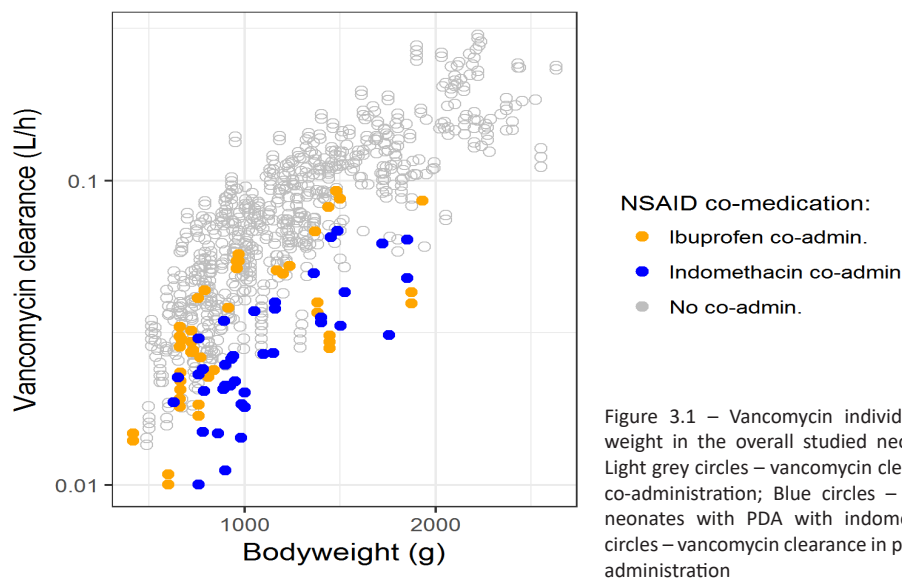


Figure 3.1 – Vancomycin individual clearance values versus body weight in the overall studied neonatal population (semi-log scale). Light grey circles – vancomycin clearance in neonates without NSAIDs co-administration; Blue circles – vancomycin clearance in preterm neonates with PDA with indomethacin co-administration; Orange circles – vancomycin clearance in preterm neonates with ibuprofen co-administration

relatively high overall inter-individual variability of 33.6% in vancomycin clearance was estimated (Table S3.1, Figure 3.1).

The model described the data with good accuracy, as confirmed by the goodness-of-fit plots, for all three patient groups (no NSAID, ibuprofen and indomethacin) (Figure S3.1), while the NPDE analysis confirmed accurate predictions (Figures S3.2 and S3.3). Estimated PK parameters had acceptable precision, as indicated by the relative standard errors (RSE%) of the estimates being well below 20%. The bootstrap analysis confirms the robustness of the model (Table S3.1).

3.4.2 Vancomycin dosing optimization

Based on the selection criteria, a one compartment model with zero-order absorption and first-order Simulations showed that, to maintain an effective vancomycin exposure (i.e., AUC_{0-24h} within 300-550 mg·h/L) when NSAIDs are co-administered in preterm neonates with PDA, different dose adjustments should be made for ibuprofen and indomethacin to compensate for the differences in decreases in vancomycin CL. Table 3.2 displays how the vancomycin dosing regimen proposed by

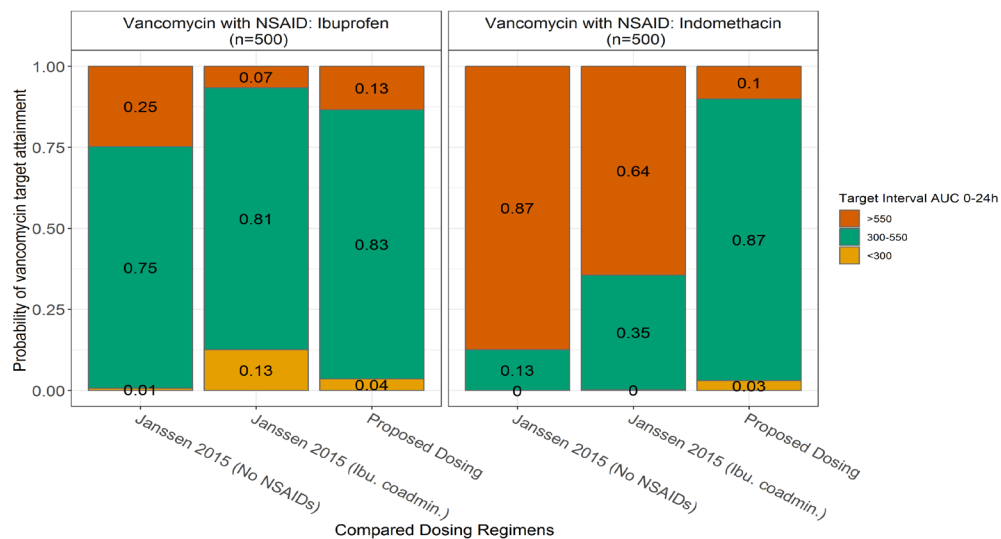


Figure 3.2 –Probability of target attainment for AUC_{0-24h} (first day of treatment) between 300 - 550 mg·h/L for vancomycin for different dosing regimens, derived from Monte Carlo simulations in virtual preterm neonates with PDA. The left panel shows the results in preterm neonates with PDA after vancomycin co-administrated with ibuprofen and the right panel for preterm neonates with PDA after vancomycin co-administrated with indomethacin. Each bar represents the results obtained with one dosing regimen (see Table 3.2 for detailed descriptions the dosing regimens).

Janssen et al. [2] for neonates without co-administration of NSAIDs (grey columns) should be adapted when NSAIDs are co-administrated, i.e. a decrease of the maintenance dose by 20 % for ibuprofen and a decrease in both the loading and the maintenance dose by 20% and 60%, respectively, for indomethacin (Table 3.2).

Monte Carlo simulations in virtual preterm neonates pharmacologically treated for PDA

Figure 3.2 shows the probabilities of attaining vancomycin exposure within, above or below the predefined target range of 300-550 mg·h/L following the dosing guidelines of Janssen et al.[2] (with and without dose reduction of 2 mg/kg/dose for ibuprofen co-administration) and our proposed dose adjustments for co-administration with ibuprofen or indomethacin (see Table 3.2), in virtual patients resampled from the available PDA patient group.

The proposed dose reduction when ibuprofen is co-administrated decreases the probability of under dosing, especially in the smallest children (Figures 3.2 and 3.3 – left panel). Using vancomycin dosing regimens with no adjustments or with the same adjustment for both NSAIDs would lead to major differences in vancomycin target attainment (Figure 3.3) and particularly increase the probability for over-exposure and, thereby, the risk of experiencing side effects.

Stochastic simulations in hypothetical preterm neonates pharmacologically treated for PDA

Figure 3.3 shows results of stochastic simulations in representative, hypothetical patients with pharmacologically treated PDA illustrating how variability in vancomycin CL is reflected into AUC_{0-24h} values following vancomycin administration with our proposed dosing (Table 3.2) and published dosing guidelines (Table S3.2), with adjustments for co-medication when available [3-6]. Remaining variability

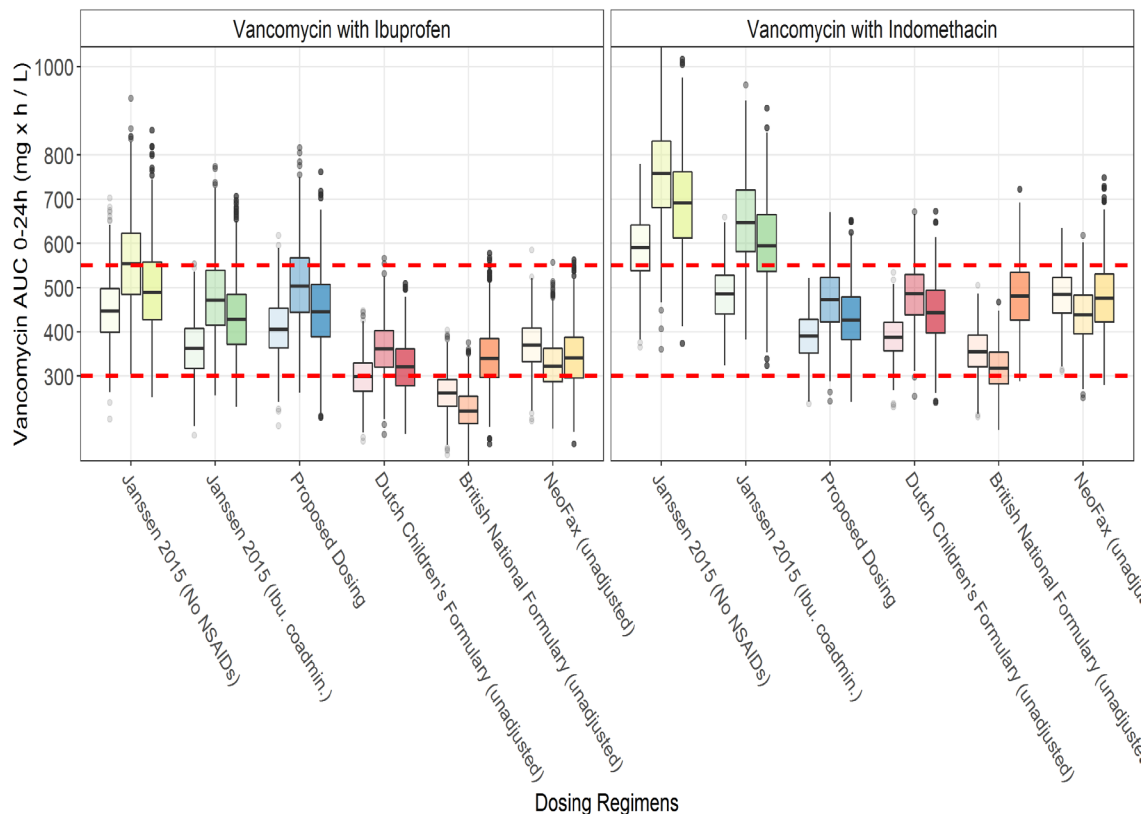


Figure 3.3 –Vancomycin AUC_{0-24h} values on the first day of treatment obtained following stochastic simulations for each dosing regimen in hypothetical individuals with birth body weights of 770 g, 1050 g and 1250 g and postnatal ages of 6, 9 and 12 days, respectively. Each color represents one dosing regimen (see Table 3.2 and Table S3.2 for details of each dosing regimen) and the colors intensify with increasing birth body weight. The left panel shows the results in preterm neonates with PDA after vancomycin co-administrated with ibuprofen and the right panel for neonates with PDA after vancomycin co-administrated with indomethacin. The dashed lines represent the target AUC_{0-24h} of 300 – 550 mg·h/L (red) and 400 mg·h/L (black)

in these plots results from random inter-individual variability in vancomycin CL, for which TDM remains necessary.

Figure 3.3 illustrates that large variability in exposure may be expected depending on both the selected dosing regimen, the birth body weight of the neonate and the NSAID involved (Figure 3.3).

3.5 Discussion

In preterm neonates treated concomitantly with ibuprofen for PDA and with vancomycin for suspected or confirmed late onset sepsis, a 16% decrease in vancomycin clearance has been reported previously [5]. In the current study, we found a 55% decrease in vancomycin clearance when PDA is treated with indomethacin. Based on these findings we propose dose adjustments to ensure a safe and effective vancomycin treatment for this special population, i.e. a decrease of the vancomycin maintenance dose by 20% when ibuprofen is co-administrated and a decrease of the loading and the maintenance dose of vancomycin by 20% and 60%, respectively, when indomethacin is co-administrated.

In the model-based simulations, AUC_{0-24h} values (between 300-550 mg·h/L) were defined as targets, as proposed in recent publications [2, 12]. However, vancomycin trough concentrations taken at the end of the first day of treatment are still commonly used as surrogate markers for vancomycin exposure. In adults, trough concentrations above 15 mg/L are associated with an effective vancomycin exposure of around 400 mg·h/L. However, Neely et al. showed, using Bayesian modeling, that 60% of adult patients with a vancomycin AUC of at least 400 mg·h/L, had a trough concentration below 15 mg/L [13]. For neonates, Frymoyer et al. showed that trough levels ranging between 7 and 10 mg/L were highly predictive of an AUC_{0-24h} above 400 mg·h/L [12]. Both these studies suggest that guiding dose individualization based on a trough concentration of 15 mg/L could lead to over-exposure and increased risk of adverse events. In addition, when correlating trough concentrations with AUC_{0-24h} , vancomycin dosing frequency should be accounted for [14].

To ensure an efficacious vancomycin treatment, a target AUC_{0-24h} around 400 mg·h/L for a pathogen MIC of 1 mg/L should be attained from the start of therapy, as this was correlated with a better treatment outcome and a shorter time to reach steady-state [15]. Therefore, we decided to aim for a therapeutic window of 300-550 mg·h/L. US guidelines recommend an AUC_{0-24h} around 700 mg·h/L for efficiency, when MIC is above 1.5 mg/L. A higher pathogen MIC indicates development of bacterial resistance and would justify the use of a higher therapeutic target [16] or an alternative drug. When aiming for an (median) AUC of 700 mg·h/L the dosing advice in Table 3.2 should be adjusted by 700/400.

Previously, Janssen et al. proposed to decrease the vancomycin dose by 2 mg/kg/dose when co-administrated with ibuprofen [2]. This recommendation was shown to have a relatively larger impact in small neonates (see Figure 3.3), who receive lower doses on average, tending towards under-exposure. This limitation has been considered in the current proposal by decreasing the dose proportionally to the decrease in CL (Table 3.2).

Even though both ibuprofen and indomethacin belong to the same drug class (NSAIDs) and are used for the same therapeutic indication, the extent to which they influence vancomycin clearance is more than 3-fold different. While it is unknown whether this results from the drug itself or a non-equivalent dose compared to this side effect, it seems that a specific dose adjustment for each NSAID should be applied for the best vancomycin treatment outcome. Ibuprofen is associated with a decreased risk of necrotizing enterocolitis and transient renal insufficiency as compared to indomethacin [17]. There are no reviews comparing how different dosing regimens or modes of administration of the different NSAIDs used to treat PDA affect the treatment outcome or the risk for side effects [18]. From these results it also seems that dose adjustments might be required for other drugs with similar physico-chemical properties to

vancomycin that are co-administrated with NSAIDs and are eliminated by glomerular filtration [5]. The proposed dosing regimen should be prospectively validated before applying them in clinical practice.

Supplemental figure S3.4-A shows the probability of target attainment for AUC_{0-24h} between 300-500 mg·h/L derived from Monte Carlo following various currently advised vancomycin dosing regimen without dose adjustments in patients with NSAID co-administration. Dosing according to the Dutch Children's Formulary, British National Formulary and NeoFax (meningitis) guidelines results in considerable under-exposure in neonates with neither PDA nor co-therapy with NSAIDs, therefore, it is important that these dosing guidelines are not further reduced using our proposal.

The results of our stochastic simulations show how the relatively high inter-individual variability in vancomycin CL is carried over to the yielded exposure, as this variability in CL cannot be accounted for a priori (Figure 3.3). The high inter-individual variability in vancomycin CL in all neonates makes dosing challenging. Therefore, even though the proposed adjustments improve the vancomycin target attainment in the population as a whole, TDM is still required to individualize dosing in clinical practice.

3.6 Conclusion

In preterm neonates with suspected or confirmed late onset sepsis and pharmacologically treated for PDA, vancomycin CL is reduced by 16% and 55% when co-administered with ibuprofen or indomethacin, respectively. To reach the same exposures as in patients without PDA and co-administration with NSAIDs, we propose dosing adjustments of 20% in maintenance dose when ibuprofen is co-administrated and reductions of 20% and 60% in loading dose and maintenance dose, respectively, when indomethacin is co-administrated, as compared to previously reported neonatal dosing guidelines [2]. Therapeutic drug monitoring is still required due to the remaining random variability on vancomycin CL that can yield high exposures which increase the risk of adverse events. PK of drugs with similar properties to vancomycin that are also eliminated by glomerular filtration may be affected to a similar extent by NSAIDs co-administration.

3.7 Acknowledgements

CAJK received support from the Innovational Research Incentives Scheme (Vidi grant, June 2013) of the Dutch Organization for Scientific Research (NWO) for the submitted work. All authors declare that they have no conflicts of interest. This work was performed within the framework of Top Institute Pharma project D2-501. The research activities of AS are supported by the Clinical Research and Education Council of the University Hospitals Leuven. The authors would like to thank Aline GJ Engbers for performing the code review for this project.

3.8 References

1. Stoll BJ, Hansen N, Fanaroff AA, Wright LL, Carlo WA, Ehrenkranz RA, Lemons JA, Donovan EF, Stark AR, Tyson JE, Oh W, Bauer CR, Korones SB, Shankaran S, Laptook AR, Stevenson DK, Papile L-A, Poole WK. 2002. Late-Onset Sepsis in Very Low Birth Weight Neonates: The Experience of the NICHD Neonatal Research Network. *Pediatrics* 110 (2 Pt 1): 285-91.
2. Janssen EJH, Väitalo PA J, Allegaert K, de Cock RFW, Simons SHP, Sherwin CMT, Mouton JW, van den Anker JN, Knibbe CA J. 2015. Towards rational dosing algorithms for vancomycin in neonates and infants based on population pharmacokinetic modeling. *Antimicrob Agents Chemother* AAC.01968-15.
3. Allegaert K, de Hoon J, Debeer A, Gewillig M. 2010. Renal side effects of non-steroidal anti-inflammatory drugs in neonates. *Pharmaceuticals* 3:393-405.

4. Lin YJ, Chen CM, Rehan VK, Florens A, Wu SY, Tsai ML, Kuo YT, Huang FK, Yeh TF. 2017. Randomized Trial to Compare Renal Function and Ductal Response between Indomethacin and Ibuprofen Treatment in Extremely Low Birth Weight Infants. *Neonatology*.111(3):195-202.
5. De Cock RFW, Allegaert K, Sherwin CMT, Nielsen EI, De Hoog M, Van Den Anker JN, Danhof M, Knibbe C a J. 2014. A Neonatal amikacin covariate model can be used to predict ontogeny of other drugs eliminated through glomerular filtration in neonates. *Pharm Res* 31:754–767.
6. Zhao W, Biran V, Jacqz-Aigrain E. 2013. Amikacin maturation model as a marker of renal maturation to predict glomerular filtration rate and vancomycin clearance in neonates. *Clin Pharmacokinet* 52:1127–1134.
7. Silva R, Reis E, Bispo MA, Almeida AM, Costa IM, Falcao F, Palminha JM, Falcao AC. 1998. The kinetic profile of vancomycin in neonates. *J Pharm Pharmacol* 50:1255–1260.
8. Young T. 2011. Neofax, 24th ed. Thomas Reuters.
9. Formulary CP. 2009. British National Formulary for children. BMJ Group, London.
10. Nederlands Kenniscentrum voor Farmacotherapie bij Kinderen. 2013. Kinderformularium.
11. Comets E, Brendel K, Mentré F. 2010. Model evaluation in nonlinear mixed effect models, with applications to pharmacokinetics. *J la Société Française Stat* 151:106–127.
12. Frymoyer A, Hersh AL, El-Komy MH, Gaskari S, Su F, Drover DR, Van Meurs K. 2014. Association between vancomycin trough concentration and area under the concentration-time curve in neonates. *Antimicrob Agents Chemother* 58:6454–6461.
13. Neely MN, Youn G, Jones B, Jelliffe RW, Drusano GL, Rodvold KA, Lodise P. 2014. Are Vancomycin Trough Concentrations Adequate for Optimal Dosing ? *Antimicrob Agents Chemother* 58:309–316.
14. Morrison AP, Melanson SEF, Carty MG, Bates DW, Szumita PM, Tanasijevic MJ. 2012. What Proportion of Vancomycin Trough Levels Are Drawn Too Early ? Frequency and Impact on Clinical Actions. *Am J Clin Pathol*. 137(3):472–478.
15. Moise-broder PA, Forrest A, Birmingham MC, Schentag JJ. 2004. Pharmacodynamics of Vancomycin and Other Antimicrobials in Patients with Staphylococcus aureus Lower Respiratory Tract Infections. *Clin Pharmacokinet*. 43(13):925–942.
16. Phillips CJ. 2014. Questioning the accuracy of trough concentrations as surrogates for area under the curve in determining vancomycin safety. *Ther Adv Drug Saf* 5:118–120.
17. Ohlsson A, Walia R, Shah SS. 2015. Ibuprofen for the treatment of patent ductus arteriosus in preterm or low birth weight (or both) infants. *Cochrane Database Syst Rev*.18;(2):CD003481.
18. Mitra S, Florez ID, Tamayo ME, Mbuagbaw L, Vanniyasingam T, Veroniki AA, Zea AM, Zhang Y, Sadeghirad B, Thabane L. 2018. Association of placebo, indomethacin, ibuprofen, and acetaminophen with closure of hemodynamically significant patent ductus arteriosus in preterm infants a systematic review and meta-analysis. *JAMA* 319(12):1221–1238

3.9 Supplementary material

Table S3.1. Parameter estimates of the final vancomycin pharmacokinetic model with relative standard errors (RSE %) obtained in the model fit and median value and 95% confidence interval obtained in the bootstrap analysis.

Vancomycin PK parameters		Bootstrap Results
Structural parameters	Value (RSE%)	Bootstrap median value (95% Confidence Interval)
$CL = CL_p \times \left(\frac{BW}{1760}\right)^{\theta_{BW}} \times \left(1 + \left(\theta_{PNA} \times \left(\frac{PNA}{2}\right)\right) \times F_{ibu} \times F_{indo}\right)$		
$CL_{(p)}$ (L/h)	0.053 FIX*	0.053 FIX*
θ_{BW}	1.34 FIX*	1.34 FIX*
θ_{PNA}	0.213 FIX*	0.213 FIX*
F_{ibu}	0.838 FIX*	0.838 FIX*
F_{indo}	0.447 (14%)	0.471 (0.33 – 0.56)
$V_i = V_p \times \left(\frac{cBW}{1750}\right)^{\theta_{WT}}$		
V_p (L)	0.913 FIX*	0.913 FIX*
θ_{WT}	0.919 FIX*	0.919 FIX*
$V_2 = V_1$		
$Q = Fr \times CL$		
Fr	0.904 FIX*	0.904 FIX*
Inter-individual Variability		
IIVCL (%)	33.6 (18%)	38.3 (22%- 41%)
Residual Error		
Proportional (%)	0.106 (8%)	0.11 (0.09- 0.12)

*values fixed to values published by De Cock et al. [5] and Janssen et al.[2]

BW - birthweight (g); PNA - postnatal age (days); cBW - current weight (g)

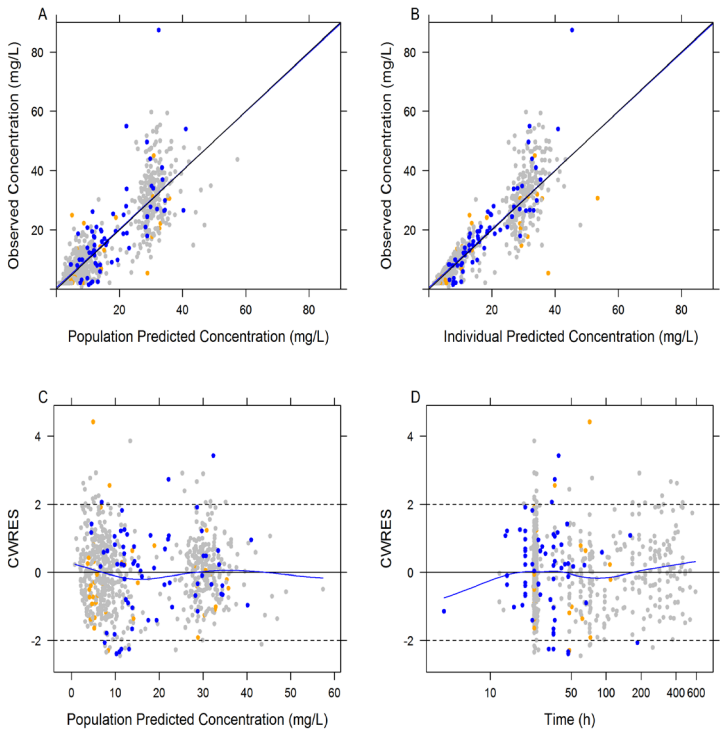


Figure S3.1 – Goodness of fit plots for the final vancomycin PK model including all groups colored by co-medication: grey – vancomycin without NSAIDs, orange vancomycin with ibuprofen and blue vancomycin with indomethacin.

Table S3.2 –Vancomycin dosing guidelines for preterm neonates with PDA that receive co-administration with ibuprofen or indomethacin used for simulations with the final model.

Dosing guideline	PMA	PNA	Dose
Dutch Children’s Formulary (2013) (10)	-	< 1 week	20 mg/kg/day in 2 doses
		1-4 weeks	30 mg/kg/day in 2 doses
		1 month – 18 years	40 mg/kg/day in 3 doses
British National Formulary for children (2009)(9) – for Gram positive bacteria	< 29 weeks	-	15 mg/kg/day in 1 dose
	29– 35 weeks		30 mg/kg/day in 2 doses
	> 35 weeks		45 mg/kg/day in 3 doses
	-	1 month – 18 years	45 mg/kg/day in 3 doses (max 2 g)
NeoFax – meningitis (2011)(8)	≤ 29 weeks	0-14 days	15 mg/kg q18h
		> 14 days	15 mg/kg q12h
	30-36 weeks	0-14 days	15 mg/kg q12h
		> 14 days	15 mg/kg q8h
	37-44 weeks	0-7 days	15 mg/kg q12h
		> 7 days	15 mg/kg q8h
	≥ 45 weeks	-	15 mg/kg q6h

PMA: postmenstrual age (gestational age + postnatal age); PNA: postnatal age

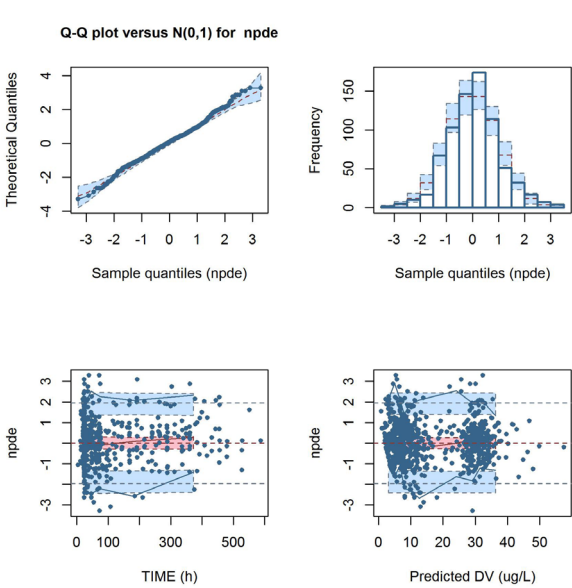


Figure S3.2 - Normalized prediction distribution errors results of the final model (N = 1000). DV stands for dependent variable, which in this case is the observed vancomycin concentrations.

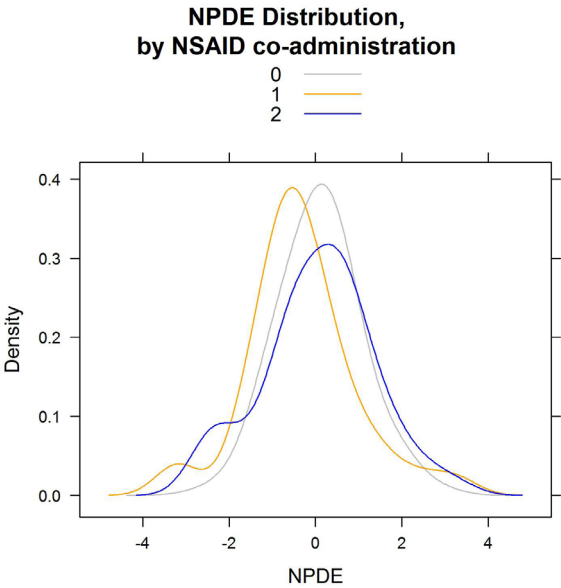


Figure S3.3 – Distribution of NPDEs for the three groups: grey: no co-medication; orange ibuprofen as co-medication; blue indomethacin as co-medication.

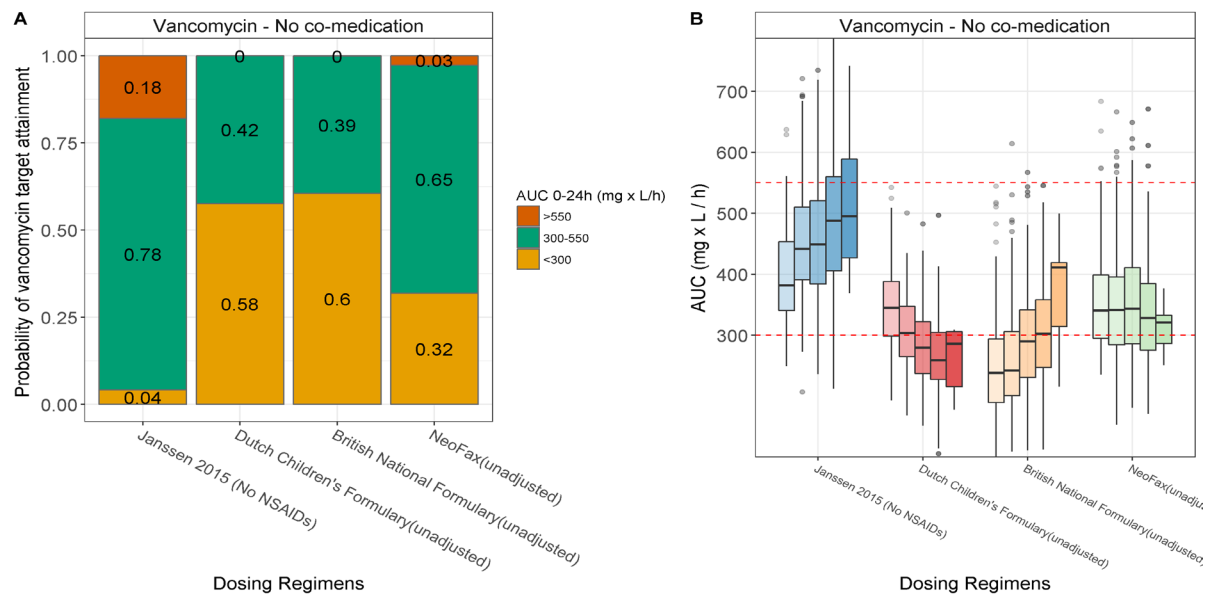


Figure S3.4 – Panel A - Probability of target attainment for AUC_{0-24h} between 300 - 550 mg·h/L for vancomycin for different dosing regimens, derived from Monte Carlo simulations in virtual neonates without PDA (no co-medication). Each bar represents the results obtained with one dosing (see Table 2 and supplemental Table S2 for details of different dosing regimens). Panel B - Vancomycin AUC_{0-24h} in the first day of treatment obtained following Monte Carlo simulations for hypothetical individuals with birthweights grouped by the dosing categories: < 700 g, 700 - 1000 g, 1000 - 1500 g, 1500 - 2500 g and > 2500 g for different vancomycin dosing regimens with no adjustments (see Tables 3.2 and S3.2 for details on different dosing regimens). Color intensifies with increasing birthweight.

3.10 Model code

```
;; 1. Based on: De Cock 2012
;; 2. Description: VANCO-IBU-INDO PRJ
$PROB Vanco + NSAIDS - IBU & INDO in PDA patients
$INPUT ID WT PMA OCC TIME RATE AMT DUR MDV DV GA PNA BW CULT VEN RS INOT
NSAI study CREA
$DATA ../DataSets/Modeling/vanco02.csv
IGNORE=@ IGNORE(ID.EQ.245) ; previously excluded

$SUBROUTINES ADVAN6 TOL=9
$MODEL
    COMP=(CENT,DEFOBS,DEFDOS) ; central cmt with obs
    COMP=(PERIPH1) ; peripheral cmt
    COMP=(AUC) ; AUC cmt

$PK
FF1 = 1 ; no ibu coadmin
FF2 = 1 ; no indo coadmin
    IF (NSAI.EQ.1) FF1 = THETA(7)
    IF (NSAI.EQ.2) FF2 = THETA(8)
TVCL = THETA(1) * ((BW / 1750) ** THETA(4)) * (1 + (PNA/ 2) * THETA(6)) *
    FF1 * FF2 ;BW in g, PNA in days
CL = TVCL * EXP(ETA(1))
TVV1 = THETA(2) * ((WT / 1760) ** THETA(5)) ;WT in g
V1 = TVV1 * EXP(ETA(2))
Q = THETA(3) * CL
V2 = V1
S1 = V1
K10 = CL / V1
K12 = Q / V1
K21 = Q / V2

$DES
DADT(1) = -K12*A(1) + K21*A(2) - K10*A(1)
DADT(2) = K12*A(1) - K21*A(2)
DADT(3) = A(1)/V1

$ERROR
AUC = A(3)
IPRED = F
Y = F*(1+ERR(1)) ; propotional error

$THETA
0.053 FIX ;1-CL
0.913 FIX ;2-V1
0.904 FIX ;3-Q
1.34 FIX; 4-BW exp on CL
0.919 FIX ;5-CW exp on V2
0.213 FIX ;6-PNA lin on CL
0.838 FIX ;7-IBU coadmin
0.6 ;8-INDO coadmin

$OMEGA
0.1 ;CL

$SIGMA
0.05

$EST METHOD=1 INTERACTION NOABORT SIGDIG=3 PRINT=5 MAXEVAL=9999 POSTHOC
$COV COMP PRINT=E
$TABLE ID TIME RATE DV MDV GA BW WT PNA PMA NSAI TVCL IPRED CL V1 V2 Q ETA1
ETA2 CWRES CREA AUC NOPRINT ONEHEADER FILE=Vancomycin130_1.tab
```


Section III. PBPK-based dosing of drugs cleared by glomerular filtration in children



**The predictive value of GFR-based scaling of
pediatric clearance and doses for drugs eliminated
by glomerular filtration with varying protein binding
properties**

S Cristea, EHJ Krekels, K Allegaert, CAJ Knibbe

4.1 Abstract

For drugs eliminated by glomerular filtration (GF), clearance (CL) is determined by GF rate (GFR) and the unbound fraction of the drug. When predicting CL of GF-eliminated drugs in children, instead of physiologically-based (PBPK) methods which consider changes in both GFR and protein binding, empiric bodyweight-based methods are often used. Here we explore the predictive value of scaling using a GFR function and compare the results to linear and allometric scaling methods for drugs with different protein binding properties.

First, different GFR maturation functions were compared to identify the GFR function that would yield the most accurate GFR predictions across the pediatric age-range as compared to published pediatric inulin/mannitol CL values. Subsequently, the accuracy of pediatric CL scaling using this GFR maturation function was assessed and compared to PBPK CL predictions for hypothetical drugs binding to varying extents to serum albumin or α -acid glycoprotein across the pediatric age range. Additionally, empiric bodyweight-based methods were assessed.

The published GFR maturation functions yielded comparable maturation profiles, with the function of Salem et al. leading to the most accurate predictions. On the basis of this function, GFR-based scaling yields reasonably accurate (percentage prediction error $\leq 50\%$) pediatric CL values for all drugs, except for some drugs highly bound to AGP in neonates. Overall, this method was more accurate than linear or 0.75 allometric bodyweight-based scaling.

When scaling CL and dose by GFR function, maturational changes in plasma proteins concentrations impact GF minimally, making this method a superior alternative to empiric bodyweight-based scaling.

4.2 Introduction

Clearance (CL) is the driving parameter for dosing as it determines steady-state and trough concentrations. For children, precise scaling of clearance without bias across the pediatric age range is paramount to reach both an effective and safe (starting) dose. This is of relevance for defining (first-in-child) doses in clinical studies particularly of drugs for which differences in dose requirements between adults and children can be attributed entirely to differences in pharmacokinetics (PK) and/or for which target concentrations in children are known [1].

CL of drugs eliminated through glomerular filtration (GF) is dependent on GF rate (GFR) and plasma protein binding. GFR maturation across the pediatric population has been described by different functions based on data either from CL of endogenous (e.g. creatinine, cystatin C) or from exogenous (e.g. inulin, iohexol, aminoglycosides) compounds, used as markers for GFR function [2–7]. With respect to plasma protein binding, changes in the unbound drug fraction (f_u) with age need to be taken into account when predicting pediatric CL via GF, as only the drug fraction that is not bound to plasma proteins can be eliminated through GF. The unbound fraction across age is dependent on the protein the drug binds to (i.e. human serum albumin or α -acid glycoprotein) and the changes in the concentrations of these proteins with age [8]. As physiologically-based pharmacokinetic (PBPK) models include drug properties (i.e. f_u) and physiological differences between adults and children (i.e. maturation of plasma proteins concentrations and GFR), these models are considered the ‘gold standard’ for pediatric CL predictions [9].

The application of PBPK approaches is however constrained by the availability of both drug-specific data, skilled personnel and resources needed to access and use different modeling platforms. Therefore, empirical bodyweight-based scaling methods such as linear scaling or allometric scaling with a fixed exponent of 0.75 are still often used to derive pediatric CL from adult CL values. However, empirical scaling methods disregard information about maturation of both GFR and protein binding. Previous work has shown that these approaches are inaccurate for certain pediatric age-groups for drugs cleared by GF [10, 11], suggesting that more mechanistic information may be needed for accurate scaling. For

this, it has been proposed to adjust the allometric scaling with a maturation function for GFR, especially in the very young [12]. Here we assess the accuracy of scaling based on GFR maturation without taking into account maturational changes in f_u . We compare this approach to two relatively straight forward scaling methods based on bodyweight alone, since these methods are still often used and perhaps even preferred because of their ease.

To this end, we first identify the GFR maturation function that yields the most accurate GFR predictions across the pediatric age-range. Subsequently, we assess the accuracy of pediatric CL and dose scaling obtained with the GFR maturation function as compared to PBPK predictions for hypothetical drugs binding to varying extents to human serum albumin (HSA) or α -acid glycoprotein (AGP) across the pediatric age range. Additionally, the results are compared to those of the two-empiric bodyweight-based methods, i.e. linear and allometric scaling with a fixed exponent of 0.75.

4.3 Methods

4.3.1 Establishing the most accurate pediatric GFR maturation function

Functions that quantify GFR maturation throughout the pediatric age-range for children with a normal renal functionality and that only used demographic characteristics as input, were collected from the literature by searching the PUBMED data base with the search term “glomerular filtration maturation children human ” or from Simcyp v18 resources. Seven [7, 13–17] functions were identified, of which six [13–17] were developed based on exogenous markers for GFR (i.e. inulin, -Cr-EDTA, mannitol, iothexol) and one [7] was derived from CL values of antibiotics that are predominantly eliminated through GF. To visually compare the different GFR maturation profiles, age-appropriate body surface area (BSA), height, and weight values were derived from the NHANES database [18] and used for GFR predictions with each of the seven functions.

In this analysis, inulin and mannitol CL values were considered the ‘gold standard’ for GF function [19, 20], hence, they were used to select the most accurate pediatric GFR maturation function. GFR predictions with each of the seven maturation functions were compared to inulin [3–6] and mannitol [2] CL values published for children, for whom the necessary demographic characteristics were reported. Individual data were either digitized with WebPlotDigitizer (<https://apps.automeris.io/wpd/>) or extracted directly from the publications. When inulin and mannitol CL values were reported relative to the standard adult BSA (i.e. normalized by 1.73 m²), they were converted to absolute values. When gestational age was missing, a gestational period of 38 weeks was imputed. Missing BSA values were calculated based on age and bodyweight with the Haycock [21] and Dubois [22] formulas for children under and over 15 kg, respectively.

For the seven GFR maturation functions, the demographic characteristics corresponding to the individuals for whom inulin [3, 4, 6] and mannitol [2] CL values were available, were used as input and the resulting predictions were compared with the reported measurements. For this, a percentage prediction error (%PE_{GFR}) between the predicted GFR with each function and the inulin [3, 4, 6] and mannitol [2] CL values was calculated according to equation 1. In addition, the root mean square percentage error (%RMSPE_{GFR}) was calculated using equation 2 for the entire pediatric population as well as for selected age-groups to show the stratified accuracy of the GFR functions for preterm neonates, term neonates at the first day, newborns between 1 day and 1 month, and children between 1 and 6 months, between 6 months and 1 year, between 1 and 5 years, and between 5 and 15 years. In equations 1 and 2, the predicted GFR are values obtained with each of the published GFR maturation functions and observed CL_{inulin/mannitol} are the published values for inulin or mannitol CL.

$$\%PE_{GFR} = \frac{\text{predicted GFR} - \text{observed CL}_{\text{inulin/mannitol}}}{\text{observed CL}_{\text{inulin/mannitol}}} \times 100 \quad [1]$$

$$\%RMSPE_{GFR} = \sqrt{\frac{1}{n} \times \sum_{i=1}^n \left(\frac{\text{predicted } GFR - \text{observed } CL_{\text{inulin/manitol}}}{\text{observed } CL_{\text{inulin/manitol}}} \right)^2} \quad [2]$$

As the predictions do not include variability or uncertainty in any of the terms, only point estimates of $\%PE_{GFR}$ and $\%RMSPE_{GFR}$ are obtained. To compensate for this, rather than applying the 2-fold rule that is commonly used in assessing the accuracy of PBPK model prediction we designated values within $\pm 30\%$ to be “accurate predictions”, values outside the $\pm 50\%$ interval to be inaccurate, and with values in between to be reasonably accurate for $\%PE_{GFR}$. For $\%RMSPE_{GFR}$, values within 0% - 30% indicate “accurate predictions”, values $> 50\%$ indicate “inaccurate predictions”, and values within 30% - 50% are “reasonably accurate”. The GFR maturation function that would lead to the narrowest range in $\%PE_{GFR}$ predictions and the smallest $\%RMSPE_{GFR}$ overall and per age-group was selected and used in the PBPK-based approach as well as in the evaluation of pediatric CL scaling.

The results here do not include findings for preterm neonates as only four [7, 13, 15] of the seven GFR maturation functions were also developed for preterm neonates. Inulin and mannitol data collected from preterm neonates [3, 5, 23] were analyzed separately together with these four functions, and the results can be found in the supplemental material.

4.3.2 Evaluation of pediatric clearance scaling

To evaluate the accuracy of pediatric CL scaling using the selected GFR function or empiric functions, a ‘true’ CL value is needed as reference. As PBPK-based approaches are considered the “gold standard” for pediatric CL predictions, the renal PBPK model in equation 3 was used to derive ‘true’ CL values. ‘True’ CL of hypothetical drugs was predicted for typical pediatric individuals at the age of 1 day, 1, 3, 6 and 9 months, 2, 5, 10, and 15 years and a 35-year-old typical adult.

$$'true' CL = GFR \times f_u \quad [3]$$

In equation 3, pediatric GFR values were obtained with the best maturation function selected above. Demographic values needed to predict pediatric GFR values with the best GFR maturation function were derived from the NHANES database [18] and from the ICRP annals [24] for children and adults, respectively.

For f_u in equation 3, a total of 20 hypothetical drugs was evaluated. For these drugs, f_u values in adults ($f_{u,adult}$) of 0.1, 0.2, 0.3, 0.4, 0.5, 0.6, 0.7, 0.8, 0.9 or 1 were used and each drug was assumed to exclusively bind to either HSA or AGP. Pediatric f_u values ($f_{u,ped}$) at each pediatric age were obtained based on the ratios between relevant binding proteins concentrations and the $f_{u,adult}$, according to equation 4 [8]:

$$f_{u,ped} = \frac{1}{1 + \frac{[P]_{ped} \times (1 - f_{u,adult})}{[P]_{adult} \times f_{u,adult}}} \quad [4]$$

in which [P] stands for the plasma concentration of the relevant binding protein (i.e. HSA or AGP).

Equations 5 and 6 [15] were used to calculate the plasma concentrations ([P]) of HSA and AGP, respectively, for typical children of different ages, with age expressed in days. Visual representations of the maturation profiles of the plasma proteins as well as of the resulting $f_{u,ped}$ values are presented in supplemental Figure S4.1.

$$[HSA(g/L)] = 1.1287 \times \ln(Age) + 33.746 \quad [5]$$

$$[AGP(g/L)] = \frac{0.887 \times Age^{0.28}}{8.89^{0.28} + Age^{0.28}} \quad [6]$$

where [HSA(g/L)] and [AGP(g/L)] represent the plasma protein concentrations and Age is the age of the typical child expressed in days[15].

GFR-based scaling of clearance

For GFR-based scaling of CL from adults to children of different ages, equation 7 is used. Here 'true' adult CL values of the drug, i.e. GFR_{adult} multiplied by $f_{u,adult}$ (for 20 hypothetical drugs, see equation 3), were scaled by the ratio between GFR_{ped} and GFR_{adult} , with GFR_{ped} calculated according the selected function (see results, Salem [17], equation 12). Note that $f_{u,adult}$ is included for obtaining the 'true' adult CL values, however, changes in f_u with age are not included when applying GFR-based scaling (equation 7).

$$GFR \text{ scaled } CL_{ped} = 'true' CL_{adult} \times \left(\frac{GFR_{ped}}{GFR_{adult}} \right) \quad [7]$$

Empiric and linear body-weight based scaling methods

For comparative purposes, the accuracy of GFR-based scaling was evaluated together with linear bodyweight-based scaling (equation 8) and bodyweight-based allometric scaling with a fixed exponent of 0.75 (equation 9), which are two commonly used empirical pediatric CL scaling methods.

$$Linear \text{ scaled } CL_{ped} = 'true' CL_{adult} \times \left(\frac{WT_{ped}}{WT_{adult}} \right) \quad [8]$$

$$Allometric \text{ scaled } CL_{ped} = 'true' CL_{adult} \times \left(\frac{WT_{ped}}{WT_{adult}} \right)^{0.75} \quad [9]$$

Comparison of different scaling methods

The accuracy of GFR-based, linear and allometric scaling with a fixed exponent of 0.75 of clearance was assessed by calculating the $\%PE_{CL}$ compared to 'true' CL_{ped} according to equation 10. Note that in 'true' CL_{ped} (equation 3) the changes in f_u with age are considered according to equations 4-6.

$$\%PE_{CL} = \frac{scaled \ CL_{ped} - 'true' \ CL_{ped}}{'true' \ CL_{ped}} \times 100 \quad [10]$$

4.3.3 Assessment of pediatric dose scaling

As CL scaling is commonly used as the basis for dose scaling, the implications of the different CL scaling methods on the accuracy of the dose-adjustments derived from them were also assessed. For each of the 20 hypothetical drugs for which 'true' adult CL values (equation 3) were calculated, equation 11 was used to derive the pediatric dose.

$$dose_{ped} = dose_{adult} \times \left(\frac{CL_{ped}}{'true' \ CL_{adult}} \right) \times 100 \quad [11]$$

in which CL_{ped} refers to CL values obtained with either of the three simplified scaling methods (GFR-based scaling, linear scaling or allometric scaling with a fixed exponent of 0.75) according to equations 7, 8 and 9, respectively. This method assumes steady-state conditions (i.e. drug exposure is only dependent on dose and CL) and that the same drug target exposure (i.e. AUC) is applicable in children and adults. As relative dose adjustments were assessed, the adult dose was expressed as 1.

The 'true' reference doses were obtained by replacing the CL_{ped} value in equation 11 by the 'true' CL_{ped} value (equation 3). The accuracy of the scaled doses was assessed by calculating the $\%PE_{dose}$ according to equation 10.

4.4 Results**4.4.1 Establishing the most accurate pediatric GFR maturation function**

Figure 4.1 shows the seven published GFR maturation profiles [7, 13–17]. All profiles are comparable

with the steepest maturation occurring in the first two years of life and plateau values being reached beyond the age of 15 years.

Figure 4.2 depicts the %PE_{GFR} between GFR predictions according to the seven different functions versus inulin [3, 4, 6] or mannitol [2] CL measurements. In addition, Table 4.1 presents the %RMSPE_{GFR} and the range in %PE_{GFR} per age-group as well as for the entire pediatric age-range. The results show that all functions tend towards over-prediction of GFR in the very young. In newborns, inter-individual variability is higher than in older children which yields the largest spread in %PE_{GFR} for all GFR functions, with values ranging between -112% and 484%. Furthermore, %RMSPE_{GFR} in newborns can reach values of 158% compared to values below 50% in older children. For all functions, the %PE_{GFR} range becomes narrower with increasing age and above 5 years most functions lead to accurate predictions (%PE_{GFR} within ±30%). The function of Salem [17] had the best predictive performance per age-group and across all pediatric ages. These GFR predictions were similar to the ones obtained with the function of Rhodin [14], as indicated by the RMSPE_{GFR} % values and %PE_{GFR} ranges for the entire population as for the different age groups. Results for preterm neonates are presented in the supplemental material (Figure S4.2, Table S4.1).

From these results, the GFR maturation function published by Salem [16] (equation 12) was selected and used in the renal PBPK model (equation 3) to determine the ‘true’ renal CL of the 20 hypothetical drugs for the typical adult and the typical pediatric individuals. These GFR values are also used in equation 7 to calculate GFR based scaled clearance values across the pediatric range.

$$GFR_{ml/min} = 112 \times \left(\frac{Weight(kg)}{70} \right)^{0.63} \times \frac{PMA^{3.3}}{PMA^{3.3} + TM_{50}^{3.3}} \quad [12]$$

with PMA defined as postmenstrual age in weeks and TM₅₀ as the PMA at which GFR reaches half of the adult levels.

4.4.2 Evaluation of pediatric clearance scaling

Figure 4.3 shows the %PE_{CL} for GFR-based scaling and for the two empirical bodyweight-based scaling methods, none of which take changes in plasma protein concentrations into account. The figure illustrates how scaling accuracy of CL with each of the three methods is impacted by f_u (color intensifies with increased f_u) and plasma protein concentrations at every investigated age. Overall, GFR-based scaling is

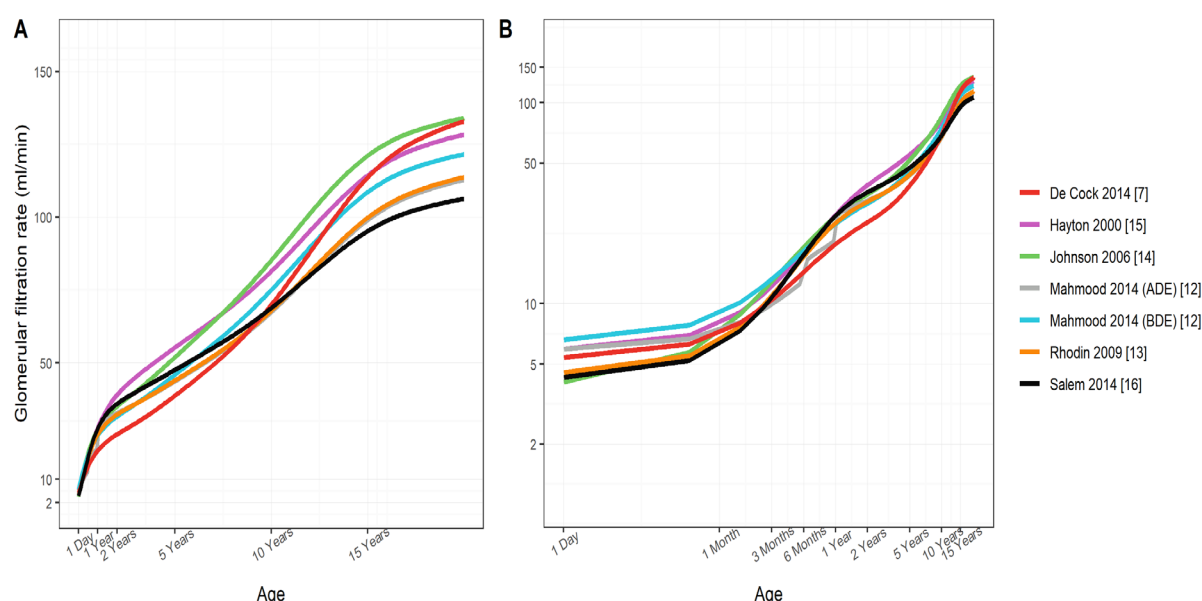


Figure 4.1 – Pediatric glomerular filtration rate (GFR) according to published GFR maturation functions [7, 13–17] throughout the pediatric age range. Panel A – semi-logarithmic scale; Panel B – double logarithmic scale.

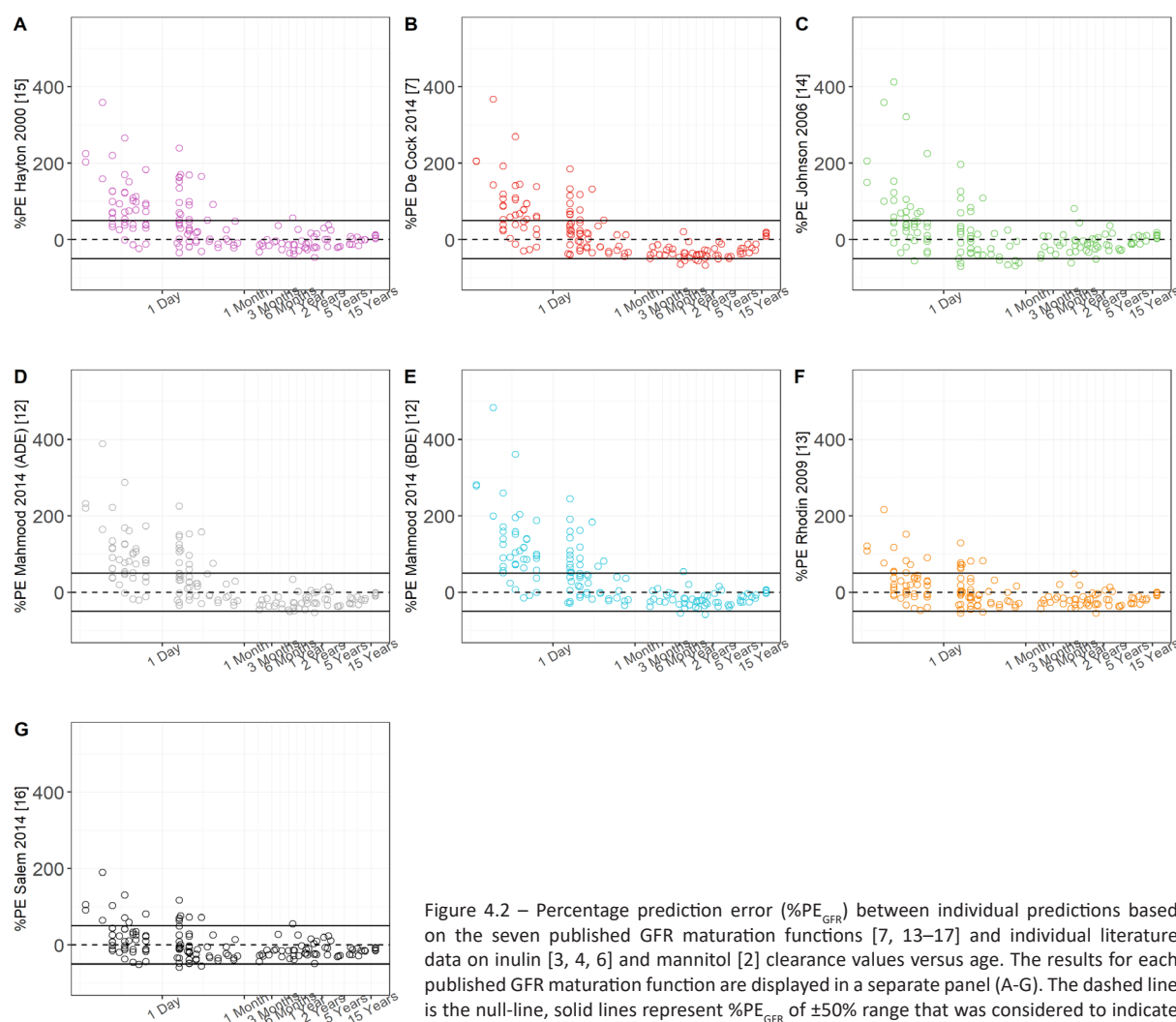


Figure 4.2 – Percentage prediction error ($\%PE_{GFR}$) between individual predictions based on the seven published GFR maturation functions [7, 13–17] and individual literature data on inulin [3, 4, 6] and mannitol [2] clearance values versus age. The results for each published GFR maturation function are displayed in a separate panel (A–G). The dashed line is the null-line, solid lines represent $\%PE_{GFR}$ of $\pm 50\%$ range that was considered to indicate reasonably accurate scaling.

more accurate than the two empirical bodyweight-based methods, leading to $\%PE_{CL}$ values within $\pm 50\%$ ($f_u \text{ adult} < 0.3$). Bodyweight-based allometric scaling with a fixed exponent of 0.75 is mostly inaccurate for individuals below 3 months. GFR-based scaling and linear scaling outperform allometric scaling for these subjects. For children between 6 months and 15 years of age, linear scaling is reasonably accurate albeit with a trend in $\%PE_{CL}$ values indicating systematic bias towards under-prediction. In this age-range similar, yet less strong, trends are seen for allometric scaling with a fixed exponent of 0.75, while GFR-based scaling is generally the most accurate of the three (Figure 4.3).

4.4.3 Assessment of pediatric dose scaling

Figure 4.4 and Table 4.2 show pediatric doses (expressed as percentage of adult dose) obtained with ‘true’ CL values versus those obtained with CL values by the three scaling methods in typical patients for 20 hypothetical drugs differing in unbound drug fraction in adults and binding to either HSA or AGP. Both the figure and table show that the ‘true’ doses predicted based on ‘true’ pediatric CL values are dependent on f_u whereas the scaled doses derived from CL values scaled with the three different scaling methods (i.e. GFR scaling, linear scaling and allometric scaling) are not. Overall, the results show that doses obtained with GFR-based scaling are lower than the ‘true’ reference doses for drugs highly bound (i.e. $f_u = 0.1$) to HSA or AGP (up to 20 to 60%, respectively). For drugs with low protein binding (i.e. $f_u = 0.9$), the differences between the ‘true’ reference dose and GFR-based scaled doses are small throughout the pediatric age-range ($< 5\%$). Using linear bodyweight-based scaling doses are also lower than the ‘true’ reference doses for children with ages between 6 months and 10 years (up to 25.5%

Table 4.1 – Root mean square percentage error (%RMSPe_{GFR}) and percentage prediction error (%PE_{GFR}) ranges for the GFR predictions by the different published GFR maturation functions, stratified by age groups.

Age groups	Salem 2014[16]		Rhodin 2002 [13]		Hayton 2000 [15]		De Cock 2014 [7]		Johnson 2006 [14]		Mahmood 2016 (ADE) [12]		Mahmood 2016 (BDE) [12]	
	%RM-SPE _{GFR}	%PE _{GFR}	%RM-SPE _{GFR}	%PE _{GFR}	%RM-SPE _{GFR}	%PE _{GFR}	%RM-SPE _{GFR}	%PE _{GFR}	%RM-SPE _{GFR}	%PE _{GFR}	%RM-SPE _{GFR}	%PE _{GFR}	%RM-SPE _{GFR}	%PE _{GFR}
		[min-max]		[min-max]		[min-max]		[min-max]		[min-max]		[min-max]		[min-max]
At first day	54	-51 190	62	-47 216	123	-23 360	113	-29 367	123	-55 413	69	-44 235	158	-15 484
Between 1 day and 1 month	36	-58 117	36.5	-55 129	181	-34 482	58	-44 185.5	62	-112 197	52	-53 141	71	-34 245
Between 1 and 6 months	26	-43 28	25	-43 20	36	-32 117	32	-49 15	26	-49 13	29	-47 7	21	-37 28
Between 6 months and 1 year	30	-38 55	32	-42 48.5	30	-38 57.5	42	-63 21	38	-60 81.5	34	-48 33	35	-55 54
Between 1 and 5 years	23	-49 24	27	-55 13	22	-47 39	41	-67 -4.3	23	-51 37	26	-55 22	29	-58 16
Between 5 and 15 years	16	-28 -6	18	-31 0.82	9	-16 13	23	-37 19	10	-12 19	13	-21 17	14	-26 7
Entire pediatric age-range	38	-58 190	41	-55 216	141	-47 482	68	-67 367	77	-112 413	50	-55 235	88.5	-58 484

to 49% lower). For younger children, the difference between doses becomes smaller (less than 30% difference). Doses obtained using bodyweight-based allometric scaling with a fixed exponent of 0.75 are generally higher than the 'true' reference doses for children younger than 6 months. For this method, the highest difference of >150% was obtained for drugs with high fraction unbound in children younger than 1 month (Figure 4.4, Table 4.2).

4.5 Discussion

This study aimed to identify the GFR maturation function that yields the most accurate GFR predictions across the entire pediatric age-range and subsequently to assess what the accuracy of GFR-based scaling of CL and dose is as compared to the gold standard (i.e. PBPK-based predictions) and to two commonly used empiric bodyweight-based scaling methods. By comparing scaled CL values to PBPK CL predictions, we studied the influence of the maturation of plasma proteins concentrations on CL and dose scaling and showed at what ages this maturation is of relevance for each scaling method. The assessed scaling methods are typically used to guide pediatric dosing when little or no information is available on a

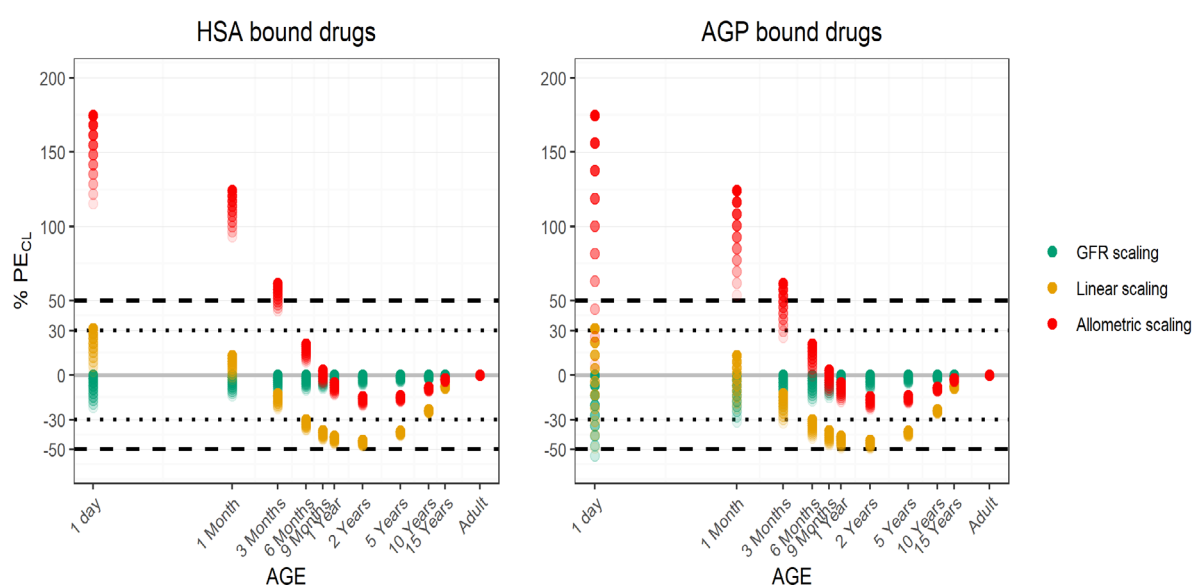


Figure 4.3 – Percentage prediction error (%PE_{CL}) between 'true' clearance (CL) values and CL values obtained with three different simplified scaling methods in typical pediatric patients for 20 hypothetical drugs differing in unbound drug fraction in adults and binding to either HSA (left panel) or AGP (right panel). Green dots indicate GFR-based scaling, orange dots indicate linear bodyweight-based scaling, red dots indicate bodyweight-based scaling with a fixed allometric exponent of 0.75. Colors intensify with increasing f_u . The grey solid line is the null-line, black dashed lines and black dotted lines represent the %PE_{CL} range of $\pm 30\%$ and $\pm 50\%$, respectively, that indicate accurate and reasonably accurate scaling, respectively.

drug in this population. As such, this work identifies drug properties (i.e. f_u) and patient characteristics (i.e. age) for which bodyweight-based scaling methods suffice and when more mechanistic information is necessary by means of either GFR-based scaling or PBPK for accurate CL and dose scaling. Our findings provide guidance for (first-in-child) clinical studies on what scaling method to use when deriving pediatric doses from adult doses of small molecules drugs that are mainly eliminated by GF.

The published GFR maturation functions we evaluated were found to have comparable profiles while the functions published by Salem [17] and by Rhodin [14] had similar accuracy in predicting inulin [3, 4, 6] and mannitol [2] CL measures, with the function by Salem [17] being overall slightly more accurate. This function (equation 12) was used in PBPK-based predictions of 'true' pediatric CL values (equation 3) and it was directly used for simplified GFR-based scaling (equation 7).

Drug CL by GF depends on GFR and plasma protein binding, which are taken into account by PBPK modeling approaches. However, the extent of protein binding and the proteins the drugs bind to may not

always be known, especially for the pediatric population. The simplified scaling functions, which include GFR-based scaling (equation 7), bodyweight-based linear scaling (equation 8), and bodyweight-based

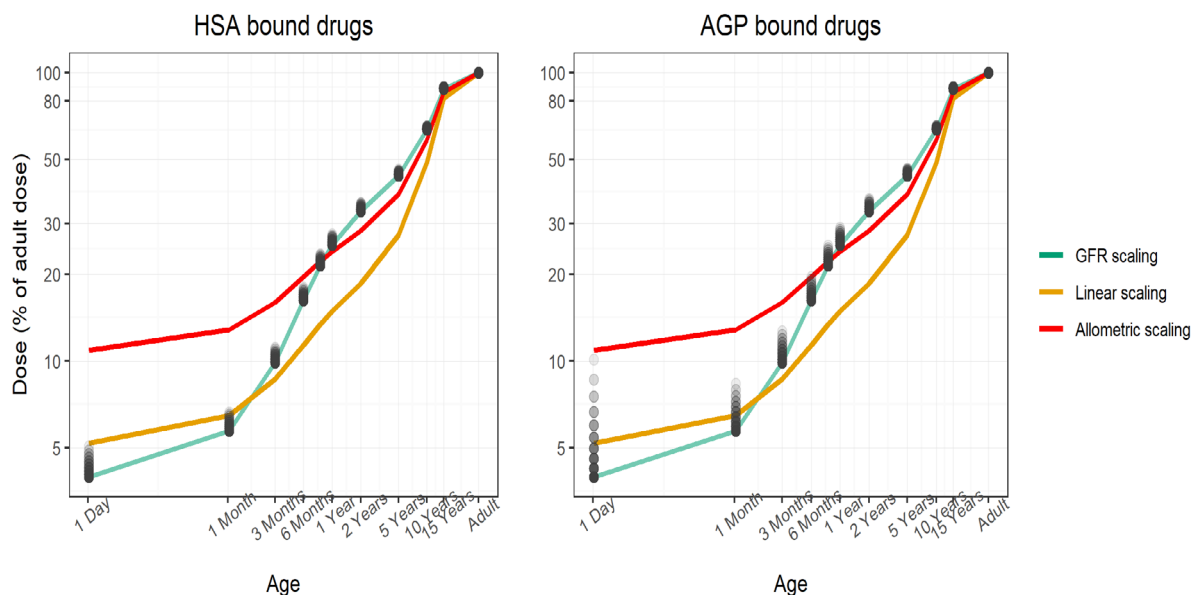


Figure 4.4 – Pediatric doses (percentage of adult dose) obtained with ‘true’ clearance (CL) values (black dots) and CL values obtained with three different simplified scaling methods (lines) in typical pediatric patients for 20 hypothetical drugs differing in unbound drug fraction in adults and binding to either HSA (left panel) or AGP (right panel). Green line indicates dose values obtained with GFR-based scaling, orange line indicates dose values obtained with linear bodyweight-based scaling, red line indicates dose values obtained with bodyweight-based scaling with a fixed allometric exponent of 0.75. The black dots indicate dose values obtained with ‘true’ CL. Color intensifies with increasing f_u

allometric scaling with a fixed exponent of 0.75 (equation 9), typically do not take changes in plasma protein binding with age into account. The difference between GFR-based scaled pediatric CL values and ‘true’ pediatric CL values reflects the impact of ignoring maturation in plasma protein concentrations on CL scaling. The current analysis showed that with GFR-based scaling this impact can be disregarded throughout the entire pediatric age-range, except in neonates for a few drugs highly bound to AGP (Figure 4.3). Prediction errors in scaled CL values are largest in neonates, especially for drugs that bind to AGP, possibly due to its steep maturation in early life (Figure S4.1). GFR-based scaling leads to under-prediction of CL in neonates and drug doses, as compared to ‘true’ CL and ‘true’ reference doses, which will result in a reduced risk of developing toxic effects, but also in an increased risk of treatment failure. Bodyweight-based allometric scaling with a fixed exponent of 0.75 tends to over-predict CL in children younger than 6 months, even though for drugs with a low f_u maturational changes in the expression of drug binding plasma proteins can still partially correct this bias. Bodyweight-based linear scaling leads to reasonably accurate CL predictions in this young population. After the age of 6 months the influence of plasma protein binding on CL scaling decreases as shown by a smaller deviation of GFR-based scaled CL from PBPK-based CL predictions. In this age-range reasonably accurate CL predictions are obtained using bodyweight-based scaling, irrespective of whether the exponent is 1 (linear scaling), 0.75 (allometric scaling), or 0.62 (GFR function from Salem et al.). As scaled CL values drive the scaled dose values, the same patterns are observed for this variable.

The CL predictions of selected drugs (>80% renal elimination) in neonates and children using the GFR maturation function of Rhodin [14], was recently described [25]. Our results are in line with these published findings, with the added advantage that our analysis captures the entire hypothetical parameter space regarding the relevant drug-specific parameters (i.e. extent and type of plasma protein binding). As such the presented analysis covers both drugs that are currently in clinical use as well as all small molecule drugs that are still to be developed. Therefore, this framework can be used to make a priori assessments on the accuracy of the pediatric CL and dose scaling methods for new drugs.

Table 4.2 – Pediatric doses presented as % of adult dose for drugs eliminated through GFR with varying f_u values. The ‘true’ doses predicted based on ‘true’ pediatric CL values are dependent on f_u , whereas the scaled doses derived from CL values scaled with the three different scaling methods (i.e. GFR scaling, linear scaling and allometric scaling) are not.

Demographic Characteristics of Typical Individuals			‘True’ dose (% of adult dose) obtained based on ‘true’ CL				Scaled dose (% of adult dose) obtained using three CL scaling methods		
Age	Weight* (kg)	GFR** (ml/min)	Drugs binding to HSA		Drugs binding to AGP		GFR scaling	Linear scaling	Allometric scaling
			$f_u = 0.1$	$f_u = 0.9$	$f_u = 0.1$	$f_u = 0.9$			
1 Day	3.4	4.3	5%	4.1 %	10.1 %	4.2 %	4 %	5.2%	11 %
1 Month	4.3	6.2	6.6 %	5.8 %	8.3 %	5.9 %	5.7 %	6.5 %	13 %
3 Months	5.8	10.7	11.1 %	10 %	12.7 %	10.1 %	9.9 %	8.6 %	16 %
6 Months	7.5	17.6	17.9 %	16.4 %	19.6 %	16.5 %	16.2 %	11.4 %	20 %
9 Months	8.9	23.2	23.5 %	21.6 %	25.1 %	21.8 %	21.4 %	13.4 %	22 %
1 Year	9.9	27.4	27.5 %	25.5 %	29.1 %	25.6 %	25.3 %	14.9 %	24 %
2 Years	12.3	35.9	35.4 %	33.3 %	36.5 %	33.4 %	33.1 %	18.6 %	28 %
5 Years	18.2	47.7	46 %	44.2 %	46.6 %	44.3 %	44 %	27.4 %	38 %
10 Years	32.5	68.9	65.4 %	63.8 %	65.6 %	63.8 %	63.6 %	48.9 %	58 %
15 Years	54.2	95.3	89.7 %	88.1 %	89.7 %	88.1 %	87.9 %	81.6 %	86 %
Adult	66.5	108.4	100 %	100 %	100 %	100 %	100 %	100 %	100 %

*weights from the NHANES database [17] for children and from the ICRP annals [23] for adults

** GFR values were predicted with Salem [16]

The current results are also in line with previous findings from our group comparing ‘true’ PBPK-based CL predictions to CL values scaled by both methods however small differences in numerical results are present. These differences are caused by two different GFR maturation functions being used in the PBPK model for the predictions of the ‘true’ CL values. For the current analysis we used the function published by Salem [17], which we now found to be most accurate, whereas, in the previous analyses the function by Johnson [15] was used.

The conclusions from our analysis are based on typical individuals and do not take inter-individual variability into account. For preterm and term neonates younger than 1 month, high variability in the inulin [3, 4, 6] and mannitol [2] CL data is observed, which poses a challenge when scaling CL and doses to this age-range. This suggests that variables other than the demographics used in GFR maturation functions are predictive of GFR-based clearance. For this special population, dosing recommendations that rely on empiric PK models of the same drug, even in slightly older children or of a similar drug that is mainly eliminated through GF in the same population, may therefore offer a better alternative [26, 27]. We emphasize that all published GFR maturation functions included in our analysis describe GFR maturation in pediatric individuals with normal renal function. These functions should therefore not be used for CL or dose scaling for pediatric patients with renal deficiencies. To account for renal impairment, functions that require a biomarker for renal function (e.g., creatinine, cystatin C, etc.) as input are more reliable and suitable to predict GFR. These functions can be implemented in the renal PBPK model in equation 3 and can also be used for GFR-based scaling. The impact of ignoring plasma protein binding in these scenarios may not be the same as observed in the current analysis, as plasma protein binding may also be altered in patients with renal deficiencies.

4.6 Conclusion

The maturation function by Salem [17] (equation 12) describes GFR most accurately throughout the pediatric age-range as compared to data on inulin and mannitol clearance. GFR-based CL and dose

scaling for drugs eliminated through GFR yields reasonably accurate pediatric CL and dose values, despite ignoring the influence of maturational changes in protein binding, except for drugs highly bound to AGP in neonates.

4.7 Acknowledgement

CAJK received support from the Innovational Research Incentives Scheme (Vidi grant, June 2013) of the Dutch Organization for Scientific Research (NWO) for the submitted work. All authors declare that they have no conflicts of interest. The authors would like to thank Linda B.S. Aulin for performing the code review.

4.8 References

1. Dunne J, Rodriguez WJ, Murphy MD, Beasley BN, Burckart GJ, Filie JD, Lewis LL, Sachs HC, Sheridan PH, Starke P, Yao LP (2011) Extrapolation of Adult Data and Other Data in Pediatric Drug-Development Programs. *Pediatrics*. <https://doi.org/10.1542/peds.2010-3487>
2. Rubin MI, Bruck E, Rapoport M, Snively M, McKay H, Baumler a (1949) Maturation of Renal Function in Childhood: Clearance Studies. *J Clin Invest* 28:1144–62 . <https://doi.org/10.1172/JCI102149>
3. Coulthard MG (1985) Maturation of glomerular filtration in preterm and mature babies. *Early Hum Dev* 11:281–292 . [https://doi.org/10.1016/0378-3782\(85\)90082-9](https://doi.org/10.1016/0378-3782(85)90082-9)
4. Dean RFA, McCance RA (1947) Inulin, diodone, creatinine and urea clearances in newborn infants. *J Physiol* 431–439
5. Leake RD, Trygstad CW, Oh W (1976) Inulin clearance in the newborn infant: Relationship to gestational and postnatal age. *Pediatr Res* 10:759–762 . <https://doi.org/10.1203/00006450-197608000-00013>
6. OH W, OH MA, LIND J (1966) Renal Function and Blood Volume in Newborn Infant Related to Placental Transfusion. *Acta Paediatr* 55:197–210 . <https://doi.org/10.1111/j.1651-2227.1966.tb15226.x>
7. De Cock RFW, Allegaert K, Brussee JM, Sherwin CMT, Mulla H, De Hoog M, Van Den Anker JN, Danhof M, Knibbe C a J (2014) Simultaneous pharmacokinetic modeling of gentamicin, tobramycin and vancomycin clearance from neonates to adults: Towards a semi-physiological function for maturation in glomerular filtration. *Pharm Res* 31:2643–2654 . <https://doi.org/10.1007/s11095-014-1361-z>
8. McNamara PJ, Alcorn J (2002) Protein binding predictions in infants. *AAPS PharmSci* 4:E4 . <https://doi.org/10.1208/ps040104>
9. Edginton AN, Schmitt W, Willmann S (2006) Development and evaluation of a generic physiologically based pharmacokinetic model for children. *Clin Pharmacokinet*. <https://doi.org/10.2165/00003088-200645100-00005>
10. Krekels EHJ, Calvier EAM, van der Graaf PH, Knibbe CAJ (2019) Children Are Not Small Adults, but Can We Treat Them As Such? *CPT Pharmacometrics Syst Pharmacol*. <https://doi.org/10.1002/psp4.12366>
11. Calvier E, Krekels E, Valitalo P, Rostami-Hodjegan A, Tibboel D, Danhof M, Knibbe CAJ (2017) Allometric scaling of clearance in paediatrics: when does the magic of 0.75 fade? *Clin Pharmacokinet* 56:273–285 . <https://doi.org/doi:10.1007/s40262-016-0436-x>
12. Anderson BJ, Holford NHG (2009) Mechanistic basis of using body size and maturation to predict clearance in humans. *Drug Metab Pharmacokinet* 24:25–36 . <https://doi.org/10.2133/dmpk.24.25>
13. Mahmood I (2014) Dosing in children: A critical review of the pharmacokinetic allometric scaling and modelling approaches in paediatric drug development and clinical settings. *Clin Pharmacokinet* 53:327–346 . <https://doi.org/10.1007/s40262-014-0134-5>
14. Rhodin MM, Anderson BJ, Peters a. M, Coulthard MG, Wilkins B, Cole M, Chatelut E, Grubb A, Veal GJ, Keir MJ, Holford NHG (2009) Human renal function maturation: A quantitative description using

- weight and postmenstrual age. *Pediatr Nephrol* 24:67–76 . <https://doi.org/10.1007/s00467-008-0997-5>
15. Johnson TN, Rostami-Hodjegan A, Tucker GT (2006) Prediction of the clearance of eleven drugs and associated variability in neonates, infants and children. *Clin Pharmacokinet* 45:931–956 . <https://doi.org/10.2165/00003088-200645090-00005>
 16. Hayton WL (2000) Maturation and growth of renal function: dosing renally cleared drugs in children. *AAPS PharmSci* 2:E3 . <https://doi.org/10.1208/ps020103>
 17. Salem F, Johnson TN, Abduljalil K, Tucker GT, Rostami-Hodjegan A (2014) A re-evaluation and validation of ontogeny functions for cytochrome P450 1A2 and 3A4 based on in vivo data. *Clin Pharmacokinet*. <https://doi.org/10.1007/s40262-014-0140-7>
 18. National Health and Nutrition Examination Survey www.cdc.gov/growthcharts/index.htm
 19. Schwartz GJ, Furth SL (2007) Glomerular filtration rate measurement and estimation in chronic kidney disease. *Pediatr Nephrol*. <https://doi.org/10.1007/s00467-006-0358-1>
 20. Kiss K, Molnár M, Söndergaard S, Molnár G, Ricksten SE (2018) Mannitol clearance for the determination of glomerular filtration rate—a validation against clearance of 51Cr-EDTA. *Clin Physiol Funct Imaging*. <https://doi.org/10.1111/cpf.12374>
 21. Haycock GB, Schwartz GJ, Wisotsky DH (1978) Geometric method for measuring body surface area: A height-weight formula validated in infants, children, and adults. *J Pediatr*. [https://doi.org/10.1016/S0022-3476\(78\)80601-5](https://doi.org/10.1016/S0022-3476(78)80601-5)
 22. Du Bois D, Du Bois EF (1916) Clinical calorimetry: Tenth paper a formula to estimate the approximate surface area if height and weight be known. *Arch Intern Med*. <https://doi.org/10.1001/archinte.1916.00080130010002>
 23. Barnett BHL, Hare K, Mcnamara H (1948) MEASUREMENT OF GLOMERULAR FILTRATION RATE IN PREMATURE INFANTS-1 2 metabolism in young infants is derived almost renal mechanisms which we are attempting to de-. 691–699
 24. International Commission on Radiological Protection (1995) Basic anatomical and physiological data for use in radiological protection - Skeleton. *Ann ICRP* 32:1–277 . [https://doi.org/10.1016/S0146-6453\(03\)00002-2](https://doi.org/10.1016/S0146-6453(03)00002-2)
 25. Wang J, Kumar SS, Sherwin CM, Ward R, Baer G, Burckart GJ, Wang Y, Yao LP (2019) Renal Clearance in Newborns and Infants: Predictive Performance of Population-Based Modeling for Drug Development. *Clin Pharmacol Ther*. <https://doi.org/10.1002/cpt.1332>
 26. Krekels EHJ, Neely M, Panoilia E, Tibboel D, Capparelli E, Danhof M, Mirochnick M, Knibbe CAJ (2012) From pediatric covariate model to semiphysiological function for maturation: Part I-extrapolation of a covariate model from morphine to zidovudine. *CPT Pharmacometrics Syst Pharmacol*. <https://doi.org/10.1038/psp.2012.11>
 27. Calvier EAM, Krekels EHJ, Yu H, Väitalo PAJ, Johnson TN, Rostami-Hodjegan A, Tibboel Di, Van Der Graaf PH, Danhof M, Knibbe CAJ (2018) Drugs being eliminated via the same pathway will not always require similar pediatric dose adjustments. *CPT Pharmacometrics Syst Pharmacol*. <https://doi.org/10.1002/psp4.12273>

4.9 Supplementary material

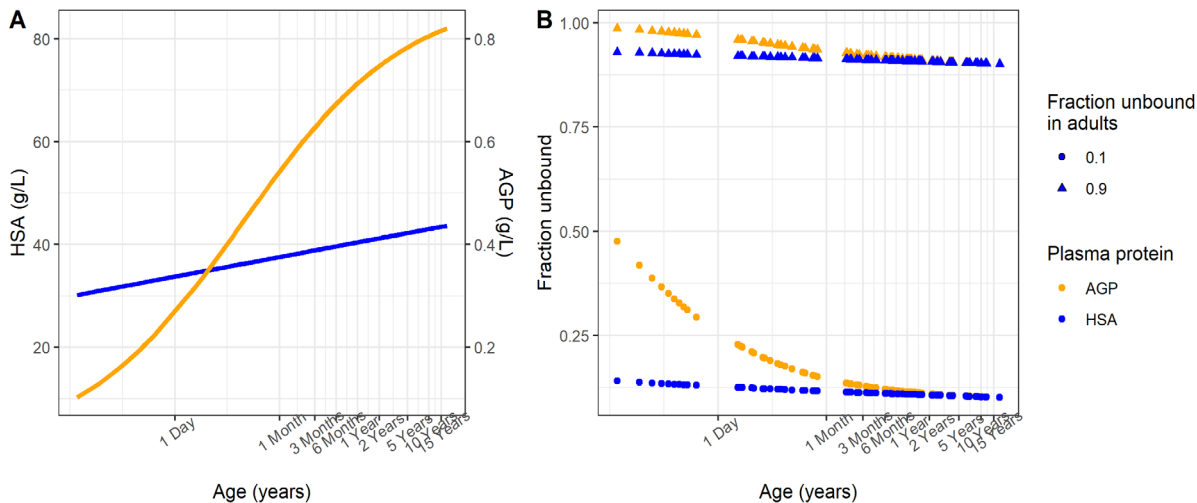


Figure S4.1 – Maturation profiles for plasma protein expression and plasma protein binding. Left panel (A) shows plasma concentrations of the plasma proteins human serum albumin (HSA) in blue and α -acid glycoprotein (AGP) in orange with age. Right panel (B) shows the changes in protein binding with age for each of the plasma proteins (AGP in orange, HSA in blue) when the fraction unbound measured in adults is either 0.1 (circles) and 0.9 (triangles).

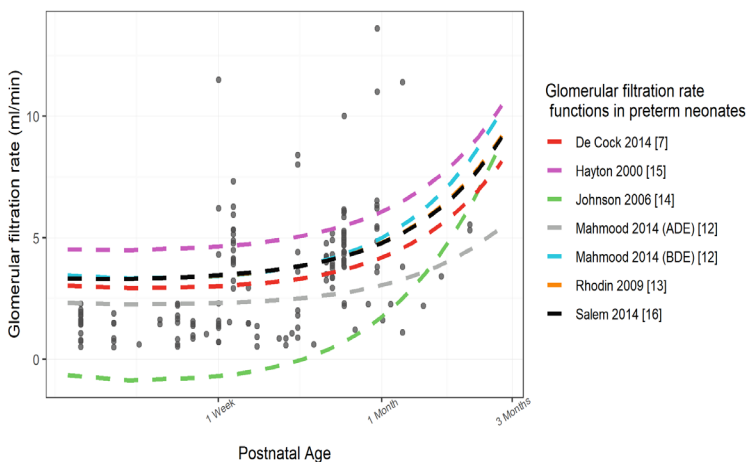


Figure S4.2 – GFR predictions using published maturation function [7, 12–16] for typical preterm neonates born at 35 weeks and a weight of 2330 g during the first 12 weeks of life [27] (dashed lines) overlaid with observed inulin clearance measurements collected from literature [3, 5, 22] (dots). Rhodin [13] and Salem [16] are overlapping.

weeks of life was used [27]. The demographics for the typical preterm neonate were selected as they most resembled the data collected from literature [3, 5, 22]. For the remaining three [13, 15, 16] GFR maturation functions that were not based on data from preterm neonates extrapolations were made. Furthermore, extrapolations were made for the functions used to characterize the maturation of plasma proteins concentrations and to obtain the unbound fractions in preterm neonates.

In Figure S4.2 we show the GFR predictions with the seven published functions for the typical preterm neonate overlaid with literature data collected for preterm neonates [3, 5, 22]. By using the demographics of the published data, we found that in preterm neonates, the prediction accuracy of the maturation function of Mahmood [12] had the lowest $\%RMSPE_{GFR}$ value of 37%, but it had a similar $\%PE_{GFR}$ range compared to Salem [16] and Rhodin [13] (Table S4.1).

Establishing the most accurate GFR maturation function in preterm neonates

As only four [7, 12, 14] of the published GFR maturation functions assessed in this manuscript were developed including data from preterm neonates and as maturation functions for physiological parameters in PBPK models are often not known in preterm neonates, the assessment of the accuracy of the published GFR maturation predictions in preterm neonates was performed separately. For this, a typical preterm neonate born at 35 weeks with a birthweight of 2330 g followed for the first 12

TaTable S4.1 – Root mean square percentage error (%RMSPE_{GFR}) and percentage prediction error% (%PE_{GFR}) ranges of the GFR predictions for preterm neonates, obtained with each of the studied GFR maturation functions.

Age groups	Salem 2014 [16]		Rhodin 2002 [13]		Hayton 2000 [15]		De Cock 2014 [7]		Johnson 2006 [14]		Mahmood 2016 (ADE) [12]		Mahmood 2016 (BDE) [12]	
	%RM-SPE _{GFR}	%PE _{GFR}	%RM-SPE _{GFR}	%PE _{GFR}	%RM-SPE _{GFR}	%PE _{GFR}	%RM-SPE _{GFR}	%PE _{GFR}	%RM-SPE _{GFR}	%PE _{GFR}	%RM-SPE _{GFR}	%PE _{GFR}	%RM-SPE _{GFR}	%PE _{GFR}
		[min-max]		[min-max]		[min-max]		[min-max]		[min-max]		[min-max]		[min-max]
Preterm	46	-72 26	45	-72 26	60	-56 299	42	-77 39	238	-1215 -73	41	-68 48	37	-78 28

4.10 Supplementary references

1. Johnson, T. N., Rostami-Hodjegan, A. & Tucker, G. T. Prediction of the clearance of eleven drugs and associated variability in neonates, infants and children. *Clin. Pharmacokinet.* 45, 931–956 (2006).
2. Mahmood, I. Dosing in children: A critical review of the pharmacokinetic allometric scaling and modelling approaches in paediatric drug development and clinical settings. *Clin. Pharmacokinet.* 53, 327–346 (2014).
3. De Cock, R. F. W. et al. Simultaneous pharmacokinetic modeling of gentamicin, tobramycin and vancomycin clearance from neonates to adults: Towards a semi-physiological function for maturation in glomerular filtration. *Pharm. Res.* 31, 2643–2654 (2014).
4. Anchieta, L. M., Xavier, C. C., Colosimo, E. A. & Souza, M. F. Weight of preterm newborns during the first twelve weeks of life. *Brazilian J. Med. Biol. Res.* (2003). doi:10.1590/S0100-879X2003000600012
5. Coulthard, M. G. Maturation of glomerular filtration in preterm and mature babies. *Early Hum. Dev.* 11, 281–292 (1985).
6. Barnett, B. H. L., Hare, K. & Mcnamara, H. MEASUREMENT OF GLOMERULAR FILTRATION RATE IN PREMATURE INFANTS-1 2 metabolism in young infants is derived almost renal mechanisms which we are attempting to de-. 691–699 (1948).
7. Leake, R. D., Trygstad, C. W. & Oh, W. Inulin clearance in the newborn infant: Relationship to gestational and postnatal age. *Pediatr. Res.* 10, 759–762 (1976).
8. Hayton, W. L. Maturation and growth of renal function: dosing renally cleared drugs in children. *AAPS PharmSci* 2, E3 (2000).
9. Rhodin, M. M. et al. Human renal function maturation: A quantitative description using weight and postmenstrual age. *Pediatr. Nephrol.* 24, 67–76 (2009).
10. Salem, F., Johnson, T. N., Abduljalil, K., Tucker, G. T. & Rostami-Hodjegan, A. A re-evaluation and validation of ontogeny functions for cytochrome P450 1A2 and 3A4 based on in vivo data. *Clin. Pharmacokinet.* (2014). doi:10.1007/s40262-014-0140-7

4.11 R code

```
# title: "Dose scaling using GFR maturation functions"
# author: "SC"
# date: "29 Apr 2019"
# output: data to be used with scripts:
# list of scripts to be added here
#'@abbrev: [GA - gestational age]
# =====

# set wd:
loc1 <- "1.Data/1.LitData/"
wd <- paste0(wd1, loc1)

# small function to read in all csv files:

data_name <- function(wd, file_name, ext = ".csv") {paste(wd,"\\", file_
name, ext, sep = "")}

# preterm datasets with comments:
# -----

# preterm female babies, healthy otherwise (?)
mydata1 <- read.csv(data_name(wd = wd, file_name = "Barnett 1948"), header
= T, sep=";", stringsAsFactors = F)
mydata1$status <- "preterm"

# preterm babies - healthy at the time of study

mydata5 <- read.csv(data_name(wd = wd, file_name = "Leak 1976"), sep=";",
header = T, stringsAsFactors = F)
mydata5$status <- "preterm"

# "healthy kidneys" babies datasets with comments:
# -----

mydata2 <- read.csv(data_name(wd = wd, file_name = "Coulthard 1975"),
header = T, sep=";", stringsAsFactors = F)
mydata2$status <- ifelse(mydata2$Gestation..wks. < 37, "preterm",
"healthy") # cut-off of 37 weeks for GA was used.

# term babies with meningo-myelocoeles with low life expectancy; postmortem
analysis of kidneys
# didn't reveal any renal impairment

mydata4 <- read.csv(data_name(wd = wd, file_name = "Dean 1947"), sep=";",
header = T, stringsAsFactors = F)
mydata4$status <- "healthy" # MM changed to healthy

# (near)term healthy neonates: 38-42 weeks of gestation;
mydata6 <- read.csv(data_name(wd = wd, file_name = "Oh 1966"), sep=";",
header = T, stringsAsFactors = F)
names(mydata6) <- as.character(mydata6[1,])
mydata6 <- mydata6[c(-1,-45),]
mydata6$status <- "healthy"

mydata7 <- read.csv(data_name(wd = wd, file_name = "Oh 1966-2"), sep=";",
header = T, stringsAsFactors = F)
mydata7$status <- "healthy"
```

```

# healthy babie, Rubin 1965:
# input by hand (not proud)

mydata8 <- data.frame(
  AGED = c(2,7,10,10,14,14,15,19,19,20,22,54,55,61,63,75,81,101,108,118,137
,138,181,190,216,223,225,229,232,268,275,314,356,371,374,395,417,456,517,51
7,532,547,578,578,782,821,912,912,943,1034,1368,1429,1521,2281,2311,2372,25
24,2554,3102,3284,3649,4197,4318,6569),
  AGEY = c(0.005,0.019,0.027,0.027,0.038,0.038,0.041,0.052,0.052,0.055,0.06
0,0.148,0.151,0.167,0.173,0.205,0.222,0.277,0.296,0.323,0.375,0.378,0.496,0
.521,0.592,0.611,0.616,0.627,0.636,0.734,0.753,0.860,0.975,1.016,1.025,1.08
3,1.141,1.250,1.416,1.416,1.458,1.500,1.583,1.583,2.141,2.250,2.499,2.499,2
.583,2.833,3.749,3.916,4.166,6.249,6.332,6.499,6.915,6.998,8.498,8.998,9.99
8,11.497,11.831,18),
  AGEM = c(0.066,0.230,0.329,0.329,0.460,0.460,0.493,0.625,0.625,0.658,0.72
3,1.776,1.809,2.006,2.072,2.466,2.664,3.321,3.551,3.880,4.505,4.538,5.952,6
.248,7.103,7.333,7.399,7.530,7.629,8.813,9.043,10.326,11.707,12.2,12.3,13,1
3.7,15,17,17,17.5,18,19,19,25.7,27,30,30,31,34,45,47,50,75,76,78,83,84,102,
108,120,138,142,216),
  PMA = c(40.286,41.000,41.429,41.429,42.000,42.000,42.143,42.714,42.714,42
.857,43.143,47.714,47.857,48.714,49.000,50.714,51.571,54.429,55.429,56.857,
59.571,59.714,65.857,67.143,70.857,71.857,72.143,72.714,73.143,78.286,79.28
6,84.857,90.857,93.000,93.435,96.476,99.517,105.164,113.853,113.853,116.025
,118.197,122.541,122.541,151.648,157.296,170.329,170.329,174.673,187.706,23
5.493,244.181,257.214,365.821,370.166,378.854,400.576,404.920,483.117,509.1
83,561.314,639.511,656.889,978.366),
  BWg = 1000 * c(2.4,3.35,3,3.2,2.7,3.8,3.7,2.8,3,3.1,3,3.75,3.5,5.3,4.3,5.
4,4.15,3.8,5.1,3.6,7.2,7.1,5,4.2,8,7.9,8.35,7.7,8,8.9,8.8,7.7,7.3,9.25,11,7
.5,9.6,6.5,10.5,11.4,9.5,13.6,10,13.2,10.3,10,10.6,11.8,15.5,17,17.8,13.6,1
6.7,25.9,19.5,18.9,20.9,22.7,28.9,24.9,25,20,35.3,70),
  BWkg = c(2.4,3.35,3,3.2,2.7,3.8,3.7,2.8,3,3.1,3,3.75,3.5,5.3,4.3,5.4,4.15
,3.8,5.1,3.6,7.2,7.1,5,4.2,8,7.9,8.35,7.7,8,8.9,8.8,7.7,7.3,9.25,11,7.5,9.6
,6.5,10.5,11.4,9.5,13.6,10,13.2,10.3,10,10.6,11.8,15.5,17,17.8,13.6,16.7,25
.9,19.5,18.9,20.9,22.7,28.9,24.9,25,20,35.3,70),
  BSA = c(0.208,0.231,0.212,0.224,0.2,0.251,0.242,0.205,0.214,0.222,0.208,0
.244,0.237,0.312,0.274,0.307,0.266,0.246,0.299,0.243,0.388,0.388,0.292,0.26
,0.423,0.421,0.436,0.413,0.423,0.459,0.452,0.413,0.399,0.467,0.524,0.405,0.
479,0.387,0.508,0.516,0.477,0.607,0.491,0.593,0.505,0.492,0.503,0.544,0.679
,0.69,0.737,0.606,0.67,0.94,0.83,0.67,0.87,0.9,1.035,0.96,0.99,0.8,1.24,1.8
3),
  GFR = c(5.16,6.28,6.44,7.51,5.32,5.37,7,7.23,6.93,4.11,6.61,11.8,8.9,11.4
,10.9,11,11.2,10.1,12.1,7,21.5,17.5,15.9,19.2,12.7,22.9,28.9,32,23.7,18.3,3
2.4,22.9,28.6,29.8,37.6,31.8,30.9,19.2,40.8,31.4,57.1,47.4,27.8,48.6,26.8,3
4.1,36.2,47.8,34.1,40.7,67.5,55.8,62.5,79.3,66.2,52.2,69.5,62.7,70.3,81.1,6
8.8,59.2,86,120)
)
mydata8$status <- "healthy"

# diseased datasets:
# -----

# dose was given in mg/kg and the children often needed 50-100% more of the
drug than the adults to achieve
# equivalent plasma concentrations; a higher clearance of amikacin in pro-
portion with BW
# dose based on BSA resulted in uniform requirements and predictable plasma
concentrations
# aplastic anemia; pelvic inflammatory disease; cystic fibrosis; acute lympho-
cytic leukemia; acute nonlymphatic
# leukemia; appendicitis; ovarian teratoma; wilms tumor;They also say that
the value they found was 20-25% higher

```

```

# than the value reported in adults

mydata9 <- read.csv(data_name(wd = wd, file_name = "Vogelstein 1977"),
  sep=";", header = T, stringsAsFactors = F)
mydata9$status <- "diseased"

# standardize datasets to merge into one:
# -----
# changes in mydata1:

mydata1$PMA.wk <- (mydata1$Age.days. / 7) + 33.4 # healthy preterm, based
on Table 1 of Anchieta et al. 2003, this assumption should be good.

# changes in mydata6:
# there are 168 hours in a week

mydata6$PMA.wk <- (as.numeric(mydata6$`Age (h)` ) / 168) + 38 # term GA = 38
weeks

#changes to mydata7
mydata7$PMA.wk <- (mydata7$Age..days./7) + 38 # term GA = 38 weeks

# merge datasets into one:
# -----
# OrID has the number of the dataset pasted in front of the original ID
# for mydataset1 made all of them factors and put 1 in front
# mydata2 and mydata3 were excluded because they produced negative clear-
ances or was data from older adults
# with decreased renal function

options(stringsAsFactors = FALSE)

all.data <- data.frame(
  OrID = c(paste("1", as.numeric(as.factor(mydata1$ID)), sep=""),
  paste("4", mydata4$ID, sep=""),
  paste("5", mydata5$study, sep=""), paste("6", mydata6$-
Case,sep=""), paste("7", mydata7$Case, sep=""),
  paste("9", mydata9$Patient.No., sep=""), paste("8", c(1:n-
row(mydata8)), sep="")),
  BW.g = c(mydata1$WT.g., mydata4$Weight, mydata5$WT.at.study..g., mydata-
6$`Birth wt (g)`, mydata7$Study.weight..g.,
  (mydata9$Weight..kg.*1000),mydata8$BWg),
  PMA.wk = c(mydata1$PMA.wk,mydata4$PMA..wks.,mydata5$PMA.wks.,mydata6$PMA.
wk,
  mydata7$PMA.wk,mydata9$PMA.with.assumed.38.weeks.of.gestation,
mydata8$PMA),
  AGE.y = c((mydata1$Age.days./365), (mydata4$AGE.days./365), (mydata-
5$weeks.at.study/52), (as.numeric(mydata6$`Age (h)`)/8760),
  (mydata7$Age..days./365), mydata9$Age.yrs., mydata8$AGEY),
  BSA = c(mydata1$BSA.sqm., mydata4$BSA, mydata5$Calc.BSA, mydata6$`BSA
(sqm)` , mydata7$BSA..sqm.,
  mydata9$BSA.sqm., mydata8$BSA),
  GFR = c(mydata1$CL.ml.min., mydata4$Inulin.clearance.ml.min, mydata5$Cin.
ml.min., mydata6$`Cin(ml/min)` ,
  mydata7$Cin.ml.min., mydata9$Inul.RC, mydata8$GFR),
  STATUS=c(mydata1$status, mydata4$status, mydata5$status, mydata6$status,
mydata7$status,
  mydata9$status, mydata8$status)
)

# Extra changes:
# -----

```

```

# mydata2
names(mydata2)<-c("ID", "GA.wk", "BrW.kg", "FPA", "PMA.wk", "GFR", "PW.kg", "SW.
kg", "status")
mydata2$AGE.y<-(mydata2$PMA.wk-mydata2$GA.wk)/52
mydata2$BW.g<-mydata2$PW.kg*1000
mydata2$BSA<-NA # made this change as BSA in this dataset returned negative
CL values for Johnson 2006

# added mydata2 to the whole dataset:

mydata2a<-mydata2[,c(1,11,5,10,12,6,9)]
names(mydata2a)<-names(all.data)
all.in<-rbind(all.data,mydata2a)
all.in$GFR<-as.numeric(all.in$GFR) # the observed GFR column made numeric
all.in$BW.g<-as.numeric(all.in$BW.g)
all.in$BSA<-as.numeric(all.in$BSA)
remove(list = c("mydata1", "mydata2", "mydata2a", "mydata4", "mydata5",
"mydata6", "mydata7", "mydata8", "mydata9", "all.data"))

# add data for the AUC, dose, cl at maintenance dose analysis:

# Generate typical demographics dataframe:
demo <- data.frame(
  lab = c("1 day", "1 Month", "3 Months", "6 Months", "9 Months", "1 Year",
"2 Years", "5 Years", "10 Years", "15 Years", "Adult"),
  age = c(1/365, 30/365, 0.25, 0.5, 0.75, 1, 2, 5, 10, 15, 35), # in years
  wt = c(3.45, 4.3, 5.75, 7.55, 8.9, 9.9, 12.35, 18.25, 32.5, 54.25, (73+60)/2),
# in kg
  kw = c(0.6, 0.7, 0.7, 0.7, 0.7, 0.7, 0.73, 0.65, 0.56, 0.51, 0.42)/100, # percen-
tege of body weight
  ht = c(49.75, 54.25, 60, 66, 70.75, 74.75, 86, 108.25, 138.25, 166, (163+176)/2),
# in cm; added to calculate the BSA needed for CO%
  mat = round(x = c(20.3, 14.9, 31.3, 46.5, 45.3, 44.2, 66.5, 73.7, 73.7,
73.7, 79.8)/79.8, digits = 3), # % of adult maximal capacity (assumption for
ages >1yr) De Voskin 2009
  hemat = c(56, 44, 35.5, 36, 36, 36, 36.5, 37, 40, 42, 44) / 100
# Hematocrite in percentage for each age (AGE), from Am Fam Physi-
cian. 2001 Oct 15;64(8):1379-86.Anemia in children.Irwin JJ
)
demo$bsa <- BSA(ht = demo$ht, age = demo$age, wt = demo$wt)
demo$wt.g <- demo$wt*1000

# end-of-script #

```



```

# title: "Dose scaling using GFR maturation functions"
# author: "SC"
# date: "29 Apr 2019"
# output: functions to be used with scripts:
#'@abbreviations: [bw - bodyweight][cl - clearance][bsa - body surface
area][bde/ade - bodyweight/age dependent exponent][pma - postmenstrual age]
#' [pe - prediction error][RMSE - root mean square error]
# =====

# 1. read in data from literature with Rmd
data_name <- function(wd, file_name, ext = ".csv") {paste(wd,"\\", file_name,
ext, sep = "")}

# GFR functions:
# -----

# all GFR predictions are in ml/min

# Roosmarijn de Cock 2014: RED
# normalized to bw of 4000 g

CL_RdC <- function(bw, cl4kg = 0.39) { # bw in g; vancomycin value;
  bde <- 2.23 * bw ^ (-0.065)
  cl <- cl4kg * (bw / 4000) ^ bde
  return(cl * 1000 / 60)
}

# 3. Mahmood BDE 2016: CYAN
# normalized to 70000 g; based on inulin clearance

CL_Mah_BDE <- function(bw) {
  bde <- 1.199 * (bw/1000) ^ (-0.157)
  cl <- 128 * (bw / 70000) ^ bde
  return(cl)
}

# 4. Mahmood ADE 2016:
CL_Mah_ADE_pre <- function(bw, age) cl <- 120 * (bw / 70000) ^ 1.15 #
function with exponent for preterm neonates

CL_Mah_ADE <- function(bw, age) {
  ade <- ifelse(age < 0.5 , 1,
               ifelse(age >= 0.5 & age <= 1, 0.9, 0.75))
  cl <- 120 * (bw / 70000) ^ ade
} # function with exponents for the term babies

# 5. Johnson 2006: GREEN

CL_J <- function(bsa) (-6.16 * bsa ^ 2) + (99.054 * bsa) - 17.74 # bsa in
m^2

# 6. Salem 2014: BLACK

CL_S <- function(bw, pma) { # bw in g; pma in weeks

  cl <- 112 * (((bw / 70000) ^ 0.632) * (pma ^ 3.3) / ((55.4 ^ 3.3) +
pma ^ 3.3))

  return(cl)
}

# 7. Rhodin 2009: ORANGE

```

```

CL_R <- function(bw, pma) { # bw in g; pma in weeks
  cl <- 121 * ((bw / 70000) ^ 0.75) * (pma ^ 3.4) / (47.7 ^ 3.4 + pma ^
3.4)
  return(cl)
}

# 8. Hayton 2000: MAGENTA

CL_H <- function(bw, age) { # bw in g; age in years
  age_mo <- age * 12 # age converted to months to use as input in funtion
  cl <- 2.6 * ((bw / 1000) ^ 0.662) * exp(-0.0822 * age_mo) + (8.14 * (bw
/ 1000) ^ 0.662) * (1 - exp(-0.0822 * age_mo))
  return(cl)
}

# Functions to calculate prediction errors:
# -----

# 10. PE% function:

pe <- function(a, b) { # a = prediction; b = observation; directly in %
  err <- 100 * (a - b) / b
  return(err)
}

# 11. RMSE:

rmse <- function(x) re <- sqrt(sum(x^2, na.rm = TRUE)/length(x[!is.na(x)]))

# Physiological maturation functions:
# -----

# 12. fraction unbound maturation functions:

# human serum albumin (HSA) (g/l): [Johnson 2006 - pg. 9 - eq. 5 & 7]

HSA <- function(age) {hsa <- 1.1287 * log(age * 365) + 33.746 ; return(h-
sa)}

fu_paed_hsa <- function(age_ad = 35, age, fu) {return(1 / (1 + (((1 - fu) *
HSA(age)) / (HSA(age_ad) * fu))))}

# alpha1-acid glycoprotein (AGP) (g/L): [Johnson 2006 - pg. 9 - eq. 6 & 7]

AAG <- function(age) {aag <- 0.887 * (age * 365) ^ 0.38 / ((8.89 ^ 0.38) +
(age * 365) ^ 0.38) ; return(aag)}

fu_paed_aag <- function(age_ad = 35, age, fu) {return(1 / (1 + (((1 - fu) *
AAG(age)) / (AAG(age_ad) * fu))))}

# Derive BSA for preterms and children of different ages:
# -----

# 13. BSA function:

BSA <- function(ht, age, wt) { # age in years
  haycock <- 0.024265 * ht ** 0.3964 * wt ** 0.5378
  dubois <- 0.007184 * ht ** 0.725 * wt ** 0.425

```

```

    return(ifelse(wt < 15, haycock, dubois)) # in m^2
    # for wt <15kg use Haycock et al. for children < or =15kg, else Dubois
    and Dubois
  }

# 14. BSA function for preterms

BSApre <- function(wt) # Furqan & Haque, 2009 m^2 (WT in kg)
{
  bsa <- (4 * wt + 7)/(90+wt) # m^2
  return(bsa)
}

# Functions for plots:

# 14. PE% plots :

pe_plot <- function(data, x, y, ylabel = "Your function name", col_name =
"black") {
  ggplot(data, aes_string(x = x, y = y))+
    geom_point(aes(shape = as.factor(STATUS)), col = col_name, size = 2) +
    scale_shape_discrete(solid = F)+
    scale_x_log10(breaks = c(0.0027, 0.08, 0.25, 0.5, 1, 2, 5, 15,
35),
                    labels = c("1 Day ", "1 Month ", "3 Months ", "6 Months
", "1 Year ", "2 Years ", "5 Years ", "15 Years ", "Adult "))+
    geom_hline(yintercept = c(-50, 0 , 50), linetype = c("solid", "dashed",
"solid"))+
    ylim(c(-100, 550))+
    ylab(paste("%PE", ylabel))+
    xlab("")+
    theme(axis.text.x = element_text(angle = 30, size = 10),
          axis.text.y = element_text(size = 14))+
    guides(shape = F)
}

```

```
#####
# Run-Time Environment:      R version 3.3.5
# Author:                   SC
# Project number:          1
# Short title:             GFR Dosing
# Purpose:                 Final figures & tables GFR dosing manuscript
#
# Date:                    2018-10-05
# Version:                 V.2.0
# Changes with prev.:      separate figures for dosing for AGP and HSA
# bound drugs
#####
# Remove all objects
rm(list=ls(all=TRUE))

# Load library
library(lattice)
library(stats)
library(ggplot2)
library(dplyr)
library(cowplot)
library(gridExtra)

# set ggplot white background theme:
theme_set(theme_bw())

# work dir
wd1 <- "D:/sinzi/work/GFR_manuscript/Code_review_Linda/"
setwd(wd1)

# call scripts with data and functions
# -----
loc0 <- "2.Rscripts/"

source(paste0(wd1, loc0, "SC01_GFR.PBPK_v08_Func.R")) # script to load
all functions
source(paste0(wd1, loc0, "SC01_GFR.PBPK_v08_Data.R")) # script to load
data from literature

loc0 <- "1.Data/2.GrowthCharts/"

source(paste0(wd1, loc0, "nhanes-dump.R")) # script with nhanes data from
literature

# growth charts data transformation:
# -----

# nhanes data transformations (only weight-age datasets used):

# combine datasets and get average weight between males and females from
birth till 20 yo
nhanes.wt.kg <- c(NHANES.LT.3ys[NHANES.LT.3ys$Ages<24&NHANES.
LT.3ys$Sex==1,4]/2+NHANES.LT.3ys[NHANES.LT.3ys$Ages<24&NHANES.LT.3ys$-
Sex==2,4]/2,
                 NHANES.GT.2ys[NHANES.GT.2ys$Sex==1,4]/2+NHANES.GT.2ys[N-
HANES.GT.2ys$Sex==2,4]/2)

# ages for the combined ds
nhanes.age.yrs <- c(NHANES.LT.3ys[NHANES.LT.3ys$Ages<24&NHANES.LT.3ys$-
Sex==1,2],NHANES.GT.2ys[NHANES.GT.2ys$Sex==1,2])/12

# format dataframe:
```

```

# -----

grow_data <- data.frame(
  typ_age = nhanes.age.yrs, # age in years
  typ_wt = nhanes.wt.kg * 1000, # wt in grams
  status = "healthy"
)

grow_data[grow_data$typ_age == 0,]$typ_age <- 1/365 # set min age to 1
day

# typical preterm neonates:
# -----

# preterm data from paper from Achieta2003 - typical ID with GA = 35 weeks:

preterm_35wks <- read.csv(file = paste0(wd1, loc0, "Preterms_GA_35wks.
csv"), header = FALSE) # age in days; wt in g
names(preterm_35wks) <- c("typ_age", "typ_wt") # change names
preterm_35wks$status <- "preterm"
preterm_35wks$typ_age <- preterm_35wks$typ_age/365 # age from days to
years

# split literature ds collection in "healthy" and "preterm"

all_preterm <- all.in[all.in$STATUS == "preterm",]
all.in <- all.in[all.in$STATUS == "healthy",]

# Figure 1: Qualitative assessment - GFR maturation profiles based on growth
charts data as input; no preterm
# -----
cols <- c("Hayton 2000 [15]"="#C95BBD", "Johnson 2006
[14]"="#6FC95B", "Mahmood 2014 (ADE) [12]"="#ADAFAD",
"Mahmood 2014 (BDE) [12]"="#2AC7DD", "Rhodin 2009 [13]" =
"#F98708", "De Cock 2014 [7]" = "#EA3027", "Salem 2014 [16]" = "#080808")
ggplot(data = grow_data)+
  geom_line(aes(x = typ_age, y = CL_H(bw = typ_wt, age = typ_age), col =
"Hayton 2000 [15]"), size = 1.25)+ # hayton (magenta)
  geom_line(aes(x = typ_age, y = CL_J(bsa = BSAPre(wt = typ_wt/1000)),
col = "Johnson 2006 [14]"), size = 1.25)+ #johnson 2006 (green)
  geom_line(aes(x = typ_age, y = CL_Mah_ADE(bw = typ_wt, age = typ_age),
col = "Mahmood 2014 (ADE) [12]"), size = 1.25)+ # mahmood 2016 ade (grey)
  geom_line(aes(x = typ_age, y = CL_Mah_BDE(bw = typ_wt), col = "Mahmood
2014 (BDE) [12]"), size = 1.25)+ # mahmood 2016 bde (cyan)
  geom_line(aes(x = typ_age, y = CL_R(bw = typ_wt, pma = (typ_age*52 +
40)), col = "Rhodin 2009 [13]"), size = 1.25)+ # rhodin 2005 (orange)
  geom_line(aes(x = typ_age, y = CL_RdC(bw = typ_wt, cl4kg = 0.39), col =
"De Cock 2014 [7]"), size = 1.25)+ # RdC 2012 (red)
  geom_line(aes(x = typ_age, y = CL_S(bw = typ_wt, pma = (typ_age*52 +
40)), col = "Salem 2014 [16]"), size = 1.25)+ # Salem 2015 (black)

  xlab("Age")+
  scale_colour_manual(name=" ", values=cols) +
  theme(axis.text.x = element_text(angle = 30, size = 8),
        axis.text.y = element_text(size = 8))+
  background_grid(major = "xy") -> base_plot1

base_plot1 +
  scale_y_continuous(breaks = c(2, 10, 50, 100, 150), limits= c(1, 160))+

```

```

    scale_x_continuous(breaks = c(0.0027, 1, 2, 5, 10, 15, 35),
                      labels = c("1 Day ", "1 Year ", "2 Years ", "5 Years
", "10 Years ", "15 Years ", "Adult ")) +
    ylab("Glomerular filtration rate (ml/min)") +
    theme(legend.position="none") -> gph1

    base_plot1 +
    scale_y_continuous(trans= "log10", breaks = c(2, 5, 10, 50, 100, 150),
limits= c(1, 200)) +
    scale_x_log10(breaks = c(0.0027, 0.08, 0.25, 0.5, 1, 2, 5, 10,
15, 35),
                      labels = c("1 Day ", "1 Month ", "3 Months ", "6 Months
", "1 Year ", "2 Years ", "5 Years ", "10 Years ", "15 Years ", "Adult ")) +
    ylab("") -> gph2

# save plot:

loc0 <- "3.Results/"

tiff(filename = paste0(wd1, loc0, "Figure_1_GFR_maturation.tiff"), width = 30,
height = 11.6, units = 'cm', res = 300)

plot_grid(gph1, gph2, labels = c('A', 'B'), nrow = 1, ncol = 2, rel_widths
= c(1, 1.5))

dev.off()

# Figure 2: Quantitative assessment - Prediction error between literature
data and the GFR functions predictions for each maturation function
# -----

all.in %>% mutate(pe = pe(a = CL_H(age = AGE.y, bw = BW.g), b = GFR)) %>%
  pe_plot(x = "AGE.y", y = "pe", ylabel = "Hayton 2000 [15]", col_name =
"#C95BBD") +
  background_grid(major = "xy") -> gg1

all.in %>% mutate(pe = pe(a = CL_RdC(bw = BW.g), b = GFR)) %>%
  pe_plot(x = "AGE.y", y = "pe", ylabel = "De Cock 2014 [7]", col_name =
"#EA3027") +
  background_grid(major = "xy") -> gg2

all.in %>% mutate(pe = pe(a = CL_J(bsa = BSA), b = GFR)) %>%
  pe_plot(x = "AGE.y", y = "pe", ylabel = "Johnson 2006 [14]", col_name =
"#6FC95B") +
  background_grid(major = "xy") -> gg3

all.in %>% mutate(pe = pe(a = CL_Mah_ADE(bw = BW.g, age = AGE.y), b = GFR))
%>%
  pe_plot(x = "AGE.y", y = "pe", ylabel = "Mahmood 2014 (ADE) [12]", col_
name = "#ADAFAD") +
  background_grid(major = "xy") -> gg4

all.in %>% mutate(pe = pe(a = CL_Mah_BDE(bw = BW.g), b = GFR)) %>%
  pe_plot(x = "AGE.y", y = "pe", ylabel = "Mahmood 2014 (BDE) [12]", col_
name = "#2AC7DD") +
  background_grid(major = "xy") -> gg5

all.in %>% mutate(pe = pe(a = CL_R(bw = BW.g, pma = PMA.wk), b = GFR)) %>%
  pe_plot(x = "AGE.y", y = "pe", ylabel = "Rhodin 2009 [13]", col_name =
"#F98708") +
  background_grid(major = "xy") -> gg6

```

```

all.in %>% mutate(pe = pe(a = CL_S(bw = BW.g, pma = PMA.wk), b = GFR)) %>%
  pe_plot(x = "AGE.y", y = "pe", ylabel = "Salem 2014 [16]", col_name =
"#080808")+
  background_grid(major = "xy")-> gg7

# save plot:
tiff(filename = paste0(wd1, loc0, "Figure_2_PE.tiff"), width = 30, height =
28, units = 'cm', res = 300)
plot_grid(gg1, gg2, gg3, gg4, gg5, gg6, gg7, labels = c('A', 'B', 'C', 'D',
'E', 'F', 'G'), nrow = 3, ncol = 3)
dev.off()

# Dosing based on the best GFR function (Salem et al. 2014)

# -----

# create the required dataset:

dose <- 100 # assume adult dose is 100 for direct output of %

demo_fu <- left_join(demo, expand_grid(age = demo$age, fu = seq(0.1, 1, by
= 0.1))) # add fraction unbound to all ages
demo_fu$fu_ped_hsa <- fu_paed_hsa(age = demo_fu$age, fu = demo_fu$fu) # fu
of HSA pediatric
demo_fu$fu_ped_agp <- fu_paed_aag(age = demo_fu$age, fu = demo_fu$fu) # fu
of AGP pediatric
demo_fu$gfr <- CL_S(bw = demo_fu$wt * 1000, pma = (demo_fu$age * 52 + 40))
# dosing is based on the GFR Salem 2015 function

# The adult demographics and dose
adult <- demo_fu %>% filter(age == 35) %>% select(fu, gfr)
names(adult) <- c("fu", "gfr_ad")
demo_fu_ext <- left_join(demo_fu, adult, by = "fu") # add this as a new
column to ease calculations

# dose scaled by PBPK clearance (based on GFR and fu maturation)
demo_fu_ext$dose_calc_hsa <- dose * (demo_fu_ext$gfr / demo_fu_ext$gfr_ad)
* (demo_fu_ext$fu_ped_hsa / demo_fu_ext$fu) # dose as % of adult dose
demo_fu_ext$dose_calc_agp <- dose * (demo_fu_ext$gfr / demo_fu_ext$gfr_ad)
* (demo_fu_ext$fu_ped_agp / demo_fu_ext$fu)

# save clearance values in dataframe:

demo_fu_ext$cl_adult <- demo_fu_ext$gfr_ad*demo_fu_ext$fu
demo_fu_ext$cl_ped_hsa <- demo_fu_ext$gfr*demo_fu_ext$fu_ped_hsa
demo_fu_ext$cl_ped_agp <- demo_fu_ext$gfr*demo_fu_ext$fu_ped_agp

# function to scale dose and clearance with AS0.75 and linear scaling

dose_ped <- function(dose_ad = 100, wt_ped, wt_ad, ex = 1) {
  ddose <- dose_ad * (wt_ped / wt_ad) ^ ex
  return(ddose)
} # dose scaling

# -----

cl_ped <- function(cl_ad = 120, wt_ped, wt_ad, ex = 1) {
  clped <- cl_ad * (wt_ped / wt_ad) ^ ex
  return(clped)
}

```

```

} # cl scaling

# add the doses calculated with the function above to the data frame
demo_fu_ext$dose_lin <- dose_ped(dose_ad = 100, wt_ped = demo_fu_ext$wt,
wt_ad = demo[demo$age == 35, "wt"], ex = 1)
demo_fu_ext$dose_as <- dose_ped(dose_ad = 100, wt_ped = demo_fu_ext$wt,
wt_ad = demo[demo$age == 35, "wt"], ex = 0.75)
demo_fu_ext$dose_r <- dose * (demo_fu_ext$gfr / demo_fu_ext$gfr_ad) #
dose based on GFR fraction

# add the scaled clearances to the data frame:

demo_fu_ext$cl_lin <- cl_ped(cl_ad = demo_fu_ext$cl_adult, wt_ped = demo_
fu_ext$wt, wt_ad = demo[demo$age == 35, "wt"], ex = 1)
demo_fu_ext$cl_as <- cl_ped(cl_ad = demo_fu_ext$cl_adult, wt_ped = demo_
fu_ext$wt, wt_ad = demo[demo$age == 35, "wt"], ex = 0.75)
demo_fu_ext$cl_gfr <- demo_fu_ext$cl_adult * (demo_fu_ext$gfr / demo_fu_
ext$gfr_ad) # dose based on GFR fraction

# Figure 3: Pediatric dose as a % of the adult dose.
# -----

# lines <- c("GFR scaling" = "solid", "Linear scaling" = "dotted", "Allo-
metric scaling" = "dashed")
col2 <- c("GFR scaling" = "#009E73", "Linear scaling" = "#E69F00", "Allo-
metric scaling" = "#FB0101")
base_plot2 <-
  demo_fu_ext %>%
  ggplot()+
  geom_line(aes(x = age, y = dose_r, col = "GFR scaling"), size = 1.2,
alpha = 0.55)+
  geom_line(aes(x = age, y = dose_lin, col = "Linear scaling"), size =
1.3)+
  geom_line(aes(x = age, y = dose_as, col = "Allometric scaling"), size =
1.2)+
  scale_y_continuous(breaks = c(0.1, 5, 10, 20, 30, 50, 80, 100), trans =
"log10")+
  xlab("Age")+
  background_grid(major = "xy")+
  guides(alpha = FALSE)+
  theme(plot.title = element_text(hjust = 0.5),
        axis.text.x = element_text(angle = 35))

base_plot2 +
  geom_point(aes(x = age, y = dose_calc_agp, alpha = factor(fu)), colour
= "#404040", shape = 19, fill = "#C0392B", size = 2.3)+
  ylab(" ") +
  theme(plot.title = element_text(hjust = 0.5))+
  scale_color_manual(name = " ", values = col2,
                     breaks = c("GFR scaling", "Linear scaling", "Al-
lometric scaling"))+
  scale_x_continuous(breaks = c(0.0027, 0.08, 0.25, 0.5, 1, 2, 5, 10, 15,
35),
                    trans = "log10",
                    labels = c("1 Day", "1 Month", "3 Months", "6
Months", "1 Year",
                             "2 Years", "5 Years", "10 Years", "15
Years", "Adult" ))+
  ggtitle("AGP bound drugs") -> gph_b

base_plot2 +

```



```

    geom_point(aes(x = age, y = dose_calc_hsa, alpha = factor(fu)), colour
= "#404040", shape = 19, fill = "#2B88C0", size = 2.3)+
    ylab("Dose (% of adult dose)")+
    ggtitle("HSA bound drugs")+
    theme(plot.title = element_text(hjust = 0.5))+
    scale_color_manual(name = " ", values = col2)+
    scale_x_continuous(breaks = c(0.0027, 0.08, 0.25, 0.5, 1, 2, 5, 10, 15,
35),
                      trans = "log10",
                      labels = c("1 Day", "1 Month", "3 Months", "6
Months", "1 Year",
                                "2 Years", "5 Years", "10 Years", "15
Years", "Adult" ))+
    theme(legend.position="none") -> gph_a

```

```

tiff(filename = paste0(wd1, loc0, "Figure_3_Pediatric_Dose.tiff"), width = 25,
height = 10, units = 'cm', res = 300)
plot_grid(gph_a, gph_b, nrow = 1, ncol = 2, rel_widths = c(1, 1.4))
dev.off()

```

```

# Figure 4_scaled CL: %PE PBPK clearance vs. scaled clearance.
# -----

col2 <- c("GFR scaling" = "#009E73", "Linear scaling" = "#E69F00", "Allo-
metric scaling" = "#FB0101")
demo_fu_ext %>% #mutate(err = pe()) %>%
  ggplot()+
  geom_hline(aes(yintercept = 0), linetype = "solid", col = "grey", size =
1)+
  geom_hline(aes(yintercept = -50), linetype = "dashed", col = "black",
size = 1)+
  geom_hline(aes(yintercept = 50), linetype = "dashed", col = "black", size
= 1)+
  geom_hline(aes(yintercept = -30), linetype = "dotted", col = "black",
size = 1)+
  geom_hline(aes(yintercept = 30), linetype = "dotted", col = "black", size
= 1)+
  #facet_grid(.~fu)+

  ylim(-60, 200)+
  xlab("AGE")+
  guides(alpha = F)+
  theme(axis.text.x = element_text(angle = 45, hjust = 1),
        plot.title = element_text(hjust = 0.5))+
  scale_color_manual(name = " ", values = col2,
                     breaks = c("GFR scaling", "Linear scaling", "Allomet-
ric scaling"))+
  background_grid(major = "y") -> basis_plot3

basis_plot3+
  geom_point(aes(x = age, y = pe(cl_gfr, cl_ped_hsa), alpha = factor(fu),
col = "GFR scaling"), size = 2.25)+
  geom_point(aes(x = age, y = pe(cl_lin, cl_ped_hsa), alpha = factor(fu),
col = "Linear scaling"), size = 2.25)+
  geom_point(aes(x = age, y = pe(cl_as, cl_ped_hsa), alpha = factor(fu),
col = "Allometric scaling"), size = 2.25)+
  ggtitle("HSA bound drugs")+
  scale_x_continuous(breaks = demo$age, labels = demo$lab, trans =
'log10')+
  theme(legend.position="none")+

```

```
scale_y_continuous(name = expression('% PE'['CL']), limits = c(-60, 200),
breaks = c(-50, -30, 0, 30, 50, 100, 150, 200)) -> gph6
```

```
basis_plot3+
  geom_point(aes(x = age, y = pe(cl_gfr, cl_ped_agp), alpha = factor(fu),
col = "GFR scaling"), size = 2.25)+
  geom_point(aes(x = age, y = pe(cl_lin, cl_ped_agp), alpha = factor(fu),
col = "Linear scaling"), size = 2.25)+
  geom_point(aes(x = age, y = pe(cl_as, cl_ped_agp), alpha = factor(fu),
col = "Allometric scaling"), size = 2.25)+
  scale_x_continuous(breaks = demo$age, labels = demo$lab, trans =
'log10')+
  scale_y_continuous(limits = c(-60, 200), breaks = c(-50, -30, 0, 30, 50,
100, 150, 200))+
  ylab(" ") +
  ggtitle("AGP bound drugs") -> gph7
```

```
tiff(filename = paste0(wd1, loc0, "Figure_4_PE_clearance_after_rev.tiff") ,
width = 25, height = 10, units = 'cm', res = 300)
plot_grid(gph6, gph7, nrow = 1, ncol = 2, rel_widths = c(1, 1.4))
dev.off()
```

```
## for the reviewer comments:
```

```
demo_fu_ext %>%
  ggplot()+
  geom_line(aes(x = age, y = cl_as, alpha = factor(fu), col = "Allometric
scaling", group = fu))+
  geom_point(aes(x = age, y = cl_ped_hsa, alpha = factor(fu), col = "GFR
scaling"))+
  geom_point(aes(x = age, y = cl_ped_agp, alpha = factor(fu), col = "Linear
scaling"))+
  scale_color_manual(name = " ", values = col2, breaks = c("GFR scaling",
"Linear scaling", "Allometric scaling"))+
  scale_x_continuous(breaks = demo$age, labels = demo$lab)#+
  # scale_y_continuous(trans = 'log10')
```

```
demo_fu_ext %>% filter(lab %in% c("1 day", "1 Month", "3 Months", "6
Months")) %>%
  ggplot()+
  geom_line(aes(x = age, y = cl_as, alpha = factor(fu), col = "Allometric
scaling", group = fu))+
  geom_point(aes(x = age, y = cl_ped_agp, alpha = factor(fu), col = "GFR
scaling"))+
  geom_point(aes(x = age, y = cl_ped_hsa, alpha = factor(fu), col = "Linear
scaling"))+
  scale_color_manual(name = " ", values = col2, breaks = c("GFR scaling",
"Linear scaling", "Allometric scaling"))+
  scale_x_continuous(breaks = demo$age[demo$lab %in% c("1 day", "1 Month",
"3 Months", "6 Months")], labels = demo$lab[demo$lab %in% c("1 day", "1
Month", "3 Months", "6 Months")], trans = 'log10')#+
  # scale_y_continuous(trans = 'log10')
```

```
# Table with first-dose recommendation based on GFR scaling, AS0.75 and lin-
ear scaling
# These tables are combined to make Table 2 for the paper.
```

```
demo_fu_ext %>% filter(fu %in% c(0.1)) %>% # results for fu = 0.1
  select(Age = lab, "Weight (kg)" = wt, "GFR (ml/min)" = gfr, "GFR ratio
dose" = dose_r, "Linear dose scaling" = dose_lin,
  "Allometric Scaled Dose" = dose_as, "CLR scaling HSA" = dose_calc_
hsa, "CLR scaling AGP" = dose_calc_agp,
```

```

"Unbound fraction HSA (pediatric)" = fu_ped_hsa, "Unbound fraction
AGP (pediatric)" = fu_ped_agp, "fu" = fu) -> tab2a
write.csv(x = tab2a, file = paste0(wd1, loc0, "Table_2a_dosing.csv"))

demo_fu_ext %>% filter(fu %in% c(0.9)) %>% # results for fu = 0.9
  select(Age = lab, "Weight (kg)" = wt, "GFR (ml/min)" = gfr, "GFR ratio
dose" = dose_r, "Linear dose scaling" = dose_lin,
  "Allometric Scaled Dose" = dose_as, "CLR scaling HSA" = dose_calc_
hsa, "CLR scaling AGP" = dose_calc_agp,
  "Unbound fraction HSA (pediatric)" = fu_ped_hsa, "Unbound fraction
AGP (pediatric)" = fu_ped_agp, "fu" = fu) -> tab2b

write.csv(x = tab2b, file = paste0(wd1, loc0, "Table_2b_dosing.csv"))

# Supplement Figure S1:
# -----
# the preterm predictions only on log scale.

ggplot()+
  geom_point(data = all_preterm, aes(x = AGE.y, y = GFR), col = "#4E4D4D",
alpha = 0.75)+
  geom_line(data = preterm_35wks[preterm_35wks$typ_age > 0.005,], aes(x =
typ_age, y = CL_H(bw = typ_wt, age = typ_age), col = "Hayton 2000 [15]"),
linetype = "dashed", size = 1.25)+ # hayton (magenta)
  geom_line(data = preterm_35wks[preterm_35wks$typ_age > 0.005,], aes(x
= typ_age, y = CL_J(bsa = BSAPre(wt = typ_wt/1000)), col = "Johnson 2006
[14]"), linetype = "dashed", size = 1.25)+ #johnson 2006 (green)
  geom_line(data = preterm_35wks[preterm_35wks$typ_age > 0.005,], aes(x =
typ_age, y = CL_Mah_ADE_pre(bw = typ_wt, age = typ_age), col = "Mahmood
2014 (ADE) [12]"), linetype = "dashed", size = 1.25)+ # mahmood 2016 ade
(grey)
  geom_line(data = preterm_35wks[preterm_35wks$typ_age > 0.005,], aes(x =
typ_age, y = CL_Mah_BDE(bw = typ_wt), col = "Mahmood 2014 (BDE) [12]"),
linetype = "dashed", size = 1.25)+ # mahmood 2016 bde (cyan)
  geom_line(data = preterm_35wks[preterm_35wks$typ_age > 0.005,], aes(x =
typ_age, y = CL_R(bw = typ_wt, pma = (typ_age * 52 + 40)), col = "Rhodin
2009 [13]"), linetype = "dashed", size = 1.25)+ # rhodin 2005 (orange)
  geom_line(data = preterm_35wks[preterm_35wks$typ_age > 0.005,], aes(x =
typ_age, y = CL_RdC(bw = typ_wt), col = "De Cock 2014 [7]"), linetype =
"dashed", size = 1.25)+ # RdC 2012 (red)
  geom_line(data = preterm_35wks[preterm_35wks$typ_age > 0.005,], aes(x =
typ_age, y = CL_S(bw = typ_wt, pma = (typ_age * 52 + 40)), col = "Salem
2014 [16]"), linetype = "dashed", size = 1.25)+ # Salem 2015 (black)
  scale_x_log10(breaks = c(0.0027, 7/365, 0.08, 0.25, 0.5, 1, 2, 5,
10, 15, 35),
  labels = c("1 Day ", "1 Week", "1 Month ", "3 Months ", "6
Months ", "1 Year ", "2 Years ", "5 Years ", "10 Years ", "15 Years ",
"Adult "))+
  # scale_y_log10(limits = c(0.5,150))+
  xlab("Postnatal Age")+
  ylab("Glomerular filtration rate (ml/min)")+
  theme(axis.text.x = element_text(angle = 30, size = 7))+
  background_grid(major = "xy")+
  scale_colour_manual(name="Glomerular filtration rate\n functions in pre-
term neonates", values=cols) -> gph2_preterm

tiff(filename = paste0(wd1, loc0, "Figure_S1_GFR_functions_preterm.tiff"),
width = 20, height = 10, units = 'cm', res = 300)
plot_grid(gph2_preterm, nrow = 1, ncol = 1)
dev.off()

```

```

# Figure with the fraction unbound and hsa/agp:
col3 <- c("HSA" = "blue", "AGP" = "orange")
ggplot(all.in)+
  geom_line(aes(x= AGE.y, y = HSA(age = AGE.y), col = "HSA"), size = 1.3)+
  geom_line(aes(x= AGE.y, y = AAG(age = AGE.y)*100, col = "AGP"), size =
1.3)+
  scale_x_continuous(trans = 'log10', name = "Age (years)",
                      breaks = c(0.0027, 0.08, 0.25, 0.5, 1, 2, 5, 10,
15, 35),
                      labels = c("1 Day ", "1 Month ", "3 Months ", "6
Months ", "1 Year ", "2 Years ", "5 Years ", "10 Years ", "15 Years ",
"Adult "))+
  scale_y_continuous(sec.axis = sec_axis(~ . / 100, name = "AGP (g/L)"),
name = "HSA (g/L)")+
  scale_color_manual(values = col3, name = "Plasma protein")+
  theme(axis.text.x = element_text(angle = 35))+
  guides(col = FALSE) -> s2a

shapel <- c("0.1" = 21, "0.9" = 24)
ggplot(all.in)+
  geom_point(aes(x= AGE.y, y = fu_paed_aag(age = AGE.y, fu = 0.1), shape =
"0.1", col = "AGP"), fill = "orange")+
  geom_point(aes(x= AGE.y, y = fu_paed_aag(age = AGE.y, fu = 0.9), shape =
"0.9", col = "AGP"), fill = "orange")+
  geom_point(aes(x= AGE.y, y = fu_paed_hsa(age = AGE.y, fu = 0.1), col =
"HSA", shape = "0.1"), fill = "blue")+
  geom_point(aes(x= AGE.y, y = fu_paed_hsa(age = AGE.y, fu = 0.9), col =
"HSA", shape = "0.9"), fill = "blue")+
  scale_x_continuous(trans = 'log10', name = "Age (years)",
                      breaks = c(0.0027, 0.08, 0.25, 0.5, 1, 2, 5, 10,
15, 35),
                      labels = c("1 Day ", "1 Month ", "3 Months ", "6
Months ", "1 Year ", "2 Years ", "5 Years ", "10 Years ", "15 Years ",
"Adult "))+
  scale_y_continuous(name = "Fraction unbound")+
  scale_color_manual(values = col3, name = "Plasma protein")+
  scale_shape_manual(values = shapel, name = "Fraction unbound\nin
adults")+
  theme(axis.text.x = element_text(angle = 35)) -> s2b

tiff(filename = paste0(wd1, loc0, "Figure_S2_Prot_bind_and_prot_mat.tiff"),
width = 25, height = 10, units = 'cm', res = 300)
plot_grid(s2a, s2b, labels = c('A', 'B'), nrow = 1, ncol = 2, rel_widths =
c(1, 1.3))
dev.off()

```


Section IV. Ontogeny of renal transporters and its impact on drug renal clearance in children



The influence of drug properties and ontogeny of transporters on pediatric renal clearance through glomerular filtration and active secretion - a simulation-based study

S Cristea, EHJ Krekels, A Rostami-Hodjegan, K Allegaert, CAJ Knibbe

AAPS J 22, 87 (2020).

Epub ahead of print, doi.org/10.1208/s12248-020-00468-7

5.1 Abstract

Glomerular filtration (GF) and active tubular secretion (ATS) contribute to renal drug elimination, with the latter remaining understudied across the pediatric age-range. Therefore, we systematically analyzed the influence of transporter ontogeny on the relative contribution of GF and ATS to renal clearance CL_R for drugs with different properties in children.

A physiology-based model for CL_R in adults was extrapolated to the pediatric population by including maturation functions for the system-specific parameters. This model was used to predict GF and ATS for hypothetical drugs with a range of drug-specific properties, including transporter-mediated intrinsic clearance ($CL_{int,T}$) values, that are substrates for renal secretion transporters with different ontogeny patterns. To assess the impact of transporter ontogeny on ATS and total CL_R , a percentage prediction difference (%PD) was calculated between the predicted CL_R in the presence and absence of transporter ontogeny.

The contribution of ATS to CL_R ranges between 41% and 90% in children depending on fraction unbound and $CL_{int,T}$ values. If ontogeny of renal transporters is <0.2 of adult values, CL_R predictions are unacceptable (%PD $> 50\%$) for the majority of drugs regardless of the pediatric age. Ignoring ontogeny patterns of secretion transporters increasing with age in children younger than 2 years results in CL_R predictions that are not systematically acceptable for all hypothetical drugs (%PD $> 50\%$ for some drugs).

This analysis identified for what drug-specific properties and at what ages the contribution of ATS on total pediatric CL_R cannot be ignored. Drugs with these properties may be sensitive in vivo probes to investigate transporter ontogeny.

5.2 Introduction

Between 21% and 31% of marketed drugs are primarily renally cleared [1]. Processes underlying renal clearance (CL_R) include glomerular filtration (GF), active tubular secretion (ATS), reabsorption and renal metabolism. Maturation of GF has been extensively studied and quantified in children. However, less is known about the impact of maturation in the other process on CL_R , partly due to the lack of specific biomarkers to distinguish between the activity of different transporters and to the overlap in specificity of transporters for different substrates. Together with GF, ATS is one of the major contributing pathways for CL_R , ontogeny of ATS is therefore the focus of the current analysis.

ATS involves different transporter systems located on the basolateral and apical sides of the proximal tubule cells of the kidney. These systems enable the efflux of drugs from the blood into the tubule where pre-urine is formed [2]. The expression of renal transporters was found to change in children [3]. However, these findings are based on a limited number of postmortem kidney samples collected throughout the pediatric age-range [3]. Furthermore, there is limited information about the relationship between transporter-specific protein expression and transporter activity [4] or whether this remains constant with age. Finally, the extent to which transporter activity impacts ATS and subsequently total CL_R has not been quantified yet for the pediatric population.

Physiology-based pharmacokinetic (PBPK) models [5] integrate prior knowledge on drug- and system-properties. This configuration can be leveraged to perform extrapolations to unstudied scenarios. For example, PBPK models can be back-extrapolated to the pediatric population by taking into account the developmental changes in system-parameters and be further used to make predictions in this special population for drugs that have not been studied in children yet. Previously, our group has used PBPK approaches in an innovative manner to systematically assess in which situations empirical scaling methods (i.e. allometric scaling, linear scaling) could be used to accurately scale plasma clearance of drugs that were eliminated by hepatic metabolism or GF for a broad range of hypothetical drugs [6,7]. However, due to limited information on the ontogeny of renal transporters, the accuracy of clearance

scaling for drugs eliminated through ATS could not be addressed.

Using a similar PBPK-based modelling approach as the one described above, we performed a systematic analysis to investigate the impact of the ontogeny of renal secretion transporters in relation with maturation of other physiological processes on the relative contribution of GF and ATS to CL_R as well as on the total CL_R. This assessment was performed throughout the pediatric age-range for a large number of hypothetical drugs with different properties covering a realistic parameter space. Moreover, to assess the impact of renal transporter ontogeny on CL_R throughout the pediatric population, we compared CL_R predictions obtained with and without including ontogeny patterns for renal transporters.

5.3 Methods

5.3.1 Expansion of a PBPK framework to predict CL_R in children

For this simulation study, a PBPK-based framework was developed analogue to the one published by Calvier et al. for plasma clearance by liver metabolism and GF [6]. R v3.5.0 under R studio 1.1.38 was used to build the framework and to perform the systematic simulations.

An existing PBPK model for predicting CL_R in adults [5] was extrapolated to the pediatric population by incorporating published maturation functions for the system-specific parameters in the model. The model assumes a serial arrangement of the two major contributing pathways, GF and ATS (equation 1).

$$CL_R = CL_{GF} + CL_{ATS} = f_u \times GFR + \frac{(Q_R - GFR) \times f_u \times CL_{int,sec}}{Q_R + f_u \times \frac{CL_{int,sec}}{BP}} \quad [1]$$

where CL_{GF} and CL_{ATS} represent the clearance by GF and ATS, respectively and f_u is the fraction unbound, GFR is the glomerular filtration rate, Q_R is renal blood flow, BP is the blood to plasma ratio of the drug, and $CL_{int,sec}$ is the intrinsic secretion clearance of the active transporters. This model assumes that only the unbound drug in plasma is available for elimination whereas drugs bound to plasma proteins or accumulated in erythrocytes are considered unavailable for elimination.

Maturation functions from literature were included for plasma concentrations of human serum albumin (HSA) and α -acid glycoprotein (AGP) [8], GFR [9], Q_R [10], hematocrit [10], kidney weight [10], and relative ontogeny for transporter-mediated intrinsic clearance (ont_T). The functions for ont_T described either hypothetical values, or published functions for individual [3] or aggregated [11,12] transporter systems.

The concentrations of the two plasma proteins impact the f_u of the drug in plasma and the hematocrit levels impact BP. $CL_{int,sec}$ was obtained as the product of transporter-mediated intrinsic clearance ($CL_{int,T}$), ont_T , the number of proximal tubule cells per gram kidney (PTCPGK), and kidney weight (KW), as shown in equation [2].

$$CL_{int,sec} = CL_{int,T} \times ont_T \times PTCPGK \times KW \quad [2]$$

$CL_{int,T}$ is the resultant of expression and activity of renal secretion transporters. While maturation functions for KW and ont_T were included in the pediatric PBPK model for CL_R, the number of proximal tubule cells per gram kidney was assumed to have the same value in children as in adults (60×10^6 cells), as no information was available about its development. KW (g) was calculated across the pediatric age by multiplying the kidney volume (L) with a kidney density of 1050 g/L as obtained from Simcyp v18. All maturation functions and parameter values on which the PBPK model for CL_R is dependent, can be found in Table 5.1. These maturation functions are depicted in Figure 5.1A.

ont_T was included in equation [2] as a fraction relative to the adult $CL_{int,T}$. In this way, pediatric $CL_{int,T}$: (1) remained fixed at the adult $CL_{int,T}$ levels ($ont_T = 1$, meaning ontogeny is absent), (2) was a constant fraction of the adult $CL_{int,T}$ throughout the entire pediatric age-range, or (3) increased with age as flexible fraction of adult $CL_{int,T}$ according to published ontogeny functions [3]. For the relative ontogeny fractions

that remained constant throughout the pediatric age, the following values were used: 0.05, 0.2, 0.5, 0.7. Ontogeny functions that increased with age were taken from literature, including 4 functions for individual transporters [3] (i.e. OAT1, OAT3, OCT2, and Pgp), and 2 functions for aggregated transporter systems [11,12]. All the relative ontogeny functions for $CL_{int,T}$ that increased with age and the details about their implementation in the model are presented in Table 5.1. In addition, the published ontogeny functions that characterize relative ontogeny for individual (i.e. OAT1, OAT3, OCT2, and Pgp) and aggregated (i.e. Hayton et al., DeWoskin et al.) transporters throughout the pediatric population relative to adult values, are visualized in Figure 5.1B.

The pediatric PBPK-based model was used to predict CL_R in typical virtual individuals. For this, patients with the following ages were selected: 1 day, 1, 3, and 6 months, 1, 2, 5, and 15 years for pediatric

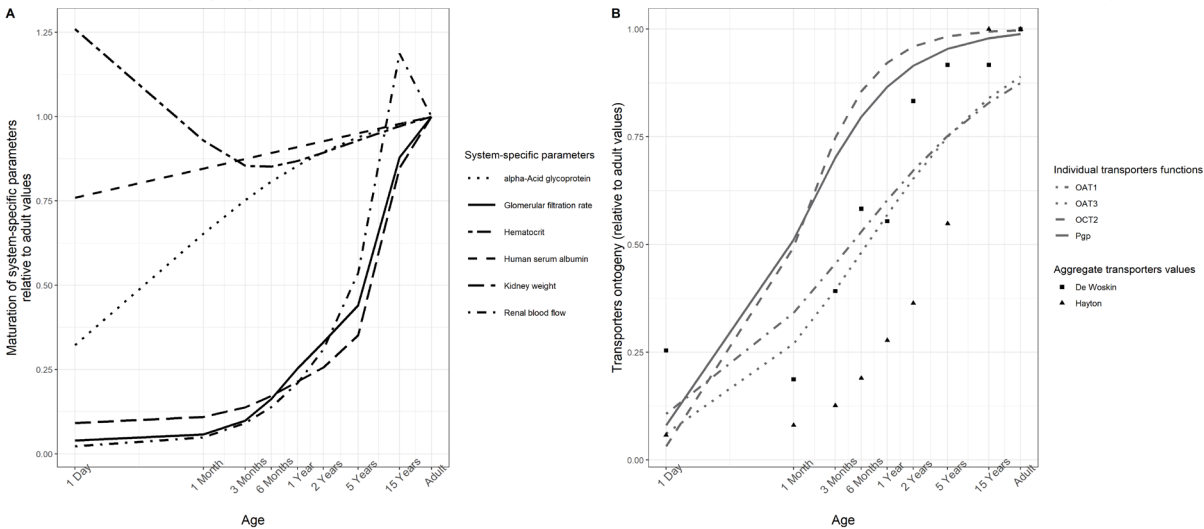


Figure 5.1 – Published functions illustrating (A) the maturation of system-specific parameters and (B) age-dependent ontogeny functions (ontT) for individual or aggregated transporter systems used with the transporter-mediated intrinsic clearance ($CL_{int,T}$) to obtain intrinsic secretion clearance ($CL_{int,sec}$). These functions were used to extend the PBPK model to the pediatric population according to the functions in Table 1.

individuals, and 35 years for the adult. The demographics for the typical pediatric individuals required to obtain the maturation functions in the PBPK-based model were derived from the NHANES database [13] and the ones for the typical adult were derived from the ICRP annals [14]. The demographic characteristics corresponding to these ages are given in Table 5.2.

For a systematic investigation of the drug-specific parameter space, hypothetical drugs with different properties were generated and their CL_R was predicted with the PBPK model for CL_R for all typical individuals. The hypothetical drugs were defined by four drug-specific properties for which ranges of realistic values were used as follows:

- The drugs were assumed to bind exclusively to either HSA or AGP.
- $f_{u,adult}$ values of 0.05, 0.15, 0.25, 0.35, 0.45, 0.55, 0.65, 0.75, 0.85, 0.95 and 1 were used for drugs binding to either HSA or AGP.
- BP was obtained from hematocrit levels and Kp values in adults of 0, 1, 2, 3 and 4 (Table 5.1) [15].
- For $CL_{int,T}$ 39 representative values were sampled within the range of 2 and 500 ml/min/mg protein.

The selected range was based on $CL_{int,T}$ values obtained from published CL_R values in adults following retrograde calculation for 53 drugs that are renally excreted by ATS. The obtained $CL_{int,T}$ represents the affinity of the drug for different transporters together with the abundances of transporters. Details about the retrograde calculation of $CL_{int,T}$ are shown in the Supplement section S5.1: Retrograde-calculation of $CL_{int,T}$ from adult CL_R values and the obtained $CL_{int,T}$ values for these drugs in adults are displayed in Figure S5.1.

Table 5.1 – Maturation functions used in equations [1] and [2] for the extrapolation of system-specific and combined system-specific and drug-specific model parameters in the physiology-based pharmacokinetic (PBPK) model for renal clearance from typical adults to typical pediatric individuals

System-specific parameters for equations [1] and [2] (abbreviation) [units]	Maturation functions included in the pediatric PBPK model for CL _R	
Glomerular filtration rate (GFR) [ml/min]	$GFR = 112 \times \left(\frac{WT}{70}\right)^{0.63} \times \left(\frac{PMA^{3.3}}{PMA^{3.3} + 55.4^{3.3}}\right)$	
Fraction unbound (fu) [-]	$[HSA]_{ped/adult} = 1.1287 \times \ln(AGE) + 33.746$ $[AGP]_{ped/adult} = \frac{0.887 \times AGE^{0.38}}{8.89^{0.38} + AGE^{0.38}}$ $\rightarrow f_{u,ped} = \frac{1}{1 + \frac{(1 - f_{u,adult}) \times [P]_{ped}}{[P]_{adult} \times f_{u,adult}}}$	
Renal blood flow (QR) [ml/min]	$CO = BSA \times (110 + 184 \times e^{-0.0378 \times AGE} - e^{-0.24477 \times AGE})$ $fr = \frac{fr_{males} + fr_{females}}{2}$ $fr_{males} = 4.53 + \left(14.63 \times \frac{AGE}{0.1888 + AGE}\right)$ $fr_{females} = 4.53 + \left(13 \times \frac{AGE^{1.15}}{0.188^{1.15} + AGE^{1.15}}\right)$ $\rightarrow QR = CO \times fr$	
Intrinsic secretion CL (CL _{int,sec}) [mL/min]	$PTCPGK = 60 \text{ (adult value)}$ $KW = 1050 \times (4.214 \times WT^{0.823} + 4.456 \times WT^{0.795})/1000$ $\rightarrow CL_{int,sec} = ont_T \times CL_{int,T} \times PTCPGK \times KW$	
Blood to plasma ratio (BP) [-]	$hemat = \frac{hemat_{male} + hemat_{female}}{2}$ $hemat_{male} = 53 - \left(43 \times \frac{AGE^{1.12}}{0.05^{1.12} + AGE^{1.12}}\right) \times \left(1 + \left(-0.93 \times \frac{AGE^{0.25}}{0.10^{0.25} + AGE^{0.25}}\right)\right)$ $hemat_{female} = 53 - \left(37.4 \times \frac{AGE^{1.12}}{0.05^{1.12} + AGE^{1.12}}\right) \times \left(1 + \left(-0.80 \times \frac{AGE^{0.25}}{0.10^{0.25} + AGE^{0.25}}\right)\right)$ $\rightarrow BP = 1 + hemat \times (f_u \times k_p - 1)$	
Published ontogeny functions for renal transporters (ont _T) [-]	$ont_{P-gp} = \frac{PNA^{0.73}}{PNA^{0.73} + 4.02^{0.73}}$ $ont_{OAT_1} = \frac{PNA^{0.43}}{PNA^{0.43} + 19.71^{0.43}}$ $ont_{OAT_3} = \frac{PNA^{0.51}}{PNA^{0.51} + 30.70^{0.51}}$ $ont_{OCT_2} = \frac{PNA^1}{PNA^1 + 4.38^{0.51}}$ $* ont_{ATSHayton} = \frac{(1.08 \times weight^{1.04} \times e^{-0.185 \times age} + 1.83 \times weight^{1.04} \times (1 - e^{-0.185 \times age}))}{ont_{ATSHayton}^{(adult)}}$ $* ont_{ATSDewoskin} = \frac{20.3}{79.8'} \frac{14.9}{79.8'} \frac{31.3}{79.8'} \frac{46.5}{79.8'} \frac{44.2}{79.8'} \frac{66.5}{79.8'} \frac{73.15}{79.8'} \frac{73.15}{79.8'} \frac{79.8}{79.8'}, \text{ at 1 Day, 1 Month, 3 Months, 6 Months, 1 Year, 2 Years, 5 Years, 15 Years, and Adult, respectively}$	
WT – bodyweight [kg] PMA – postmenstrual age [weeks] HSA – human serum albumin [g/L] AGP – α-acid glycoprotein [g/L] [P] – plasma binding protein (e.g. HSA or AGP [g/L]) CO – cardiac output [mL/min] hemat – hematocrit fr – fraction of cardiac output directed to renal artery BSA – body surface area (m2)		AGE – age in [days] for the maturation of [P] and in [years] for the fraction of cardiac output and hematocrit levels PTCPGK – proximal tubule cells per gram kidney [x 106 cells] KW – kidney weight [g] ont _T – transporters ontogeny relative to adult levels [-] CL _{int,T} – transporter-mediated active clearance [ml/min] k _p – blood-to-plasma partitioning coefficient of a drug PNA-postnatal age [weeks]
*Hayton et al. developed a continuous function using age in years and weight in kg, based on the data published by Rubin et al. [17]. The function covers the pediatric age-range up to 12 years and values obtained at 12 years were considered mature and assigned to the typical 15-year-old and adult (ont _{ATSHayton(adult)}). *DeWoskin et al. collected literature data on tubular secretion rates and categorized it in different age groups, from neonates up to adults. For children older than 1 year and younger than 18 years, the average between the values published for children and adults was interpolated.		

Table 5.2 – Demographics of the typical virtual pediatric individuals¹³ and adult¹⁴ included in this analysis.

Age	Height	Weight	Hematocrit	Body Surface Area
	(cm)	(kg)	(%)	(m ²)
1 Day	49.75	3.5	56	0.22
1 Month	54.25	4.3	44	0.25
3 Months	60	5.75	35.5	0.31
6 Months	66	7.55	36	0.37
1 Year	74.75	9.9	36	0.46
2 Years	86	12.35	36.5	0.54
5 Years	108.25	18.25	37	0.73
15 Years	166	54.25	42	1.59
Adult	169.5	66.5	44	1.76

Generating all possible combinations between the values given to the four drug properties yielded 3800 hypothetical drugs that were included in the current systematic analysis.

5.3.2 Contribution of GF and ATS to pediatric CL_R for drugs with different properties

The PBPK-framework was used to simulate CL_R for the 3800 hypothetical drugs for each typical virtual individual. Simulations with a relative ontogeny fixed at adult levels ($ont_T = 1$) were used to assess the impact of drug-specific properties on CL_R in the absence of transporter ontogeny. For each drug, the relative contribution of GFR and ATS to CL_R was determined according to equations [3a] and [3b], respectively.

$$GFR_{contribution} \% = \frac{CL_{GFR}}{CL_R} \times 100 \quad [3a]$$

$$ATS_{contribution} \% = \frac{CL_{ATS}}{CL_R} \times 100 \quad [3b]$$

5.3.3 Influence of renal transporters ontogeny on pediatric CL_R

To assess the influence of ontogeny of kidney transporters on pediatric CL_R we implemented transporter ontogeny fractions relative to adult values in the pediatric PBPK model for CL_R (equations [1] and [2]) such that ontogeny of $CL_{int,T}$: (1) remained fixed at adult levels, (2) was a constant fraction of adult values throughout the pediatric age-range, or (3) increased with age as a flexible fraction of adult values. The use of these implementations to describe the ontogeny of transporters, enabled us to explore different values and patterns for transporter ontogeny to ultimately quantify the impact of these changes on ATS and CL_R throughout the pediatric age-range. To quantify the influence of transporter ontogeny on pediatric CL_R predictions, a percentage prediction difference (%PD) was calculated between CL_R predictions without ontogeny ($CL_{R,adult,ont_T}$) (i.e. $ont_T = 1$) and CL_R predictions with transporter ontogeny that either remained constant or increased with age ($CL_{R,pediatric,ont_T}$) according to equation [4].

$$\%PD = \frac{CL_{R,adult,ont_T} - CL_{R,pediatric,ont_T}}{CL_{R,pediatric,ont_T}} \times 100 \quad [4]$$

The %PD obtained upon ignoring the ontogeny of kidney transporters was classified as leading to acceptable CL_R predictions for %PD below 30%, reasonably acceptable CL_R predictions for %PD between 30% and 50%, and unacceptable CL_R predictions for %PD above 50%. As published transporters ontogeny patterns only increase with age (i.e. ont_T is always between 0 and 1) until they reach adult $CL_{int,T}$ levels (i.e. $ont_T = 1$), the %PD will always be positive.

In addition, %PD was used to assess the systematic accuracy of CL_R predictions obtained while ignoring transporter ontogeny. CL_R at a certain age would have systematically acceptable predictions for a transporter pathway when the maximum %PD value for all 3800 hypothetical drugs at that pediatric age was below 30%. In this case, ontogeny of transporters was expected to have a limited role in predicting CL_R for any drug at that age. When CL_R predictions obtained in the absence of transporter ontogeny were reasonably acceptable or unacceptable for one or more hypothetical drugs, CL_R predictions were no longer considered systematically acceptable. In this case CL_R predictions might still be acceptable for some of the hypothetical drugs however it cannot be known a priori whether CL_R predictions are acceptable or not for individual drugs, without taking drug properties into account. As such, systematically acceptable scenarios were a means to identify the pediatric ages for which the ontogeny of individual or aggregated transporters cannot be ignored, as it could lead to biased CL_R predictions.

5.4 Results

5.4.1 Contribution of GF and ATS to pediatric CL_R for drugs with different properties

The contributions of GF and ATS to CL_R over age is shown in Figure 5.2 for a selection of 9 hypothetical drugs with varying $CL_{int,T}$ and $f_{u,adult}$ values. These drugs represent the mean and the extremes of the assessed ranges for these parameter values. Here ont_T was fixed at 1, meaning that results show the influence of maturation of system-specific parameters other than transporter ontogeny on CL_R . Very similar results were obtained for drugs binding to AGP (Figure S5.2).

Figure 5.2 and S5.2 show that GF and ATS increase nonlinearly throughout the pediatric age-range with the steepest increase in the first year of life and continue to increase moderately up to the age of 15 years. Clearance by GF is strictly dependent on the maturation of GFR and on the concentrations of drug binding plasma proteins, which impact f_u . Clearance by ATS changes with age and it depends on the maturation of Q_R , KW , concentrations of drug binding plasma proteins, and hematocrit levels, the latter of which impact BP (Table 5.1).

The relative contribution of GF and ATS to CL_R is strongly impacted by $CL_{int,T}$. For drugs mainly cleared by GF (e.g. $CL_{int,T} = 5 \mu\text{L}/\text{min}/\text{mg}$ protein), the relative contribution of ATS to CL_R is on average 41% and it decreases with age from 52% in neonates to 35% between ages 2 to 15 years. As $CL_{int,T}$ increases, ATS becomes the main pathway for CL_R . A 10-fold increase in $CL_{int,T}$ from 5 to 50 $\mu\text{L}/\text{min}/\text{mg}$ protein increases the relative contribution of ATS, on average, from 41% to 80%. When $CL_{int,T}$ is further increased up to 500 $\mu\text{L}/\text{min}/\text{mg}$ protein, ATS relative contribution increases up to 90%.

Changes in CL_R are dependent on age-related changes in system-specific parameters as well as on differences in drug-specific parameters. Drugs mainly cleared by GF (e.g. $CL_{int,T} = 5 \mu\text{L}/\text{min}/\text{mg}$ protein) show, on average, a 15-fold increase in CL_R (from 3 ml/min to 46 ml/min) with $f_{u,adult}$ increasing from 0.05 to 0.95. For drugs mainly cleared by ATS with a $CL_{int,T}$ of 50 $\mu\text{L}/\text{min}/\text{mg}$ protein, the same increase in $f_{u,adult}$ yields, on average, a 12-fold increase in CL_R (from 11 ml/min to 130 ml/min). For drugs that are mainly cleared by ATS and are largely unbound from plasma proteins ($f_{u,adult} = 0.95$), a 10-fold increase in $CL_{int,T}$ (from 5 to 50 $\mu\text{L}/\text{min}/\text{mg}$ protein) yields, on average, a 2.8-fold increase in CL_R (from 46 ml/min to 130 ml/min). For drugs with very high $CL_{int,T}$ values, the same fold-difference in $CL_{int,T}$ (from 50 to 500 $\mu\text{L}/\text{min}/\text{mg}$ protein) yields, on average, a lower increase in CL_R of only 1.8-fold (from 130 ml/min to 238 ml/min).

Changes in K_p (and implicitly in BP) may only become moderately relevant for drugs with very large $CL_{int,T}$ values and medium to high $f_{u,adult}$ values. When K_p increases from 1 to 4, CL_R increased, on average, only by 1.15 fold for drugs with $CL_{int,T} = 50 \mu\text{L}/\text{min}/\text{mg}$ protein and $f_{u,adult} = 0.55$ and reached a maximum increase of 1.25-fold for drugs with $CL_{int,T} = 500 \mu\text{L}/\text{min}/\text{mg}$ protein and $f_{u,adult} = 0.95$.

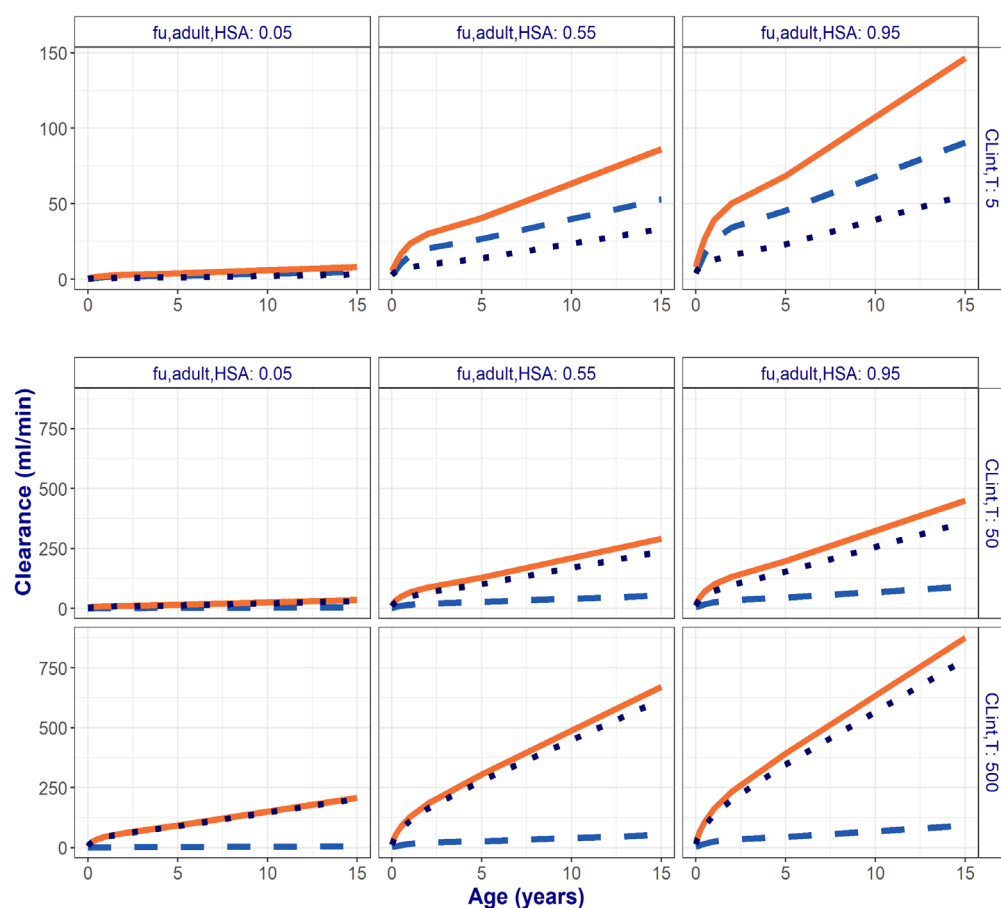


Figure 5.2 – Developmental changes in total renal clearance (CL_R – solid orange lines) and the contribution of glomerular filtration (GF – light blue dashed lines) and active tubular secretion (dark blue dotted lines) vs. age for 9 representative hypothetical drugs. These drugs bind to albumin (HSA) and have low, medium or high unbound fractions in adults ($f_{u,adult}$ – horizontal panels) that change with age, dependent on the HSA plasma concentrations. Transporter-mediated intrinsic clearance values ($CL_{int,T}$) were assumed to remain constant with age at the indicated values (vertical panels). Note the different scales on the y-axes for the graphs in the top row (range 0-150 ml/min) compared to middle and bottom row (range 0-750 ml/min).

5.4.2 Influence of renal transporters ontogeny on CL_R

The role of transporter ontogeny on CL_R was quantified by calculating the %PD between CL_R predictions with the transporter relative ontogeny fixed at adult levels ($CL_{R,adult,ontT} = 1$) and CL_R predictions with relative transporter ontogeny that either remains at a constant fraction of adult values or increases over age for individual transporters, as published for OAT1, OAT3, OCT2, Pgp [3], and aggregated transporters [11,12] ($CL_{R,pediatric,ontT}$).

Figure 5.3 shows the results for the same 9 hypothetical drugs as in Figure 5.2, with four age-constant ontogeny fractions for the renal transporters (i.e. $ont_T = 0.05, 0.2, 0.5, 0.7$). Similar results are observed for drugs binding to AGP (Figure S5.3). When transporters are underdeveloped ($ont_T < 0.2$), ontogeny of renal transporters cannot be ignored as it would lead to unacceptable CL_R predictions for all investigated hypothetical drugs regardless of age. The shapes of the %PD profiles for the 9 selected drugs differ from one another, depending on whether the primary elimination pathway contributing to CL_R is GF or ATS. This is related to the maturation of other system-specific parameters that are underlying GF and ATS.

For drugs that are mainly cleared by GF ($CL_{int,T} = 5 \mu\text{L}/\text{min}/\text{mg protein}$), in children younger than 6 months and relative transporter ontogeny lower than 0.2, ignoring ontogeny of kidney transporters would lead to unacceptable CL_R predictions (%PD = 53%- 113%). For children older than 6 months, with relative ontogeny higher than 0.05, reasonably acceptable CL_R predictions are obtained for all drugs mainly cleared by GF.

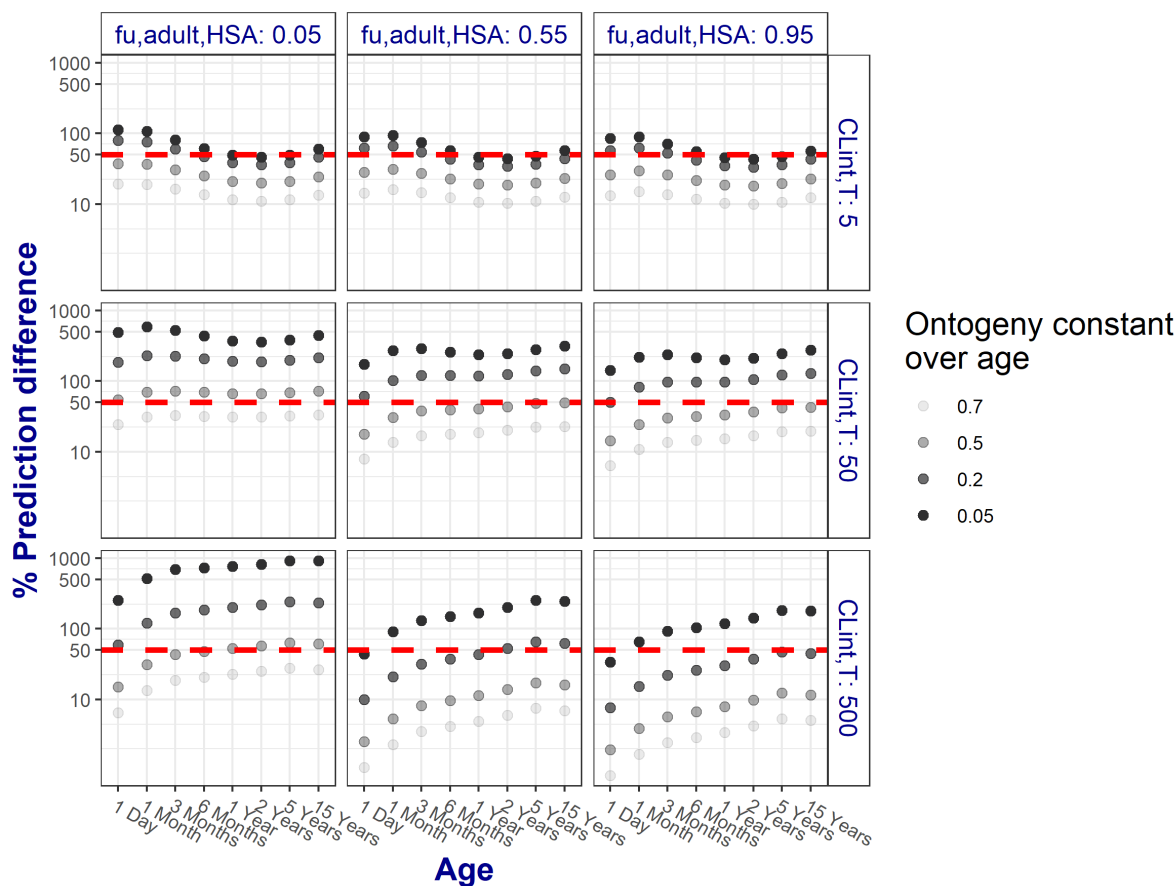


Figure 5.3 – Percentage prediction difference (%PD) for 9 representative hypothetical drugs calculated between renal clearance (CL_R) predictions obtained with the pediatric renal PBPK model that included or excluded hypothetical transporter ontogeny (ont_T) values that remained constant over age. These hypothetical drugs bind to albumin (HSA) and have low, medium or high unbound fractions in adults ($f_{u,adult}$ - horizontal panels) that change with age, dependent on the HSA plasma concentrations. Transporter-mediated intrinsic clearance values ($CL_{int,T}$) were assumed to remain constant with age at the indicated values (vertical panels). The colors of the %PD increases with decreasing transporter ontogeny values (ont_T). The dashed red line represents the threshold of reasonably acceptable CL_R prediction of 50%. Results are displayed on a log-log scale.

For drugs that are mainly cleared by ATS and have a low fraction unbound ($CL_{int,T} \geq 50 \mu\text{L}/\text{min}/\text{mg}$ protein with $f_{u,adult} = 0.05$) ignoring the ontogeny of transporters would lead to unacceptable CL_R predictions (%PD: 53%- 918%) for all pediatric individuals with a low transporter ontogeny ($ont_T \leq 0.5$). For drugs with $CL_{int,T} = 50 \mu\text{L}/\text{min}/\text{mg}$ protein and increasing $f_{u,adult}$, reasonably acceptable CL_R predictions are obtained for all ages when relative transporter ontogeny is high ($ont_T > 0.5$). For these drugs, %PD can reach values between 50% and 316% when transporter ontogeny is low ($ont_T \leq 0.2$). For drugs with a very large $CL_{int,T}$ and high $f_{u,adult}$ ($CL_{int,T} = 500 \mu\text{L}/\text{min}/\text{mg}$ protein with $f_{u,adult} = 0.95$) the influence of transporter ontogeny on CL_R decreases, as indicated by the reasonably acceptable %PD values.

The results shown in Figure 5.4 complement the previous findings by illustrating the implications for CL_R predictions for drugs that are substrates for transporters for which ontogeny functions have been published. Figure 5.4 shows when CL_R predictions are systematically acceptable with or without transporter ontogeny functions (i.e. CL_R values obtained with ont_T values varying with age according to individual [3] or aggregated [11,12] transporters functions for ontogeny and CL_R values obtained with ont_T fixed to the adult levels ($ont_T = 1$)). In both simulations, system-specific parameters and transporter ontogeny functions changed with age as shown in the Table 5.1 and Figure 5.1.

Figure 5.4 displays the results as a heat-map, where the numbers in each box represent the minimum, median and maximum %PD values obtained for all 3800 hypothetical drugs that are substrates for the indicated individual transporter or aggregated transporters at every pediatric age. Systematically

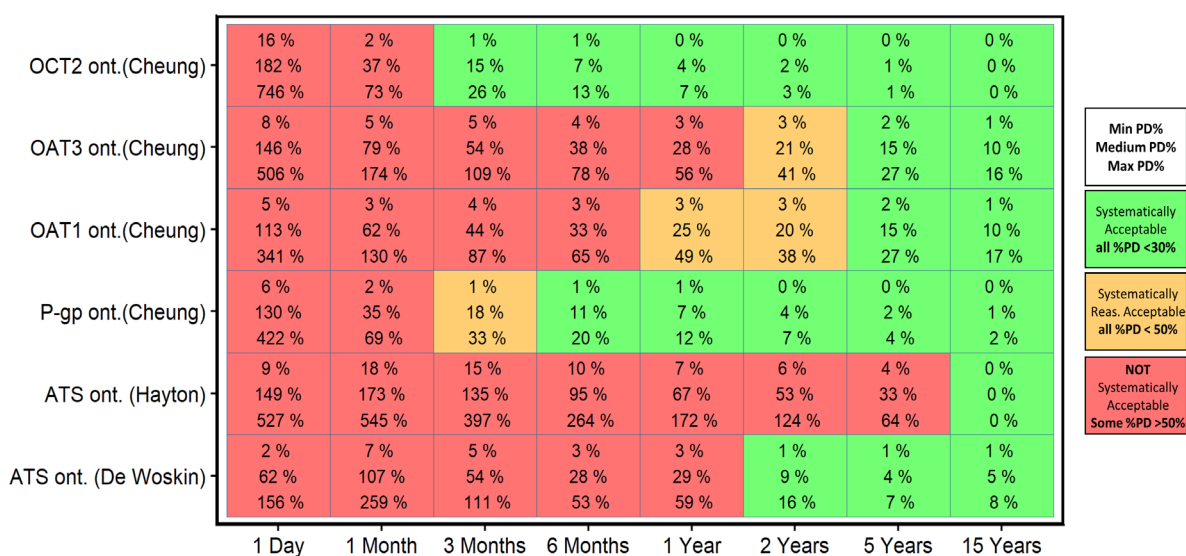


Figure 5.4 –Percentage prediction difference (%PD) between CL_R predictions obtained with the pediatric PBPK model that does not include transporter ontogeny ($ont_i = 1$, reflecting adult values) and the model that includes age-specific pediatric ont_i values for each of the indicated transporter systems. In each box, the minimum (top), median (middle) and maximum (bottom) %PD is displayed to summarize the findings for all hypothetical drugs per typical pediatric individual at different ages. Systematically acceptable scenarios have %PD for all drugs < 30% (green box), reasonable acceptable scenarios have %PD for all drugs < 50% (orange box), and absence of systematic acceptance means that at least one drug has a %PD > 50% (red box).

acceptable scenarios are achieved when CL_R predictions for all 3800 hypothetical drugs lead to %PD values below 30% in the absence of transporter ontogeny. This is indicated by the green boxes, while orange and red boxes indicate CL_R predictions that are reasonably acceptable (highest %PD between 30% and 50%) and unacceptable (highest %PD > 50%), respectively, for one or more drugs. Nonetheless, when CL_R predictions are not systematically acceptable it does not imply that %PD values below 30% were not observed, rather it indicates that predictions for one or more drugs are biased at the indicated age. Hence, it cannot be predicted a priori whether the predictions without including ontogeny of transporters will be acceptable or not, without taking drug properties into account.

When the relative transporter ontogeny varied with age according to the functions of Cheung et al. (i.e. for OAT1, OAT3, OCT2, and P-gp) [3], ignoring ontogeny lead to CL_R predictions that were not systematically acceptable for all transporters in newborns of 1 month and younger. CL_R predictions of drugs that are substrates of OAT transporters are not systematically acceptable below the age of 1 year. For children of 2 years and older ignoring the ontogeny of transporters lead to CL_R predictions that were reasonably acceptable or acceptable for all transporters – individual or aggregated- and all substrates, except when ontogeny follows the aggregated transporters ontogeny function as published by Hayton et al..

5.5 Discussion

A PBPK-based framework was used to predict CL_R of hypothetical drugs with various properties that are substrates for renal secretion transporters throughout the pediatric age-range. This approach provided insight on the contribution of GF and ATS to total pediatric CL_R . In addition, the impact of ignoring this transporter ontogeny in predicting CL_R in children was quantified.

The physiology-based model for CL_R used in the presented framework was developed based on a model published for adults [5] that was extended to the pediatric population by including maturation functions for the system-specific parameters as shown in Table 5.1 and illustrated in Figure 5.1A. This model included two major contributing pathways to CL_R : GF and ATS. Based on this model we could quantify the impact of transporter ontogeny on pediatric drug clearance for all current and future small molecule

drugs, based on drug-specific properties alone. We found that the contribution of these pathways to CL_R increases non-linearly throughout the pediatric age-range, with the steepest increase during the first year of life, even in the absence of transporter ontogeny. These changes in pediatric CL_R are determined by the influence of maturation in the system-specific parameters underlying GF and ATS as well as by drug-specific properties (Figure 5.2). Both GF and ATS increase with increasing f_u , while ATS also increases with increasing $CL_{int,T}$ values.

Drug f_u was found to have a major influence on CL_R through both investigated pathways, but especially on CL_R through GF. $CL_{int,T}$ has a major influence on CL_R only through ATS. Drugs with 10-fold different $CL_{int,T}$ values and low binding to plasma proteins ($f_{u,adult} = 0.95$) yield different contributions of ATS to CL_R . When ATS contribution to CL_R is limited only by the activity and the abundance of transporters (i.e. $CL_{int,T}$ changes between 5 and 50 $\mu\text{L}/\text{min}/\text{mg}$ protein) an increase of 1.9-fold in average ATS contribution was observed. As $CL_{int,T}$ changes between 50 and 500 $\mu\text{L}/\text{min}/\text{mg}$ protein) we observed a lower increase in average ATS contribution of only 1.1-fold¹⁶. This behavior could be explained by the fact that f_u and $CL_{int,sec}$ are rate limiting factors for ATS when $CL_{int,sec} \times f_u$ is low relative to Q_R (i.e. permeability limited process). Q_R becomes the rate limiting factor for ATS when $CL_{int,sec} \times f_u$ is high relative to Q_R (i.e. perfusion limited process). This also explains why the impact of ignoring transporter ontogeny decreases for drugs with very high $CL_{int,T}$, as shown by the lower %PD values in Figure 5.3. It is important to mention that whether ATS is permeability limited ($CL_R/Q_R < 0.3$) or perfusion limited ($CL_R/Q_R > 0.7$) or a combination between the two processes ($0.3 < CL_R/Q_R < 0.7$) may change with age, as shown in Figure 5.5.

The present framework explored a broad parameter space for ontogeny of transporters. By keeping ontogeny of transporters constant with age, the potential impact of ignoring ontogeny on predicting CL_R was systematically explored (Figure 5.3). This exploration highlights that an ontogeny below 0.2 of the adult value cannot be ignored for the majority of drugs regardless of the pediatric age. In this situation, the assumption that there are no differences in transporter ontogeny between children and adults would lead to unacceptable CL_R predictions. Data characterizing how ontogeny of individual kidney transporters changes across the pediatric age is scarce in literature. Cheung et al. [3] recently took the first steps in quantifying the ontogeny of protein abundance for individual renal transporters. According to this report, which is based on a limited sample size, BCRP, MATE1, MATE2-K, and GLUT2 have protein abundance levels similar to the adult levels throughout the studied pediatric age-range [3], meaning that $ont_T = 1$ for children of all ages and that transporter ontogeny is not a factor of influence in predicting CL_R for substrates of these transporters. Including these ontogeny profiles in the current framework increased our understanding on the role of age-dependent ontogeny in predicting CL_R (Figure 5.4). As reported by Cheung et al., the ontogeny of OAT1 and OAT3 is slower than the ontogeny of OCT2 and P-gp. Ignoring OCT2 ontogeny yields systematically acceptable pediatric CL_R values for all its hypothetical substrates in children from 3 months and older. For P-gp substrates, the same holds true in children from 6 months and older. Ontogeny of OATs however cannot be ignored for children younger than 2 years as CL_R predictions are not systematically acceptable for substrates of this transporter. The CL_R predictions obtained with the aggregate transporter function published by DeWoskin et al. [11] are in line with the results for OATs. The aggregate function of Hayton et al. [12] suggest a much slower ontogeny leading to CL_R predictions that are not systematically acceptable in children up to and including 5 years. CL_R predictions with Hayton et al. [12] diverge from the predictions obtained with the other transporter ontogeny functions since it was the first function to quantify the ontogeny of ATS and has a different profile than all the other studied functions. Disregarding ontogeny of transporters leads to over-predictions of CL_R in the young patients. If these predicted CL_R values were used as the basis for pediatric dose adjustments, these could lead to over-exposure to drugs and, eventually, increase the risk of toxic events.

As our analysis identifies drugs for which CL_R is sensitive to transporter ontogeny, the proposed framework can also be used to find and select drugs with relevant properties to serve as *in vivo* probes

for the quantification of the ontogeny of transporters underlying ATS. From the results of the current analysis we could conclude that the best probe drugs should have a $CL_{int,T}$ of 5-50 $\mu\text{L}/\text{min}/\text{mg}$ protein and medium to high fraction unbound in adults ($f_{u,adults} = 0.55 - 0.95$). Drugs for which GF is the main elimination pathway or drugs with extremely high $CL_{int,T}$ that cause renal blood flow to be limiting for elimination, will have a limited use in characterizing ontogeny profiles. These guidelines could be the basis for future research aiming to derive ontogeny of individual renal transporters *in vivo*.

Our results rely on the validity of the PBPK approach, which is currently considered the “gold standard” for clearance predictions in the absence of clinical data. This approach gives an overview of the impact of system- and drug-specific parameters on CL_R . The explored arrays of ontogeny fractions and of drug properties were realistic, however, unrealistic combinations of drug properties could have been generated. As with the previously published hepatic PBPK framework [6], this analysis does not include measures for the variability or uncertainty of the parameters that constitute the PBPK model, to highlight the impact of system- and drug-specific changes in the absence of variability and uncertainty. Our approach could be extended for investigations on the impact of variability and uncertainty by including variability terms on the system-specific parameters and performing stochastic simulations. Finally, PBPK modelling is ideally suitable to study the impact of specific physiological processes in a way that is not possible *in vivo*. In the *in vivo* situation, studies are limited to drugs that are currently available on the market and prescribed to children. However, generally these drugs are not eliminated in totality by one single pathway. Moreover, the accuracy of these observations is impacted by aspects related to study design, sampling and analytical methods. Our current model-based analysis is not impacted by these limitations. The physiology-based model for CL_R used here only included GF and ATS, but not passive permeability, reabsorption, or renal metabolism. This enabled the study of GF and ATS in isolation and reduced the noise and complexity of the results. The influence of ontogeny on transporters working in tandem or of reabsorption and kidney metabolism together with their dependencies on physiological

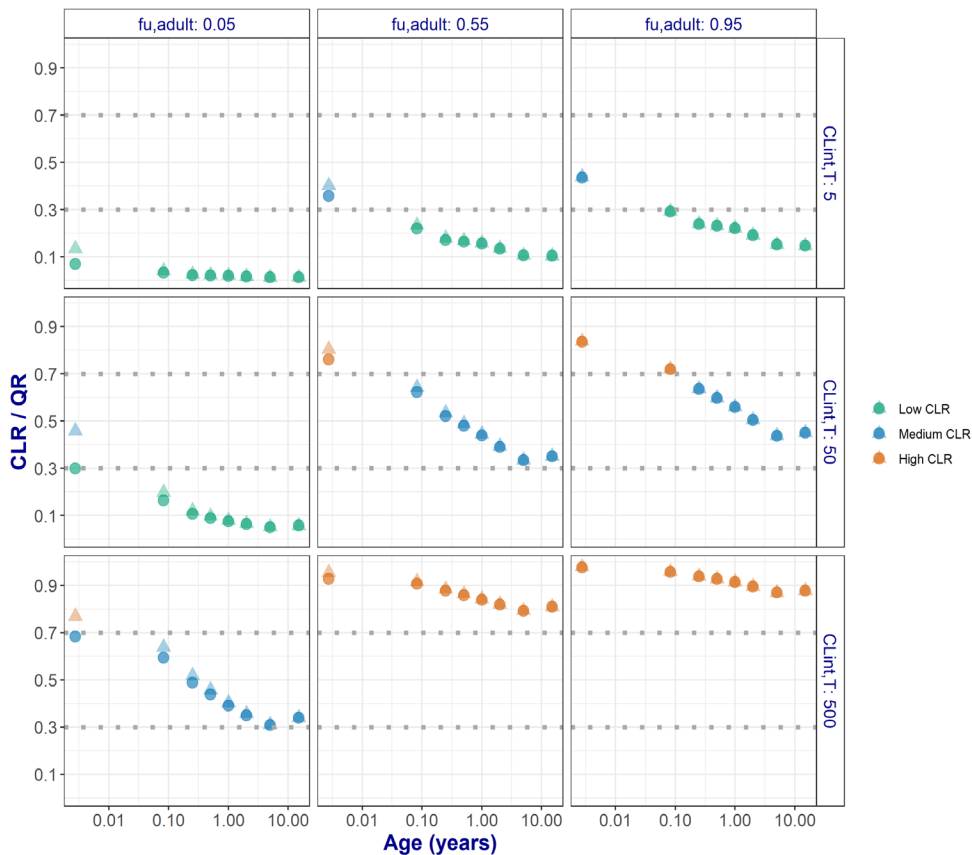


Figure 5.5 – Ratio of total renal clearance (CLR) and renal blood flow (Q) for 9 representative hypothetical drugs. Results are presented for drugs binding to human serum albumin (HSA) (circles) or to α -acid glycoprotein (AGP) (faded triangles).

properties like pH at the tubule side, ionization, enzyme abundance, affinity, and maturation, could be explored in a similar manner in subsequent analyses.

5.6 Conclusion

A PBPK-based framework was used to determine the role of drug properties and ontogeny of transporters in predicting pediatric CL_R . The contribution of GFR to CL_R is influenced by drug f_u and contribution of ATS to CL_R is influenced by f_u and $CL_{int,T}$. Transporters play a major role in predicting CL_R . Discordance in the CL_R predictions when ignoring maturation in ATS, shows when accurate predictions of total pediatric CL_R from the adults if extrapolation solely relied on changes in GF with age, are not possible. Ignoring transporter ontogeny, especially when it is below 0.2 of the adult values, leads to inaccurate CL_R predictions for the majority of drugs, regardless of age. Given known age-dependent patterns, transporter ontogeny cannot be ignored in children younger than 2 years. Drugs with properties that lead to high %PE when ignoring ATS ontogeny may serve as sensitive *in vivo* probes to further investigate transporter ontogeny.

5.7 Acknowledgements

The authors would like to thank Muhammed Saleh for reviewing the R code used for this work.

5.8 References

1. Morrissey, K. M., Stocker, S. L., Wittwer, M. B., Xu, L. & Giacomini, K. M. Renal transporters in drug development. *Annu Rev Pharmacol Toxicol.* 503–29 (2013). doi:10.1146/annurev-pharmtox-011112-140317
2. Kunze, A., Huwyler, J., Poller, B., Gutmann, H. & Camenisch, G. In vitro-in vivo extrapolation method to predict human renal clearance of drugs. *J. Pharm. Sci.* (2014). doi:10.1002/jps.23851
3. Cheung, K. W. K. et al. A Comprehensive Analysis of Ontogeny of Renal Drug Transporters: mRNA Analyses, Quantitative Proteomics, and Localization. *Clin. Pharmacol. Ther.* (2019). doi:10.1002/cpt.1516
4. Elmorsi, Y., Barber, J. & Rostami-Hodjegan, A. Ontogeny of hepatic drug transporters and relevance to drugs used in pediatrics. *Drug Metabolism and Disposition* (2016). doi:10.1124/dmd.115.067801
5. Rowland Yeo, K., Aarabi, M., Jamei, M. & Rostami-Hodjegan, a. Modeling and predicting drug pharmacokinetics in patients with renal impairment. *Expert Rev Clin Pharmacol* 4, 261–274 (2011).
6. Calvier, E. et al. Allometric scaling of clearance in paediatrics: when does the magic of 0.75 fade? *Clin Pharmacokinet.* 56, 273–285 (2017).
7. Krekels, E. H. J., Calvier, E. A. M., van der Graaf, P. H. & Knibbe, C. A. J. Children Are Not Small Adults, but Can We Treat Them As Such? *CPT Pharmacometrics Syst. Pharmacol.* (2019). doi:10.1002/psp4.12366
8. Johnson, T. N., Rostami-Hodjegan, A. & Tucker, G. T. Prediction of the clearance of eleven drugs and associated variability in neonates, infants and children. *Clin. Pharmacokinet.* 45, 931–956 (2006).
9. Salem, F., Johnson, T. N., Abduljalil, K., Tucker, G. T. & Rostami-Hodjegan, A. A re-evaluation and validation of ontogeny functions for cytochrome P450 1A2 and 3A4 based on in vivo data. *Clin. Pharmacokinet.* 53, 625–636 (2014).
10. Simcyp (a Certara Company). Simcyp v18. (2018).
11. DeWoskin, R. S. & Thompson, C. M. Renal clearance parameters for PBPK model analysis of early lifestage differences in the disposition of environmental toxicants. *Regul. Toxicol. Pharmacol.* 51, 66–86 (2008).
12. Hayton, W. L. Maturation and growth of renal function: dosing renally cleared drugs in children. *AAPS PharmSci* 2, E3 (2000).
13. National Health and Nutrition Examination Survey. www.cdc.gov/growthcharts/index.htm.
14. International Commission on Radiological Protection. Basic anatomical and physiological data for

use in radiological protection- Skeleton. Ann. ICRP 32, 1–277 (1995).

15. Rowland, M. & Tozer, T. N. Clinical Pharmacokinetics and Pharmacodynamics: Concepts and Applications. (Wolters Kluwer Health/Lippincott William & Wilkins, 2011).
16. Tucker, G. Measurement of the renal clearance of drugs. Br. J. Clin. Pharmacol. (1981). doi:10.1111/j.1365-2125.1981.tb01304.x

5.9 Supplementary material

S5.1: Retrograde calculation of transporter-mediated intrinsic clearance from adult renal clearance values

Following an extensive literature search, Scotcher et al. [1] published data on renal clearance (CL_R) of 157 drugs in adults. These drugs were classified according to the publication of Varma et al. [2] into (i) compounds with net renal reabsorption ($CL_R < 0.8 \times f_u \times GFR$), (ii) compounds with net renal secretion ($CL_R > 1.2 \times f_u \times GFR$) and (iii) compounds with no net reabsorption or secretion ($0.8 \times f_u \times GFR < CL_R < 1.2 \times f_u \times GFR$). Only findings on the 53 net secretion drugs were used in this analysis [2].

By solving equation [S1] for $CL_{int,sec}$ we obtain [S1A], where all terms are known and all parameter values take adult values.

$$CL_R = f_u \times GFR + \frac{(Q_R - GFR) \times f_u \times CL_{int,sec}}{Q_R + f_u \times \frac{CL_{int,sec}}{BP}} \quad [S1]$$

$$CL_{int,sec} = \frac{(CL_R - f_u \times GFR) \times Q_R}{((Q_R - GFR) \times f_u - (CL_R - f_u \times GFR) \times \frac{f_u}{BP})} \quad [S1A]$$

To get $CL_{int,T}$ we solved equation [S2] for $CL_{int,T}$ and obtained the form in [S2A], where all parameter values take adult values and $CL_{int,sec}$ from equation [S1A] is used in equation [S7A].

$$CL_{int,sec} = ont_T \times CL_{int,T} \times PTCPGK \times KW \quad [S2]$$

$$CL_{int,T} = \frac{CL_{int,sec}}{ont_T \times PTCPGK \times KW} \quad [S2A]$$

The $CL_{int,T}$ values obtained for 53 drugs classified as net secretion drugs following the retrograde calculation are shown in Figure S5.1.

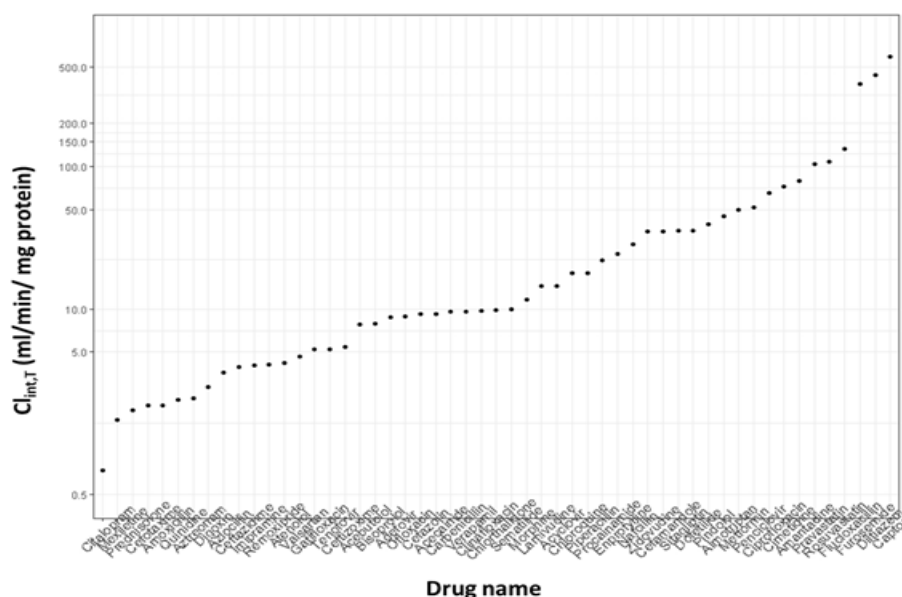


Figure S5.1 – Intrinsic clearance ($CL_{int,T}$) values obtained for 53 drugs classified as net secretion drugs collected from literature. Drugs are ordered by $CL_{int,T}$ values. Y-axis is logarithmic.

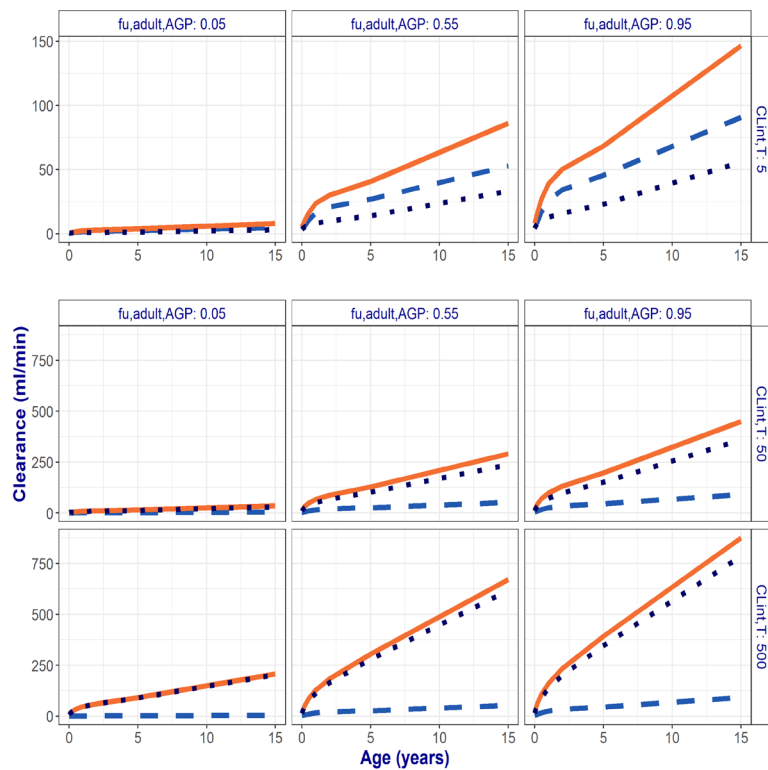
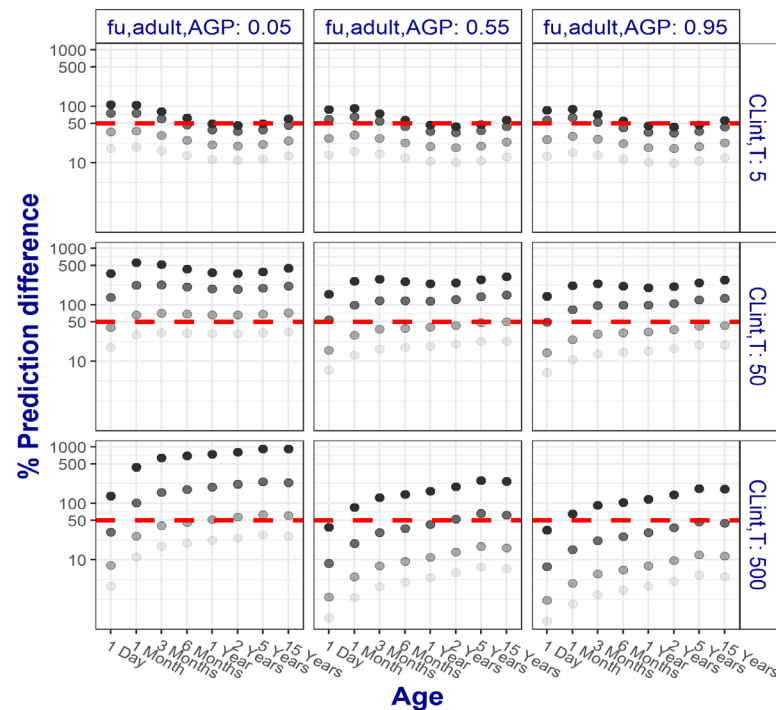


Figure S5.2 – Developmental changes in total renal clearance (CL_R – solid orange lines) and the contribution of glomerular filtration (GF – light blue dashed lines) and active tubular secretion (dark blue dotted lines) vs. age for 9 representative hypothetical drugs. These drugs bind to α -acid glycoprotein (AGP) and have low, medium or high unbound fractions in adults ($f_{u,adult}$ – horizontal panels) that change with age, dependent on the AGP plasma concentrations. Transporter-mediated intrinsic clearance values ($CL_{int,T}$) were assumed to remain constant with age at the indicated values (vertical panels). Note the different scales on the y-axes for the graphs in the top row (range 0-150 ml/min) compared to middle and bottom row (range 0-750 ml/min).



Ontogeny constant over age

- 0.7
- 0.5
- 0.2
- 0.05

Figure S5.3 – Percentage Prediction difference (%PD) for 9 representative hypothetical drugs calculated between renal clearance (CL_R) predictions obtained with the renal PBPK model that included or excluded hypothetical transporter ontogeny (ont_T) values that remained constant over age. These drugs bind to α -acid glycoprotein (AGP) and have low, medium or high unbound fractions in adults ($f_{u,adult}$ – horizontal panels) that change with age, dependent on the AGP plasma concentrations. Transporter-mediated intrinsic clearance values ($CL_{int,T}$) were assumed to remain constant with age at the indicated values (vertical panels). The colors of the %PD increases with decreasing transporter ontogeny values (ont_T). The dashed red line represents the threshold of reasonably acceptable CL_R prediction of 50%. Results are displayed on a log-log scale.

5.10 References Supplementary material

1. Scotcher D, Jones C, Rostami-Hodjegan A, Galetin A (2016) Novel minimal physiologically-based model for the prediction of passive tubular reabsorption and renal excretion clearance. *Eur J Pharm Sci.* <https://doi.org/10.1016/j.ejps.2016.03.018>
2. Varma MVS, Feng B, Obach RS, Troutman MD, Chupka J, Miller HR, El-Kattan A (2009) Physicochemical determinants of human renal clearance. *J Med Chem* 52:4844–4852 . <https://doi.org/10.1021/jm900403j>

5.11 R code

```
# Script: PBPK Framework - Renal
# Version: 12
# Last Update: 6-2-2020
# Author: SC
#=====
# change with previous version: Removed interim plots;
#
# Create the dataframe with all required combinations
#=====
# remove all from environment:
rm(list=ls(all=TRUE))
# change for parth

memory.limit(200*1024*1024*1024)
# Load Libraries
library(dplyr)      # operations with dataframes
library(ggplot2)    # plotting
library(gridExtra)  # multiplot
library(reshape2)   # melt and cast
library(cowplot)    # extra options for ggplot plots
#=====

# Input the wd (change home location and wd as needed):

home <- ""
wd <- "1.Scripts\\"

# Call script with functions that are needed:
# ---

source(file = paste(home, wd, "SC04_PBPKFrame_functions.R", sep = ""))

# Generate demographics dataframe:
demo <- data.frame(
  lab = c("1 Day", "1 Month", "3 Months", "6 Months", "9 Months", "1 Year",
"2 Years", "5 Years", "10 Years", "15 Years", "Adult"), #labels for plotting
  age = c(1/365, 30/365, 0.25, 0.5, 0.75, 1, 2, 5, 10, 15, 35), # in years
  wt = c(3.45, 4.3, 5.75, 7.55, 8.9, 9.9, 12.35, 18.25, 32.5, 54.25, (73+60)/2),
# in kg
  ht = c(49.75, 54.25, 60, 66, 70.75, 74.75, 86, 108.25, 138.25, 166, (163+176)/2),
# in cm; added to calculate the BSA needed for CO%
  hemat = c(56, 44, 35.5, 36, 36, 36, 36.5, 37, 40, 42, 44) / 100,
  # Hematocrite in percentage for each age (AGE), from Am Fam Physi-
  cian. 2001 Oct 15;64(8):1379-86. Anemia in children. Irwin JJ
  mat_w = round(x = c(20.3, 14.9, 31.3, 46.5, 45.3, 44.2, 66.5, 73.15,
73.15, 73.15, 79.8)/79.8, digits = 3) # aggregated ATS ontogeny function de-
  rived from deWoskin
)

# Generate age specific renal blood flow (qr), glomerular filtration rate
(gfr), kidney weight (kw in g)
# ---

demo$kw <- KW(demo$wt)
demo$qr <- QR_new(age = demo$age, ht = demo$ht, wt = demo$wt)
demo$gfr <- GFR(wt = demo$wt, age = demo$age)

# Include age-specific functions for ontogeny:
# ---
```

```

# aggregated ontogeny function of Hayton 2000:

demo$mat_h <- rfp(wt = demo$wt, age = demo$age)/rfp(wt = demo$wt[demo$lab
== "10 Years"], age = demo$age[demo$lab == "10 Years"]) # % of 5yo maximal
capacity (assumption for ages > 15yr is 100%) Hayton 2000 not defined above
12 year, 35.5 kgs
demo$mat_h[demo$lab %in% c("15 Years", "Adult")] <- 1 # assume 15 yo and
adult to have 100% maturation since they are out of range.

# individual transporter ontogeny functions:

demo$mat_pgp <- pgp(demo$age)
demo$mat_oat1 <- oat1(demo$age)
demo$mat_oat3 <- oat3(demo$age)
demo$mat_oct2 <- oct2(demo$age)

# assumed maturation as fraction of adult value (fixed to 1; to use later in
impact of ont heatmap)

mat <- 1 #c(0.1, 0.25, 0.5, 0.75, 1)

# For manuscript/review purposes remove a few ages:
# ---

demo <- demo[!demo$lab %in% c("9 Months", "10 Years"),]

# Vectors with arrays for generating the hypothetical drug
# ---

fu <- round(seq(0.05,1, by =0.1), digits = 2) # reference/ adult plasma
fraction unbound values
kp <- c(0, 1, 2, 3, 4) # range from Tozer and Rowland book
freab <- 0 # fraction reabsorbed

# Used back-calculated clint values from Varma 2009 and D.Scotcher adult
CLR values, class: "Net Secretion"
# to determine realistic range to investigate
# ---
clint <- c(seq(0, 20, by = 1), seq(30, 70, by = 5), seq(80, 100, by =
10), 150, seq(200, 600, by = 100)) # uL/min

# Expanded dataset with all possible combinations; keep system parameters
unchanged:
# ---

d <- expand.grid(age = demo$age, fu = fu, kp = kp, freab = freab, clint =
clint, mat = mat)
d <- left_join(x = demo, y = d, by = "age")

# Add maturation functions for fu dependent on plasma proteins concs.
# ---

d$fu_paed_hsa <- fu_paed_hsa(age_ad = demo[demo$lab == "Adult", "age"],
age = d$age, fu = d$fu) # HSA
d$fu_paed_aag <- fu_paed_aag(age_ad = demo[demo$lab == "Adult", "age"],
age = d$age, fu = d$fu) # AGP

# Plots
# ---
wd <- "2.Figures\\"

```

```

# Figure with ontogeny transporters functions:
# -- log normal data:

linety <- c("Pgp" = 1, "OCT2" = 2, "OAT3" = 3, "OAT1" = 4)
sha <- c("De Woskin" = 15, "Hayton" = 17)

tiff(paste0(home, wd, "SC_Figure_S2_TransportersOntog_func.tiff"), width = 22,
height = 10, res = 300, units = "cm")

ggplot(demo)+
  geom_line(aes(age, mat_pgp, linetype = "Pgp"), size = 1.2, col =
"#68686b")+
  geom_line(aes(age, mat_oct2, linetype = "OCT2"), size = 1.2, col =
"#68686b")+
  geom_line(aes(age, mat_oat3, linetype = "OAT3"), size = 1.2, col =
"#68686b")+
  geom_line(aes(age, mat_oat1, linetype = "OAT1"), size = 1.2, col =
"#68686b")+
  geom_point(aes(age, mat_w, shape = "De Woskin"), size = 1.75, col =
"black")+
  geom_point(aes(age, mat_h, shape = "Hayton"), size = 1.75, col =
"black")+
  scale_x_continuous(breaks = demo$age, labels = demo$lab, trans =
"log10")+
  scale_linetype_manual(name = "Individual transporters functions", val-
ues = linety)+
  scale_shape_manual(name = "Aggregate transporters values", values =
sha)+
  xlab("Age (years)")+
  ylab("Transporters ontogeny (relative to adult values)")+
  theme(axis.title.x = element_text(size = 10),
        axis.title.y = element_text(size = 10),
        axis.text.x = element_text(angle = 15))

dev.off()

# melt dataframe to be able to group by transporter:

d_melt <- melt(d, id.vars = c("lab", "age", "wt", "kw", "ht", "hemat",
"qr", "gfr", "fu", "kp", "freab",
                        "clint", "fu_paed_hsa", "fu_paed_aag"), var-
iable.name = "transp", value.name = "mat_fr")
d <- d_melt
d$mat_flag <- ifelse(d$mat_fr > 0 & d$mat_fr <= 0.25, "0-25%",
                    ifelse(d$mat_fr > 0.25 & d$mat_fr <= 0.5, "25-50%",
                           ifelse(d$mat_fr > 0.5 & d$mat_fr <= 0.75, "50-
75%", "75-100%")))

# PBPK clearance simulations for the pediatric population for each plasma
protein:

d$cl_mat_hsa <- CL(qr = d$qr, wt = d$wt, age = d$age, fu = d$fu_paed_hsa,
fre = d$freab, #fu HSA
                 clsec = CLSEC(jmax.t = d$clint, km.t = 1, kwt = d$kw
, mat = d$mat_fr),
                 bp = BP(hemat = d$hemat, fu = d$fu_paed_hsa, kp = d$kp))

d$cl_mat_aag <- CL(qr = d$qr, wt = d$wt, age = d$age, fu = d$fu_paed_aag,
fre = d$freab, # fu AGP
                 clsec = CLSEC(jmax.t = d$clint, km.t = 1, kwt = d$kw, mat
= d$mat_fr),
                 bp = BP(hemat = d$hemat, fu = d$fu_paed_aag, kp = d$kp))

```

```

# PBPK clearance with mat = 1:
# ---

d$cl_mat_hsa_1 <- CL(qr = d$qr, wt = d$wt, age = d$age, fu = d$fu_paed_hsa,
fre = d$freab, #fu HSA
                    clsec = CLSEC(jmax.t = d$clint, km.t = 1, kwt = d$kw,
mat = 1),
                    bp = BP(hemat = d$hemat, fu = d$fu_paed_hsa, kp = d$kp))

d$cl_mat_aag_1 <- CL(qr = d$qr, wt = d$wt, age = d$age, fu = d$fu_paed_aag,
fre = d$freab, # fu AGP
                    clsec = CLSEC(jmax.t = d$clint, km.t = 1, kwt = d$kw, mat
= 1),
                    bp = BP(hemat = d$hemat, fu = d$fu_paed_aag, kp = d$kp))

# prediction error (with and without ontogeny):
# ---

d$pe_hsa <- PE(a = d$cl_mat_hsa_1, b = d$cl_mat_hsa)
d$pe_aag <- PE(a = d$cl_mat_aag_1, b = d$cl_mat_aag)

# Systematic bias:
# ---

tiff(paste0(home, wd, "SC_Figure_3_All_drugs_Systematic_bias_per_function_
and_age_min_med_max.tiff"), width = 20, height = 10, units = "cm", res =
300)

d %>%
  # changes to ds:

  filter(lab != "Adult") %>% filter(transp != "mat" & clint != 0) %>% #mat ==
1 GFR only drugs (clint = 0) are excluded
  melt(id.vars = names(d)[c(-22, -23)], variable.name = "plasma_prot", val-
ue.name = "pe") %>% # all pes in 1 column
  group_by(transp, mat_fr, lab) %>% summarize(maxPE = max(pe), medPE = me-
dian(pe), minPE = min(pe)) %>% # summary stats on %pe for each age and tram-
sp
  mutate(peCol = ifelse(maxPE <= 30, 1, ifelse(maxPE > 30 & maxPE <= 50, 2,
3))) %>% # colour tiles

  ggplot(aes(x = factor(lab, levels = c("1 Day", "1 Month", "3 Months",
"6 Months", "9 Months", "1 Year", "2 Years", "5 Years", "10 Years", "15
Years")), y = factor(transp))) +
  geom_tile(aes(fill = peCol, alpha = 1, colour=1))+
  scale_fill_gradientn(colours = c("green", "orange", "red"))+
  geom_text(aes(label = paste(round(minPE, 0), "%", "\n", round(medPE,
0), "%", "\n", round(maxPE, 0), "%")), size = 3)+
  scale_y_discrete(labels = c("ATS ont. (De Woskin)", "ATS ont. (Hay-
ton)", "P-gp ont. (Cheung)", "OAT1 ont. (Cheung)", "OAT3 ont. (Cheung)", "OCT2
ont. (Cheung)"))+
  theme_bw()+
  xlab("")+
  ylab("")+
  guides(col = FALSE, alpha = FALSE)+
  theme_cowplot(12)+
  theme(panel.spacing=unit(.05, "lines"),
        panel.border = element_rect(color = "black", fill = NA, size =
1.2),
        legend.position = "none")

dev.off()

```

```

# Script: General functions for PBPK Framework - Renal
# Version: 2
# Last Update: 6-2-2020
# Author: SC
#=====
#
# Renal blood flow (Qr):
#=====
## This is dependent on body surface area, so there is a function for BSA
here too:
# references names used
BSA <- function(ht, age, wt) { # age in years
  haycock <- 0.024265 * ht**0.3964 * wt**0.5378
  dubois <- 0.007184 * ht**0.725 * wt**0.425
  return(ifelse(wt < 15, haycock, dubois)) # in m^2
  # for wt <15kg use Haycock et al. for children < or =15kg, else Dubois
and Dubois
}

## Then add the blood flow (Qr) as a % of CO function:
QR <- function(age, ht, wt) { # CO in L/h if /60
  co <- BSA(ht, age, wt) * (110 + 184 * exp(-0.0378 * age) - exp(-0.24477 *
age)) * 1000 / 60
  return(0.19 * co) # in L/h
}

# this has to be optimize to work differently for males and females:

QR_new <- function(age, ht, wt) { # CO in L/h
  co <- BSA(ht, age, wt) * (110 + (184.974 * (exp(-0.0378 * age) - exp(-
0.24477 * age)))) * 1000 / 60
  fr_qr_male <- 4.53 + (14.63 * age ^ 1.0 / (0.188 ^ 1.0 + age ^ 1.0))
  fr_qr_female <- 4.53 + (13.00 * age ^ 1.15 / (0.188 ^ 1.15 + age ^ 1.15))
  return(rowMeans(as.data.frame(list(fr_qr_male, fr_qr_female)))/100* co) #
in L/h
}

# Kidney weight:
# ---

KW <- function(wt) 1050 * (4.214 * wt ^ 0.823 + 4.456 * wt ^ 0.795) / 1000

# GFR:
#=====
## GFR maturation function (my poster from PAGE 2015 --> Salem 2014); wt is
#in g and age is PMA
## here age should be as PMA (GA + PNA in wks): 40 (wks of GA)+age/7 (if
the age-range is in days)

GFR <- function(wt, age) { # wt in kg and age in years
  return(112 * (((wt * 1000 / 70000) ^ 0.632) * ((40 + age * 365 / 7) ^
3.3) / ((55.4 ^ 3.3) + (40 + age * 365 / 7) ^ 3.3)))
} # ml/min

# Calculation of CL determined by GFR (net GFR)
CLGFR <- function(wt, age, fu) { GFR(wt, age) * fu }

# fraction unbound maturation functions:
#-----
# HSA (g/l):
HSA <- function(age) {hsa <- 1.1287 * log(age * 365) + 33.746 ; return(h-

```

```

sa)})
fu_paed_hsa <- function(age_ad = 35, age, fu) {return(1 / (1 + (((1 - fu) *
HSA(age)) / (HSA(age_ad) * fu))))})

#alpha1-acid glycoprotein (AAG):
AAG <- function(age) {aag <- 0.887 * (age * 365) ^ 0.38 / ((8.89 ^ 0.38) +
(age * 365) ^ 0.38) ; return(aag)}
fu_paed_aag <- function(age_ad = 35, age, fu) {return(1 / (1 + (((1 - fu) *
AAG(age)) / (AAG(age_ad) * fu))))})

# BP - blood to plasma partition coeficient:
#-----
# hemat is required as input; took from simcyp v.18.r.1
# age in years:
hemat <-function(age) {
  hemat_male <- 53 - ((43.0 * age ^ 1.12 / (0.05 ^ 1.12 + age ^ 1.12)) * (1
+ (-0.93 * age ^ 0.25 / (0.10 ^ 0.25 + age ^ 0.25))))
  hemat_female <- 53 - ((37.4 * age ^ 1.12 / (0.05 ^ 1.12 + age ^ 1.12)) *
(1 + (-0.80 * age ^ 0.25 / (0.10 ^ 0.25 + age ^ 0.25))))
  return(rowMeans(as.data.frame(list(hemat_male/100, hemat_female/100)))) #
in fraction
}

BP <- function(hemat, fu, kp) { bp <- 1 + hemat * (fu * kp - 1)}

#Secretion clearance and CLint as used in SimCYP mechkim.
# =====

# instead of jmax.t and km.t I will use jmax.t = clint and fix km.t=1
CLSEC <- function(isef.t = 1, jmax.t, km.t, raf = 1,ptcpgk = 60, kwt, mat =
1) # jmax/km is equivalent to ul/min; kwt in g
{ # jmax.t is used interchangeably with clint; dependent on the type of in-
put.
  clsec <- (mat * (isef.t * jmax.t * raf) / km.t) * ptcpgk * kwt / 1000 #
conversion to ml/min from ul/min
  return(clsec) #ml/min
}

# secretion clearance
CL_ACTIV <- function(qr, fu, gfr, clsec, bp){(qr - gfr) * fu * clsec / (qr
+ fu * clsec / bp )} # the function without fu^2; unit ml/min; https://sci-
hub.tw/10.1124/dmd.106.013359

# Well-stirred renal clearance model (double correction) Rowland Yeo (2014)
according to Jamei 2009
CL <- function(qr, wt, age, fu, clsec, bp = 1, fre = 0.01) { # unit is ml/
min
  gfr <- GFR(wt, age)
  clgfr <- CLGFR(wt, age, fu)
  clactiv <- CL_ACTIV(qr, fu, gfr, clsec, bp)
  return(qr * (clgfr / qr + clactiv/qr) * (1 - fre))
}

# Clearances generated using the allometric scaling
CL_AS <- function(cl_ad, wt, wt_ad) {
  cl_ad * (wt / wt_ad) ^ 0.75
}

# Clearances generated using the linear scaling
CL_LIN <- function(cl_ad, wt, wt_ad) {
  cl_ad * (wt / wt_ad)
}

```

```

# Hayton maturation function form 2 days (2.15 kg) till 12 yo (35.5 kg) for
OAT1 #
rfp <- function(wt, age) { # mg/min
  1.08 * (wt ^ 1.04) * exp(-0.185 * (age * 12)) + 1.83 * (wt ^ 1.04) * (1 -
exp(-0.185 * (age * 12)))
}

# -- functions for transporters taken from https://ascpt.onlinelibrary.
wiley.com/doi/epdf/10.1002/cpt.1516
pgp <- function(age) {
  (age * 52) ^ 0.73 / ((age * 52) ^ 0.73 + 4.02 ^ 0.73)
}

oat1 <- function(age) {
  (age * 52) ^ 0.43 / ((age * 52) ^ 0.43 + 19.71 ^ 0.43)
}

oat3 <- function(age) {
  (age * 52) ^ 0.51 / ((age * 52) ^ 0.51 + 30.07 ^ 0.51)
}

oct2 <- function(age) {
  (age * 52) ^ 1 / ((age * 52) ^ 1 + 4.38 ^ 1)
}

# prediction error calculation:
# -----
PE<-function(a,b) (a-b) / b *100 # a- function to compare; b - function to
compare it to

# calculated allometric scaling coefficient (without GFR maturation func-
tion):
# -----
---
coeff <- function(cl_ped, cl_ad, wt_ped, wt_ad) {
  return(log(cl_ped/cl_ad)/log(wt_ped/wt_ad))
}

```


Estimation of ontogeny functions for renal transporters using a combined population pharmacokinetic and physiology-based pharmacokinetic approach: application to OAT3

S Cristea, EHJ Krekels, K Allegaert, P De Cock,
P De Paepe, A de Jaeger, CAJ Knibbe

AAPS J 23, 65 (2021)

Epub ahead of print, doi.org/10.1208/s12248-021-00595-9

6.1 Abstract

To date, information on the ontogeny of renal transporters is limited. Here we propose to estimate the *in vivo* ontogeny of transporters using a combined population pharmacokinetic (popPK) and physiology-based pharmacokinetic (PBPK) approach (popPBPK). Clavulanic acid and amoxicillin were used as probes for glomerular filtration and for combined glomerular filtration and active secretion through OAT3, respectively. The predictive value of the estimated OAT3 ontogeny function was assessed by PBPK predictions of renal clearance (CL_R) of other OAT3 substrates: cefazolin and piperacillin.

Individual CL_R post-hoc values, obtained from a published popPK model on the concomitant use of clavulanic acid and amoxicillin in children between 1 month to 15 years, were used as dependent variables in the popPBPK analysis. CL_R was re-parameterized according to PBPK principles, resulting in the estimation of OAT3-mediated intrinsic clearance ($CL_{int,OAT3,in vivo}$) and its ontogeny.

$CL_{int,OAT3,in vivo}$ ontogeny was described by a sigmoidal function, reaching half of adult level around 7 months of age, comparable to findings based on renal transporter-specific protein expression data. PBPK-based CL_R predictions including this ontogeny function were reasonably accurate for piperacillin in a similar age range (2.5 months – 15 years) as well as for cefazolin in neonates as compared to published data (%RMSPE of 21.2% and 22.8%, respectively and %PE within $\pm 50\%$).

Using this novel approach we estimated an *in vivo* ontogeny function for $CL_{int,OAT3,in vivo}$ that yields accurate CL_R predictions for different OAT3 substrates across different ages. This approach deserves further study on ontogeny of other transporters.

6.2 Introduction

Pediatric renal clearance (CL_R) is driven by physiology related changes to kidney size, number of glomeruli and nephron filtration capacity, renal blood flow, expression of drug binding plasma proteins and expression of transporters. Throughout the pediatric age-range, the maturation of glomerular filtration rate (GFR) has been extensively studied by various groups [1–6] however less is known about the development of other processes contributing to CL_R such as active tubular secretion (ATS), which is mediated through transporters in the kidneys.

Recently, the ontogeny of individual renal transporters has been quantified by directly measuring transporter-specific protein expressions in postmortem kidney samples from children of different ages [7]. However, there is limited information about how protein expression relates to *in vivo* transporter activity and whether this relationship remains constant with age. Alternatively, ontogeny of ATS has been quantified *in vivo* as net secretion of drugs with non-selective affinity for transporters. Net secretion aggregates the activity of all active secretion transporters involved in renal excretion and of reabsorption [3,8]. Since ontogeny patterns may differ between transporters, their relative contributions to CL_R will also differ throughout the pediatric age-range, as drugs may have a broad spectrum in transporter affinity and can be transported by one or more transporters at once. Therefore, it would be of relevance to separately quantify the ontogeny of each renal transporter *in vivo*.

Empirically, clinical pharmacokinetic (PK) data (i.e. concentration-time data) are analyzed using population PK (popPK) models. When analyzing pediatric PK data, the inter-individual variability in different parameters is driven by differences in underlying developing physiological processes. These differences are usually captured by a function that describes the relation between the individual deviations in parameter values from typical parameter values and a relatively small set of demographic variables that vary with age, i.e. covariate relation. In pediatric physiology-based PK (PBPK) modelling, quantitative knowledge on developing physiology is included a priori in functions that describe changes

in system-specific parameters. Subsequently, these models describe the interaction between drugs with certain physicochemical properties and this system. The parameters in a PBPK model can be derived from various data sources (e.g. in vitro experiments, clinical studies, etc.). Recently, combined popPK and PBPK (popPBPK) approaches have been proposed to derive physiological measures for PBPK models that cannot be obtained through direct measures, by leveraging concentration-time data [9]. When selecting drugs that are predominantly eliminated by one main pathway, inferences can be made regarding system-specific parameters that are particular for that pathway.

In this study, the ontogeny of *in vivo* renal organic anion transporter 3 (OAT3) activity was characterized with this popPBPK approach. To this end, PK data obtained in children of different ages after the concomitant administration of clavulanic acid and amoxicillin was used. Each drug was assumed a probe for their specific elimination pathway, i.e. clavulanic acid for glomerular filtration (GF) and amoxicillin for a combination of GF and ATS through OAT3 [10,11]. With this methodology the ontogeny function of OAT3 could be estimated. Its predictive value was assessed by including the ontogeny function in a pediatric PBPK model to predict CLR of two other OAT3 substrates including cefazolin and piperacillin.

6.3 Methods

6.3.1 Software

For the present analysis we used NONMEM v7.3 integrated with Pirana v2.9.9 for developing the model and R v3.5 integrated with RStudio for graphics and evaluation.

6.3.2 Quantifying the ontogeny function of OAT3 *in vivo*

Individual post-hoc CL_R values for clavulanic acid and amoxicillin in pediatric patients were obtained from a population PK model of De Cock et al. [12]. In short, a simultaneous popPK analysis was performed for both drugs based on data obtained after the administration of a fixed dose ratio of 1:10 (clavulanic acid : amoxicillin) in 50 intensive care pediatric patients with ages between 1 month and 15 years (median age of 2.6 years)[12]. The PK of clavulanic acid and amoxicillin were described by a two- and a three-compartment model, respectively, with inter-individual variability (IIV) on CL_R and central volume of distribution. The covariate analysis identified current weight as a statistically significant predictor for the IIV on both central volume of distribution and CL_R , whereas vasopressor treatment and cystatin C were found to be statistically significant predictors only for the IIV on CL_R [12].

In a sequential step, CL_R was re-parameterized according to PBPK principles to reflect clearance through glomerular filtration (CL_{GF}) and through active tubular secretion (CL_{ATS}). The PBPK-based model for CL_R assumes a serial arrangement for GF and ATS, in which CL_R of clavulanic acid was described by CL_{GF} only ($CL_{ATS} = 0$), while CL_R of amoxicillin was described by a combination of CL_{GF} and CL_{ATS} .

$$CL_R = CL_{GF} + CL_{ATS} = (GFR \times f_u) + \left(\frac{(Q_R - GFR) \times f_u \times CL_{sec,OAT3}}{Q_R + f_u \times \frac{CL_{sec,OAT3}}{BP}} \right) \quad [1]$$

$$CL_{sec,OAT3} = CL_{int,OAT3,in vivo} \times ont_{OAT3} \times PTCPGK \times KW \quad [2]$$

In equation 1, GFR stands for glomerular filtration rate, f_u for drug fraction unbound, Q_R for renal blood flow, $CL_{sec,OAT3}$ for secretion clearance through OAT3, and BP for blood to plasma ratio. Equation 2 shows how $CL_{sec,OAT3}$ is obtained by multiplying $CL_{int,OAT3,in vivo}$ that stands for OAT3-mediated *in vivo* intrinsic clearance in adults, with ont_{OAT3} that stands for the ontogeny function for OAT3, PTCPGK that stands for proximal tubule cells per gram kidney, and KW that stands for kidney weight in grams.

The adult PBPK-based model for CL_R through a combination of GF and ATS (equations 1 and 2) was extrapolated to the pediatric population. For this, published functions that describe the age-related changes of the system-specific parameters (i.e. GFR [14], renal blood flow [15], and kidney weight [15]) and of the drug-specific parameters impacted by changes in system-specific parameters (i.e. serum

albumin concentrations [4] that influence the fraction unbound [16], and hematocrit levels that influence BP [15]) were inputted, as shown in Table S6.1. Values for f_u [17] and BP_{amox} [18] as reported in adults were used ($f_{u,clav.acid} = 0.75$; $f_{u,amox} = 0.82$; $BP_{amox} = 0.55$). $CL_{int,OAT3,in vivo}$ reflects both the expression and activity of the OAT3 transporter in adults. Assuming PTCPGK to remain constant at adult values, this only leaves $CL_{int,OAT3,in vivo}$ and its ontogeny function (ont_{OAT3}) to be estimated. This was done using the individual CL_R values from the population model as dependent variables and deriving the system-specific PBPK parameters based on the individual patient characteristics for each patient.

Pediatric typical CL_{GF} values were obtained using a published GFR maturation function developed for children with a normal renal function [14]. However, when compared to normal CL_{GF} values, CL_R of both drugs as estimated with the population PK models, were found to be increased in the intensive care children included in the dataset of the current analysis [12]. Hence, the PBPK-based re-parameterization of CL_{GF} included a typical GF correction factor (θ_{corr}) with IIV (η_{GFR}) to account for this difference (equations 3).

$$CL_{R,clavulanic\ acid,i} = GFR \times f_{u,clav.\ acid} \times \theta_{corr} \times e^{\eta_{GFR}} \quad [3]$$

As both amoxicillin and clavulanic acid were administered simultaneously to each child, from the data on clavulanic acid the GF correction factor and IIV on GFR for each patient was estimated. According to equations 4 and 5, the difference between the individual values for CL_R of amoxicillin and CL_R of clavulanic acid were used to estimate CL_{AT3} , which was the basis for the estimation of the IIV on the *in vivo* $CL_{sec,OAT3}$ value and subsequently the OAT3 ontogeny function (ont_{OAT3}).

$$CL_{R,amoxicillin,i} = GFR \times f_{u,amox} \times \theta_{corr} \times e^{\eta_{GFR}} + \frac{(Q_R - GFR) \times f_{u,amox} \times CL_{sec,OAT3,i}}{Q_R + f_{u,amox} \times \frac{CL_{sec,OAT3,i}}{BP_{amox}}} \quad [4]$$

$$CL_{sec,OAT3,i} = \theta_{CLint,OAT3,in vivo} \times e^{\eta_{CLint,OAT3,in vivo}} \times ont_{OAT3} \times PTCPGK \times KW \quad [5]$$

To quantify the ontogeny profile of $CL_{int,OAT3,in vivo}$, different covariates (i.e. postnatal age, postmenstrual age, weight) were explored using sigmoid relationships (equation 6) or a simplification of this equation (i.e. an exponential equation). In equation 6, *hill* is the *hill* coefficient, which quantifies the steepness of the ontogeny slope and TM_{50} quantifies the age at which OAT3 reaches half of the adult value.

$$ont_{OAT3} = \frac{COV^{hill}}{COV^{hill} + TM_{50}^{hill}} \quad [6]$$

The statistical significance of including the ont_{OAT3} function in the equation for $CL_{sec,OAT3,i}$ to obtain CL_R of amoxicillin was assessed according to the likelihood ratio test on the difference in objective function value. Under the assumption of a χ^2 distribution, the objective function value of a model with one more degree of freedom had to be 3.84 points lower, with a corresponding $p < 0.05$ to indicate statistical significance [19]. For graphical goodness-of-fit, a plot was made to check for prediction bias of the individual CL_R values obtained either with the PBPK model or the individual post hoc values from the population PK model that served as the dependent variable in these fits. In addition, ETA (η_{GFR} , $\eta_{CLint,OAT3,in vivo}$) vs. covariate plots (age, weight) are made to check for structural accuracy in PK parameters.

6.3.2 Predictive properties of the OAT3 ontogeny function for new substrates

To assess the predictive performance of the obtained OAT3 maturation function, the PBPK model that includes the estimated ontogeny function for OAT3 (equations 1 and 2) was used for pediatric CL_R predictions of piperacillin and cefazolin, two other substrates of the OAT3 transporter. PBPK predictions of CL_R were compared to published pediatric CL_R values of the same drugs. To obtain the pediatric PBPK predictions for CL_R , we collected literature values for f_u , adult of 0.8 (20) and 0.31 (18) for piperacillin and cefazolin, respectively and for BP adult of 0.55 for both drugs. $CL_{int,OAT3,in vivo}$ in equation 2 had to be derived first for both drugs. This was done based on published *in vitro* activity data as measured in assays with OAT3 transfected cells (1.95 μ l/min/mg protein [20] and 7.1 μ l/min/mg protein [18] for piperacillin and cefazolin respectively). These values were used as input for *in vitro-in vivo* extrapolation

(IVIVE). More details on IVIVE are provided in the supplemental materials.

The drug-specific $CL_{int,OAT3, in vivo}$ values obtained in the IVIVE step were used in equations 1 and 2 of the renal PBPK model to obtain pediatric CL_R predictions for cefazolin and piperacillin. Pediatric CL_R predictions for piperacillin and cefazolin were made for typical individuals with the same demographic characteristics as the individual patients reported in the original publications describing the pediatric population PK models of these drugs [12],[21]. This means that, for piperacillin, typical CL_R values were estimated for 47 pediatric patients with ages between 2.5 months and 15 years (median age of 2.83 years). For cefazolin, the typical CL_R values were estimated for 26 near-term neonates with gestational age higher than 35 weeks and postnatal age (PNA) between 1 – 30 days (median of 8 days). For this, the OAT3 ontogeny function obtained above for children of 1 month and older based on data from clavulanic acid and amoxicillin was extrapolated to the neonatal population.

Pediatric PBPK CL_R predictions were visually and quantitatively compared to typical estimates obtained with published population PK models for these two OAT3 substrates. Precision was quantified as percentage root mean square prediction error (%RMSPE) (equation 7) and bias as percentage prediction error (%PE) (equation 8).

$$\%RMSPE = \sqrt{\frac{1}{N} \times \sum_{i=1}^N \left(\frac{CL_{R,PBPK} - CL_{R,reference}}{CL_{R,reference}} \right)^2} \times 100 \quad [7]$$

$$\%PE = \left(\frac{CL_{R,PBPK} - CL_{R,reference}}{CL_{R,reference}} \right) \times 100 \quad [8]$$

In both equations, $CL_{R,PBPK}$ are the CL_R predictions obtained with the renal PBPK model in pediatrics and $CL_{R,reference}$ represents the CL_R values for typical CL_R predictions obtained with the published population PK models [21,22]. %RMSPE and %PE were calculated separately for piperacillin and cefazolin and reported overall as well as per age group. CL_R was considered to be accurately predicted if %RMSPE and %PE was within $\pm 30\%$, reasonably accurately predicted between -30% – -50% and 30% – 50% and inaccurate when %RMSPE and %PE were outside $\pm 50\%$. Note that %RMSPE can only take positive values.

6.4 Results

6.4.1 Quantifying the ontogeny function of OAT3

With the popPBPK approach, CL_{GF} was separated from CL_{ATS} such that $CL_{int,OAT3, in vivo}$ and its ontogeny profile could be estimated in children as young as 1-month up to 15 years of age. Figure 6.1 shows the ontogeny profile of OAT3 as best described by a sigmoidal relationship based on PNA. $CL_{int,OAT3, in vivo}$ was estimated to be 15.8 ml/h/g kidney (RSE% of 5%) at 15 years with an IIV of 78.5%. This high IIV suggests large differences between individual values obtained for $CL_{int,OAT3, in vivo}$. $CL_{int,OAT3, in vivo}$ was found to reach half of the adult capacity at a PNA of 27.3 weeks (RSE of 28%), which is around 7 months. The rapid ontogeny of OAT3 was captured by a *hill* exponent of 1.17 (%RSE of 36%). The estimated transporter ontogeny fractions range from 0.1 at 1 month and 1 at 15 years. The GF correction factor used to account for the increased CL_R in intensive care children was estimated at 1.83 (RSE of 4%) with an IIV of 24.4%.

The goodness-of-fit plots did not show any bias for CL_R predictions obtained with CL_R re-parameterized according to PBPK principles. Neither Figure S6.1, which depicts popPBPK CL_R predictions vs. the popPK CL_R predictions, nor Figure S6.2, which depicts the η_{GF} and $\eta_{CL_{int,OAT3, in vivo}}$ vs. covariates (i.e. weight and age) show any bias. This suggests that the PBPK-based re-parameterization as CL_{GF} (equation 3) can predict individual clavulanic acid CL_R values accurately and that the reparameterization for CL_{GF} together with CL_{ATS} (equation 4) can accurately predict the CL_R of amoxicillin as excreted by GF and ATS through OAT3.

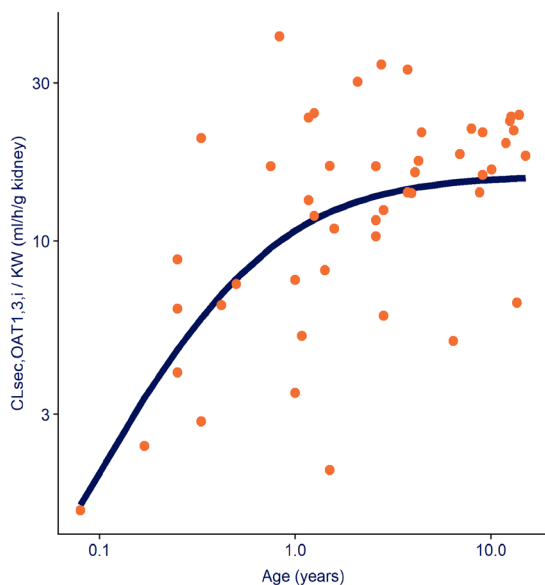


Figure 6.1 Ontogeny function for OAT3-mediated intrinsic clearance normalized by kidney weight ($CL_{sec,OAT3}$ – blue line) described by a sigmoidal function based on age and displayed throughout the studied pediatric age-range (1 month to 15 years), on a double-log scale. The orange dots represent the individual secretion clearance estimates normalized by kidney weight. See equation [5] for more details.

Figure 6.2 shows the total CL_R for amoxicillin and the contribution of CL_{GF} and CL_{ATS} to CL_R for each individual. Total CL_R increases almost 7-fold between neonates younger than 1 year and children of 10 years and older (median of 1.64 L/h and 12 L/h respectively). The median contribution of ATS to amoxicillin CL_R for the studied pediatric population was 22% (range: 4%–40%). Even if variability in ATS contribution was high within groups of individuals with similar ages, the ATS contribution increased with age, on average, from 14% in children younger than 1 year to 18% in children of 1–2 years, 21% for children of 2–5 years, 24% for children 5–10 years, reaching 29% for children older than 10 years.

6.4.2 Predictive properties of the OAT3 ontogeny function for new substrates

Figure 6.2 shows the pediatric CL_R predictions for piperacillin and cefazolin obtained with the PBPK-based model and the identified OAT3 ontogeny function based on clavulanic acid and amoxicillin overlaid with the typical clearance estimates obtained

with the published population PK models. The %RMSPE calculated between PBPK CL_R and typical CL_R predictions for piperacillin (Figure 6.3A) over the entire age-range (2.5 months to 15 years) was 21.8% with a %PE interval between –33.2%–25.4%. When stratified per age groups (i.e. younger than 1 year, 1–2 years, 2–5 years, 5–10 years and older than 10 years) %RMSPE is generally higher for children under 5 years (23.3%, 22.2%, and 27.4% vs. 14.9%, 18.8%). For neonates (Figure 6.3B), the %RMSPE calculated between PBPK CL_R and typical CL_R predictions for cefazolin was 22.2% with %PE interval between –34.4%–46%.

For both pediatric populations the PBPK-based CL_R predictions can be considered reasonably accurate

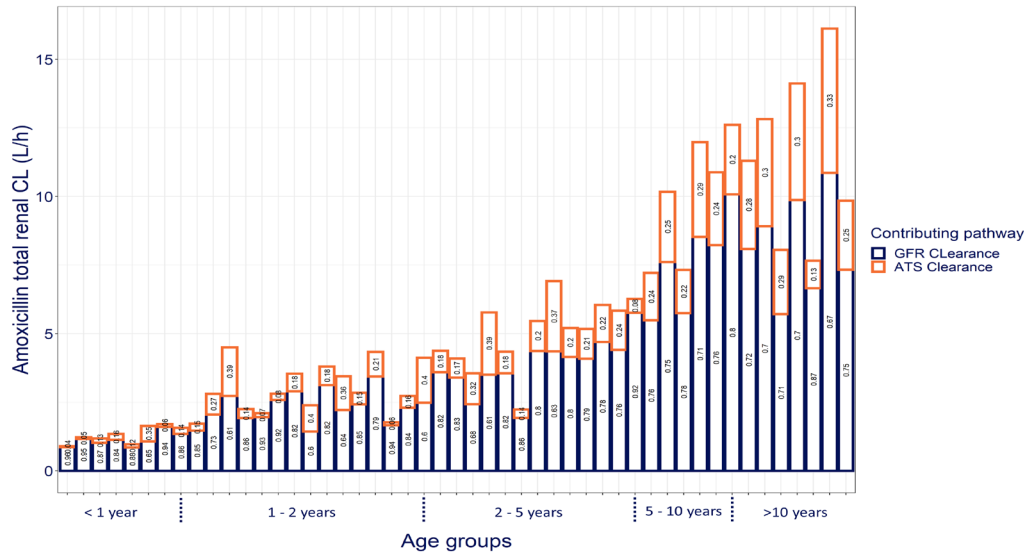


Figure 6.2 Contribution of clearance through glomerular filtration (CL_{GF} – bottom blue boxes) and through active tubular secretion (CL_{ATS} – top orange boxes) to total renal clearance of amoxicillin (CL_R – sum of blue and orange boxes) for each pediatric patient of the studied population sorted and grouped by age. The numbers in each box show the relative contribution of CL_{GF} and CL_{ATS} to total CL_R for each individual

with %RMPE < 30% and %PE within $\pm 50\%$. For piperacillin, the PBPK-based CL_R predictions tend towards overprediction (Figure 6.3A), with all %PE values below 0% although percentages deviation were acceptable [%PE between -13.3% and -28.8%] for children older than 1 year. For cefazolin in neonates, predictions are reasonably accurate (Figure 6.3B), with PBPK-based CL_R predictions tending towards underprediction [%PE between 18.1% and 46%] for children older than 10 days.

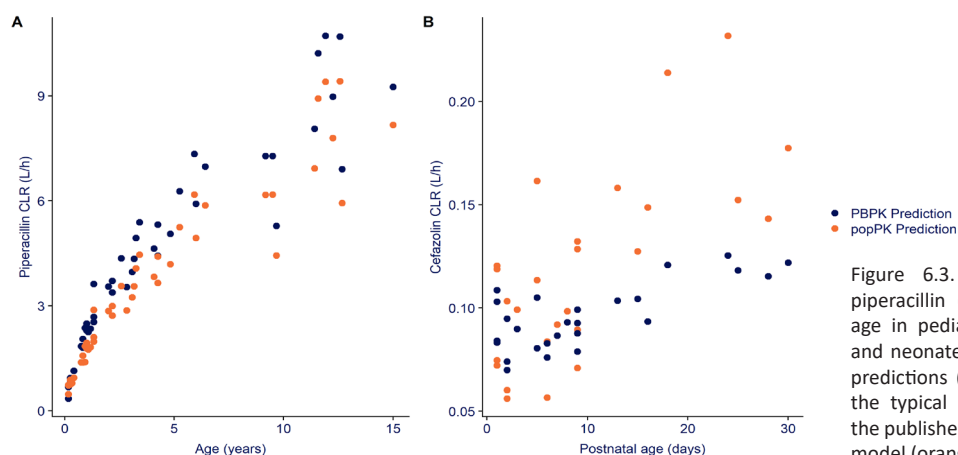


Figure 6.3. Renal clearance (CL_R) of piperacillin (A) and cefazolin (B) versus age in pediatric patients in children (A) and neonates (B). The pediatric PBPK CL_R predictions (dark blue) are overlaid with the typical CL_R estimates obtained with the published population pharmacokinetic model (orange).

6.5 Discussion

With a combined population PK with PBPK approach we estimated the *in vivo* ontogeny function for OAT3, a parameter that cannot be obtained through direct measurements, down to the age of 1 month. With the clinical data available for both clavulanic acid – a descriptor for GF- and amoxicillin – a descriptor for GF and ATS through OAT3- after administration to the same patients simultaneously, we were able to separate the ontogeny in both of these processes. Using a population PK approach, we derived the individual CL_R values for both drugs that served as dependent variable for the popPBPK approach. CL_R was re-parameterized according to PBPK principles to take advantage of existing information about drug- and system-specific properties while estimating the ontogeny of OAT3 *in vivo* and the variability on GFR and on OAT3-mediated intrinsic clearance *in vivo* ($CL_{int,OAT3, in vivo}$).

OAT3 ontogeny for the OAT3-mediated intrinsic clearance is steep in the first year of life, attaining half of the adult value around 7 months of age. This estimated ontogeny function was included in the pediatric PBPK-based model for CL_R through GF and ATS and predicted the CL_R for other drugs that are substrates for OAT3 reasonably accurate, as compared to popPK CL_R predictions for these drugs. Assuming clearance to be only mediated by GF and ATS, for piperacillin the PBPK CL_R predictions over an age-range of 2.5 months to 15 years lead to a %RMSPE of 21.8% [%PE: -33.2%– 25.4%] with a trend towards over-prediction for children older than 1 year. For cefazolin, extrapolation of CL_R predictions to near term neonates with ages between 1- and 30-days lead to a %RMSPE of 22.2% [%PE: -34.4%– 46%], with a trend towards under-prediction for children older than 10 days.

Recently, ontogeny profiles of renal transporters have been quantified based on direct measurements of the expression of transporter-specific proteins in kidney samples taken postmortem from children of various ages, as described in detail by Cheung *et al.* [7]. This group characterized the ontogeny of OAT3 as a sigmoidal function based on PNA in weeks with children reaching half of the adults values around 8 months of age (TM50 = 30.7 weeks [95% CI: 16.64 – 50.97]) and the steepness of the ontogeny slope given by a *hill* coefficient of 0.51 (95% CI: 0.35 – 0.71). While our findings align with Cheung *et al.* regarding the age at which half of the adult level is reached, which was estimated to be around 7 months with our function, we found a steeper ontogeny for OAT3, as shown by a 2-fold higher estimated *hill* coefficient. The impact of these differences on the ontogeny profiles is illustrated in Figure 6.4. This figure shows relatively similar OAT3 ontogeny found by both methods at ages above the TM50 values, but for younger ages the function quantified in our work shows lower ontogeny values. Given the

relatively low number of observed values in both analyses at these younger ages, the uncertainty around the ontogeny below 7 months of age is high for both analyses.

The ontogeny function for OAT3 found in our analysis was included in the pediatric PBPK-based model for CL_R through GF and ATS and used to predict pediatric CL_R for two other substrates for OAT3, namely piperacillin and cefazolin. Despite small trends towards over and under-prediction respectively,

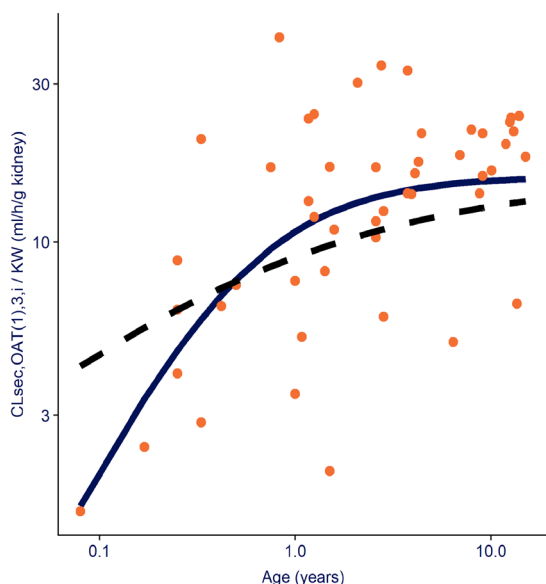


Figure 6.4 Ontogeny functions for OAT3-mediated intrinsic clearance normalized by kidney weight ($CL_{\text{int,OAT3, in vivo}}$) throughout the studied pediatric age-range (1 month to 15 years). The solid line shows the sigmoidal function estimated in the current analysis whereas the dashed line shows the function as published by Cheung *et al.* [7]. The orange dots represent the individual secretion clearance estimates normalized by kidney weight derived from amoxicillin CL_R values obtained with the current analysis. See equation [5] for more details.

CL_R predictions for piperacillin and cefazolin were reasonably accurate with %RMSPE of 21.8% and 22.2%, which is well below the 2-fold error, which is the generally accepted criterion for accuracy of PBPK predictions. The tendency towards over-prediction of pediatric PBPK CL_R for piperacillin could be explained by other processes involved in renal elimination that are not accounted for in the PBPK model. It could, for instance, be that there is passive or active reuptake of these drugs in the kidneys. Alternatively, the authors of the popPK model that served as the reference values, reported a (temporary) impairment of the renal maturation function [22] which could explain the lower CL_R values obtained with the popPK model as compared to the PBPK CL_R predictions, the latter of which does not take (potential) renal impairment into account. A second drug, cefazolin, was used to assess the accuracy of this function for extrapolations to term newborns below 1 month of age. Remarkably, despite a small trend towards under-prediction of CL_R values for cefazolin in part of the newborns, all predictions can still be considered accurate.

Our group recently developed a PBPK simulation framework for investigating the impact of ontogeny of renal secretion transporters on CL_R by predicting pediatric CL_R for hypothetical drugs with an array of drug properties [23]. By looking at the difference between PBPK CL_R predictions with or without inclusion of the ontogeny function, probe drugs for quantifying the ontogeny of transporters were identified. According to the findings with this framework, amoxicillin, which has an estimated $CL_{\text{int,OAT3, in vivo}}$ of 4.4 $\mu\text{l}/\text{min}/\text{mg}$ protein and a f_u of 0.82 [24], has the potential of serving as a probe to quantify OAT3 ontogeny. Furthermore, the clinical data available for probe drugs for GF and a combination of GF and ATS (clavulanic acid and amoxicillin, respectively) administrated to the same individuals was paramount to separate between these two processes.

6.6 Conclusion

The ontogeny of *in vivo* OAT3 activity was quantified by using a combined population PK and PBPK approach. This popPBPK approach leverages the knowledge on underlying physiological processes included in PBPK models and information carried by individual PK parameters as quantified with a population approach, to derive parameters that cannot be measured *in vivo*. With this methodology we derived the renal OAT3 transporter ontogeny *in vivo*. This ontogeny function was included in the pediatric PBPK-based model CL_R for two other OAT3 substrates and on average predicted CL_R throughout the entire pediatric age-range accurately. This methodology could be applied to other transporters substrates to characterize the *in vivo* ontogeny of the remaining renal transporters to further increase our understanding on renal development and increase the accuracy in predicting pediatric CL_R .

6.7 Acknowledgements

The authors would like to thank Dr. Parth Upadhyay for reviewing the code that was used for the analysis presented in this manuscript.

6.8 References

1. Rhodin MM, Anderson BJ, Peters a. M, Coulthard MG, Wilkins B, Cole M, Chatelut E, Grubb A, Veal GJ, Keir MJ, Holford NHG (2009) Human renal function maturation: A quantitative description using weight and postmenstrual age. *Pediatr Nephrol* 24:67–76 . <https://doi.org/10.1007/s00467-008-0997-5>
2. Salem F, Johnson TN, Abduljalil K, Tucker GT, Rostami-Hodjegan A (2014) A re-evaluation and validation of ontogeny functions for cytochrome P450 1A2 and 3A4 based on in vivo data. *Clin Pharmacokinet*. <https://doi.org/10.1007/s40262-014-0140-7>
3. Hayton WL (2000) Maturation and growth of renal function: dosing renally cleared drugs in children. *AAPS PharmSci* 2:E3 . <https://doi.org/10.1208/ps020103>
4. Johnson TN, Rostami-Hodjegan A, Tucker GT (2006) Prediction of the clearance of eleven drugs and associated variability in neonates, infants and children. *Clin Pharmacokinet* 45:931–956 . <https://doi.org/10.2165/00003088-200645090-00005>
5. Mahmood I (2014) Dosing in children: A critical review of the pharmacokinetic allometric scaling and modelling approaches in paediatric drug development and clinical settings. *Clin Pharmacokinet* 53:327–346 . <https://doi.org/10.1007/s40262-014-0134-5>
6. De Cock RFW, Allegaert K, Brussee JM, Sherwin CMT, Mulla H, De Hoog M, Van Den Anker JN, Danhof M, Knibbe C a J (2014) Simultaneous pharmacokinetic modeling of gentamicin, tobramycin and vancomycin clearance from neonates to adults: Towards a semi-physiological function for maturation in glomerular filtration. *Pharm Res* 31:2643–2654 . <https://doi.org/10.1007/s11095-014-1361-z>
7. Cheung KWK, van Groen BD, Spaans E, van Borselen MD, de Bruijn ACJM, Simons-Oosterhuis Y, Tibboel D, Samsom JN, Verdijk RM, Smeets B, Zhang L, Huang SM, Giacomini KM, de Wildt SN (2019) A Comprehensive Analysis of Ontogeny of Renal Drug Transporters: mRNA Analyses, Quantitative Proteomics, and Localization. *Clin Pharmacol Ther*. <https://doi.org/10.1002/cpt.1516>
8. Rubin MI, Bruck E, Rapoport M, Snively M, McKay H, Baumler a (1949) Maturation of Renal Function in Childhood: Clearance Studies. *J Clin Invest* 28:1144–62 . <https://doi.org/10.1172/JCI102149>
9. Tsamandouras N, Rostami-Hodjegan A, Aarons L (2015) Combining the “bottom up” and “top down” approaches in pharmacokinetic modelling: Fitting PBPK models to observed clinical data. *Br J Clin Pharmacol*. <https://doi.org/10.1111/bcp.12234>
10. Parvez MM, Kaiser N, Shin HJ, Jae Lee Y, Shin J-G (2018) Comprehensive Substrate Characterization of 22 Antituberculosis Drugs for Multiple Solute Carrier (SLC) Uptake Transporters In Vitro. *Antimicrob Agents Chemother* 62:1–12
11. Horber FF, Frey FJ, Descroedres C, Murray AT, Reubi FC (1986) Differential effect of impaired renal function on the kinetics of clavulanic acid and amoxicillin. *Antimicrob Agents Chemother*. <https://doi.org/10.1128/AAC.29.4.614>
12. De Cock PAJG, Standing JF, Barker CIS, De Jaeger A, Dhont E, Carlier M, Verstraete AG, Delanghe JR, Robays H, De Paepe P (2015) Augmented Renal Clearance Implies a Need for Increased Amoxicillin-Clavulanic Acid Dosing in Critically Ill Children. *Antimicrobial Agents and Chemotherapy* Oct 2015, 59 (11) 7027-7035; DOI: 10.1128/AAC.01368-15
13. Salem F, Johnson TN, Abduljalil K, Tucker GT, Rostami-Hodjegan A (2014) A re-evaluation and validation of ontogeny functions for cytochrome P450 1A2 and 3A4 based on in vivo data. *Clin Pharmacokinet* 53:625–636 . <https://doi.org/10.1007/s40262-014-0140-7>

14. Simcyp (a Certara Company) (2018) Simcyp v18
15. McNamara PJ, Alcorn J (2002) Protein binding predictions in infants. *AAPS PharmSci*. <https://doi.org/10.1208/ps040104>
16. FDA Augumentin ES-600: Prescribing information. https://www.accessdata.fda.gov/drugsatfda_docs/label/2009/050755s014lbl.pdf
17. Mathialagan S, Piotrowski MA, Tess DA, Feng B, Litchfield J, Varma M V. (2017) Quantitative prediction of human renal clearance and drug-drug interactions of organic anion transporter substrates using in vitro transport data: A relative activity factor approach. *Drug Metab Dispos*. <https://doi.org/10.1124/dmd.116.074294>
18. Nguyen THT, Mouksassi MS, Holford N, Al-Huniti N, Freedman I, Hooker AC, John J, Karlsson MO, Mould DR, Perez Ruixo JJ, Plan EL, Savic R, Van Hasselt JGC, Weber B, Zhou C, Comets E, Mentre F (2017) Model evaluation of continuous data pharmacometric models: Metrics and graphics. *CPT Pharmacometrics Syst Pharmacol*. <https://doi.org/10.1002/psp4.12161>
19. Wen S, Wang C, Duan Y, Huo X, Meng Q, Liu Z, Yang S, Zhu Y, Sun H, Ma X, Yang S, Liu K (2018) OAT1 and OAT3 also mediate the drug-drug interaction between piperacillin and tazobactam. *Int J Pharm*. <https://doi.org/10.1016/j.ijpharm.2017.12.037>
20. De Cock RFW, Smits a., Allegaert K, de Hoon J, Saegeman V, Danhof M, Knibbe C a J (2014) Population pharmacokinetic modelling of total and unbound cefazolin plasma concentrations as a guide for dosing in preterm and term neonates. *J Antimicrob Chemother* 69:1330–1338 . <https://doi.org/10.1093/jac/dkt527>
21. De Cock PAJG, van Dijkman SC, de Jaeger A, Willems J, Carlier M, Verstraete AG, Delanghe JR, Robays H, Walle J Vande, Della Pasqua OE, De Paepe PD (2017) Dose optimization of piperacillin/tazobactam in critically ill children. *J Antimicrob Chemother* 72:2002–2011 . <https://doi.org/10.1093/jac/dkx093>
22. Cristea S, Calvier EAM, Rostami-Hodjegan A, Krekels EHJ, Knibbe CAJ (2015) Impact of renal transporters on pediatric renal clearance using PBPK modelling Discover the World at Leiden University. 2015
23. FDA (2008) AUGMENTIN® (amoxicillin/clavulanate potassium) Powder for Oral Suspension and Chewable Tablets. https://www.accessdata.fda.gov/drugsatfda_docs/label/2008/050575s037550597s044050725s025050726s019lbl.pdf
24. T'jollyn H, Snoeys J, Van Bocxlaer J, De Bock L, Annaert P, Van Peer A, Allegaert K, Mannens G, Vermeulen A, Boussery K (2017) Strategies for Determining Correct Cytochrome P450 Contributions in Hepatic Clearance Predictions: In Vitro–In Vivo Extrapolation as Modelling Approach and Tramadol as Proof-of Concept Compound. *Eur J Drug Metab Pharmacokinet*. <https://doi.org/10.1007/s13318-016-0355-0>
25. Brill MJE, Houwink API, Schmidt S, Van dongen EP a, Hazebroek EJ, Van ramshorst B, Deneer VH, Mouton JW, Knibbe C a J (2014) Reduced subcutaneous tissue distribution of cefazolin in morbidly obese versus non-obese patients determined using clinical microdialysis. *J Antimicrob Chemother* 69:715–723 . <https://doi.org/10.1093/jac/dkt444>
26. Butterfield JM, Lodise TP, Beegle S, Rosen J, Farkas J, Pai MP (2014) Pharmacokinetics and pharmacodynamics of extended-infusion piperacillin/tazobactam in adult patients with cystic fibrosis-related acute pulmonary exacerbations. *J Antimicrob Chemother*. <https://doi.org/10.1093/jac/dkt300>

6.9 Supplementary material

Table S6.1 Functions describing age-related changes of system-specific parameters and variables required by the PBPK model for pediatric CL_R predictions

System-specific parameters for equation [1] (abbreviation) [units]	Maturation functions included in the pediatric PBPK model for CL _R
Glomerular filtration rate (GFR) [ml/min]	$GFR = 112 \times \left(\frac{WT}{70}\right)^{0.63} \times \left(\frac{PMA^{3.3}}{PMA^{3.3} + 55.4^{3.3}}\right)$
Fraction unbound (fu) [-]	$[HSA]_{ped/adult} = 1.1287 \times \ln(AGE) + 33.746$ $f_{u,clav.acid} = 0.75; f_{u,amox.} = 0.82 \text{ (adult values)}$ $\rightarrow f_{u,ped} = \frac{1}{1 + \frac{(1-f_{u,drug}) \times [HSA]_{ped}}{[HSA]_{adult} \times f_{u,drug}}}$
Renal blood flow (QR) [ml/min]	$CO = BSA \times (110 + 184 \times e^{-0.0378 \times AGE} - e^{-0.24477 \times AGE})$ $fr = \frac{fr_{males} + fr_{females}}{2}$ $fr_{males} = 4.53 + \left(14.63 \times \frac{AGE}{0.1888 + AGE}\right)$ $fr_{females} = 4.53 + \left(13 \times \frac{AGE^{1.15}}{0.188^{1.15} + AGE^{1.15}}\right)$ $\rightarrow QR = CO \times fr$
Intrinsic secretion CL (CL _{sec,OAT3}) [mL/min]	$PTCPKG = 60 \text{ (adult value)}$ $KW = 1050 \times (4.214 \times WT^{0.823} + 4.456 \times WT^{0.795}) / 1000$ $\rightarrow CL_{sec,OAT3} = CL_{int,OAT3,in vivo} \times ont_{OAT3} \times PTCPKG \times KW$
Blood to plasma ratio (BP _{amoxicillin}) [-]	$hemat = \frac{hemat_{male} + hemat_{female}}{2}$ $hemat_{male} = 53 - \left(\left(43 \times \frac{AGE^{1.12}}{0.05^{1.12} + AGE^{1.12}} \right) \times \left(1 + \left(-0.93 \times \frac{AGE^{0.25}}{0.10^{0.25} + AGE^{0.25}} \right) \right) \right)$ $hemat_{female} = 53 - \left(\left(37.4 \times \frac{AGE^{1.12}}{0.05^{1.12} + AGE^{1.12}} \right) \times \left(1 + \left(-0.80 \times \frac{AGE^{0.25}}{0.10^{0.25} + AGE^{0.25}} \right) \right) \right)$ $\rightarrow BP = 1 + hemat \times (f_u \times k_p - 1)$

WT – bodyweight [kg]

PMA – postmenstrual age [weeks]

[HSA] – human serum albumin [g/L]

CO – cardiac output [mL/min]

hemat – hematocrit

fr – fraction of cardiac output directed to renal artery

AGE – age in [days] for the maturation of [HSA] and in [years] for the fraction of cardiac output and hematocrit levels

BSA – body surface area (m²)

PTCPKG – proximal tubule cells per gram kidney [x 106 cells]

KW – kidney weight [g]

ont_{OAT3} – OAT3 ontogeny relative to adult levels [-]

CL_{int,OAT3} – OAT3-mediated active clearance [mL/min]

k_p – blood-to-plasma partitioning coefficient of a drug

S6.8.1 In vitro – in vivo extrapolation (IVIVE)

The CL_{int,OAT3,in vivo} values required for the PBPK-based model for CL_R (equation 1 and 2 of the main document), were obtained following *in vitro-in vivo* extrapolation, as shown in equation S1. Published *in vitro* values for OAT3-mediated intrinsic clearance (CL_{int,OAT3,in vitro}) for piperacillin and cefazolin [20],[18] obtained from tissue samples from adults (Table 6.8.1.1), were extrapolated to CL_{int,OAT3,in vivo} based on the protein expression correction factor (relative active factor (RAF)) between the OAT-transfected cells in the *in vitro* assay and the in proximal tubule cells and an activity adjustment factor (AAF).

$$CL_{int,OAT3,in vivo} = CL_{int,OAT3,in vitro} \times \text{protein correction} \times \text{RAF} \times \text{AAF}, \quad [S1]$$

In equation S1, protein correction represents the total amount of proteins in 106 cells obtained from the *in vitro* sample, under the assumption that 106 cells from this sample is equivalent to 106 proximal tubule cells in the kidney. RAF is an activity correction factor between the *in vitro* and the *in vivo* OAT3 transporter activity. These first two parameters are specific to the *in vitro* assay and independent of the

studied drug. AAF is the activity adjustment factor, which is included as a correction factor for $CL_{int,OAT3,in\ vitro}$ to account for the discrepancy between the CL_R obtained with adult PBPK model and the reported CL_R values in literature [25].

For performing IVIVE, a protein expression value of 0.25 mg protein per 106 Human Embryonic Kidney 293 (HEK293) OAT-transfected cells was used as measured and reported by Mathialagan [18] for their uptake assay [18]. For cefazoline, $CL_{int,OAT3,in\ vitro}$ was measured by the same group, whereas for piperacillin this value was obtained from a similar system but developed by another research group (Wen et al. [20]). Since the protein expression value is not reported for Wen et al. [20], the protein expression value was assumed to be the same between cell systems and included as such for the IVIVE.

The RAF value used for OAT3 was previously determined by Mathialagan [18] by using selective substrates for OAT transporters to account for the difference between the scaled *in vitro* and *in vivo* intrinsic secretion clearance ($CL_{sec,OAT}$ – equation 2 of the main document). For OAT3, the reported value was 4.6 and this drug-independent value was included as such in equation S1.

AAF was obtained by back-calculation to match the literature values collected for CL_R . Using the literature adult CL_R , the PBPK model was then solved for $CL_{sec,OAT3}$ as shown in equation S2A. The result was used in equation S3A, which was solved for $CL_{int,OAT3,in\ vivo}$. The obtained $CL_{int,OAT3,in\ vivo}$ was used as input in equation S4A, solved for AAF. This factor was then multiplied with the relevant parameter to obtain the *in vivo* OAT3-mediated intrinsic clearance. AAF accounts for any activity differences between *in vitro* assays and *in vivo* derived activity in adults [25].

$$CL_{R,lit.} = f_u \times GFR + \frac{(Q_R - GFR) \times f_u \times CL_{sec,OAT3}}{Q_R + f_u \times \frac{CL_{sec,OAT3}}{BP}} \quad [S2]$$

$$CL_{sec,OAT3} = \frac{(CL_{R,lit.} - f_u \times GFR) \times Q_R}{((Q_R - GFR) \times f_u - (CL_R - f_u \times GFR) \times \frac{f_u}{BP})} \quad [S2A]$$

$$CL_{sec,OAT3} = ont_{OAT3} \times CL_{int,OAT3} \times PTCPGK \times KW \quad [S3]$$

$$CL_{int,OAT3} = \frac{CL_{sec,OAT3}}{ont_{OAT3} \times PTCPGK \times KW} \quad [S3A]$$

$$CL_{int,OAT3,in\ vivo} = CL_{int,OAT3,in\ vitro} \times protein\ expression \times RAF \times AAF, \quad [S4]$$

$$AAF = \frac{CL_{int,OAT3,in\ vivo}}{CL_{int,OAT3,in\ vitro} \times protein\ expression \times RAF} \quad [S4A]$$

The drug-specific parameters required as input for the PBPK-based model (i.e. f_u and BP) were collected from literature for each drug [26,27] (Table S6.2). Literature values of adult CL_R for cefazolin and piperacillin were collected together with the reported median values of the demographic characteristics in these reports (i.e. weight, age) (Table S6.2), as these values were needed to derive the system-specific parameters required in equations S2 and S3 (i.e. GFR, QR, KW, HSA concentration). As the PBPK model is for adults, ont_{OAT3} was fixed at the adult level ($ont_{OAT3} = 1$). The $CL_{int,OAT3,in\ vivo}$ obtained after the IVIVE step in adults was included in the pediatric PBPK model for CL_R .

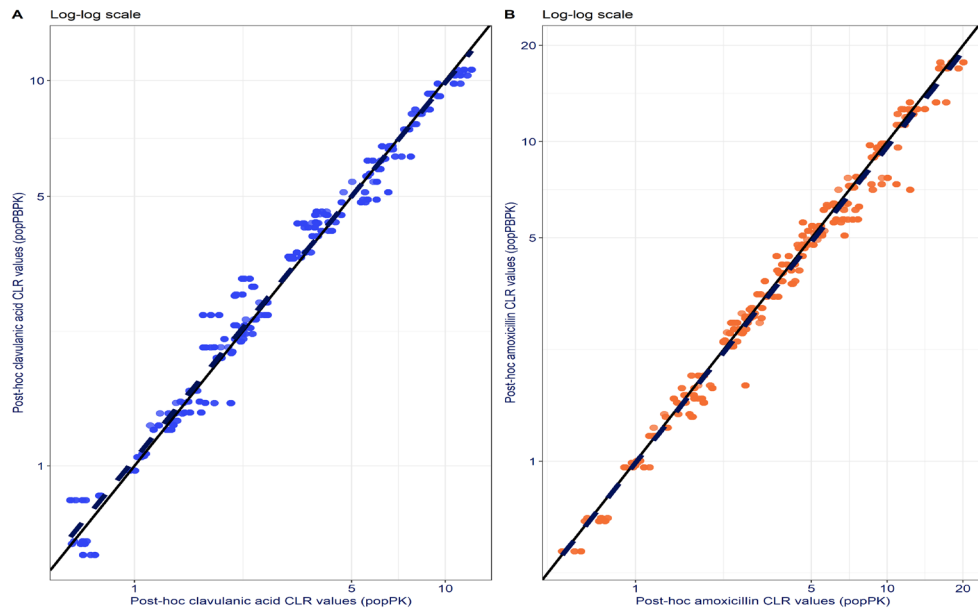


Figure S6.1 Individual post-hoc CL_R predictions of clavulanic acid (left panel) and amoxicillin (right panel) obtained with the population PK approach vs. individual post-hoc CL_R predictions obtained with the combined population and PBPK approach (popPBPK). A line of identity (solid line) and a linear regression line (dashed line) are added to the graph. The data points are scattered around the line of identity without bias. Plots are on a double-log scale.

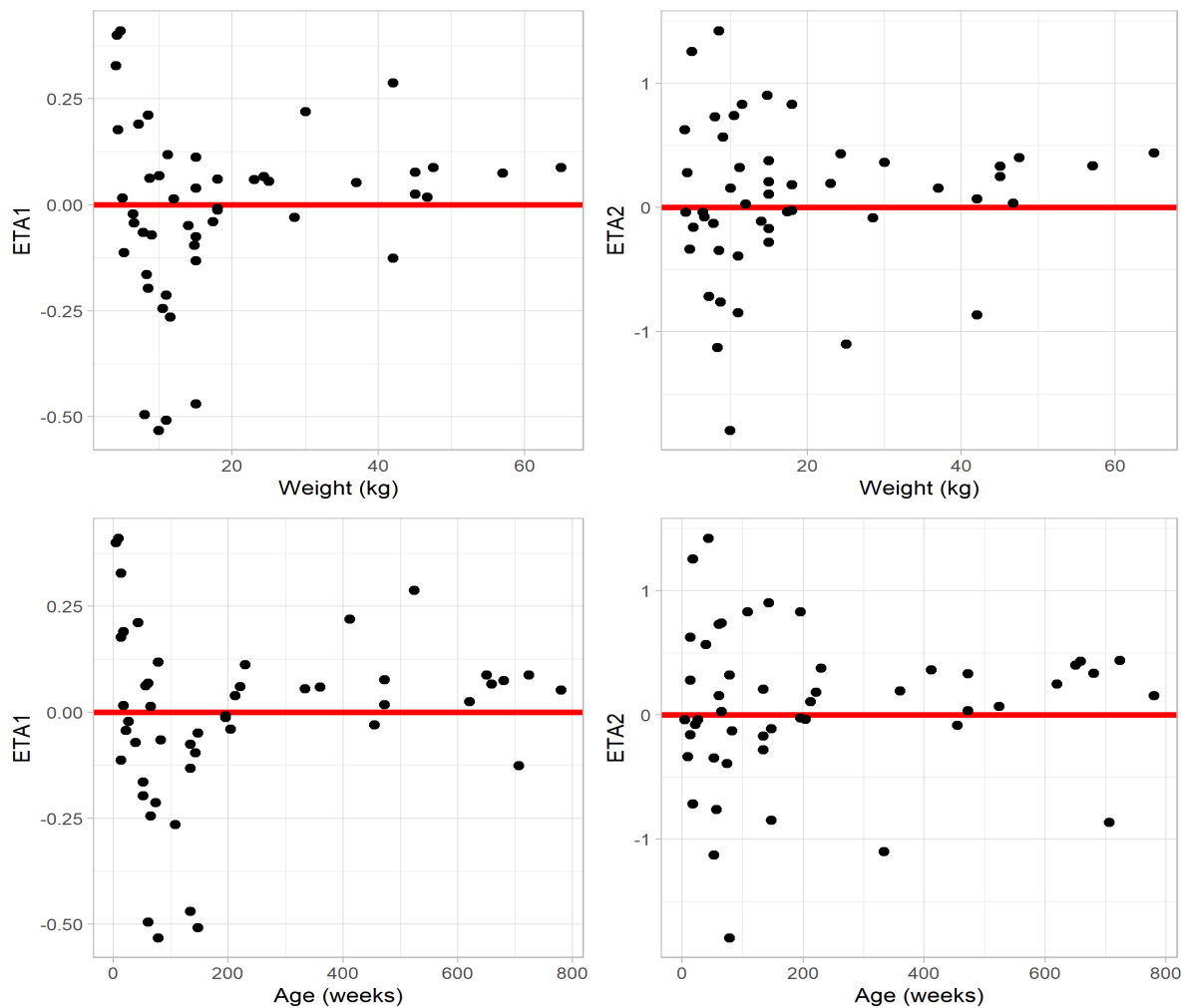


Figure S6.2 ETA vs. covariates correlation plots. This shows the correlation between $\eta_{CL_{int,OAT3,in vivo}}$ (ETA1) and η_{GFR} (ETA2) as estimated with the popPBPK approach and weight and postnatal age in weeks, in the model including the ontogeny function for OAT3. Red line is the zero line, the theoretical mean of the ETAs

Table S6.2 Adult demographic characteristics and drug-specific parameters used for PBPK-based CL_R predictions as well as published typical CL_R values for adults as obtained with popPK models, for piperacillin and cefazolin.

		Piperacillin value [unit]	Cefazolin value [unit]
Demographic characteristics	Weight	53.6 [kg]	109 [kg]
	Age	33 [years]	47 [years]
Drug-specific parameter	$CL_{int,OAT3, \text{ in vitro}}$	1.95 [$\mu\text{l}/\text{min}/\text{mg protein}$][20]	7.1 [$\mu\text{l}/\text{min}/\text{mg protein}$][18]
CL_R values	Total CL_R (literature)	13.6 [L/h](27)	4.5 [L/h](26)
	Activity adjustment factor (AAF)	11.6	0.65

6.10 NONMEM model code

```

$PROBLEM Estimation of transporters ontogeny
$INPUT ID TIME DV MDV CL3i CL4i CL5i V1i V2i V3i V4i V5i DOSN SEX AGE PMA
LENGTH WT BSA PRISM PELOD BLQ CMT COVCYS1i COVCYS2i COVVASi CYSC AMT RATE
INF L2 EVID
$DATA coamox_sinzi_indivparms_4.csv IGNORE=#; input datafile
      IGNORE(ID.EQ.25)
$SUBROUTINE ADVAN13 TOL=9

$MODEL
NCOMP = 5
COMP(CENTRAL)
COMP(PERIPH1)
COMP(PERIPH2)
COMP(CENTRAL)
COMP(PERIPH)

$PK
; include/align units for covariates needed -----

WTG = WT * 1000      ; weight from kg to g
AGED = AGE * 365     ; age in days
HSA_AD = 44          ; g/dl
FU_CLAV = 0.75       ; between 0.7-0.8 for clavulanic acid
FU_AMOX = 0.82       ; determined in vitro
BP2 = 0.55           ; blood-to-plasma partition coefficient for amoxicillin

; fixed PBPK functions -----

; GFR -----
GFR = 112 * ((WTG/70000) ** 0.632) * (PMA ** 3.3) / ((PMA ** 3.3) + (55.4 **
3.3)) * 0.06          ; GFR in L/h
HSA = 1.1287 * LOG(AGED) + 33.764      ; HSA pediatrics
FU1 = 1 / (1 + ((1 - FU_CLAV) * HSA) / (HSA_AD * FU_CLAV)) ; fu clavulanic acid
FU2 = 1 / (1 + ((1 - FU_AMOX) * HSA) / (HSA_AD * FU_AMOX)) ; fu amoxicillin

; active tubular secretion -----
CO = BSA * (110 + 184 * EXP(-0.0378 * AGE) - EXP(-0.24477 * AGE)) ; L/h
IF(SEX.EQ.0) THEN      ; fraction of CO for females
      FRCO = 4.53 + (13.00 * AGE ** 1.15 / (0.188 ** 1.15 + AGE ** 1.15))
ENDIF

IF(SEX.EQ.1) THEN ; fraction of CO for male
      FRCO = 4.53 + (14.63 * AGE ** 1.0 / (0.188 ** 1.0 + AGE ** 1.0))
ENDIF

QR = FRCO * CO ; L/h ; renal blood flow

; density of kidney x kidney volume = kidney weight in grams
KW = 1050 * (4.214 * WT ** 0.823 + 4.456 * WT ** 0.795) / 1000

; covs relationships fixed from PPK model -----
COVCYS1 = COVCYS1i ; (CYSC/0.63) ** THETA(11) ; amoxicillin
COVCYS2 = COVCYS2i ; (CYSC/0.63) ** THETA(12) ; clavulanic acid
COVVAS = COVVASi

; parms to be estimated -----
MAT = THETA(3) + (THETA(4) - THETA(3)) * (AGED/7) ** THETA(5) / (THETA(6) **
THETA(5) + (AGED/7) ** THETA(5)) ; maturation func OAT3

```

```

CLINT = THETA(2)/100 * MAT * KW ; intrinsic CL scaled by 100
ATS = ((QR - GFR) * FU2 * CLINT / (QR + FU2 * CLINT/BP2)) * EXP(ETA(2))
GFRCL = (GFR * THETA(1) * FU2) * EXP(ETA(1))
CL1 = (GFRCL + ATS) * COVCYS1 * COVVAS ; CL amoxicillin
CL2 = (GFR * THETA(1) * FU1) * EXP(ETA(1)) * COVCYS2 ; CL clavulanic acid

; --- posthoc estimates from PPK model
Q11 = CL3i ; intercompartmental CL amox
Q21 = CL4i ; intercompartmental CL clav. ac.
Q12 = CL5i ; intercompartmental CL amox (2)
V11 = V1i ; central volume amox.
V21 = V2i ; central volume clav. ac.
V12 = V3i ; peripheral volume amox. (1)
V22 = V4i ; peripheral volume clav. ac.
V13 = V5i ; peripheral volume amox. (2)

K10 = CL1/V11 ; elimination rate amox
K20 = CL2/V21 ; elimination rate for clav. ac.
K13 = Q11/V11 ; intercompartmental rate amox. central -> periph 1
K15 = Q12/V11 ; intercompartmental rate amox. central -> periph 2
K24 = Q21/V21 ; intercompartmental rate clav. ac. central -> periph
K31 = Q11/V12 ; intercompartmental rate amox. periph 1 -> central
K42 = Q21/V22 ; intercompartmental rate clav. ac. periph -> central
K51 = Q12/V13 ; intercompartmental rate amox. periph 2 -> central

S1 = V11 ; scaling amoxi.
S2 = V21 ; scaling clav. ac.

$DES
DADT(1) = A(3) * K31 + A(5) * K51 - A(1) * (K10+K13+K15) ; 1 central amox.
DADT(2) = A(4) * K42 - A(2) * (K20 + K24) ; 2 central clav. ac.
DADT(3) = A(1) * K13 - A(3) * K31 ; 3 periph. cmp. amox.
DADT(4) = A(2) * K24 - A(4) * K42 ; 4 periph. cmp. clav. ac.
DADT(5) = A(1) * K15 - A(5) * K51 ; 5 periph. cmp. (2) amox.

$ERROR
IPRED = F

C1 = A(1) / V11 ; conc. amox.
C2 = A(2) / V21 ; conc. clav.

IND1 = 0
IND2 = 0
IF(CMT.EQ.1) IND1 = 1
IF(CMT.EQ.2) IND2 = 1
Y1 = C1 * (1 + ERR(1))
Y2 = C2 * (1 + ERR(2))
Y = Y1*IND1 + Y2*IND2

; Initial estimates (lower boundary, initial) for typical parameters
$THETA
(0, 2) ; 1- augmented CL amox.
(0, 2) ; 2- CL clav. ac.
0 FIX ; 3- Fbirth
1 FIX ; 4- Adult max
(0, 0.5) ; 5- HILL
(0, 31) ; 6- Age of half maturation

; Initial estimates between-subject variability variance
$OMEGA
0.06 ; IIV CL amox.
0.6 ; IIV CL clav. ac.

```

```

; Residual variability
$SIGMA BLOCK(2)      ;covariance for prop. residual random effects
0.11
0.009 0.12

; Estimation method
$ESTIMATION METHOD=1 INTER MAXEVAL=9999 NOABORT SIG=3 PRINT=1 POSTHOC

; Covariance step
$COVARIANCE PRINT = E

; Output table
$TABLE ID TIME DV IPRED PRED CWRES CWRESI MDV CL1 CL2 Q12 Q21 Q11 V11 V21
V12 V13 V22 ETA1 ETA2 C1 C2 GFR FU1 FU2 HSA CO QR SEX AGE PMA WT BSA PRISM
PELOD COVCYS1 COVCYS2 COVVAS BLQ CYSC MAT CMT RES WRES CLINT ATS GFRCL
NOPRINT NOAPPEND ONEHEADER FILE=run303_6_201.tab

```


Section V. Summary, conclusion, and perspectives



Chapter 7

Summary, conclusion, and perspectives

7.1 Exploring renal clearance in children

Differences in size and physiological development between adults and children are known to influence several aspects of drug disposition. This thesis focuses on the disposition of renally excreted drugs, which, among others, relates to changes in kidney size, number of glomeruli and of proximal tubule cells and transporter expression. As introduced in **chapter 1**, this thesis explores how the changes in size and physiology throughout the pediatric age-range influence the contribution of glomerular filtration (GF) and active tubular secretion (ATS) to renal clearance (CL_R) using both population pharmacokinetic (popPK) and physiologically-based pharmacokinetic (PBPK) approaches. The extent to which these developmental changes impact CL_R and, subsequently, drug dosing, was explored in pediatric populations either for existing drugs using clinical data or for hypothetical drugs with an array of different properties excreted by either GF or both GF and ATS to meet the following research objectives:

1. Further development of population pharmacokinetic models by characterizing the maturation in CL_R for antibiotics (i.e. amikacin, vancomycin) mainly excreted by GF in (pre)term neonates and quantify the influence of disease and co-therapy on CL_R . These models are subsequently used to propose dosing recommendations for the antibiotics administrated to these special populations (**section II**).
2. Establish a general scaling method for CL_R from adults to children for drugs eliminated by GF and systematically investigate how maturation of plasma protein concentrations influence the unbound fraction of drugs, and subsequently, scaling of pediatric CL_R and drug doses (**section III**).
3. Use a pediatric PBPK-based model for CL_R to systematically investigate the influence of transporter ontogeny on the contribution of ATS to CL_R and illustrate how a combined population PBPK approach could be used to derive in vivo ontogeny functions for renal transporters involved in ATS (**section IV**).

7.2 Population PK modelling to guide dosing of renally excreted drugs in preterm neonates

To meet our first objective, in **section II (chapters 2 and 3)** PK data were used to build covariate models that explain inter-individual variability and capture changes in PK parameters related to development, co-therapy, and disease status.

In **chapter 2**, amikacin PK was studied in neonates with perinatal asphyxia treated with therapeutic hypothermia (TH). Perinatal asphyxia is expected to have an impact on amikacin PK. Therefore, we quantified the differences in amikacin PK between neonates with and without perinatal asphyxia using popPK modelling, to propose suitable dosing recommendations. To this end, PK data for amikacin collected retrospectively from routine therapeutic drug monitoring of neonates with perinatal asphyxia during TH was combined with a previously published amikacin PK dataset in (pre)term neonates without other co-therapy to assess the impact of perinatal asphyxia with TH on amikacin PK. Subsequently, model simulations were performed to establish amikacin exposures in neonates with perinatal asphyxia during TH after dosing according to the current guidelines and according to proposed model-derived dosing guidelines. Peak and trough plasma concentrations were used as a measure of efficacy and safety. Peak levels within 24–35 mg/L and trough levels strictly under 5 mg/L were aimed for to ensure a safe and effective treatment. Amikacin clearance was found to be decreased by 40% in neonates with perinatal asphyxia with TH, with no changes in volume of distribution. Simulations showed that, increasing the dosing interval with 12 hours results in a decrease in percentage of neonates reaching toxic trough levels (> 5 mg/L) from 40–76% to 14–25%, while still reaching target peak concentrations, as compared to current dosing regimens. The range in percentage represents the maximum percentage of patients reaching toxic levels obtained with different dosing regimen and for different weight groups.

In **chapter 3** dose adjustments were proposed for vancomycin when administrated together with either

ibuprofen or indomethacin. Both are used to induce patent ductus arteriosus (PDA) closure in (pre)term neonates. Previously, a popPK model for vancomycin co-administered with ibuprofen was developed for (pre)term neonates (suspected) of sepsis and PDA. In that analysis, co-administration of ibuprofen for PDA was found to reduce vancomycin clearance by 16%. PK data of vancomycin administered with indomethacin was collected and added to the existing modelling dataset. In the current analysis, co-administration of indomethacin was found to decrease vancomycin clearance by 55%. The updated vancomycin popPK model was used to revise and propose dose adjustments that yield effective vancomycin exposure (i.e. AUC_{0-24h} between 300-550 mg·h/L) in preterm neonates with PDA treated with ibuprofen or indomethacin. Model simulations showed that, as compared to a dosing regimen for vancomycin in neonates without co-administration of ibuprofen or indomethacin, a 20% and 60% decrease of the loading and maintenance dose of vancomycin, respectively, is required when aiming for optimized exposure in the neonatal population with PDA treated with either ibuprofen or indomethacin, respectively.

Both amikacin and vancomycin are eliminated mainly by GF. Previously, a covariate model for amikacin has been used to describe the maturation of CL_R in neonates for other antibiotics mainly cleared by GF (i.e. gentamycin, tobramycin) [1]. Therefore, it is likely that the CL_R of other drugs cleared by GF could be impaired by perinatal asphyxia during TH or co-administration of NSAIDs.

7.2.1 Key messages

- Population PK models can be used to describe the maturation of CLR resulting from all changes in underlying physiological processes.
- Based on CLR and the combined effect of disease and/or co-therapy on CLR, dose adjustments were derived for (pre)term neonates with perinatal asphyxia during TH or PDA treated with NSAIDs either by extending the dosing interval or reducing the dose, respectively.

7.3 PBPK-based dosing of GFR cleared drugs in children

In literature, the maturation of GFR throughout the entire pediatric age-range has been characterized by different functions. However, it has not been established yet which GFR maturation function predicts CL_R most accurately throughout the whole pediatric age-range. Therefore, in **section III (chapter 4)**, different published GFR maturation functions were compared to measured levels of GFR markers (i.e. inulin and mannitol). For drugs eliminated by GF, CL_R is not only determined by GFR but also by unbound fraction of the drug in plasma. Therefore, the accuracy of pediatric CL_R scaling using the best GFR maturation function was assessed and compared to PBPK CL_R predictions for hypothetical drugs binding to varying extends to serum albumin or α -acid glycoprotein. Additionally, the accuracy of empiric bodyweight-based scaling methods was also assessed.

The published GFR maturation functions yielded comparable maturation profiles, with the function of Salem *et al.* [2] leading to the most accurate predictions across all ages. This function was used for PBPK-based predictions of pediatric PBPK CL_R values and it was directly used for simplified GFR-based scaling. This GFR-based scaling was found to systematically yield reasonably accurate (percentage prediction error $\leq 50\%$) pediatric CL_R values for all drugs cleared by this route, except in neonates for some drugs highly bound to AGP. Since the difference between pediatric PBPK CL_R values and CL_R obtained with GFR-based scaling is directly related to the maturation of f_u , these results also imply that after the neonatal period, the maturational changes in plasma protein concentrations have a minimal impact on CL_R scaling of GF excreted drugs. This means that a reliable measure of unbound drug fraction obtained in adults is enough to perform GFR-based scaling from adults to children for CL_R and dose. GFR-based scaling was overall more accurate than linear or 0.75 allometric bodyweight-based scaling.

As proposed in **chapter 3**, Table 3.2, CL_R predictions could be used to inform dosing for drugs eliminated by GF for typical pediatric patients of different ages as a percentage of the established adult dose. Nonetheless, these pediatric dose approximations should be carefully validated. Moreover, the limitations of the scaling method used to derive pediatric CL_R and the afferent dose should be well understood and clearly stated.

7.3.1 Key messages

- The most accurate maturation function for GFR throughout the whole pediatric age-range is quantified by Salem et al.[2].
- Knowing unbound drug fractions in adults is sufficient to use the GFR maturation function to scale CL_R and dose from adults to children for drugs that are mainly cleared through GF.

7.4 Ontogeny of renal transporters and its impact on renal clearance in children

In addition to GF, other processes such as ATS, renal metabolism, and reabsorption, may also contribute to CL_R . In **section IV (chapter 5)** we focused on ATS, as this process remains understudied across the pediatric age-range. It has been reported before that the expression of renal transporters changes in children due to development [3]. Therefore, we systematically analyzed the influence of transporter ontogeny in children on the relative contribution of GF and ATS to CL_R for drugs with different properties. To do so, a PBPK-based model developed to obtain adult CL_R was extrapolated to the pediatric population by including maturation functions for the system-specific parameters. This model was used to predict GF and ATS for hypothetical drugs with a range of drug-specific properties, including transporter-mediated intrinsic clearance ($CL_{int,T}$) values, that are substrates for renal secretion transporters with different ontogeny patterns. The impact of transporter ontogeny on ATS and total CL_R was assessed using a % prediction difference calculated between the predicted CL_R in the presence and absence of transporter ontogeny. Transporter ontogeny was included as either a hypothetical fraction of adult activity or as a fraction of adult activity derived from reported pediatric expression profiles as measured for a few transporters (i.e. OAT1, OAT3, OCT2, Pgp) in pediatric kidney samples. Our analysis showed that the contribution of ATS to CL_R ranges between 41% and 90% in children, depending on f_u and $CL_{int,T}$ values. Predictions of CL_R are inaccurate for the majority of drugs that undergo ATS in the absence of transporter ontogeny, regardless of the pediatric age, if the real ontogeny of renal transporters is <0.2 of adult values. Ignoring ontogeny patterns for secretion transporters results in CL_R predictions that are not systematically accurate for all hypothetical drugs (% prediction discrepancy $> 50\%$ for some drugs) in children younger than 2 years.

Recently, Cheung et al. [3] published ontogeny functions for 8 renal transporters following direct measurements of protein expression specific for each transporter. According to this report, BCRP, MATE1, MATE2-K, and GLUT2 have expression levels similar to the adult throughout the studied pediatric age-range, whereas, the ontogeny of OAT1, OAT3, OCT2 and Pgp increases with increasing age [3]. As the ontogeny profiles of individual transporters are different, the contribution of these transporters to the ATS of a drug changes differently with age as well. OAT1 and OAT3 have a slow rate of ontogeny, reaching adult levels around 2 years of age, whereas expression of OCT2 and Pgp is fully developed after 3 and 6 months, respectively [3]. Disregarding ontogeny of transporters leads to over-predictions of CL_R in young patients. If these predictions were used as the basis for pediatric dose adjustments, they could lead to over exposure to drugs and to an increase in risk of toxic events.

Drugs that lead to high % prediction discrepancy could potentially be used as sensitive in vivo probes to derive transporter ontogeny and complement research similar to what has been performed by Cheung et al.. Following the proposed framework in **chapter 5**, the best probe drugs should have a $CL_{int,T}$ of 5-50 $\mu\text{L}/\text{min}/\text{mg}$ protein and medium to high fraction unbound in adults ($f_u = 0.55 - 0.95$). Drugs for which GF is the main elimination pathway or drugs with a high enough $CL_{int,T}$ to have their elimination

limited by renal blood flow, will have a limited use in characterizing ontogeny profiles.

The ontogeny of different renal transporters has been quantified based on specific protein expression levels measured in a limited number of kidney samples. However, it remains unknown whether the ontogeny of protein levels reflects the ontogeny of *in vivo* transporter activity. Hence, in **section IV, chapter 6**, a combined population and physiologically-based PK modelling approach (popPBPK) was proposed to derive the transporters ontogeny *in vivo*. To obtain the ontogeny function for OAT3, PK data on two probe drugs administered simultaneously- clavulanic acid, which is mainly cleared by GF, and amoxicillin, which is mainly cleared by a combination of GF and ATS by OAT3- were used to differentiate between clearance through GF and OAT3-mediated ATS. First, individual post-hoc values for pediatric CL_R values for clavulanic acid and amoxicillin were obtained with a previously published popPK model developed for those data and these were used as dependent variables for the popPBPK approach. Then, CL_R was re-parameterized according to PBPK principles, using known maturation profiles for all system-specific parameters, while only leaving the OAT3-mediated intrinsic clearance ($CL_{int,OAT3,in vivo}$) and its ontogeny profile to be estimated. The estimated ontogeny function for OAT3 was included in a pediatric PBPK-based model for CL_R and used to scale CL_R of other OAT3 substrates (i.e. cefazolin, piperacillin). *In vivo* $CL_{int,OAT3}$ for these drugs in adults, was obtained following *in vitro-in vivo* extrapolation and adjusted by comparing adult PBPK CL_R predictions to literature values. Subsequently, pediatric PBPK CL_R values were compared to typical CL_R estimates, as obtained with published popPK models for each drug. As described by a sigmoidal Emax function based on PNA in weeks, $CL_{int,OAT3,in vivo}$ reached half of adult levels around 7 months of age. Estimating the *in vivo* ontogeny of OAT3 lead to similar results to those measured by Cheung et al. [3] as protein expression levels. The ontogeny of OAT3 between 1 month and 15 years was characterized, with a minimal quantified ontogeny of 0.1 of the adult value at 1 month and reaching adult values at 15 years. Adding the OAT3 ontogeny to the PBPK-based model yielded accurate CL_R predictions for cefazolin and piperacillin (%RMSPE of 21% and 12%).

With this popPBPK approach, $CL_{int,OAT3,in vivo}$ for amoxicillin in adults was estimated at 4.4 $\mu\text{L}/\text{min}/\text{mg}$ protein which is in line with the published value of 4.3 $\mu\text{L}/\text{min}/\text{mg}$ protein [5]. Judging by the $CL_{int,OAT3}$ value and f_u of 0.826, amoxicillin has the potential of quantifying OAT3 ontogeny in a popPBPK approach because according to **chapter 5** the best probe drugs should have a $CL_{int,T}$ of 5-50 $\mu\text{L}/\text{min}/\text{mg}$ protein and medium to high fraction unbound in adults ($f_u = 0.55 - 0.95$). Here, since amoxicillin was given together with clavulanic acid, we were able to disentangle the two routes that contribute to CL_R (i.e. GF and ATS) and quantify the ontogeny of OAT3 activity for a broad pediatric age-range between 1 month and 15 years. With this methodology the ontogeny of renal transporters can be derived *in vivo*, also for other transporter substrates for which data that allows the differentiation between GF and ATS is available. In addition, this methodology does not require direct kidney samples to quantify transporter ontogeny of remaining transporters.

7.4.1 Key messages

- Realistic combinations of f_u and $CL_{int,T}$ values lead to contributions of ATS to CL_R between 41% and 90% in children.
- If ontogeny of renal transporters is <0.2 of adult values, predictions of CL_R in the absence of transporter ontogeny are inaccurate for the majority of drugs, regardless of the pediatric age.
- The *in vivo* ontogeny of OAT3, estimated using population PBPK modelling on amoxicillin data in children, reaches half of adult levels of activity around 7 months of age.
- PBPK-based predictions based on this *in vivo* OAT3 ontogeny function were accurate for other OAT3 substrates such as cefazolin and piperacillin throughout the pediatric age-range.
- The proposed popPBPK approach could be used to derive *in vivo* transporter ontogeny of other renal transporters.

7.5 Perspectives

Based on the models and approaches developed in this thesis we have explored how these could be used to answer additional clinically relevant research questions. We focus on three specific topics in this perspectives section:

1. How predictive are trough concentrations as surrogates for vancomycin exposure, considering the correlation between vancomycin trough concentrations and exposure (i.e. AUC_{24h}) for different pediatric age groups and dosing regimens.
2. How well do empirical scaling methods based on bodyweight and GFR-based function perform for scaling CL_R of drugs that are not only cleared through GF (as described in **chapter 5**), but are also actively secreted by renal transporters.
3. How to estimate with the use of a combined population PK and PBPK approach parameters with high impact that are difficult to measure in children.

7.5.1 How predictive are vancomycin trough samples as a surrogate for exposure across age?

In **chapters 2** and **3**, we show how peak and trough levels (amikacin) or only trough levels (vancomycin) collected in clinical practice for therapeutic drug monitoring (TDM) are used as to ensure a safe and effective exposure to these antibiotics during treatment for (suspected) septicemia. In the case of vancomycin, trough levels are surrogates for AUC_{24h} which is the most predictive index for safe and/or effective exposures. However, the correlation between vancomycin trough levels and AUC_{24h} is assumed to remain constant across dosing regimens and all ages. In this analysis, this assumption is challenged by assessing how the correlation between trough levels and vancomycin exposure at 24 h (i.e. AUC_{24h}) changes for different pediatric patients treated with vancomycin following dosing guidelines that include different dosing frequencies and/or a loading dose.

The model presented in **chapter 3** is suitable for such an analysis and was used to simulate typical vancomycin PK profiles for 6 representative pediatric individuals: neonates of 14 days and gestational ages of 24, 34 and 40 weeks, and children of 6 months, 4 and 12 years of age following treatment with a recently validated dosing regimen [7] (Table 7.1). The relationships between the simulated vancomycin trough concentrations and corresponding AUC_{24h} were compared between dosing regimens with and without a loading dose (see Table 7.1) and for regimens with different dosing frequencies (i.e. for the dosing regimen in Table 7.1 the number of doses per day of the maintenance dose was changed to 4, 3 and 2, corresponding to dosing intervals of 6h, 8h and 12h, respectively). These relationships were compared at the end of the first day of treatment and at steady-state (after 7 days of treatment).

Table 7.1 Vancomycin dosing regimen for neonates and children aiming for a target AUC_{24h} of 300 - 500 mg·h/liter

Clinical characteristics			Vancomycin Dosing [7]	
PNA (days)	BW (g)	CW (kg)	Loading Dose	Maintenance Dose*
0-7	≤700		16 mg/kg	15 mg/kg/day in 3 doses
	700-1000			21 mg/kg/day in 3 doses
	1000-1500			27 mg/kg/day in 3 doses
	1500-2500			30 mg/kg/day in 4 doses
8-14	≤700		20 mg/kg	21 mg/kg/day in 3 doses
	700-1000			27 mg/kg/day in 3 doses
	1000-1500			36 mg/kg/day in 3 doses
	1500-2500			40 mg/kg/day in 4 doses

Clinical characteristics			Vancomycin Dosing [7]	
PNA (days)	BW (g)	CW (kg)	Loading Dose	Maintenance Dose*
14-28	≤700		23 mg/kg	24 mg/kg/day in 3 doses
	700-1000			42 mg/kg/day in 3 doses
	1000-1500			45 mg/kg/day in 3 doses
	1500-2500			52 mg/kg/day in 4 doses
21-28	≤700		26 mg/kg	24 mg/kg/day in 3 doses
	700-1000			42 mg/kg/day in 3 doses
	1000-1500			45 mg/kg/day in 3 doses
	1500-2500			52 mg/kg/day in 4 doses
>28		< 2.5	18 mg/kg	32 mg/kg/day in 4 doses
		2.5-5	24 mg/kg	40 mg/kg/day in 4 doses
		5-10	27 mg/kg	52 mg/kg/day in 4 doses
		> 10	30 mg/kg	60 mg/kg/day in 4 doses

*the maintenance dose was adapted for dosing frequencies in 2, 3, 4 doses in a day for frequencies of 12h, 8h, 6h, respectively

In addition, to assess the influence of inter-individual variability (IIV) in CL_R on the trough concentrations and corresponding AUC_{24h} , we performed stochastic simulations for the representative individuals treated with the vancomycin dosing regimen of Table 7.1 (more details on stochastic simulations see **chapter 3**) [7]. Briefly, for each representative individual we performed 1000 stochastic simulations with the model taking into account the IIV in CL_R . The simulated vancomycin concentration-time profiles were used to calculate the AUC_{24h} . The results are summarized for each representative individual for AUC_{24h} target intervals between 350-550 mg·h/L as well as for the commonly used > 400 mg·h/L (with a toxic level of 700 mg·h/L) [8] in Table 7.2.

Finally, to assess the influence of variability in demographic characteristics within the pediatric population on CL_R , Monte Carlo simulations were performed for the entire pediatric age-range using demographic characteristics from patients included in a previous study [9]. The probability of target attainment between 350-550 mg·h/L was calculated for each age-group (i.e. neonates, infants, children, adolescents). Briefly, a virtual pediatric population was created by resampling with replacement 1000 patients demographics from a previous study [9]. The model with IIV on CL_R was used to simulate vancomycin concentration-time profiles which served as basis to calculate the 24 h exposure (i.e. AUC_{0-24h}).

Table 7.2 - Results of stochastic simulations upon dosing according to table 1 (with loading dose) to understand the impact of inter-individual variability in CL on the 24h exposure and corresponding trough concentration at the end of day 1.

	Representative individuals	Vancomycin AUC_{0-24h} % within 300 – 550 mg·h/L	Vancomycin trough (mg/L) corresponding to AUC_{0-24h} within 300 – 550 mg·h/L (median [min-max])	Vancomycin AUC_{0-24h} % within 400 – 700 mg·h/L	Vancomycin trough (mg/L) corresponding to AUC_{0-24h} within 400 – 700 mg·h/L (median [min-max])
1	GA=24 weeks PNA=14 days	87%	11.2 [6.9 – 17.2]	55%	13.2 [10.7- 23.3]
2	GA=34 weeks PNA=14 days	84%	12.4 [7.3 – 18.1]	68%	14.2 [11.0- 25.9]
3	GA=40 weeks PNA=14 days	78%	12.1 [6.6 – 17.7]	60%	14.4 [10.8- 23.9]
4	PNA=6 months	70%	11.2 [6.1 – 16.5]	67%	14.3 [10.0- 23.7]
5	PNA=4 years	62.5%	10.3 [5.6 – 15.5]	66%	13.8 [9.31- 22.5]
6	PNA=12 years	65%	10.8 [5.6 – 15.6]	65%	13.2 [9.19- 21.2]

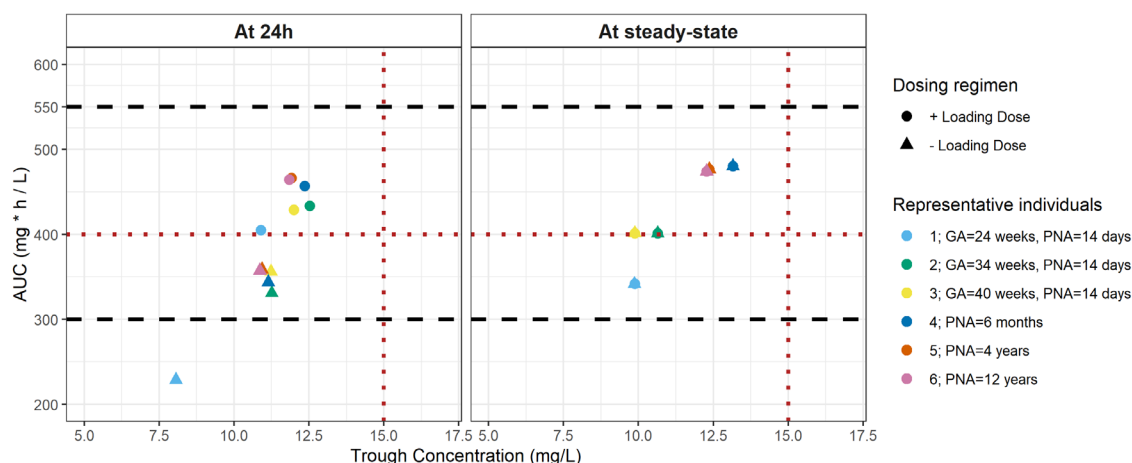


Figure 7.1 - AUC_{24h} vs. trough concentrations of vancomycin in the first day of dosing (left panel) and at steady-state (right panel) upon dosages according to Table 7.1. Different colors correspond to different ages. Symbols distinguish between the dosing regimen with (circles) and without (triangles) a loading dose (Table 7.1). Horizontal interrupted lines show the desired exposure thresholds, i.e. between 300 – 550 mg·h/L with black dashed lines, and 400 mg·h/L with a red dotted line. The vertical red dotted line marks the 15 mg/L trough concentration as previously suggested to correlate with an AUC_{24h} of >400 mg·h/L in adults.

Figure 7.1 shows the relationship between vancomycin trough and corresponding AUC_{24h} at the end of the first day of treatment following the dosing regimen in (Table 7.1) with or without administering a loading dose. Trough levels are comparable between regimens with and without a loading dose, i.e. they vary between 11 – 12.5 mg/L and 8 – 11.3, respectively, with the lowest level attributed to the smallest preterm individual. Nonetheless, the corresponding AUC_{24h} is systematically higher for the regimen with a loading dose ($AUC_{24h} > 400$ mg·h/L for all representative individuals). Once steady-state is reached, there is no difference in the two exposure measures between the regimens with and without a loading dose. Regarding safety and efficacy, Figure 7.1 shows that all patients reach AUC_{24h} within the 300 – 550 mg·h/L in the first 24 h of vancomycin treatment except for the smallest preterm neonate (i.e. GA of 24 weeks) that did not receive a loading dose. Therefore, the efficacy of vancomycin treatment in preterm neonates could be improved by using the dosing regimen with a loading dose, particularly for small preterm neonates.

Figure 7.1 shows that following the vancomycin dosing in Table 7.1, trough levels between 8 and 13 mg/L correspond to effective AUC_{24h} levels in the representative individuals. By decreasing dosing frequency of the regimen without a loading dose, in Figure 7.2 we show that trough levels also decrease, while yielding similar AUC_{24h} for all typical pediatric individuals after the first day of vancomycin treatment. In this example the daily dose remains unchanged while dosing frequencies change to every 6h, 8h and 12h. At the end of the first day of treatment, while corresponding to similar AUC_{24h} , trough levels decrease from 9-11.3 mg/L to 7.5-8 mg/L by decreasing the dosing frequency from every 6 h (4 times

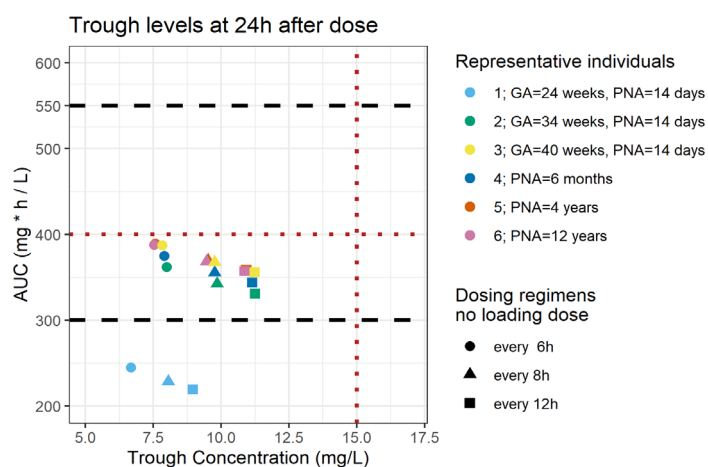


Figure 7.2 - AUC_{24h} vs. trough concentrations of vancomycin on the first day of dosing upon dosages according to Table 7.1 (without a loading dose) for different dosing frequencies represented by different symbols: squares for every 12 h, circles for every 8 h and triangles for every 6 hours. Different colors correspond to different ages. Horizontal interrupted lines show the desired exposure thresholds, i.e. between 300 – 550 mg·h/L with black dashed lines, and 400 mg·h/L with a red dotted line. The vertical red dotted line marks the 15 mg/L trough concentration as previously suggested to correlate with an AUC_{24h} of >400 mg·h/L in adults.

daily) to every 12 h (2 times daily). Regarding safety and efficacy of treatment, all patients achieve AUC_{24h} within 300 – 550 mg·h/L in the first 24 h except the smallest preterm neonate that does not reach effective AUC_{24h} levels (Figure 7.2, results given for dosing regimen without a loading dose).

After including IIV on CL_R for the same representative individuals, the trough concentrations and corresponding AUC_{24h} resulting after treatment with the dosing regimen with loading dose (Table 7.5.1.1) were explored and compared to literature values. In literature, vancomycin trough levels of at least 15 mg/L [8] for adults and between 7-11 mg/L [10] for neonates were reported to be associated with an exposure above 400 mg·h/L. The results in Table 7.5.1.2 following stochastic simulations with the model developed in **chapter 3** show that, when aiming for an exposure between 400 and 700 mg·h/L, the median trough concentrations for both neonates and children is between 13.2 and 14.4 mg/L, which is higher than the interval recommended for neonates and closer to the recommended trough value for adults. Even when aiming for a lower AUC_{24h} (i.e. 300- 550 mg·h/L), representative neonates have a median trough concentration above 11 mg/L (between 11.2 – 12.1 mg/L). Moreover, the unexplained IIV on CL_R alone leads to very broad intervals for trough levels that correspond to an effective AUC_{24h} for each representative individual.

In addition to the IIV in CL_R , Monte Carlo simulations include also the variability coming from the distribution of patient demographics for different age groups. Figure 7.3 illustrates the probability of attaining an AUC_{24h} within 300 – 550 mg·h/L based on the trough levels in the end of day 1 of vancomycin treatment following the dosing regimen in Table 7.1 with a loading dose for 4 different age groups. In clinical practice, the trough concentration guides dose adjustments while aiming for a certain target AUC_{24h} . The figure shows that for all age groups, when trough levels are between 7.5 and 12.5 mg/L, the probability of reaching the target exposure is above 0.8. For all age groups, the probability of target attainment decreases when trough levels are above 15 mg/L (< 0.75 for all age-groups except neonates) because the probability of reaching AUC_{24h} values above 550 mg·h/L increases. This indicates an increased risk of adverse events. On a population level, neonates appear to have a high chance of reaching the target exposure for a broader range of trough levels (5 – 15 mg/L), as compared to the other age groups. Even though the range of possible trough levels that would result in an effective AUC_{24h} is broader, this does not imply that effective levels will always be achieved at the individual level. With increasing age, the trough levels indicating an effective exposure become narrower (7.5- 12.5 mg/L for adolescents). This could be explained by the decrease in IIV for CL_R in older children as compared to neonates. As compared to literature values, the trough levels obtained for neonates are similar to the published 7-11 mg/L, however, levels obtained for adolescents are below the reported value in adults of 15 mg/L.

As shown by the results of the stochastic and Monte Carlo simulations, a large range of trough concentrations corresponds to an effective AUC_{24h} . Therefore, in order to know whether a measured trough concentration indeed corresponds to the target AUC_{24h} , TDM samples should be obtained and analyzed with Bayesian software in order to obtain individual PK parameters and AUC_{24h} . To ensure safe and effective treatment despite the high inter-individual variability, TDM samples could be taken earlier (e.g. samples after the first dose) instead of the last trough of the first day of treatment. Furthermore, with the new data the Bayesian model can be refined over time. By individualizing therapy both bacterial resistance and risk for adverse events could potentially be reduced.

To summarize, vancomycin trough concentrations corresponding to effective exposure change with age and with dosing regimens (i.e. with and without loading dose or with different dosing frequencies). This aspect should be taken into account when performing TDM on trough levels to guide dosing. Correlating a trough level with an effective AUC_{24h} is challenging as it is difficult to establish cut-off values that would always correlate with a successful outcome. However, when dosing using the guidelines in Table 7.1 with loading dose a probability above 0.8 of reaching an effective AUC_{24h} between 300 – 550 mg·h/L

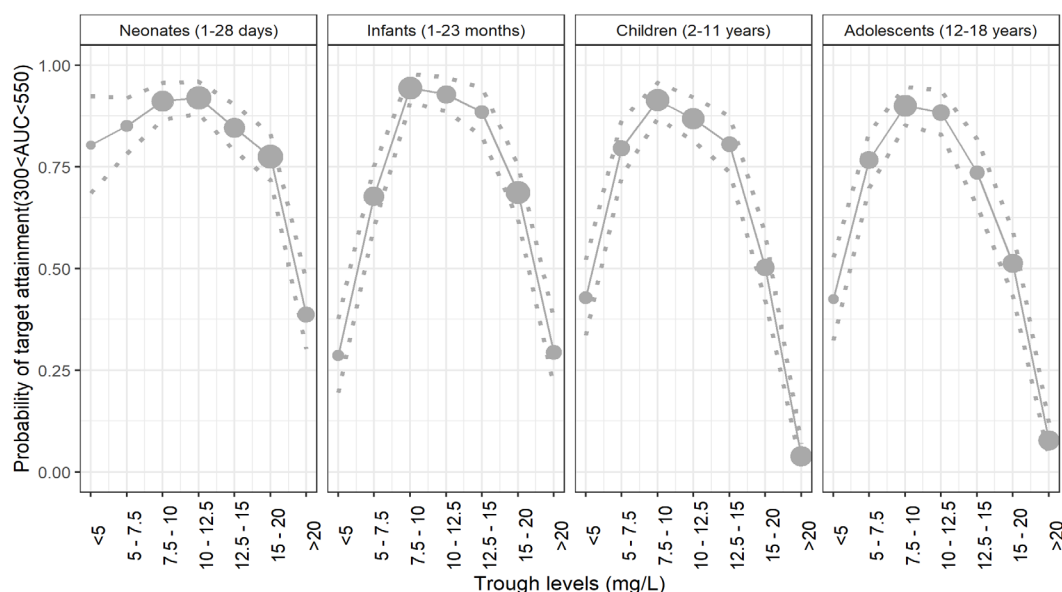


Figure 7.3 - Results of a Monte Carlo simulation for which the vancomycin dosing with loading dose was administrated according to Table 7.1. The circles show the probability of AUC_{24h} target attainment (between 300 – 550 mg·h/L) for each vancomycin trough concentration interval in different age groups on the first day of treatment. The 90% confidence interval of the probabilities is shown by the dotted line. The size of the circles is correlated to the number of individuals in each trough interval on the x-axis for which the probability is calculated.

corresponds to a trough range between 7.5 and 12.5 mg/L.

7.5.2 How can we scale CL_R of drugs eliminated by GF and ATS?

In **section III, chapter 4**, we showed that CL_R of drugs exclusively eliminated by GF can be scaled accurately by using a GFR based function throughout the whole pediatric age range, except in neonates for drugs highly bound to AGP. Here, we use a similar pediatric PBPK framework as in **chapter 4** to determine whether scaling based on a GFR maturation function can be used for drugs eliminated by GF and ATS. For comparative purposes, the accuracy of this GFR-based scaling was evaluated together with linear bodyweight-based scaling and bodyweight-based allometric scaling with a fixed exponent of 0.75, two commonly used empirical pediatric CL_R scaling methods. Age-appropriate body surface area (BSA), height, and weight values were derived from the NHANES database [10] and used for pediatric PBPK CL_R predictions with ages ranging from term newborn to 15 years.

Since information about the ontogeny profiles of transporters is scarce in literature, different hypothetical ontogeny fractions and hypothetical drugs with different properties were used here to obtain the PBPK-based CL_R predictions, as described in detail in **section IV, chapter 5**. Briefly, pediatric PBPK CL_R predictions for 3800 hypothetical drugs which differ in type of binding plasma protein, fraction unbound, blood to plasma ratio, and transporter-mediated intrinsic clearance. Ontogeny levels were explored as relative ontogeny fractions to adult levels that remained constant throughout the pediatric age with the following values: 0.05, 0.2, 0.5, 0.7 and 1.

$$CL_R = CL_{GF} + CL_{ATS} = f_u \times GFR + \frac{(Q_R - GFR) \times f_u \times CL_{int,sec}}{Q_R + f_u \times \frac{CL_{int,sec}}{BP}} \quad [1]$$

where CL_{GF} and CL_{ATS} represent the clearance by GF and ATS, respectively and f_u is the fraction unbound, GFR is the glomerular filtration rate, Q_R is renal blood flow, BP is the blood to plasma ratio of the drug, and $CL_{int,sec}$ is the intrinsic secretion clearance of the active transporters.

$$CL_{int,sec} = CL_{int,T} \times ont_T \times PTCPGK \times KW \quad [2]$$

$CL_{int,sec}$ was obtained as the product of transporter-mediated intrinsic clearance ($CL_{int,T}$), transporter

ontogeny levels (ont_r), the number of proximal tubule cells per gram kidney (PTCPGK), and kidney weight (KW), as shown in equation [2].

The pediatric CL_R obtained using equations 1-2 were compared to scaled CL_R values by GFR function (equation [3]), and the two empirical bodyweight-based relations (i.e. linear and allometric equations [5][6]). The 'true' adult CL_R predictions required for equations 3-5 were obtained with equations [1] and [2] by using the adult values for system-specific parameters as input.

$$GFR \text{ scaled } CL_{ped} = 'true' CL_{adult} \times \left(\frac{GFR_{ped}}{GFR_{adult}} \right) \quad [3]$$

$$Linear \text{ scaled } CL_{ped} = 'true' CL_{adult} \times \left(\frac{WT_{ped}}{WT_{adult}} \right) \quad [4]$$

$$Allometric \text{ scaled } CL_{ped} = 'true' CL_{adult} \times \left(\frac{WT_{ped}}{WT_{adult}} \right)^{0.75} \quad [5]$$

The criteria for accurate scaling was consistent between the previous analysis (**section II, chapter 4**) and the current analysis. By calculating a percentage prediction error (%PE- equation [6]) relative to PBPK CL_R predictions, the scaled CL_R values were considered accurate when %PE was within the range of $\pm 30\%$, inaccurate when %PE outside the range of $\pm 50\%$ and reasonably accurate in-between (i.e.-50%-30%-30%-50%).

$$\%PE_{CL} = \frac{scaled \ CL_{ped} - 'true' \ CL_{ped}}{'true' \ CL_{ped}} \times 100 \quad [6]$$

Figure 7.4 summarizes the performance of GFR-based scaling for CL_R as proposed in **chapter 4 of section II** of drugs eliminated by both GF and ATS and provides general guidance for applying GFR-based scaling throughout the pediatric age-range. GFR-based scaling leads to accurate CL_R values down to 5 years of age and reasonably accurate CL_R values down to 1 year of age when transporter ontogeny is mature (> 0.7 of the adult values) and for drugs with f_u in adults higher than 0.15. Down to 1 year of age and at ontogeny levels of 0.7 GFR-based scaling performs similarly to linear scaling (Appendix, Figure S7.1). However, scaling by GFR maturation has a worse performance than linear and allometric scaling (Appendix, Figures S7.1. and S7.2) when ontogeny is as low as 0.5 of adult values, with no more than 20- 48% of drugs leading to accurate CL_R scaling down to 1 year of age. These drugs have in general low to medium $CL_{int,T}$ (8-100 $\mu\text{L}/\text{min}/\text{g}$ kidney). For drugs with a lower f_u in adults, the percent of inaccurately scaled drugs is higher. For children younger than 3 months and ontogeny of 0.5 of adult values, GFR-based scaling leads to accurate predictions in all typical individuals with the exception of newborns. In newborns GFR-based scaling led to inaccurate predictions for 13% and 17% of drugs bound to HSA and AGP, respectively. Similar results are obtained for linear scaling (Appendix, Figure S7.1). When transporter ontogeny is ≤ 0.2 , for newborns up to 1-month GFR-based scaling leads to accurate CL_R values for 8-46% of drugs, which is more than either linear (2 – 28%) or allometric scaling (0%). However, these are drugs mainly eliminated by GF. For drugs for which ontogeny of transporters plays a major role, GFR-based scaling becomes highly inaccurate for all ages. This is the case for allometric and linear scaling as well.

In the appendix, Figures S7.1. and S7.2 summarize the performance of linear and allometric scaling for drugs cleared by GF and ATS in a similar manner as presented in Figure 7.1. This work was added to the results published by our group for scaling clearance of drugs undergoing hepatic elimination [11,12]. It has to be noted that these three scaling methods are mostly useful for scaling CL_R when no PK data is available for the pediatric population for the drug of interest. As shown here and previously by our group [11,12], drug clearance through different routes has to be scaled differently, depending on the pathway(s) involved.

To summarize, CL_R of drugs eliminated by GF and ATS can be reasonably accurately scaled using the GFR

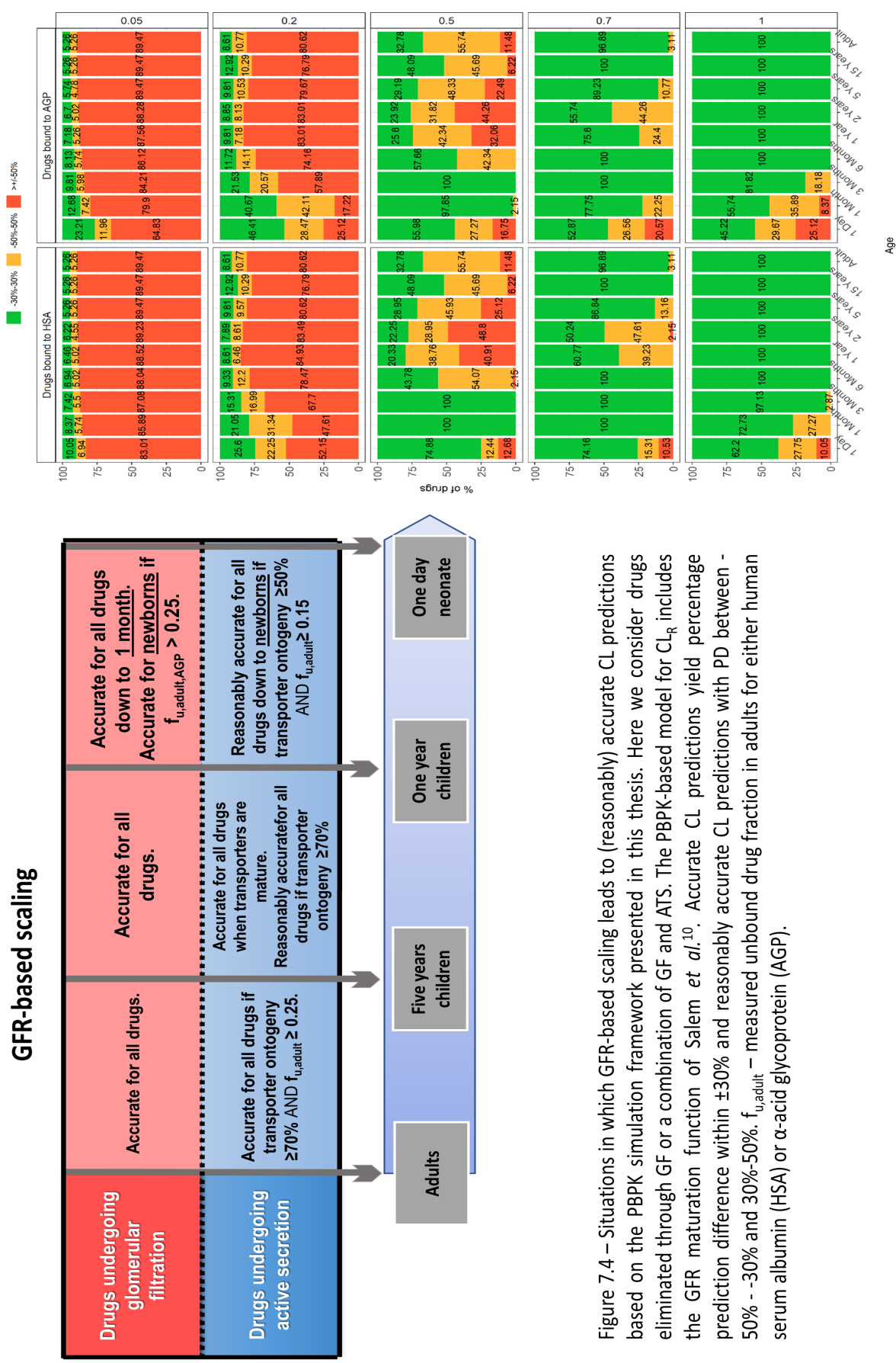


Figure 7.4 – Situations in which GFR-based scaling leads to (reasonably) accurate CL predictions based on the PBPK simulation framework presented in this thesis. Here we consider drugs eliminated through GF or a combination of GF and ATS. The PBPK-based model for CL_R includes the GFR maturation function of Salem *et al.*¹⁰. Accurate CL predictions yield percentage prediction difference within $\pm 30\%$ and reasonably accurate CL predictions with PD between -50% - -30% and 30% - 50% . $f_{u,adult}$ – measured unbound drug fraction in adults for either human serum albumin (HSA) or α -acid glycoprotein (AGP).

maturation function of Salem *et al.* down to 1 year of age when transporter ontogeny is > 0.7 of the adult levels for drugs with a f_u in adults > 0.15 . For children younger than 1 year, GFR-based scaling can be applied if transporter ontogeny is > 0.5 and f_u in adults > 0.15 . By using the guidelines presented in Figure 7.1 (reasonably) accurate initial estimates can be obtained for pediatric CL_R . These guidelines could be extended further with renal metabolism and reabsorption.

7.5.3. How to use popPBPK to derive parameters with high impact but difficult to measure?

In **section III, chapter 4** we proposed a general dosing table for drugs eliminated exclusively by GF (Table 7.2) in which the dose was expressed as a percentage of the adult dose and resulted from scaling by a GFR maturation function [2]. Developing this dosing guideline was possible because all the impactful parameters and their maturation profiles involved in predicting CL_R of drugs eliminated by GF have been extensively researched throughout the pediatric age-range. Nonetheless, in addition to GF there could be other processes involved in CL_R such as active renal tubular transport which remains understudied, especially in the pediatric population. To be able to predict this component of CL_R more information on the ontogeny of renal transporters throughout the pediatric age range is needed. This kind of information is based on protein expression levels measured in renal tissue from children.

Table 7.2 - Pediatric doses presented as % of adult dose for drugs eliminated through GFR with varying f_u values. The 'true' doses predicted based on 'true' pediatric CL values are dependent on f_u whereas the scaled doses derived from CL values scaled with the three different scaling methods (i.e. GFR scaling, linear scaling and allometric scaling) are not.

Demographic Characteristics of Typical Individuals			'True' dose (% of adult dose) obtained based on 'true' CL				Scaled dose (% of adult dose) obtained using three CL scaling methods		
Age	Weight (kg)	GFR (ml/min)	Drugs binding to HSA		Drugs binding to AGP		GFR scaling	Linear scaling	Allometric scaling
			$f_u=0.1$	$f_u=0.9$	$f_u=0.1$	$f_u=0.9$			
1 Day	3.4	4.3	5%	4.1 %	10.1 %	4.2 %	4 %	5.2%	11 %
1 Month	4.3	6.2	6.6 %	5.8 %	8.3 %	5.9 %	5.7 %	6.5 %	13 %
3 Months	5.8	10.7	11.1 %	10 %	12.7 %	10.1 %	9.9 %	8.6 %	16 %
6 Months	7.5	17.6	17.9 %	16.4 %	19.6 %	16.5 %	16.2 %	11.4 %	20 %
9 Months	8.9	23.2	23.5 %	21.6 %	25.1 %	21.8 %	21.4 %	13.4 %	22 %
1 Year	9.9	27.4	27.5 %	25.5 %	29.1 %	25.6 %	25.3 %	14.9 %	24 %
2 Years	12.3	35.9	35.4 %	33.3 %	36.5 %	33.4 %	33.1 %	18.6 %	28 %
5 Years	18.2	47.7	46 %	44.2 %	46.6 %	44.3 %	44 %	27.4 %	38 %
10 Years	32.5	68.9	65.4 %	63.8 %	65.6 %	63.8 %	63.6 %	48.9 %	58 %
15 Years	54.2	95.3	89.7 %	88.1 %	89.7 %	88.1 %	87.9 %	81.6 %	86 %
Adult	66.5	108.4	100 %	100 %	100 %	100 %	100 %	100 %	100 %

In **section IV, chapter 6** we show that a combined population PK and PBPK approach can be used to derive values for parameters that cannot be measured *in vivo* by leveraging the knowledge included in PBPK models on underlying physiological processes and information that can be derived from concentration-time profiles in patients with a population approach. By applying this methodology on informative clinical data, we were able to derive the renal OAT3 transporter ontogeny *in vivo*. The clinical data used for this case-study included both a descriptor of GF- clavulanic acid – and a descriptor of GF and ATS through OAT3- amoxicillin – obtained after the administration of both drugs simultaneously, in the same formulation, to each patient. Having PK data of both drugs administrated to the same patient facilitated the separation between GF and ATS for each individual and allowed the estimation of ontogeny for the OAT3. The resulting ontogeny function for OAT3 was included in the pediatric PBPK-based model for CL_R (equations [1] and [2]) for two new OAT3 substrates that lead to accurate predictions of CL_R throughout the entire pediatric age-range (% root mean square prediction error of 21% and 12% for cefazoline and piperacillin).

Even though having clinical data that includes probe drugs for both GF and ATS in the same individual is desirable, the combined population PK and PBPK approach can also be applied for only one probe drug for a specific renal transporter. In **section IV, chapter 5** we propose basic selection guidelines for drugs with relevant properties to serve as *in vivo* probes for quantifying the ontogeny of transporters underlying ATS. From the results in **chapter 5** we concluded that the best probe drugs should have a $CL_{int,T}$ of 5-50 $\mu\text{L}/\text{min}/\text{mg}$ protein and medium to high fraction unbound in adults ($f_{u,adults} = 0.55 - 0.95$). Drugs for which GF is the main elimination pathway or drugs with extremely high $CL_{int,T}$ that cause renal blood flow to be limiting for elimination, will have a limited use in characterizing ontogeny profiles of renal transporters.

Quantifying the individual transporters would be of great value, as it would improve the PBPK predictions of drugs for which ATS plays an important role, especially when ontogeny is immature (<0.2 of the adult value) or for children younger than 2 years. The combined population PK and PBPK approach could be used with existing clinical data on other substrates of renal transporters to characterize the *in vivo* ontogeny of the remaining renal transporters. In addition, more studies as the one presented in **chapter 6**, including specific drug probes for more than one underlying transporters would provide information about the IIV of CL_R through ATS. These results would complement and confirm existing findings, such as the *in vitro* results of Cheung et al. [3]. Once ontogeny of individual transporters becomes available, generalized dosing tables such as the one presented in **chapter 3** could be developed not only for drugs substrates specific for one transporter pathway but also for combinations of transporters working in tandem.

This type of research should not be limited to active transport only. In addition, renal reabsorption and metabolism together with their dependencies on physiological properties like pH at the tubule side, ionization, enzyme abundance, affinity, and maturation, could be explored in a similar manner in subsequent analyses.

7.6 Conclusions

Predicting PK in children, especially in children under the age of 5 years who are still developing, remains challenging. Throughout this thesis we used different modeling and simulation techniques to guide pediatric dosing when clinical data is available (population PK models) or in the absence of such data (PBPK methods). Population PK methods (i.e. covariate analyses) were used to characterize the changes in CL_R as a function of developmental changes. Obtained population PK models could be used to guide dose adjustments in vulnerable pediatric sub-populations to ensure a safe and effective treatment from the start of therapy. When PK data is scarce or unavailable, pediatric CL_R can be obtained using the information already included in PBPK models and used to derive pediatric doses. Furthermore, performing sensitivity analyses on established PBPK models for CL_R allowed the study of active tubular secretion and how this process is influenced by underlying physiological development (e.g. ontogeny of renal secretion transporters) for a broad array of drugs with different properties. Finally, the information included in the PBPK model for CL_R was further extended by integration with relevant clinical data (popPBPK). With this approach poorly characterized parameters and/or ontogeny/maturation functions were derived from data collected *in vivo*. The results presented in this thesis can serve as a basis for similar explorations to disentangle the remaining relevant processes involved in CL_R and translate relevant findings into guides for safe and effective pediatric dosing.

7.7 References

1. De Cock RFW, Allegaert K, Sherwin CMT, Nielsen EI, De Hoog M, Van Den Anker JN, Danhof M, Knibbe C a J (2014) A Neonatal amikacin covariate model can be used to predict ontogeny of other drugs eliminated through glomerular filtration in neonates. *Pharm Res* 31:754–767 . <https://doi.org/10.1007/s11095-013-1197-y>
2. Salem F, Johnson TN, Abduljalil K, Tucker GT, Rostami-Hodjegan A (2014) A re-evaluation and validation of ontogeny functions for cytochrome P450 1A2 and 3A4 based on in vivo data. *Clin Pharmacokinet*. <https://doi.org/10.1007/s40262-014-0140-7>
3. Cheung KWK, van Groen BD, Spaans E, van Borselen MD, de Bruijn ACJM, Simons-Oosterhuis Y, Tibboel D, Samsom JN, Verdijk RM, Smeets B, Zhang L, Huang SM, Giacomini KM, de Wildt SN (2019) A Comprehensive Analysis of Ontogeny of Renal Drug Transporters: mRNA Analyses, Quantitative Proteomics, and Localization. *Clin Pharmacol Ther*. <https://doi.org/10.1002/cpt.1516>
4. Mathialagan S, Piotrowski MA, Tess DA, Feng B, Litchfield J, Varma M V. (2017) Quantitative prediction of human renal clearance and drug-drug interactions of organic anion transporter substrates using in vitro transport data: A relative activity factor approach. *Drug Metab Dispos*. <https://doi.org/10.1124/dmd.116.074294>
5. FDA (2008) AUGMENTIN® (amoxicillin/clavulanate potassium) Powder for Oral Suspension and Chewable Tablets. https://www.accessdata.fda.gov/drugsatfda_docs/label/2008/050575s037550597s044050725s025050726s019lbl.pdf
6. Janssen EIJ, Väitalo P a. J, Allegaert K, de Cock RFW, Simons SHP, Sherwin CMT, Mouton JW, van den Anker JN, Knibbe C a. J (2015) Towards rational dosing algorithms for vancomycin in neonates and infants based on population pharmacokinetic modeling. *Antimicrob Agents Chemother* AAC.01968-15 . <https://doi.org/10.1128/AAC.01968-15>
7. Neely MN, Youn G, Jones B, Jelliffe RW, Drusano GL, Rodvold KA, Lodise P (2014) Are Vancomycin Trough Concentrations Adequate for Optimal Dosing ? 58:309–316 . <https://doi.org/10.1128/AAC.01653-13>
8. De Cock RFW, Allegaert K, Brussee JM, Sherwin CMT, Mulla H, De Hoog M, Van Den Anker JN, Danhof M, Knibbe C a J (2014) Simultaneous pharmacokinetic modeling of gentamicin, tobramycin and vancomycin clearance from neonates to adults: Towards a semi-physiological function for maturation in glomerular filtration. *Pharm Res* 31:2643–2654 . <https://doi.org/10.1007/s11095-014-1361-z>
9. Frymoyer A, Hersh AL, El-Komy MH, Gaskari S, Su F, Drover DR, Van Meurs K (2014) Association between vancomycin trough concentration and area under the concentration-time curve in neonates. *Antimicrob Agents Chemother* 58:6454–6461 . <https://doi.org/10.1128/AAC.03620-14>
10. National Health and Nutrition Examination Survey www.cdc.gov/growthcharts/index.htm
11. Calvier E, Krekels E, Valitalo P, Rostami-Hodjegan A, Tibboel D, Danhof M, Knibbe CAJ (2017) Allometric scaling of clearance in paediatrics: when does the magic of 0.75 fade? *Clin Pharmacokinet* 56:273–285 . <https://doi.org/doi:10.1007/s40262-016-0436-x>
12. Krekels EHJ, Calvier EAM, van der Graaf PH, Knibbe CAJ (2019) Children Are Not Small Adults, but Can We Treat Them As Such? *CPT Pharmacometrics Syst Pharmacol*. <https://doi.org/10.1002/psp4.12366>

7.8 Supplementary material

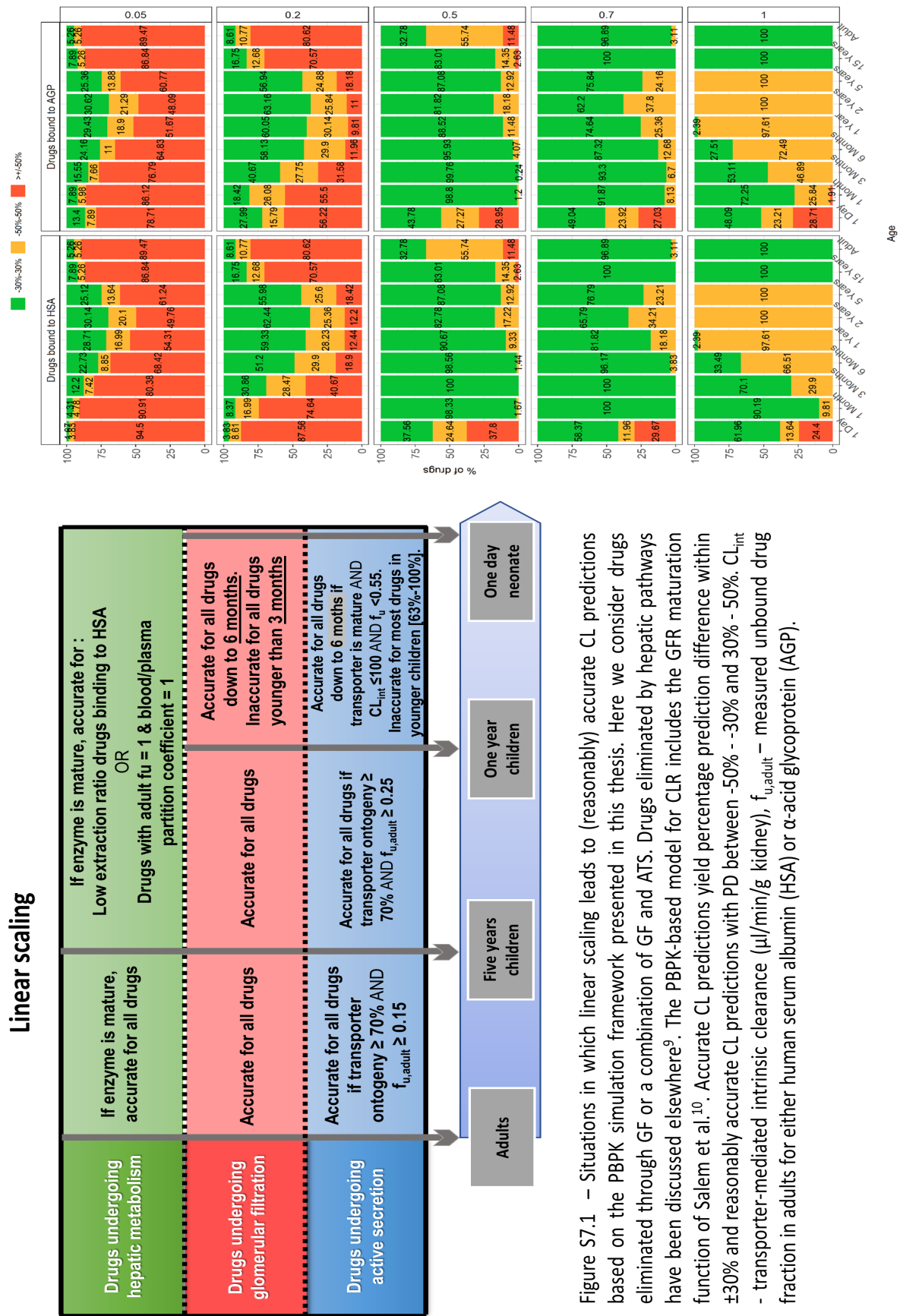


Figure S7.1 – Situations in which linear scaling leads to (reasonably) accurate CL predictions based on the PBPK simulation framework presented in this thesis. Here we consider drugs eliminated through GF or a combination of GF and ATS. Drugs eliminated by hepatic pathways have been discussed elsewhere⁹. The PBPK-based model for CLR includes the GFR maturation function of Salem et al.¹⁰. Accurate CL predictions yield percentage prediction difference within $\pm 30\%$ and reasonably accurate CL predictions with PD between -50% - -30% and 30% - 50% . CL_{int} - transporter-mediated intrinsic clearance ($\mu\text{l}/\text{min}/\text{g}$ kidney), $f_{u,adult}$ - measured unbound drug fraction in adults for either human serum albumin (HSA) or α -acid glycoprotein (AGP).

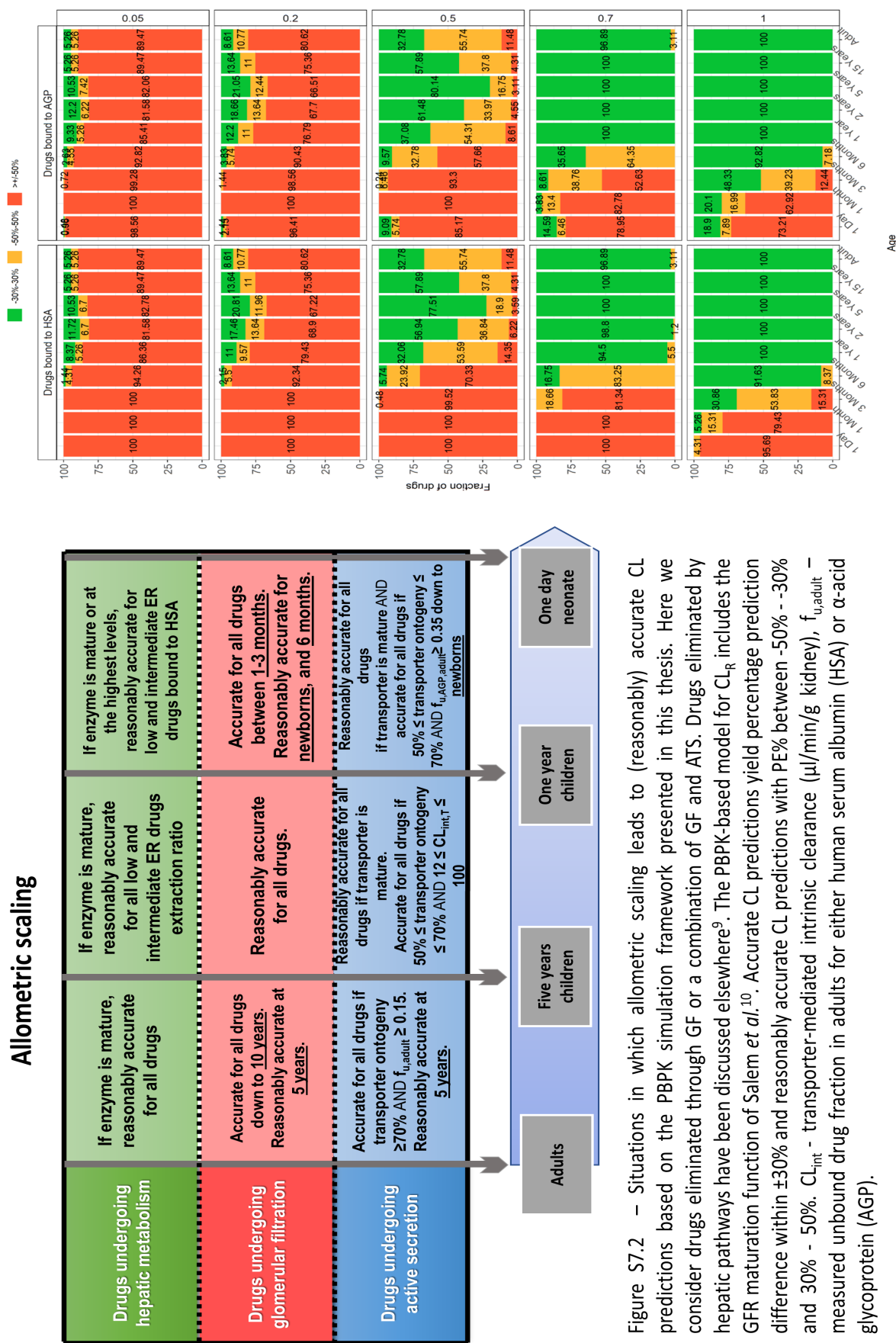


Figure S7.2 – Situations in which allometric scaling leads to (reasonably) accurate CL predictions based on the PBPK simulation framework presented in this thesis. Here we consider drugs eliminated through GF or a combination of GF and ATS. Drugs eliminated by hepatic pathways have been discussed elsewhere⁹. The PBPK-based model for CL_q includes the GFR maturation function of Salem *et al.*¹⁰. Accurate CL predictions yield percentage prediction difference within $\pm 30\%$ and reasonably accurate CL predictions with PE% between -50% - -30% and 30% - 50% . CL_{int} - transporter-mediated intrinsic clearance ($\mu\text{L}/\text{min}/\text{g}$ kidney), $f_{u,adult}$ - measured unbound drug fraction in adults for either human serum albumin (HSA) or α -acid glycoprotein (AGP).

Hoofdstuk 8

Nederlandse samenvatting

8.1 Beknopte samenvatting

Zoals reeds kort geïntroduceerd in Sectie I werden in deze thesis populatie farmacokinetisch (popPK) en fysiologisch-gebaseerde farmacokinetische (PBPK) benaderingen toegepast om de invloed van glomerulaire filtratie (GF) en actieve tubulaire secretie (ATS) op renale klaring (CLR) in kinderen te onderzoeken. Voor dit onderzoek werden de bijdragen van passieve (bijv. GF) en actieve (bijv. ATS) processen op CLR bekeken. Beide processen dragen bij aan pediatrisch CLR en worden naar verwachting beïnvloed door ontwikkelings-veranderingen.

Dus, de mate waarin deze ontwikkelingsveranderingen de impact van CLR veranderen wordt onderzocht in pediatrische populaties door gebruik te maken van klinische data van bestaande geneesmiddelen, en met behulp van een PBPK-gebaseerd framework voor hypothetische geneesmiddelen met een reeks van verschillende eigenschappen uitgescheiden door hetzij GF of zowel GF en ATS. De projecten werden uitgevoerd teneinde de onderstaande onderzoeksdolen te bereiken:

1. Verdere ontwikkeling van populatie farmacokinetische modellen door de rijping in CLR voor antibiotica (bijv. amikacine, vancomycine) uitgescheiden door GF in (pre)term neonaten en het kwantificeren van de invloed van ziekte en co-therapie op CLR. deze modellen worden vervolgens gebruikt om doseringsaanbevelingen voor te stellen voor antibiotia voorgeschreven aan deze special populaties (sectie II).
2. Het vaststellen van een algemene schalingsmethode voor CLR van volwassenen tot kinderen voor geneesmiddelen die geëlimineerd worden door GF en systematisch onderzoeken hoe rijping van plasma eiwitconcentraties de ongebonden fractie van geneesmiddelen beïnvloeden, en vervolgens het schalen van pediatrische CLR en geneesmiddeldoseringen (sectie III).
3. Het gebruik van een pediatrisch PBPK-gebaseerd model voor CLR om systematisch de invloed van ontogenie transporter op de bijdrage van ATS op CLR te onderzoeken en om te illustreren hoe een gecombineerde populatie PBPK benadering zou kunnen worden gebruikt om in vivo ontogenie functie voor renale transporters betrokken in ATS af te leiden (sectie IV).

In Sectie II werden datasets van bestaande popPK modellen uitgebreid met nieuwe data en gebruikt voor het optimaliseren van doseringsvoorschriften voor voornamelijk door GF geklaarde antibiotica. In Hoofdstuk 2, werd de invloed van perinatale asfyxie met therapeutische hypothermie (TH) gekwantificeerd op amikacine CLR en gebruikt om doseringsvoorschriften te ontwikkelen voor (pre) term neonaten. Amikacine CLR bleek met 40% te zijn verminderd in neonaten met perinatale asfyxie met TH, zonder veranderingen in distributievolume. Modelsimulaties toonden dat toename van de doseringsinterval met 12 uur resulteerde in een geoptimaliseerde blootstelling voor neonaten met perinatale asfyxie met TH, in vergelijking met behandeling met amikacine te worden met amikacine volgens het niet-aangepaste doseringsvoorschrift. In hoofdstuk 3 werd de invloed van co-administraties van indometacine of ibuprofen om de sluiting van de patent ductus arteriosus (PDA) te induceren gekwantificeerd op vancomycine CLR, en dit werd gebruikt om een doseeradvies te ontwikkelen in deze neonatale populatie. Co-administratie van indometacine verminderde de vancomycine klaring met 55% terwijl ibuprofen de CLR met slechts 16% verminderde. Simulaties lieten zien dat een verlaging van de initiële en de onderhoudsdosis van vancomycine met respectievelijk 20% en 60% in vergelijking met het originele doseerschema vereist was om de vancomycine blootstelling in neonaten met PDA te optimaliseren. Samenvattend: Populatie PK modellen konden in sectie II accuraat de netto maturatie van de CLR beschrijven als resultaat van veranderingen in de onderliggende fysiologische processen. Het gekwantificeerde effect van de combinatie van ziekte en co-medicatie op de CLR werd gebruikt om doseerschema's aan te passen voor (pre)terme neonaten met PATH of PDA onder behandeling met NSAIDs.

Terwijl sectie II gericht was op het gebruik van popPK benaderingen om de dosering te informeren gebaseerd op beschikbare klinische data, de volgende secties (secties III en IV) presenteerden algemene

methodes om pediatrische dosering te informeren door het schalen van CLR van volwassenen naar kinderen voor de situatie waar PK data beschikbaar is. In deze situatie worden vaak empirische schalingsmethodes gebaseerd op lichaamsgewicht gebruikt. Echter, de opkomst van PBPK methodes hebben geleid tot het succesvol voorspellen van pediatrische PK parameters² en een systematische analyse van bestaande empirische schalingsmethodes.

In sectie III (hoofdstuk 4) werd er een schalingsmethode voor CLR voor geneesmiddelen die geëlimineerd worden door GF voorgesteld die accuraat is voor het gehele pediatrische leeftijdsbereik. De functie van Salem et al. werd gebruikt voor GFR-gebaseerde schaling, nadat was aangetoond dat deze accuraat was voor de voorspelling van GFR over het hele pediatrische leeftijdsbereik. CLR door GF is afhankelijk van de GFR en de ongebonden fractie (f_u) van het geneesmiddel. Door het gebruik van hypothetische geneesmiddelen die enkel geklaard worden door GF en die enkel verschillen in hun f_u en type bindingseiwit in plasma (humaan serum albumine, α -1-zuur glycoproteïne) kon een systematische benadering gebruikt worden om te onderzoeken hoe de maturatie van plasma eiwit de schaling van CLR over het pediatrische leeftijdsbereik beïnvloedt. Aangezien het verschil tussen CLR waarden uit pediatrische PBPK modellen en uit GFR-gebaseerde schaling direct gerelateerd is aan de maturatie van f_u impliceren deze resultaten dat maturatie-gedreven veranderingen in plasma eiwit concentraties een minimale impact hebben op CLR schaling van geneesmiddelen uitgescheiden door GF. Dit betekent dat een betrouwbare meting van de ongebonden fractie in volwassenen voldoende is om GFR-gebaseerde schaling uit te voeren van volwassen naar kinderen voor CLR en de dosis. GFR-gebaseerde schaling was uiteindelijk accurater dan lineaire of allometrische, lichaamsgewicht-gebaseerde schaling met een exponent van 0.75.

Naast de impact van GF op de eliminatie van geneesmiddelen hebben we in sectie IV de impact van ATS op de CLR in een pediatrische populatie onderzocht. Dit onderzoek was hoognodig aangezien weinig onderzoek is gedaan naar de ontwikkeling van de CLR in deze leeftijdscategorie. Daarom hebben we, in hoofdstuk 5, een systematische analyse gedaan om de invloed van de ontwikkelingsfysiologie van transporters op de GF en ATS in kaart te brengen. Voor deze analyse is een pediatrisch PBPK model gebruikt dat geschikt was voor het maken van een schatting van de GF en ATS voor een groot aantal hypothetische geneesmiddelen met een breed scala aan eigenschappen, waaronder verschillen in transported-mediated intrinsic clearance ($CL_{int,T}$). Deze geneesmiddelen werden zo gekozen dat ze een substraat waren voor verschillende transporters, wat resulteerde in de identificatie van een bijdrage van ATS op de CLR tussen de 41% en de 90% in kinderen, afhankelijk van de f_u en $CL_{int,T}$ waarden. Wanneer er geen correctie voor de maturatie van ATS in het model aanwezig was en als de ontwikkeling van renale transporters minder was dan 20% van het niveau in de volwassenen waarde kon de CLR van de meerderheid van de geneesmiddelen niet goed voorspeld worden. Wanneer de ontwikkelingsfysiologie van secretie transporters niet meegenomen werd kon het niet op voorhand bepaald worden of de geschatte CLR waarden een accurate weergave gaven in kinderen jonger dan 2 jaar voor de onderzochte hypothetische geneesmiddelen.

Recentelijk heeft Cheung et al.² de wiskundige functies voor de ontwikkelingsfysiologie voor 8 renale transporters gerapporteerd, door middel van directe metingen van de eiwit expressie, specifiek voor elke transporter. Echter is het niet bekend in welke mate deze eiwit expressie overeenkomt met de ontwikkelingsfysiologie in vivo. De systematische analyse in hoofdstuk 5 kan helpen om deze vraag te beantwoorden door te bekijken bij welke geneesmiddelen de CLR voorspelling afhankelijk was van de ontwikkeling van een transporter. Deze geneesmiddelen kunnen dan gebruikt worden als een in vivo modelstof om de ontwikkelingsfysiologie beter te bestuderen. De meest geschikte modelstoffen zouden een $CL_{int,T}$ van 5–50 $\mu\text{L}/\text{min}/\text{mg}$ eiwitten middel tot hoge f_u moeten hebben in volwassenen ($f_u = 0.55–0.95$). Geneesmiddelen die voornamelijk door GF worden uitgescheiden of waarbij de $CL_{int,T}$ zo hoog is dat de renale bloedstroom de limitatie is zouden juist minder geschikt zijn in onderzoek naar de ontwikkelingsfysiologie.

In hoofdstuk 6 werd een gecombineerde populatie en fysiologisch-gebaseerde PK-modelaanpak (popPBPK) voorgesteld met als doel de ontogenie van transporters in vivo te bepalen op basis van concentratie-tijd data verzameld in kinderen. Om te differentiëren tussen GF en ATS werden PK-data gebruikt van twee modelmedicijnen die simultaan werden toegediend aan elke patient. Clavulaanzuur, voornamelijk geklaard door GF, en amoxicilline, voornamelijk geklaard door een combinatie van GF en ATS door OAT3. Door deze methode werd de in vivo OAT3 ontogeniefunctie bepaald. De ontogenie van OAT3 tussen 1 maand en 15 jaar bevond zich tussen 0.1 en 1 van de volwassen waarde, en bereikte de volwassen waarde bij 15 jaar. OAT3 levels bereikten de helft van de volwassen waarde rond de leeftijd van 7 maanden, zoals gekwantificeerd met een sigmoidale functie gebaseerd op PNA (in weken), hetgeen in lijn was met eerdere bevindingen². Daarnaast werd de ontwikkelde ontogeniefunctie voor OAT3 toegevoegd aan een pediatrisch PBPK-model voor CLR en gebruikt om de CLR van andere OAT3 substraten (i.e. cefazoline, piperacilline) te schalen. Met de in vivo OAT3 ontogeniefunctie leverde het PBPK-gebaseerde model accurate CLR-voorspellingen voor cefazoline en piperacilline (percentuele vierkantswortel van de gemiddelde kwadratische fout van 21% en 12%). Dit type analyse kan gebruikt worden om de in vivo transporterontogenie van andere renale transporters te bepalen.

8.2 Conclusie

Het blijft uitdagend om PK in kinderen te voorspellen, in het bijzonder voor kinderen jonger dan 2 jaar. In dit proefschrift werden verschillende modelleer- en simuleertechnieken gebruikt om pediatrische dosering te ondersteunen wanneer klinische data beschikbaar zijn (populatie PK-modellen) of wanneer deze data niet beschikbaar zijn (PBPK-methoden). Gebaseerd op klinische data kunnen populatie PK-methoden doseeraanpassingen ondersteunen in kwetsbare pediatrische subpopulaties (i.e. neonaten die hypothermische behandeling ondergaan, of met PDA) op basis van de bepaalde CLR-waarden. In het geval dat PK-data schaars of afwezig zijn, kunnen pediatrische doses bepaald worden op basis van CLR-waarden die zijn verkregen met empirische methoden of met meer actuele PBPK-methoden, zoals geïllustreerd voor medicijnen die alleen worden geëlimineerd door GF. Huidige PBPK-modellen voor CLR bevatten zowel GF als ATS. Door een gevoeligheidsanalyse uit te voeren op dit gevestigde model, konden we de invloed van ontogenie van renale transporters op actieve tubulaire secretie kwantificeren voor een brede selectie van medicijnen met verschillende eigenschappen. Tot slot werd de informatie in het PBPK-model voor CLR verder uitgebreid door het te integreren met relevante klinische data (popPBPK). Met deze aanpak werden voorheen slecht gekarakteriseerde parameters en/of ontogenie-/maturatiefuncties bepaald op basis van in vivo verzamelde data. De resultaten in dit proefschrift kunnen de basis vormen voor vergelijkbare verkenningen om de overgebleven relevante processen voor CLR te ontrafelen en de relevante bevindingen te vertalen naar richtlijnen voor veilige en effectieve pediatrische medicijndosering.

Section VI. Appendices



Curriculum vitae

Sinziana Cristea (1988, Suceava, Romania) started her academic education in 2007 with the Faculty of Pharmacy program at the University of Medicine and Pharmacy “Carol Davila” in Bucharest Romania. Sinziana obtained her Pharmacy degree in 2012 after completing her research internship at the Department of Physical-Chemistry on formulation studies for complexes with antitumoral action under the supervision of Dr. Mihaela Ghica and Prof. Dr. Cristina Dinu-Pirvu.

In 2013 Sinziana started her Master of Science program Bio Pharmaceutical Sciences with an internship at the Department of Pharmacology under the supervision of Dirk-Jan van den Berg and Prof. Dr. Elizabeth de Lange where she was trained in developing analytical analysis methods. Her second internship was at the Centre for Human Drug Research under the supervision of Dr. Jasper Stevens where she gained experience in modeling clinical data.

In 2015 Sinziana became a Research Assistant at Simcyp (a Certara company) in Sheffield, UK, where she further developed her skills in modeling approaches and contributed to the dermal absorption module of the Simcyp Simulator. In December 2015 Sinziana returned to Leiden University as a PhD student under the supervision of Dr. Elke Krekels, Prof. Dr. Karel Allegaert and Prof. Dr. Catherijne Knibbe where she applied modeling and simulation techniques to optimize pediatric drug dosing.

In April 2020 Sinziana joined the Integrated Drug Development team at Certara as a pharmacometrician and is specializing in using modeling and simulation to identify and address key decisions in drug development.

List of publications

Publications related to this thesis

Cristea, S., Krekels, E.H.J., Allegaert, K., De Paepe, P., de Jaeger, A., De Cock, P.A.J.G., Knibbe, C.A.J. Estimation of ontogeny functions for renal transporters using a combined population pharmacokinetic and physiology-based pharmacokinetic approach: application of OAT3. *AAPS J* 23, 65 (2021) <https://doi.org/10.1208/s12248-021-00595-9>

Cristea, S., Krekels, E.H.J., Rostami-Hodjegan, A., Allegaert, K., Knibbe, C.A.J. The Influence of Drug Properties and Ontogeny of Transporters on Pediatric Renal Clearance through Glomerular Filtration and Active Secretion: a Simulation-Based Study. *AAPS J* 22, 87 (2020). <https://doi.org/10.1208/s12248-020-00468-7>

Cristea, S., Krekels, E.H.J., Allegaert, K., Knibbe, C.A.J. The Predictive Value of Glomerular Filtration Rate-Based Scaling of Pediatric Clearance and Doses for Drugs Eliminated by Glomerular Filtration with Varying Protein-Binding Properties. *Clin Pharmacokinet* (2020). <https://doi.org/10.1007/s40262-020-00890-2>

Cristea S, Allegaert K, Falcao AC, Falcao F, Silva R, Smits A, Knibbe CAJ, Krekels EHJ. Larger Dose Reductions of Vancomycin Required in Neonates with Patent Ductus Arteriosus Receiving Indomethacin versus Ibuprofen. *Antimicrob Agents Chemother*. 2019 Jul 25;63(8):e00853-19.

Cristea S, Smits A, Kulo A, Knibbe CAJ, van Weissenbruch M, Krekels EHJ, Allegaert K. Amikacin Pharmacokinetics To Optimize Dosing in Neonates with Perinatal Asphyxia Treated with Hypothermia. *Antimicrob Agents Chemother*. 2017 Nov 22;61(12):e01282-17.

Publications unrelated to this thesis

Shimizu S., Hoedt S.M. den, Mangas-Sanjuan V., **Cristea S.**, Geuer J.K., Berg D.-J. van den, Hartman R., Bellanti F. & Lange E.C.M. de. Target-Site Investigation for the Plasma Prolactin Response: Mechanism-Based Pharmacokinetic-Pharmacodynamic Analysis of Risperidone and Paliperidone in the Rat. *Drug Metabolism and Disposition* February 2017, 45 (2) 152-159

Patel, N.K.; Clarke, J.; Arora, S.; Martins, F.; Salem, F.; Abdulla, T.; Tsakalozou, E.; Hodgkinson, A.; Tash, O.A.; **Cristea, S.**; et al. Multi-Phase Multi-LAYER Mechanistic Dermal Absorption (MPML MechDermA) Model to Predict Local and Systemic Exposure of Dermally Applied Drug Products 1: Model Structure and Parameterization (*Manuscript under Preparation*).

Affiliations of authors

Karel Allegaert	<i>Department of Development and Regeneration, KU Leuven, Belgium Department of Pharmacy and Pharmaceutical Sciences, KU Leuven, Belgium Department of Clinical Pharmacy, Erasmus MC, Rotterdam, The Netherlands</i>
Pieter A.J.G. De Cock	<i>Department of Pediatric Intensive Care, Ghent University Hospital, Belgium Heymans Institute of Pharmacology, Ghent University, Belgium Department of Pharmacy, Ghent University Hospital, Ghent, Belgium</i>
Peter De Paepe	<i>Department of Pediatric Intensive Care, Ghent University Hospital, Belgium</i>
Amílcar C Falcão	<i>Faculty of Pharmacy, University of Coimbra, Coimbra, Portugal</i>
Fátima Falcão	<i>Faculty of Pharmacy, University of Coimbra, Coimbra, Portugal Pharmacy Department, Centro Hospitalar de Lisboa Ocidental, Lisbon, Portugal</i>
Annick de Jaeger	<i>Heymans Institute of Pharmacology, Ghent University, Belgium</i>
Catherijne A.J. Knibbe	<i>Systems Biomedicine and Pharmacology, Leiden Academic Centre for Drug Research, Leiden University, Leiden, The Netherlands Department of Clinical Pharmacy, St. Antonius Hospital, Nieuwegein, The Netherlands</i>
Elke H.J. Krekels	<i>Systems Biomedicine and Pharmacology, Leiden Academic Centre for Drug Research, Leiden University, Leiden, The Netherlands</i>
Aida Kulo	<i>Institute of Pharmacology, Clinical Pharmacology and Toxicology, Medical Faculty, University of Sarajevo, Sarajevo, Bosnia and Herzegovina</i>
Amin Rostami-Hodjegan	<i>Simcyp Limited, Sheffield, UK Centre for Applied Pharmacokinetic Research (CAPKR), University of Manchester, Manchester, UK</i>
Rita Silva	<i>Pharmacy Department, Centro Hospitalar de Lisboa Ocidental, Lisbon, Portugal</i>
Anne Smits	<i>Department of Development and Regeneration, KU Leuven, Leuven, Belgium Neonatal Intensive Care Unit, University Hospitals Leuven, Leuven, Belgium</i>
Mirjam v. Weissenbruch	<i>Neonatal Intensive Care Unit, VU University Medical Center Amsterdam, Amsterdam, The Netherlands</i>

Acknowledgements

I would like to thank everyone who contributed to the finalization of this thesis.

This work could not have never been completed without the guidance of my promotor, Catherijne Knibbe and Karel Allegaert, and co-promotor, Elke Krekels. I am very grateful for the opportunity to collaborate on such engaging projects that resulted in this PhD thesis. Catherijne, thank you for your support and guidance and for always focusing on the positive side despite the challenges that came along with the research questions. Karel, thank you for your availability and for guiding the modeling results towards clinical applicability. Elke, as my daily supervisor, you were the victim of my first manuscript drafts and my unappealing choice of colors for graphics. Working with you has given me the chance to build confidence in my abilities. Thank you for your patience and guidance.

I would like to thank all the co-authors for their contributions, critical and constructive assessment of the scientific content of this work and for sharing their data and extensive knowledge in their respective fields.

I am especially grateful to have had such wonderful colleagues at LACDR. We have all been there for one another, had fun with great falafel, cheese, beers and bitterballen and ruminated on challenging modeling questions.

To my students, thank you for doing your best to contribute to this work. You helped me become a better mentor.

Aline, Bas, Linda, Mohammed, Parth and Swantje I greatly appreciate you critically reviewing my NONMEM and R code to ensure the quality and validity of this work.

A special thank you for Aline, Michiel, Rob, Wilbert and Paola for translating the Dutch Summary.

I'm thankful to my lovely and carrying friends for making my life fuller and richer in new experiences.

Părinților mei, vă mulțumesc că m-ați susținut în tot acest timp și că v-ați asigurat întotdeauna că am suficientă mâncare. Miky, îți mulțumesc că mi-ai fost alături și prin simțul umorului tipic nouă. Nu aș fi reușit fără voi!

(Translation: To my parents, thank you for your support through all this time and for making sure that I always had enough food. Miky, thank you for being there for me also through a sense of humor characteristic for the two of us. I could not have done it without you!)

Adrian, I could never thank you enough for your love and support throughout the many years we spent together and I hope the adventure will never end

Thank you.